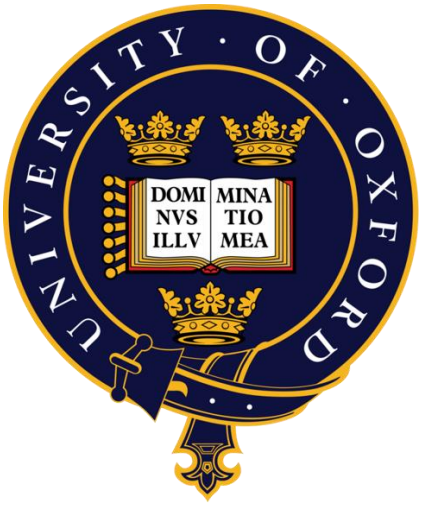
# Investigation into techniques to isolate and develop human germ cells *in vitro*




Eleni Papadopoulou

Kellogg College

University of Oxford

A Thesis submitted for the degree of

*Doctor of Philosophy*

Trinity Term 2020

**I dedicate this thesis to children who are deprived of liberty and education…**

Πάντα στὸ νοῦ σου νἄχῃς τὴν Ἰθάκη.
Τὸ φθάσιμον ἐκεῖ εἶν᾽ ὁ προορισμός σου.

Ἀλλὰ μὴ βιάζῃς τὸ ταξείδι διόλου.
Καλλίτερα χρόνια πολλὰ νὰ διαρκέσει.
Καὶ γέρος πιὰ ν᾽ ἀράξῃς στὸ νησί,
πλούσιος μὲ ὅσα κέρδισες στὸν δρόμο,
μὴ προσδοκώντας πλούτη νὰ σὲ δώσῃ ἡ Ἰθάκη.

Ἡ Ἰθάκη σ᾽ ἔδωσε τ᾽ ὡραῖο ταξίδι.
Χωρὶς αὐτὴν δὲν θἄβγαινες στὸν δρόμο

- Κωνσταντίνος Καβάφης

Keep Ithaka always in your mind.
Arriving there is what you are destined for.

But do not hurry the journey at all.
Better if it lasts for years,
so you are old by the time you reach the island,
wealthy with all you have gained on the way,
not expecting Ithaka to make you rich.

Ithaka gave you the marvellous journey.
Without her you would not have set out.

- Constantine P. Cavafy

# Abstract

Premature ovarian insufficiency (POI) occurs in 1% of women younger than 40 years of age. The manifestation of this condition varies considerably ranging from ovaries devoid of follicles (afollicular POI) to ovaries containing follicles at various stages of development (follicular POI). No methods exist in mainstream healthcare to restore ovarian function for POI patients and ≥70% of POI cases are idiopathic. The Reaggregated Ovary (RO) method, as established for mice, enables investigation into the developmental potential of oocytes by replacing dysfunctional ovarian cells. This approach could enable us to develop a potential treatment for patients with follicular POI. Investigations carried out in this thesis led to the establishment of key processes required to adapt the RO method for human tissue. A method was developed to dissociate human ovarian tissue remnants (surplus after tissue cryopreservation) and frozen/thawed ovarian cortex obtained from pre-pubertal and post-pubertal patients. Analyses revealed that age affected the efficacy of dissociation of frozen/thawed ovarian cortical tissue. To detect germ cells in a single cell suspension of ovarian cells, a method was developed for flow cytometry using a monoclonal antibody that recognises the (cytoplasmic) N-terminus region of DDX4. To assess the use of an alternative somatic cell source to support oocyte development, human dermal fibroblasts were aggregated with mouse oocytes and follicle-like structures were formed after 7-day in culture. These findings will contribute to developing the use of the RO using human oocytes and a human somatic cell alternative. The RO method once adapted for human tissue could be used to replace the dysfunctional ovarian somatic cells in POI patients and potentially restore follicle development for pre-pubertal and post-pubertal POI patients.

# Acknowledgements

My DPhil was an incredible journey. I was lucky enough to share this amazing experience with great people I met along the way.

I would like to express my sincerest thanks to Prof Suzannah Williams, who took me under her wings and helped me develop as a scientist, and Dr Rebecca Dragovic who was always there to guide me; thank you both from the bottom of my heart for always supporting me.

I wouldn't be able to pursue this DPhil if it wasn't for my family. I will always be grateful to you for believing in me even when I didn't, and for your unconditional love. A big thank you, too, to those of you that were part of this journey and kept me motivated to overcome any obstacle I encountered.

I would also like to say a big thank you to Dr Karl Morten and Dr Jen Southcombe who were always there to help me troubleshooting and supported me when I needed it. Many thanks to Prof. Jo Poulton, Janet Carver, and Celine Jones who contributed to this work, thank you so much!

And of course, I could not forget my amazing team. Sairah, Charlotte, Xi, Briet, Tomi, Aleona, and Ruth, thank you so much for being part of this journey; I couldn't have asked for better teammates. Belinda, you were an amazing mentor and friend during my first year in Oxford, thank you for everything! My crazy friends Carolina and Helena, thank you for everything we shared. I would also like to thank my flow expert Monica who was always available to answer my random questions with a generous smile and share moments at the end office…

Finally, I would like to thank all the people working at the department for being so pleasant and cheerful on our day-to-day, and of course all the students with whom I spent a significant time of my life.

# Table of Contents


ABSTRACT ..... 4
ACKNOWLEDGEMENTS ..... 5
LIST OF ABBREVIATIONS ..... 11
CHAPTER 1 ..... 15
1.1. OVERVIEW ..... 15
1.2. OVARIAN FUNCTION ..... 16
1.2.1. The mammalian ovary and its structure ..... 16
1.2.2. Oogenesis and folliculogenesis ..... 18
1.2.3. Follicle development ..... 19
1.2.3.1. Initial stages of development ..... 20
1.2.3.2. Pre-antral follicle development ..... 21
1.2.3.3. Antral follicle development and transition into the pre-ovulatory stage in humans ..... 23
1.2.3.4. Selection and ovulation of the dominant follicle in humans ..... 25
1.2.4. Oocyte meiotic and developmental competence ..... 25
1.2.5. Factors involved in the regulation of follicle development ..... 26
1.2.5.1. Early stages of follicle development ..... 26
1.2.5.2. Later stages of follicle development ..... 27
1.3. PREMATURE OVARIAN INSUFFICIENCY ..... 32
1.3.1 Aetiology for POI ..... 34
1.3.1.1 Genetic causes ..... 35
1.3.1.2 Autoimmune causes ..... 38
1.3.1.3 Iatrogenic causes ..... 39
1.3.2 Subclassification of POI ..... 39
1.3.3 Mechanisms underlying POI ..... 42
1.3.3.1 Follicle depletion ..... 44
1.3.3.2 Follicle dysfunction ..... 44
1.3.4 Available treatments for women and young girls diagnosed with POI ..... 46
1.3.4.1 Considerations ..... 49
1.3.5 The Reaggregated Ovary method as a potential technique to restore follicle development for dysfunctional ovaries ..... 50
1.4. AIMS ..... 52
CHAPTER 2 ..... 53
2.1. HUMAN OVARIAN TISSUE SAMPLES ..... 53
2.1.1. Sourcing tissue from the Oxford Cell and Tissue Biobank ..... 53
2.1.2. Information on patient characteristics ..... 54
2.1.3. Inclusion and exclusion criteria ..... 54
2.1.4. Collection and cryopreservation of ovarian tissue ..... 54
2.2. OBTAINING HUMAN OVARIAN TISSUE SAMPLES ..... 56
2.2.1. Fresh ovarian cortex from whole ovaries ..... 56
2.2.2. Ovarian remnant tissue after cortical tissue dissection prior to cryopreservation ..... 56
2.2.3. Frozen/stored ovarian cortical tissue ..... 57
2.3. THAWING OF HUMAN OVARIAN CORTICAL STRIPS ..... 57
2.4. CALCULATING NET WEIGHT OF HUMAN OVARIAN CORTICAL STRIPS ..... 58
2.5. MOUSE COLONIES ..... 58
2.6. THE REAGGREGATED OVARY TECHNIQUE ..... 61
2.6.1. Generation of Reaggregated Ovaries ..... 61
2.6.2. Cell viability assessment ..... 62
2.6.3. Reaggregated Ovary culture ..... 65
2.7. TISSUE PROCESSING ..... 66
2.7.1. Tissue collection and fixation methods ..... 66

2.7.2. Embedding process ..... 67
2.7.2.1. Dehydration ..... 67
2.7.2.2. Embedding ..... 68
2.7.2.3. Sectioning ..... 69
2.8. HISTOLOGICAL PROCESS ..... 69
2.8.1. Haematoxylin and Eosin staining ..... 69
2.9. ASSESSMENT OF FOLLICLE DEVELOPMENT IN ROS ..... 70
CHAPTER 3 ..... 72
3.1 INTRODUCTION ..... 72
3.1.1 Overview ..... 72
3.1.2 Background ..... 73
3.1.3 Commercially available enzymes ..... 74
3.1.3.1. Considerations ..... 76
3.1.4 Anti-apoptotic factors ..... 79
3.2 AIMS ..... 80
3.3 MATERIALS & METHODS ..... 81
3.3.1 Ovarian tissue source ..... 81
3.3.1.1. Types of human ovarian tissue used ..... 81
3.3.2 Exclusion criteria for tissue donors ..... 82
3.3.3 Overview of the methodology applied to dissociate human ovarian tissue ..... 82
3.3.4 Human fresh ovarian cortical tissue dissociation ..... 83
3.3.4.1 Variables tested to investigate the dissociation of fresh cortex ..... 83
3.3.4.2 Methodology applied to explore the efficacy of trypsin and collagenase to dissociate fresh cortical tissue (Protocol A) ..... 85
3.3.4.3 Methodology to explore the efficacy of mechanical dissociation using a shaker to dissociate fresh cortical tissue (Protocol B) ..... 87
3.3.4.4 Methodology to explore the efficacy of anti-apoptotic factors to improve dissociation of human fresh ovarian cortical tissue using Protocol B ..... 88
3.3.5 Human ovarian remnant tissue dissociation ..... 88
3.3.5.1. Variables tested to investigate the dissociation of human fresh ovarian remnant tissue. 89
3.3.5.2. Methodology used to dissociate human fresh ovarian remnant tissue (Protocol C) ..... 89
3.3.6 Methodology used to dissociate human frozen/thawed ovarian cortical tissue (Protocol D) .... 91
3.3.7 Normalisation of cell numbers ..... 94
3.3.8 Statistical analysis ..... 94
3.4 RESULTS ..... 95
3.4.1 Age and characteristics of the patients included ..... 95
3.4.2 Efficacy of control trypsin compared with collagenase to dissociate human fresh ovarian cortex (Protocol A) ..... 96
3.4.3 Enzymatic digestion combined with mechanical dissociation for fresh ovarian cortex (Protocol B) ..... 98
3.4.4 Enzymatic digestion combined with mechanical dissociation for human fresh ovarian remnant tissue (Protocol C) ..... 102
3.4.5 Exploring a method to dissociate human frozen/thawed ovarian cortex ..... 104
3.5 DISCUSSION ..... 110
3.5.1 Human fresh ovarian cortical tissue ..... 110
3.5.2 Human fresh ovarian remnant tissue ..... 111
3.5.3 Human frozen/thawed ovarian cortical tissue ..... 112
3.6 CONCLUSIONS ..... 113
CHAPTER 4 ..... 115
4.1 INTRODUCTION ..... 115
4.1.1 Overview ..... 115
4.1.2 Ovarian age ..... 116
4.2 AIMS ..... 117
4.3 MATERIALS & METHODS ..... 118

4.3.1. Ovarian tissue source and exclusion criteria ..... 118
4.3.2. Human fresh ovarian remnant tissue ..... 118
4.3.2.1. Process of ovarian remnants and cell debris prior to tissue dissociation ..... 118
4.3.2.2. Dissociation of ovarian remnant tissues ..... 118
4.3.3. Human frozen/thawed ovarian cortical tissue ..... 119
4.3.3.1. Dissection of frozen/thawed ovarian cortical tissue ..... 119
4.3.3.2. Dissociation of frozen/thawed ovarian cortical tissue ..... 119
4.3.4. Cell numbers ..... 121
4.3.5. Exploring the efficacy of different dissociation methods in younger and older patients ..... 121
4.3.6. Exploring the effect of age on the dissociation of frozen/thawed ovarian cortex ..... 122
4.3.7. Statistical analysis ..... 122
4.4 RESULTS ..... 124
4.4.1. Patient age and characteristics ..... 124
4.4.2. Cell viability was maintained after dissociation of human fresh ovarian remnants ..... 125
4.4.3. Comparison of three methods to dissociate human frozen/thawed ovarian cortex: 'Shaker L15', 'L15' and 'PBS' ..... 127
4.4.4. Comparing the efficacy of 'Sh.L15', 'L15', and 'PBS' to dissociate human frozen/thawed ovarian cortex from younger and older patients ..... 129
4.4.5. The efficacy of dissociation across different ages ..... 132
4.5 DISCUSSION ..... 134
4.5.1. Overview ..... 134
4.5.2. Factors that may affect dissociation of human frozen/thawed ovarian cortex ..... 134
4.5.3. The effect of age on the dissociation of human frozen/thawed ovarian cortical tissue ..... 136
4.5.4. Conclusions ..... 139
CHAPTER 5 ..... 140
5.1. INTRODUCTION ..... 140
5.1.1. Basic principles of flow cytometry ..... 141
5.1.1.1. Flow cytometer instrument components ..... 142
5.1.1.2. Fluorochromes and fluorescence principles in flow cytometry ..... 144
5.1.1.3. Monoclonal antibodies in flow cytometry ..... 144
5.1.1.4. Viability assessment by flow cytometry ..... 145
5.1.1.5. Flow cytometry analysis ..... 146
5.1.2. DEAD-box helicase 4 germ line regulator ..... 147
5.1.2.1. DDX4 localisation ..... 148
5.1.3. The role of HeLa cells and human ovarian remnant tissue in this chapter ..... 156
5.2. AIMS ..... 157
5.3. MATERIALS AND METHODS ..... 158
5.3.1. HeLa cell viability analysis using flow cytometry ..... 158
5.3.2. Immunolabelling of intracellular cytokeratin 13 in HeLa cells ..... 159
5.3.3. Immunolabelling of intracellular DDX4 in HeLa cells ..... 160
5.3.4. Ovarian tissue source and exclusion criteria ..... 161
5.3.5. Patient age and characteristics ..... 161
5.3.6. Ovarian single cell suspension obtained from human fresh ovarian remnant tissue ..... 162
5.3.7. Red-blood-cell lysis of cells from human fresh remnant tissue ..... 162
5.3.8. Ovarian single cell suspension from human frozen/thawed ovarian cortical tissue ..... 163
5.3.9. Live/Dead cell discrimination for flow cytometry analysis ..... 163
5.3.10. Fixation and permeabilisation for flow cytometry analysis ..... 163
5.3.11. Immunolabelling of cytoplasmic DDX4 in human ovarian cells using flow cytometry ..... 164
5.3.12. Flow cytometry analysis ..... 165
5.3.13. Statistical analysis ..... 166
5.4. RESULTS ..... 167
5.4.1. Part 1 - HeLa cells ..... 167
5.4.1.1. Live/dead cell discrimination using HeLa cells ..... 167
5.4.1.2. Efficacy of fixation/permeabilisation using HeLa cells ..... 169
5.4.1.3. Flow cytometry gating strategy to detect intracellular DDX4 using HeLa cells ..... 170

5.4.1.4. Detection of intracellular DDX4 in HeLa cells ..... 172
5.4.2. Part 2 – Human fresh ovarian remnant tissue ..... 173
5.4.2.1. Flow cytometry gating strategy to identify viable cells from human fresh ovarian remnant tissue ..... 173
5.4.2.2. Detection of viable cells from human ovarian remnants ..... 174
5.4.2.3. Detection of DDX4-positive cells from human fresh ovarian remnant tissue ..... 178
5.4.3. Part 3 – Human frozen/thawed ovarian cortical tissue ..... 184
5.4.3.1. Flow cytometry gating strategy to identify viable cells from human frozen/thawed ovarian cortical tissue ..... 184
5.4.3.2. Viable cells from human frozen/thawed ovarian cortical tissue ..... 186
5.4.3.3. Detection of DDX4-positive cells from human frozen/thawed ovarian cortical tissue ..... 188
5.5. DISCUSSION ..... 194
5.5.1. Overview ..... 194
5.5.2. Establishment of a flow cytometry gating strategy to detect the intracellular germ cell marker DDX4 ..... 194
5.5.3. Verification of the specificity of the monoclonal anti-DDX4 antibody used ..... 197
5.5.4. Further assessment of the DDX4-positive cell population ..... 198
5.5.4.1. Perivascular cells in the ovarian cell suspensions analysed ..... 201
5.5.5. Pubertal status did not affect DDX4 labelling ..... 202
5.5.6. Barriers to this study ..... 202
5.5.7. Conclusions ..... 203
CHAPTER 6 ..... 204
6.1. INTRODUCTION ..... 204
6.1.1 Background ..... 204
6.1.2 The 'artificial ovary' ..... 207
6.1.3 Germ cell source ..... 209
6.1.4 The potential of human dermal fibroblasts ..... 210
6.2. AIMS ..... 213
6.3. MATERIALS AND METHODS ..... 214
6.3.1. Source of cells to generate fibroblast-ROs ..... 214
6.3.2. Human dermal fibroblast cell culture ..... 214
6.3.3. Generating Control-ROs and fibroblast-ROs *in vitro* ..... 215
6.3.4. *In vitro* culture of Control-ROs and FibROs ..... 216
6.3.5. Tissue fixation, Embedding and Sectioning ..... 216
6.3.6. Histological analysis ..... 216
6.3.7. AMH detection using immunohistochemistry ..... 216
6.3.8. Analysis of AMH in FibROs and Control-ROs ..... 220
6.3.9. Assessment of follicle development in Control-ROs and follicle-like structure formation in FibROs ..... 220
6.4. RESULTS ..... 221
6.4.1 Generation of fibroblast-RO *in vitro* ..... 221
6.4.2 Histological analysis revealed follicle-like structures in FibROs ..... 223
6.4.3 Analysis of AMH in Control-ROs and FibROs ..... 226
6.5. DISCUSSION ..... 228
6.5.1 Fibroblast-RO structure ..... 229
6.5.2 Follicle-like structures in fibroblast-RO ..... 230
6.5.3 No AMH detection in fibroblast-RO ..... 233
6.5.4 The FibRO as a promising tool to restore follicle development for POI patients with follicle dysfunction ..... 235
6.5.5 Conclusions ..... 236
CHAPTER 7 ..... 237
7.1 MAIN FINDINGS FROM THIS THESIS ..... 238
7.2 FUTURE WORK ..... 239
7.3 FINAL REMARKS ..... 247

LIST OF FIGURES AND TABLES ..... 249
BIBLIOGRAPHY ..... 252
APPENDIX I. ..... 274
APPENDIX IIA. ..... 280
APPENDIX IIB. ..... 283
APPENDIX III ..... 286

# List of abbreviations

| | |
|---|---|
| 3D | 3-dimensional |
| 3βHSD | 3β-hydroxysteroid dehydrogenase |
| AAF | Anti-apoptotic factors |
| ABC | Avidin-biotin-peroxidase complex |
| ALK | Activin receptor-like kinase |
| aMEM | Alpha minimal essential media |
| AMH | Anti-müllerian hormone |
| APS | Autoimmune polyglandular syndrome |
| AR | Androgen receptor |
| ArKO | Aromatase knockout mouse model |
| ATP | Adenosine triphosphate |
| BIRC1 | Baculoviral IAP repeat containing protein 1 |
| BMP-15 | Bone morphogenetic protein 15 |
| BMPRII | Bone morphogenetic protein receptor II |
| BP | Band pass |
| BSA | Bovine serum albumin |
| BV-510 | Brilliant violet 510 |
| cAMP | Cyclic adenosine monophosphate |
| CTGF | Connective tissue growth factor |
| CL | Corpus luteum |
| COC | Cumulus oocyte complex |
| Cyt.13 | Cytokeratin 13 |
| D | Digested |
| DDX4 | DEAD-box helicase 4 |
| DHEA | Dehydroepiandrosterone |
| DM | Double mutant |
| DM | Dissection media |
| DMSO | Dimethyl sulfoxide |
| DPBS | Dulbecco's phosphate buffered saline |
| $E_2$ | Oestradiol |
| ECM | Extracellular matrix |
| EDTA | Ethylenediamine tetraacetic acid |
| ER | Oestrogen receptors |
| ERα | Oestrogen receptor alpha |
| ERβ | Oestrogen receptor beta |
| ERαKO | Oestrogen receptor alpha Knock out |
| ERβKO | Oestrogen receptor beta Knock out |
| ES | Enzymatic solution |

| | |
|---|---|
| FACS | Fluorescence-activating cell sorting |
| FBS | Fetal bovine serum |
| FC | Flow cytometry |
| FF | Follicular fluid |
| FibRO | Fibroblast-RO |
| FMR1 | FMRP translational regulator 1 |
| FMRP | Fragile X mental retardation protein |
| FOXL2 | Forkhead box L2 |
| FOXO3α | Forkhead box O3a |
| FP | Fertility preservation |
| FSC | Forward scatter |
| FSC-A | Forward scatter-area |
| FSC-H | Forward scatter-height |
| FSC-W | Forward scatter-weight |
| FSH | Follicle stimulating hormone |
| FSHR | Follicle stimulating hormone receptor |
| GCs | Granulosa cells |
| GDF-9 | Growth differentiation factor 9 |
| GFP | Green fluorescence protein |
| GJs | Gap junctions |
| GnRH | Gonadotropin releasing hormone |
| HSA | Human serum albumin |
| HDFs | Human dermal fibroblasts |
| $H_E$:$H_{HESomCs}$ | Human eggs to human dermal fibroblasts |
| $H_E$:$H_{iPSCs}$ | Human eggs to human induced pluripotent stem cells |
| $H_E$:$M_{OS}$ | Human eggs to mouse ovarian somatic cells |
| hESCs | Human embryonic stem cells |
| HPG | Hypothalamic-pituitary-gonadal (axis) |
| HSPs | Heat-shock proteins |
| ICSI | Intracytoplasmic sperm injection |
| IEGs | Immediate early gene products |
| INHA | Inhibin subunit alpha |
| IP | Immunoprecipitation |
| iPSCs | Induced pluripotent stem cells |
| ITS | Insulin-transferrin-selenium |
| IVA | *In vitro* activation |
| IVF | *In vitro* fertilisation |
| IVM | *In vitro* maturation |
| LH | Luteinising hormone |
| LHR | Luteinising hormone receptor |
| LP | Long pass |

| | |
|---|---|
| M199 | Medium 199 |
| mAbs | Monoclonal antibodies |
| MDFs | Mouse dermal fibroblasts |
| $M_E$:$H_{HDFs}$ | Mouse eggs to human dermal fibroblasts |
| MMP | Matrix metalloproteinases |
| MS | Mass spectrometry |
| ND | Not digested |
| NP-40 | Nonyl phenoxypolyethoxylethanol |
| O/N | Overnight |
| OCTB | Oxford cell and tissue biobank |
| OHSS | Ovarian hyperstimulation |
| OSCs | Oogonia stem cells |
| OTC | Ovarian tissue cryopreservation |
| pAbs | Polyclonal antibodies |
| PCOS | Polycystic ovarian syndrome |
| PE-A | R-phycoerythrin-area |
| PGCs | Primordial germ cells |
| PHA-P | Phytohemagglutinin |
| PI3K | Phosphoinositide-3-kinase |
| PMTs | Photomultiplier tubes |
| POI | Premature ovarian insufficiency |
| P | Progesterone |
| PR-A | Progesterone receptor A |
| PR-B | Progesterone receptor B |
| PTEN | Phosphatase and tensin homolog |
| RBC | Red blood cell |
| RT | Room temperature |
| RO | Reaggregated ovary |
| ROCK | Rho associated coiled-coil containing kinase |
| rOvary | Artificial ovary |
| R-PE or RPE | R-phycoerythrin |
| SCF | Stem cell factor (KIT ligand) |
| SSC | Side scatter |
| SSC-A | Side scatter-area |
| SSC-H | Side scatter-height |
| SSC-W | Side scatter-weight |
| TCs | Theca cells |
| TDE | Tumour dissociation enzyme |
| TGF-β | Transforming growth factor beta superfamily |
| TS | Turner syndrome |
| T-syn | β1,3-galactosyltransferase |

| | |
|---|---|
| TZPs | Transzonal projections |
| WB | Western blot |
| WT | Wild type |
| YAP | Yes associated transcriptional regulator |
| YBX2 | Y-box binding protein 2 |
| ZA | Zombie aqua |
| ZP | Zona pellucida |
| LHX8 | LIM homeobox 8 |
| EtOH | Ethanol |

# CHAPTER 1

# *Introduction*

## 1.1. Overview

Premature ovarian insufficiency (POI) is a common cause for infertility/subfertility and affects ~1% of women younger than 40 years (Coulam et al. 1986). Unfortunately, current knowledge of the causes underlying POI is limited; ~70%-90% of the cases are idiopathic (Shelling 2010; Nelson et al. 2005; Woad et al. 2006; Nelson 2009) and there are no established options to restore ovarian function in young girls and women diagnosed with POI in healthcare. More information is required to elucidate the mechanisms underlying POI in order to be able to develop more options to restore normal ovarian function for POI patients. The investigations presented in this thesis will contribute to the development of methods that could potentially be used to restore follicle development for patients diagnosed with POI, and follicle dysfunction.

## 1.2. Ovarian function

### 1.2.1. The mammalian ovary and its structure

The mammalian ovary is a dynamic organ with key roles in reproduction. Human ovaries are the female reproductive organs, have an ovoid shape, and are located in the pelvic area close to the lateral pelvic wall (one on each side of the uterus). Externally, human ovaries appear pink-white and weigh approximately 4 g each but size depends on age and varies considerably among individuals (Blaustein 1982). The two primary functions of the ovary are the generation and release of a mature egg and the production of hormones to support puberty and prospective pregnancies (Hirshfield 1991; McGee et al. 2000). The ovary contains oocytes surrounded by somatic cells (e.g. granulosa, theca, cumulus), stromal, immune, endothelial, perivascular and epithelial cells, as well as fibroblasts, extracellular matrix, and blood vessels (Hummitzsch et al. 2015; Wagner et al. 2020). The outermost layer of the human ovary is a single layer of squamous mesothelium cells, the surface epithelium. Underneath the surface epithelium there is a highly dense and collagen-rich area, the cortex (discussed in Chapter 3); the ovarian cortical tissue has a critical role in female fertility preservation as it hosts the fixed ovarian reserve. The human cortex (~1mm to 2mm thick) is separated from the surface epithelium by the basal lamina (tunica albuginea). The innermost part of the ovary, the medulla, is a less dense area compared to cortex, and highly vascularised (Blaustein 1982) (Figure 1. 1).

The basic functional unit of the ovary is the follicle. A single follicle is comprised of the oocyte surrounded by somatic cells essential to nurture and support oocyte development into a mature and fertilisable egg. In the human ovary, follicles are

localised at different areas within the ovary depending on the developmental stage. It is thought that the high density of cortical tissue is comparatively non-permissive and does not allow for follicle growth. Hence, follicles at the earliest stage of follicle development (primordial follicles) are found in the cortex of the human ovary, while growing follicles (primary up to antral) are found in the inner part of the human ovary which is less dense and highly vascularised, the medulla (Woodruff et al. 2011) (Figure 1. 1). Pre-ovulatory follicles are seen close to the cortex; the mature egg is released into the fallopian tube during ovulation (Figure 1. 1).

Follicle development in humans is discussed in detail in the following sections.

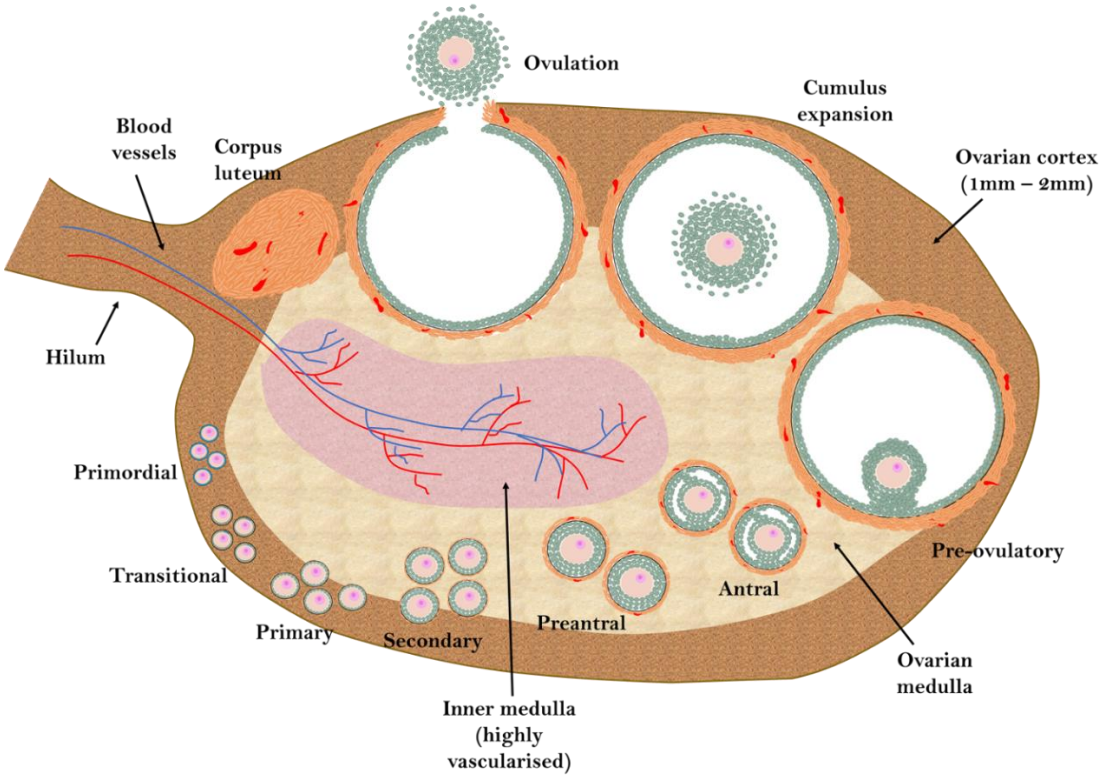



**Figure 1. 1 Follicle development in the human ovary.** Primordial follicles lie in the ovarian cortex. Once activated, the primordial follicle transitions into the primary stage after >120 days of growth, and both oocyte and follicle growth are initiated. Growing follicles are found in the medulla during development but close to the cortex later to release the egg into the fallopian tube (preovulatory and ruptured follicle). The middle of the medulla is a highly vascularised area with no follicles.

### 1.2.2. Oogenesis and folliculogenesis

The earliest known form of the oocyte is the primordial germ cell (PGC) (Wartenberg 1982). In human embryos, PGCs first appear at week 2 of gestation at an extragonadal site, the wall of the yolk sac (Marlow 2015; De Felici 2013). At week 4 of development, PGCs migrate to the gonadal ridges through the dorsal mesentery (Kozhukhar 2011) and have colonized the gonadal ridges during week 6 of gestation (Motta et al. 1997) before female sex determination occurs (at week 8 of gestation (Wartenberg 1982)). Prior to migration of PGCs, cells at the mesonephros epithelium (gonadal-ridge epithelial like cells) proliferate whereby PGCs, and mesonephric stromal cells, penetrate to form the gonadal ridge (Hummitzsch et al. 2015). At the gonadal ridge, PGCs differentiate into oogonia, which have high mitotic activity, and form clusters of dividing cells; germ cell nests (Gondos et al. 1986; Ruby et al. 1970).

Oogonia proliferate mitotically until the 5$^{th}$ month of gestation. This process overlaps with entry into meiosis and arrest; by entering into meiosis, oogonia differentiate into primary oocytes (De Felici 2013; Rosario et al. 2017). Primary oocytes arrest at prophase I of the diplotene stage. This is followed by germ cell nest breakdown whereby somatic cells invade the nests and surround the primary oocyte to form a primordial follicle (Pepling et al. 2001). These somatic cells, known as flattened pre-granulosa cells, are believed to originate from the ovarian surface epithelium (Niu et al. 2020), and their progenitors are believed to be the gonadal-ridge epithelial like cells (GREL cells) (Hummitzsch et al. 2015).

Not all germ cells in the nests will become primordial follicles; around two-thirds of oogonia will become atretic at the time of germ cell nest breakdown through apoptotic

mechanisms (Pepling et al. 2001). Even though meiotic arrest after formation can last for decades if follicles are not recruited into the growing pool (discussed below), once the primordial follicle activates (discussed below), the primary oocyte keeps growing and gains meiotic and developmental competence through follicle development until ovulation (Rosario et al. 2017).

In humans, the primordial follicle pool, and thus the ovarian reserve, is formed during embryonic development and determined by birth (Findlay et al. 2015). Prepuberty, the primordial follicle leaves the dormant stage when it is activated to initiate follicle growth. Follicles entering recruitment will reach the preantral stage and eventually become atretic if during the prepubertal years (McGee et al. 2000).

### 1.2.3. Follicle development

Development of the ovarian follicle is a complex process. Constant changes inside the nucleus and cytoplasm of the oocyte occur to generate a mature and fertilisable egg (Baca et al. 1967).

Follicle development is characterised by growth of the oocyte and its associated follicle. In humans, primordial follicle diameter is 0.026-0.040 mm (Himelstein et al. 1976), which increases to ~10 mm in antral follicles and ~20 mm in pre-ovulatory follicles (Gougeon 1986). The oocyte is ~36 µm at the primordial stage but this size increases to ~120 µm in antral and pre-ovulatory follicles (Griffin et al. 2006). The estimated timeline for follicle development in humans is illustrated in (Figure 1. 2).

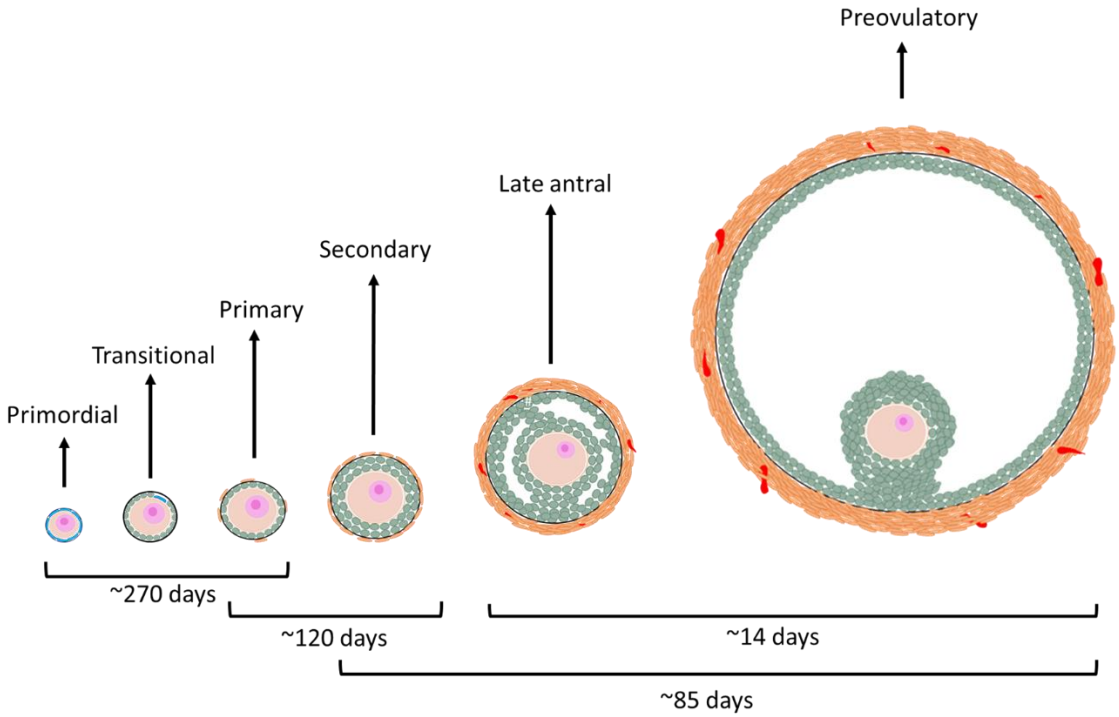



**Figure 1. 2 Estimated timeline for follicle development in humans. Transition from the primordial stage** (a single flattened layer of pre-granulosa cells) to primary stage (a single layer of cuboidal granulosa cells (GCs) takes ~270 days (Gougeon 1986). Transition from the primary to the secondary stage (two layers of GCs) takes more than 120 days (Gougeon 1986). Follicle development from the secondary to preovulatory stage (large antral cavity) takes ~85 days (Alain Gougeon 1996), and progression from the antral to preovulatory stage occurs across the 14-day follicular phase of the menstrual cycle (Alain Gougeon 1996).

Reciprocal communication between the oocyte and surrounding somatic cells is a prerequisite for follicle development (Anderson et al. 1976). The oocyte is closely bound to the follicular somatic cells through the formation of transzonal projections (TZPs) (actin filaments) (Anderson et al 1976; El-Hayek et al. 2018) which increase in number as the follicle develops (El-Hayek et al. 2018).

### 1.2.3.1. Initial stages of development

Staging of follicle development was first proposed for mouse (Pedersen et al. 1968) and then adapted for human (Gougeon 1986). In humans, primordial follicles can remain inert at a meiotically dormant state for years or be activated immediately after

formation. Activation of some follicles is believed to be a continuous process that starts after follicle formation. Oocytes that do not form follicles are believed to degenerate (Ohno et al. 1964). Throughout a woman's reproductive life, when the number of primordial follicles is reduced to a critical threshold of ~1000, reproduction ceases and they enter menopause (Faddy et al. 1996; Richardson et al. 1987) with the average menopausal age being 51 years (Faddy et al. 1996).

Primordial follicle activation entails differentiation of flattened pre-granulosa cells (single layer) into cuboidal granulosa cells (GCs) (Figure 1. 2). The intermediate stage where the oocyte is surrounded by a mixed single layer of flattened pre-granulosa and cuboidal GCs is characterised as the transitional follicle (Figure 1. 2). When a complete single layer of cuboidal granulosa cell is formed around the oocyte, transition into the primary stage (primary follicle) is complete (Figure 1. 2). Through this stage, the zona pellucida (ZP), an extracellular matrix coat comprised of glycoproteins, forms to surround the oocyte as a thin layer (Gook et al. 2008; Baca et al. 1967). In humans, ZP glycoproteins are secreted by the oocyte cytoplasm from the primordial stage onwards (Gook et al. 2008). A thin incomplete ring of ZP1 and ZP3 only forms around the oocyte at the primordial stage; through the primary stage, ZP2 is also expressed (Gook et al. 2008). This extracellular matrix coat (ZP) becomes thicker at the secondary stage and through to the antral stage in humans (Gook et al. 2008).

#### 1.2.3.2. Pre-antral follicle development

At the primary stage onwards, the oocyte continues to grow, the zona pellucida is formed, and GCs proliferate to form multiple layers (Baca et al. 1967). In secondary follicles, the oocyte is surrounded by up to 2 complete layers of GCs (Baca et al. 1967;

Faddy et al. 1996) (Figure 1. 2). Oocyte growth continues and GCs keep proliferating to form multiple layers in the preantral follicle (Faddy et al. 1996) (Figure 1. 2). Follicle development is gonadotropin responsive (gonadotropin receptors are expressed on GCs but follicle growth does not require gonadotropins) from the secondary stage through to the antral stage whereby antral follicle development is gonadotropin dependent (follicle growth requires gonadotropins) (Craig et al. 2007; Oktay et al. 1997). Although FSH receptors (FSHR) are expressed in follicles prior to gonadotropin-dependence, FSH does not play an essential role in follicle growth until the antral stage (Craig et al. 2007; Oktay et al. 1997).

*Theca cells*

Theca cells (TCs) have a crucial role in follicle development as they support follicle structure and blood supply and produce the ovarian androgens (Braw-Tal et al. 2005) that are the necessary substrates for oestradiol production (discussed below). In humans and mice, at around the primary stage of development, fibroblast-like theca cell precursors are recruited from the stroma near the basal lamina; these become aligned parallel to one another and form a layer which appears around the secondary stage of development (Skinner 2005). The major components of the basal lamina, which encapsulates the oocyte and pre-GCs or GCs, are proteoglycans and glycoproteins, including type IV collagen, laminin, fibronectin, and heparin sulphate (Heeren et al. 2015). The basal lamina is formed at the primordial follicle stage (Heeren et al. 2015).

At the primary stage, TC precursors do not express luteinizing hormone (LH) receptors, and are thus not responsive to LH, and are not steroidogenic (Braw-Tal et al. 2005).

Differentiation of theca precursors into TCs occurs when GCs form two or more layers (secondary), and the theca interna, which express the LH receptors, and theca externa layers are evident in the preantral follicle which has grown to 0.1 – 0.2 mm in humans (Gougeon 1986).

#### 1.2.3.3. Antral follicle development and transition into the pre-ovulatory stage in humans

In humans, after the onset of puberty, early antral follicles are capable of developing further into late antral follicles (Figure 1. 1 and Figure 1. 2) supported by FSH in every reproductive cycle (cyclic recruitment) (McGee et al. 2000). FSH is secreted by the pituitary gland and augments granulosa cell proliferation. A cohort of antral follicles continue growing from 0.2 – 0.4 mm in diameter (early antral) to 10 – 16 mm (late antral) (Gougeon 1986). At this stage, the oocyte has already reached its maximum size (~120 μm) and remains arrested at prophase I (Griffin et al. 2006).

The antral follicle is characterised by the presence of a follicular antrum, known as the follicular fluid (FF), which is formed within the multiple layers of GCs within the follicle (Figure 1. 3). FF contains products of blood plasma that have crossed the blood follicular barrier including a plethora of molecules necessary for oocyte growth and maturation such as progesterone, estradiol, LH and FSH, antioxidants and metabolites (Hennet et al. 2012) (Figure 1. 3). As the antral follicle grows, the antral cavity becomes bigger and separates the GCs into those surrounding the oocyte which differentiate into cumulus cells while GCs close to the basal lamina differentiate into mural cells (Pedersen et al. 1968; Hirshfield 1991) (Figure 1. 3). Cumulus cells have a pivotal role in maintaining the oocyte in meiotic arrest (Tanghe et al. 2002; Pan et al. 2019) (discussed below).

Cell communication within the follicle is facilitated by gap junctions (GJs) (mainly connexin (Willecke et al. 2002)) between cumulus cells, and TZPs (i.e. actin filaments (Barrett et al. 2010)) extending from cumulus cells through ZP (Figure 1. 3).

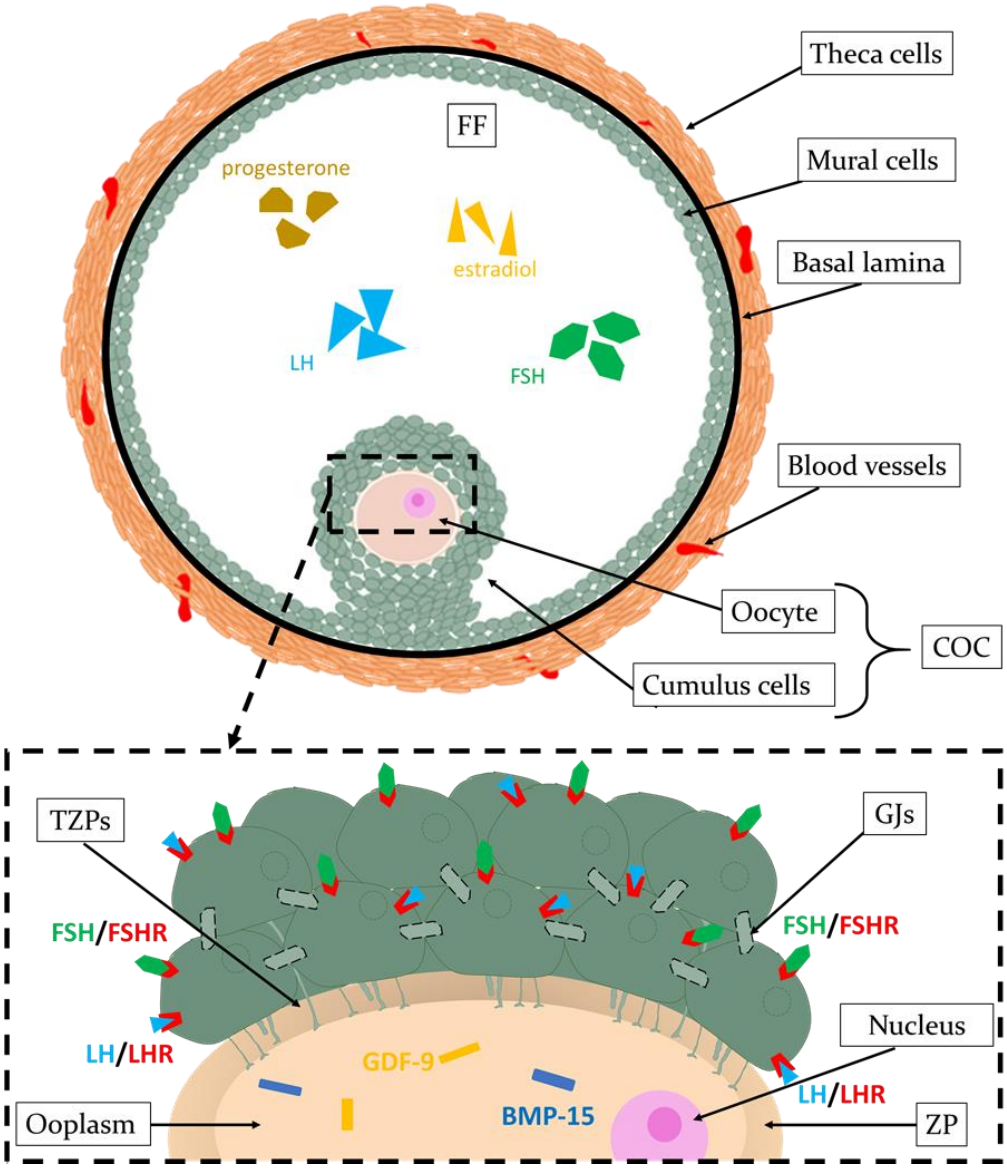



**Figure 1. 3 The structure of the antral follicle.** The FF in an antral follicle contains molecules such as progesterone, estradiol, FSH and LH. Within the cumulus-oocyte-complex (COC), transzonal projections (TZPs) facilitate communication between cumulus cells and the oocyte, while gap junctions (GJs) connect cumulus cells. FF: follicular fluid; ZP: zona pellucida; BMP-15: bone morphogenetic protein 15; GDF-9: growth differentiation factor 9; FSH: follicle stimulating hormone; FSHR: follicle stimulating hormone receptor; LH: luteinising hormone; LHR: luteinising hormone receptor.

#### 1.2.3.4. Selection and ovulation of the dominant follicle in humans

Development of a single dominant follicle into the pre-ovulatory stage is closely associated with high follicular oestradiol ($E_2$) levels, which peak at the pre-ovulatory stage. A large antral follicle at the most developed stage, among others in the antral follicle cohort will respond first to the increased FSH levels and gain dominance. Thus, development of the other antral follicles is inhibited by the dominant follicle as it will determine the FSH threshold (Mihm et al. 2008; Schipper et al. 1998). Once it becomes dominant, GCs in this single follicle produce oestrogens at higher levels (compared to non-dominant growing follicles); this has an inhibitory effect on the secretion of gonadotropins by the pituitary (Shaw et al. 2010). The dominant follicle is dependent on FSH and has a high responsiveness to FSH and becomes more resistant to gonadotropin withdrawal. Thus, as it matures, the dominant follicle requires lower levels of FSH (Shaw et al. 2010), until ovulation, whereby LH surge is critical for follicle rupture and release of the mature oocyte into the fallopian tube (Drummond 2006). The ovulatory LH surge induces cumulus expansion. Transport of the ovulated egg into the oviduct is facilitated by the cumulus cells (Figure 1. 3).

### 1.2.4. Oocyte meiotic and developmental competence

Cytoplasmic and nuclear changes, involving accumulation of mRNA and proteins, take place towards the completion of meiotic, cytoplasmic and molecular maturation, and have a key role in facilitating oocyte differentiation that results in a developmentally competent egg (Sirard et al. 2006). In the pre-ovulatory follicle, the oocyte is meiotically competent and ready to complete meiosis I at ovulation when it will remain arrested at metaphase II until fertilisation (Picton et al. 1998). Re-organisation of organelles is

another characteristic of oocyte cytoplasmic maturation (Picton et al. 1998) with a dramatic increase in the replicates of mitochondria (Wassarman et al. 1978).

### 1.2.5. Factors involved in the regulation of follicle development

The coordinated action of autocrine and paracrine intraovarian factors with pituitary-secreted hormones orchestrates follicle development. There are many factors involved in the regulation of follicle development. In this thesis, only a few of these factors are discussed as considered most relevant to this work.

#### 1.2.5.1. Early stages of follicle development

Activation of primordial follicles is believed to be regulated by many intraovarian pathways, activators such as growth differentiation factor 9 (GDF-9), stem cell factor (SCF or Kit), or suppressors such as phosphatase and tensin homolog (PTEN), anti-müllerian hormone (AMH) and forkhead box O3a (FOXO3a) (McGee et al. 2000; Lee et al. 2019; Thomas et al. 2006). The (PI3K) signalling pathway has drawn attention as a key regulatory pathway in the maintenance of primordial follicles in the dormant state through the forkhead transcription factor Foxo3 (John et al. 2008). What is more, it has been suggested that disruption of the Hippo signalling pathway has a key role in primordial follicle activation. Grosbois et al. showed that mechanical fragmentation of human frozen/thawed ovarian cortical tissue caused disruption of the Hippo pathway within the GCs. This disruption in turn stimulated the activation of Yes-associated protein (YAP) and its translocation to the nucleus where it promoted the transcription of connective tissue growth factor (CTGF) and Baculoviral IAP repeat-containing protein 1 (BIRC1); these factors are involved in granulosa cell proliferation resulting in primordial follicle activation (Grosbois et al. 2018).

### 1.2.5.2. Later stages of follicle development

Gonadotropin-releasing hormone (GnRH) is a key regulator in the hypothalamic-pituitary-gonadal (HPG) axis secreted by the hypothalamic neurons in the arcuate nucleus. GnRH binds and activates the GnRH receptor located at the anterior pituitary whereby it stimulates secretion of gonadotropins FSH and LH in a pulsatile manner into the circulation (Antunes et al. 1979; Marques et al. 2000).

LH and FSH are glycoproteins composed of an α (common) and a β subunit (specific). LH receptors (LHR) and FSH receptors (FSHR) are G-coupled receptors and are found on TCs (LHR) and on GCs (FSHR) with the exception of pre-ovulatory follicles where expression of LHR on GCs is stimulated by FSH (Camp et al. 1991; Fauser et al. 1997; Kessel et al. 1985). Levels of FSH and LH are regulated by other factors such as oestrogens, progesterone, AMH and inhibin (A and B) that are secreted by GCs, through negative or positive feedback during follicle development (discussed below).

Activation of primordial follicles is independent (Dierich et al. 1998; Oktay et al. 1997) of gonadotropins (Peters et al. 1973). Even though FSH and LH receptors are detectable in early preantral stages of follicle development (Braw-Tal et al. 2005; Oktay et al. 1997), this process is gonadotropin independent as demonstrated by female mice lacking follicle-stimulating hormone β (FSHβ) (Kumar et al. 1997) or FSH receptor (FSHR) (Dierich et al. 1998) which only develop follicles up to the preantral follicle stage. In contrast, development of the early antral follicles into the late antral stage requires gonadotropin support (Touraine et al. 1999; Dierich et al. 1998; Craig et al. 2007) .

### 1.2.5.2.1. The two cell-two gonadotropin theory

The paracrine interaction between GCs and TCs and between FSH and LH are required for oestradiol synthesis; the two cell-two gonadotropin theory establishes that oestrogens are synthesized from cholesterol through the interactions of theca and granulosa cells (Figure 1. 4) (Erickson et al. 1985; Drummond 2006).

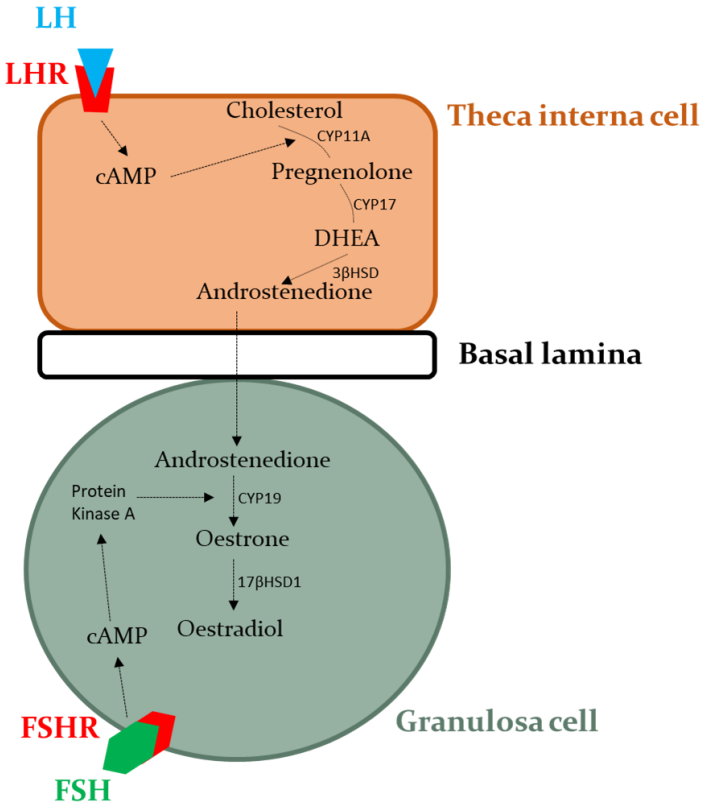



**Figure 1. 4 The two cell-two gonadotropin theory for oestradiol production**. Oestrogens are synthesized from cholesterol through the cooperative interactions of theca (TCs) and granulosa cells (GCs). Binding of the LH to its receptor (LHR) on TCs stimulates the adenylyl cyclase pathway (cAMP) resulting in the conversion of cholesterol to androstenedione by a number of enzymes in TCs in a cascade of steps. Androstenedione diffuses through the basal lamina into GCs whereby binding of FSH to its receptor (FSHR) activates the cAMP pathway resulting in production of aromatase (CYP19) by GCs. Androstenedione in GCs is then converted to oestrone by CYP19 and then to oestradiol by 17β-Hydroxysteroid dehydrogenase 1 (17βHSD1). CYP11A: cytochrome P450 Family 11 Subfamily A; CYP17: cytochrome P450 family 17 subfamily; 3βHSD: 3β-hydroxysteroid dehydrogenase; DHEA: dehydroepiandrosterone; FSH: follicle stimulating hormone; FSHR: follicle stimulating hormone receptor; LH: luteinising hormone; LHR: luteinising hormone receptor.

#### 1.2.5.2.2. Oestrogens

The production of oestradiol, the main oestrogen in follicle development (Drummond et al. 1999) has been discussed (Section 1.2.5.2.1). Oestrogens are first produced at the secondary stage of follicle development where the human follicle has acquired all the components of the two cell- two-gonadotropin model, but due to the largest number of GCs in the pre-ovulatory follicle and its ability to aromatise androgens, the highest level of oestradiol production is detected in the pre-ovulatory stage of development (McNatty et al. 1975). Oestrogens have a mitogenic effect on GCs (Billig et al. 1993), and act through a positive feedback mechanism to enhance follicle responsiveness to FSH by stimulating FSHR levels and mediating LHR expression on GCs (Knecht et al. 1984).

The role of oestrogens in ovarian function was revealed in studies in an aromatase knockout mouse model (ArKO) (Britt et al. 2004, 2000; Fisher et al. 1998). ArKO mice lack aromatase and therefore do not produce oestrogens. These mice were infertile due to a block at the antral stage of development resulting in anovulation. Ovulation was restored by administration of oestrogen (Fisher et al. 1998; Britt et al. 2000). ArKO female mice eventually undergo POI due to depletion of the primordial follicle pool (Britt et al. 2004; Fisher et al. 1998; Britt et al. 2000); AMH expression levels were similar between ArKO and wild-type ovaries (Britt et al. 2004). This observation suggests a potential role of oestrogens in the maintenance of the follicular reserve (Fisher et al. 1998; Britt et al. 2000, 2004).

Oestrogens act through binding to receptors (ER). Insight into the role of these two forms of ER receptors came from studies in ERα (ERαKO) and ERβ (ERβKO) knock out mouse models (Couse et al. 1997). Abnormal follicle growth observed in ERαKO mice

resulted in infertile females, and due to defects in ovulation ERβKO female mice were subfertile (Schomberg et al. 1999; Krege et al. 1998).

#### 1.2.5.2.3. Androgens

Aside from their role as a substrate for oestrogen production (discussed in Section 1.2.5.2.1), androgens also have an inhibitory role on FSH-stimulated LHR expression by GCs (Jia et al. 1985) which is crucial for ovulation, and in contrast to oestrogens, promote GC apoptosis (Billig et al. 1993). Administration of a non-aromatisable androgen (dihydrotestosterone) into mice resulted in subfertility due to a decline in the number of large antral follicles (Nandedkar et al. 1981). In another study, reduced ovulation in mice lacking the androgen receptor (AR) resulted in subfertile females due to defects in follicle development (Hu et al. 2004).

#### 1.2.5.2.4. Progesterone

Progesterone (P) is secreted by the corpus luteum which is formed after ovulation and has a key role in ovulation, embryo implantation and maintenance of pregnancy (Graham et al. 1997). Progesterone acts through binding to its receptor (PR) that exists in two forms; PR-A and PR-B which arise from the same gene; however, PR-A and PR-B are hypothesised to have different roles in ovarian function (Conneely et al. 2003). Cellular responsiveness to progesterone is determined by the balance between PR-A and PR-B, and findings obtained from *in vitro* studies support the inhibitory effect of PR-A on PR-B (Tung et al. 1993; Vegeto et al. 1993). Studies using a PR-A (PR-AKO) and PR-B (PR-BKO) knockout mouse model indicated that PR-A has a pivotal role in ovulation; PR-AKO female mice are infertile as they do not ovulate, evident by an increased

number of unruptured pre-ovulatory follicles whereas fertility is not impaired in PR-BKO females (Mulac-Jericevic et al. 2003; Mulac-Jericevic et al. 2000).

#### 1.2.5.2.5. The TGF-β superfamily

*Anti-Müllerian Hormone*

Anti-Müllerian Hormone (AMH) is a glycoprotein that belongs to the TGF-β family and has been identified in humans (Weenen et al. 2004) and mice (Durlinger et al. 1999). It was first demonstrated that AMH induced regression of the Müllerian duct during male sex differentiation in mouse embryos (Josso et al. 1993). Later, AMH was also detected in GCs of primary follicles and secondary follicles while its levels are increased in preantral and small antral follicles (Weenen et al. 2004).

AMH is thought to act as an inhibitor of primordial follicle activation (Pankhurst 2017). This hypothesis was studied using AMH-knock out mice where in the absence of AMH, follicle recruitment was increased resulting to primordial follicle depletion, indicating that AMH inhibits primordial follicle activation (Durlinger et al. 1999). Studies *in vitro* revealed that AMH inhibited primordial follicle activation in cultured human (Schmidt et al. 2005) and mouse (Durlinger et al. 2002) ovarian tissue.

*Oocyte secreted GDF-9, BMP-15 and cumulin*

Both growth differentiation factor 9 (GDF-9) and bone morphogenetic protein 15 (BMP-15) are glycoproteins expressed by the oocyte from the primary follicle stage through to ovulation (Moore et al. 2003; Aaltonen et al. 1999; Dube et al. 1998). GDF-9 and BMP-15 act in a synergistic way (Moore et al. 2003; Peng et al. 2013); GDF-9 acts through activation of the intracellular SMAD2/3 pathway mediated by the BMP receptor II (BMPRII) and activin receptor-like kinase 5 (ALK5) (Roh et al. 2003; Kaivo-Oja et al. 2003),

whilst BMP-15 activates the SMAD1/5/8 pathway through receptors BMPRII and ALK6 (Moore et al. 2003). BMP-15 and GDF-9 can form homodimers or heterodimers (BMP-15-GDF-9) (Peng et al. 2013) known as cumulin (Rossetti et al. 2020).

Studies using GDF-9 and BMP-15 knock out mouse models explored the role of these two oocyte secreted factors. BMP-15 deficient *(Bmp-15-/-)* mice were subfertile manifesting reduced ovulation and fertilisation rates (Yan et al. 2001) whilst Gdf-9 deficient *(Gdf-9-/-)* female mice were infertile due to a block in follicle development at the primary stage (Dong et al. 1996). However, further investigation into the role of GDF-9 in follicle development demonstrated that these effects are the results of upregulation of Inhibin A (secreted by GCs) since in mice lacking both GDF-9 and Inhibin A preantral follicles were observed (Wu et al. 2004). This finding reveals that even though GDF-9 may not regulate follicular growth directly, it acts by suppressing Inhibin A which in turn regulates follicle development. Mutations in GDF-9 and BMP-15 identified in women have been associated with POI (Dixit et al. 2006; Laissue et al. 2006; Patino et al. 2017; Rossetti et al. 2020).

## 1.3. Premature ovarian insufficiency

Premature ovarian insufficiency (POI) is a common cause of infertility (or subfertility) in women younger than 40 years of age (Webber et al. 2016). The prevalence of POI increases with age; 1 in 10,000 (0.01%) for women aged 18-25 years, 1 in 1,000 (0.1%) for women aged 26-30 years and 1 in 100 (1%) for women between 35-40 years (Coulam et al. 1986). POI is characterised by elevated levels of gonadotropins, hypoestrogenism, and amenorrhoea (primary or secondary) before the age of 40, which is about a decade

earlier than the average age of menopause in women (~51 years of age) (Faddy et al. 1996; Webber et al. 2016; Coulam et al. 1986). Elevated urinary gonadotrophins in non-cycling women, described as premature menopausal cases, were first reported in the 1930s (Heller et al. 1939) and later termed primary ovarian insufficiency by Fuller Albright in 1942 (Albright et al. 1942). Because of the common features between POI and menopause, POI is often characterised as premature menopause; though, it should be noted that less advanced stages of POI are reversable with a 5%-10% chance of a spontaneous pregnancy (Van Kasteren et al. 1999), whereas menopause is the manifestation of loss of the residual follicles and signifies the cessation of menstrual cycles.

The most well characterised features of POI include the inability to conceive, amenorrhoea, menstrual irregularities (oligomenorrhoea or sudden onset of secondary amenorrhoea) and menopausal symptoms (e.g. hot flushes) (Webber et al. 2016). However, the clinical presentation and symptoms of POI can vary highly between cases. Also, there are additional signs of the developing condition such as anxiety, depression, fatigue, hair loss and even changes in skin pigmentation (Torrealday et al. 2019).

Besides implications in fertility, POI can have long-term effects on health. Deprivation of oestrogen in POI can result in an increased bone fracture risk later in life (Webber et al. 2016; Popat et al. 2009); women with POI had reduced bone mineral density (Popat et al. 2009). What is more, POI patients are at a higher risk of developing cardiovascular diseases than normal menopausal women (Podfigurna et al. 2018). Last but not least,

psychological wellbeing and quality of life is another important implication in women diagnosed with POI (Webber et al. 2016).

### 1.3.1 Aetiology for POI

POI is a heterogenous condition and many causes have been identified (e.g. genetic, autoimmune, iatrogenic) but the majority of cases (~70%) are idiopathic (Nelson 2009; Torrealday et al. 2019) (Figure 1. 5).

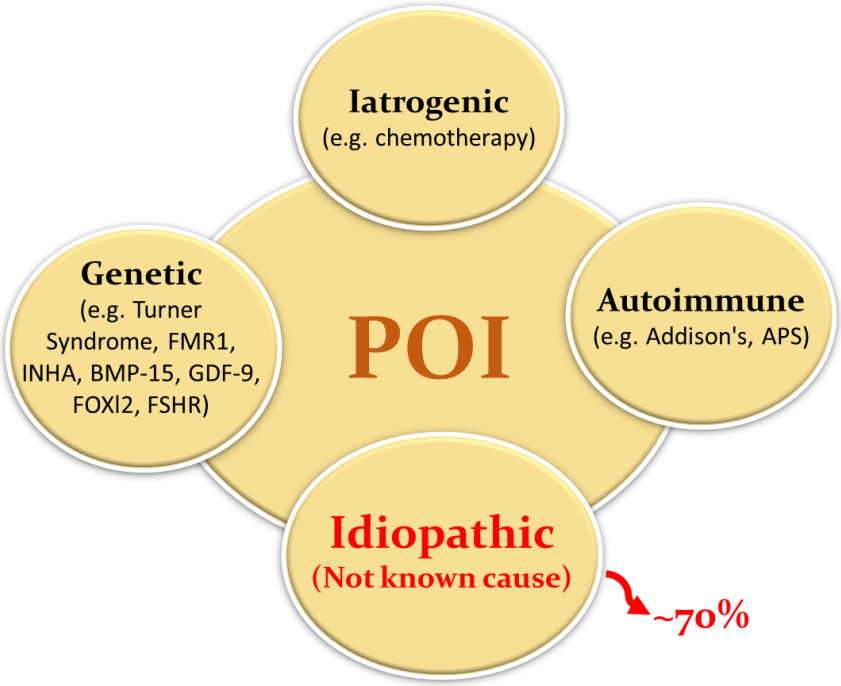



**Figure 1. 5 Categories of causes of POI.** There are many causes of POI but ~70% of cases are idiopathic. Chemotherapy is a known cause of iatrogenic POI. Some of the known causes of non-iatrogenic POI are autoimmune conditions such as Addison's disorder (a condition of adrenal insufficiency). Genetic abnormalities have been identified as causative conditions. FMR-1: fragile X mental retardation protein; INHA: inhibin subunit alpha; APS: autoimmune polyglandular syndrome; BMP-15: bone morphogenetic protein 15; GDF-9 growth differentiation factor 9; FOXL2: forkhead-box L2; FSHR: follicle stimulating hormone receptor.

#### 1.3.1.1 Genetic causes

Genetic factors identified as genetic causes of POI can be divided into two categories: chromosomal and genetic abnormalities (Shelling 2010; Rudnicka et al. 2018; Torrealday et al. 2009).

*Chromosomal abnormalities*

X chromosome abnormalities are usually identified as a genetic cause of POI. Turner Syndrome (TS) has been identified as a chromosomal abnormality associated with POI tested by karyotype analysis (Shelling 2000; Elsheikh et al. 2002). TS (monosomy 45,X0) affects 1 in 2,500 live female births and is associated with short stature, cognitive lymphedema, bone abnormalities, osteoporosis and gonadal dysgenesis (Elsheikh et al. 2002; Woad et al. 2006; Shelling 2000). In TS patients, ovaries are normally developed until around the 3$^{rd}$ month of gestation and contain primordial follicles (Weiss 1971). However, due to accelerated oocyte degeneration due to apoptosis in TS patients, follicle depletion occurs within the first months or years of life and eventually, POI (Modi et al. 2003). Other known genetic causes of POI are trisomy X (Jacobs et al. 1960) and mosaicism (Sugawara et al. 2013). In mosaic Turner Syndrome (46,XX/45,X), the ovary is populated by two populations of oogonia, one containing two X chromosomes (46,XX) and one missing an X chromosome (45,X), and thus, the number of oocytes at birth will be substantially greater than seen in ovaries of a single line of monosomy X (45,X) (Oktay et al. 2016). The pool of primordial follicles in 46,XX/45,X mosaics might then be large enough for a young woman to undergo menarche and normal pubertal development (Pasquino et al. 1997). However, these women will exhaust their supply of primordial follicles at a faster rate than age-comparable women with a normal 46,XX genotype, and are at a high risk of developing POI.

*Autosomal genetic abnormalities*

Mutations in the inhibin α (*INHA*) gene (chromosome 2) have been associated with POI. The general consensus is that carriers of these mutations are at a higher risk of POI than the general population. The mutation rate of these genes seems to differ between ethnicities and therefore, may affect populations differently depending on their background; an association of an *INHA* mutation with POI was found in populations from New Zealand (Shelling et al. 2000), Italy (Marozzi et al. 2002) and India (Dixit et al. 2004) in contrast to populations from Argentina (Christofolini et al. 2017), Korea (Sundblad et al. 2006) and Brazil (Christofolini et al. 2017). However, a larger scale study (Corre et al. 2009) and meta-analysis (Chand et al. 2009) revealed discrepancies with regards to the association of *INHA* mutations with POI.

Variants of the FSHR gene have been reported. Some of these variants are believed to affect fertility in females by inactivating or activating the FSHR. Inactivating FSHR mutations result in premature ovarian insufficiency (Desai et al. 2013); these mutations displayed decreased hormone binding specificity of the receptor, as these mutant receptors also responded to human chorionic gonadotropin (hCG) (Vasseur et al. 2003; Montanelli et al. 2004). Activating FSHR mutations result in ovarian hyperstimulation syndrome (Desai et al. 2013); these mutations reduced the ligand-binding ability, probably due to reduced expression on the cell membrane (Touraine et al. 1999; Doherty et al. 2002), but did not reduced the ligand-binding affinity (Aittomäki et al. 1995).

In a small proportion of women (Aittomaki et al. 1996), and also in a mouse model (Dierich et al. 1998), inactivating FSHR mutations exhibit the presence of follicles,

usually before the antral stage, that are unable to respond to FSH stimulation. However, the impact of FSHR mutations on fertility varies between ethnicities (Jiang et al. 1998; Woad et al. 2013; Huang et al. 2019).

Transcription factor (TF) forkhead box L2 gene (FOXL2) mutations are responsible for the blepharophimosis ptosis epicanthus inversus syndrome (type I and II), a dominant condition characterised by palpebral malformations; type I blepharophimosis ptosis epicanthus inversus syndrome is associated with POI (Georges et al. 2014). Analysis of $Foxl2^{-/-}$ mouse ovaries showed that, the ovaries developed normally until birth; however, 2 weeks after birth, follicles contained large oocytes surrounded by a single layer of flat GCs, while no normal follicles were observed at later stages of maturation (Schmidt et al. 2004; Uda et al. 2004). In the following weeks, 'follicle activation' occurred, but no cuboidal GCs are observed. The oocytes of these 'activated' follicles underwent apoptosis resulting in follicle depletion (Schmidt et al. 2004; Uda et al. 2004).

Mutations in the GDF-9 (chromosome 5) and BMP-15 (X chromosome) gene have been identified in patients with POI (Liu et al. 2019; Patino et al. 2017; Dixit et al. 2006; Laissue et al. 2006). Reports have demonstrated that BMP-15 mutations can result in disrupted ovarian function and female infertility due to reduced BMP-15 expression, activity and synergy with GDF-9 (Patino et al. 2017).

*X chromosome gene abnormalities*

The fragile X mental retardation 1 gene (*FMR1)* is located on the X chromosome (Sullivan et al. 2011). Repeats of the CGG trinucleotide in the 5' untranslated region of the *FMR1* gene results in the fragile X syndrome; the phenotype in affected males is mental

retardation and autism while females manifest POI (Sullivan et al. 2011; Murray et al. 2014; Torrealday et al. 2019). The normal repeat length of *FMR1* is less than 40 repeats, the pre-mutation is defined as 55 to 200 repeats, and over 200 repeats is the full mutation (Sullivan et al. 2011; Murray et al. 2014). Interestingly, the full mutation of the gene is associated with a less severe fragile X syndrome phenotype in female patients compared to full mutation male carriers and pre-mutation carriers in females. In the full mutation, the *FMR1* gene is not expressed. In the pre-mutation, while there are normal expression levels of the FMR protein (FMRP), there is an excessive amount of mRNA (Murray et al. 2014). The exact mechanisms that cause POI in fragile X syndrome are unknown, but since the FRMP is expressed in human (Rifé et al. 2004; Rosario et al. 2016) and mouse germ cells (Lu et al. 2012), it is thought that the excess amount of mRNA might cause ovarian damage.

#### 1.3.1.2 Autoimmune causes

Autoimmune diseases have also been found to be associated with POI with the rate reported varying from 10%-30% of cases (Shelling 2010; Rudnicka et al. 2018). The available methods to detect autoimmune ovarian antibodies lack high sensitivity and specificity (Novosad et al. 2003) and thus, diagnosis is difficult. POI may be associated with more than one autoimmune condition in a patient; this case is known as the autoimmune polyglandular syndrome; APS (APS-I, APS-II and APS-III). In APS-I, hypoparathyroidism (in 80% to 85% of autoimmune-POI cases) and Addison's disease (in 60% to 70% of autoimmune-POI cases) are the most common conditions. In APS-II, thyroid disease (in 70% to 75% of autoimmune-POI cases) and type 1 diabetes (50% to 60% of autoimmune-POI cases) are the most common disorders associated with POI

(Dittmar et al. 2003). APS-III condition is similar to APS-II with regards to the autoimmune diseases present in the same patient except for Addison's disease which is not present in APS-III (Goswami et al. 2005).

#### 1.3.1.3 Iatrogenic causes

Advancement in chemotherapy treatments have resulted in improvement of cancer survival rates (Cancer Research UK 2014; Trama et al. 2019; Arnold et al. 2019; Meirow 2000). However, iatrogenic POI is a side effect of chemotherapy (Bedoschi et al. 2016; Byrne et al. 1992). Chemotherapeutic agents can have long-term detrimental effects on fertility for cancer survivors (Kreuser et al. 1990). Other factors such as age, dose and regimen of treatment as well as the type of drug also affect the risk of developing POI with older patients being at a higher risk of ovarian failure (Meirow 2000). Alkylating agents (most toxic) and platinum derivatives impose a higher risk of developing POI than other drugs (i.e. plant alkaloids) (Meirow 2000). Chemotherapeutic agents act by destroying growing follicles (proliferating cells), and therefore the inhibitory signal for primordial follicle activation such as AMH secretion (Pankhurst 2017) is significantly reduced resulting in follicle exhaustion and eventually POI (Meirow 2000; Familiari et al. 1993). This mechanism is known as the 'burnout effect' (Roness et al. 2013) (discussed below). Chemotherapy-induced ovarian cortical fibrosis and blood-vessel damage is another potential mechanism for developing POI by damaging ovarian tissue (Meirow et al. 2007).

### 1.3.2 Subclassification of POI

POI can be an intermittent condition (Bidet et al. 2011), and ovarian function can be unpredictable in POI patients. Bidet et al. reported a reduced number of primordial

follicles or no follicles in human embryos with TS after histological analysis (Reynaud et al. 2004). In contrast, spontaneous pregnancies in POI patients have been reported in other cases (Fraison et al. 2019), as well as resumption of ovarian function with subsequent arrest in a follow-up study (Bachelot et al. 2017). Most women diagnosed with POI will have a normal menstrual history (Guzel et al. 2017) and may have been fertile. Others, despite aberrant follicle development, can conceive spontaneously (Bidet et al. 2008). Premature luteinisation of preovulatory follicles is also a manifestation of POI (follicle dysfunction) (Nelson et al. 2014). Considering the spectrum of POI manifestations, current limited knowledge of this condition and high percentage of idiopathic POI, it is difficult to precisely categorise cases of POI in such a manner that could assist studies exploring the mechanisms underlying POI and developing potential treatments.

The terms 'follicular' and 'afollicular' POI were introduced by Fox in 1992 to describe POI based on the presence of follicles in patients diagnosed with POI (Society, European and Human Reproduction 2015). Later, Welt (Welt 2008) subdivided the clinical states of POI into four categories according to FSH levels, fecundity and amenorrhoea (Table 1. 1).

**Table 1. 1 Clinical states of POI according to FSH levels, fecundity and amenorrhoea** (Welt 2008)**.**

| | FSH levels | Fecundity | Amenorrhoea | Reversible |
|---|---|---|---|---|
| Occult | Normal | Normal | No | Yes |
| Biochemical | Normal | Reduced | No | Yes |
| Overt | Elevated | Reduced | No | Yes |
| Ovarian failure (POF) | Elevated | Reduced | Yes | No |

The classification by Welt, nicely covers the spectrum of clinical manifestations of POI, but Fox's suggestion (follicular or afollicular) may provide more insightful information and contribute to furthering our understanding of the mechanisms underlying POI by identifying a group of patients with ovarian potential (follicular POI), and those with no ovarian reserve (afollicular POI). It is worth noting, that follicular POI ultimately results in afollicular POI, which as mentioned above, is an irreversible state of ovarian failure due to follicle exhaustion.

Since this thesis contributes to the development of a method that could be used in fertility preservation for patients diagnosed with follicular POI, and specifically follicle dysfunction (discussed below), I use the term 'afollicular POI' (the ovary is devoid of follicles; Figure 1. 6B), or follicular POI (the ovary contains follicles; Figure 1. 6C).

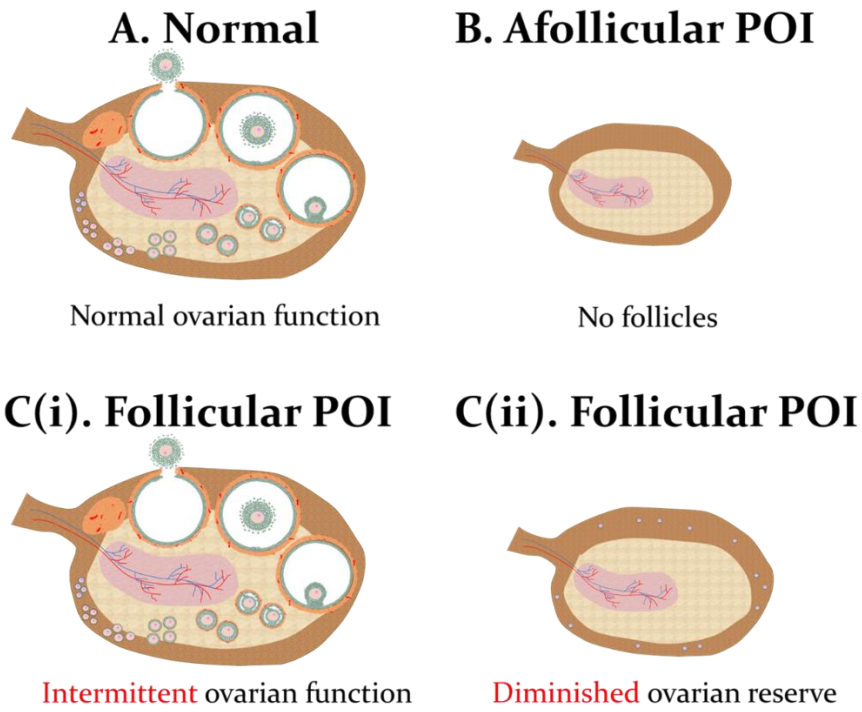



**Figure 1. 6 Categories of ovarian function in POI.** The majority of the women diagnosed with POI undergo normal puberty and are fertile (A). In afollicular POI (B), the ovarian reserve is depleted, and women are infertile. In follicular POI (C(i)), ovaries can function in an intermittent manner allowing for the generation of antral follicles and ovulation. In other cases of follicular POI (C(ii)) the ovarian reserve is diminished with only a few primordial follicles present.

### 1.3.3 Mechanisms underlying POI

Based on clinical trials and studies using mouse models, there are two known mechanisms for developing POI: follicle depletion and follicle dysfunction (Figure 1. 7).

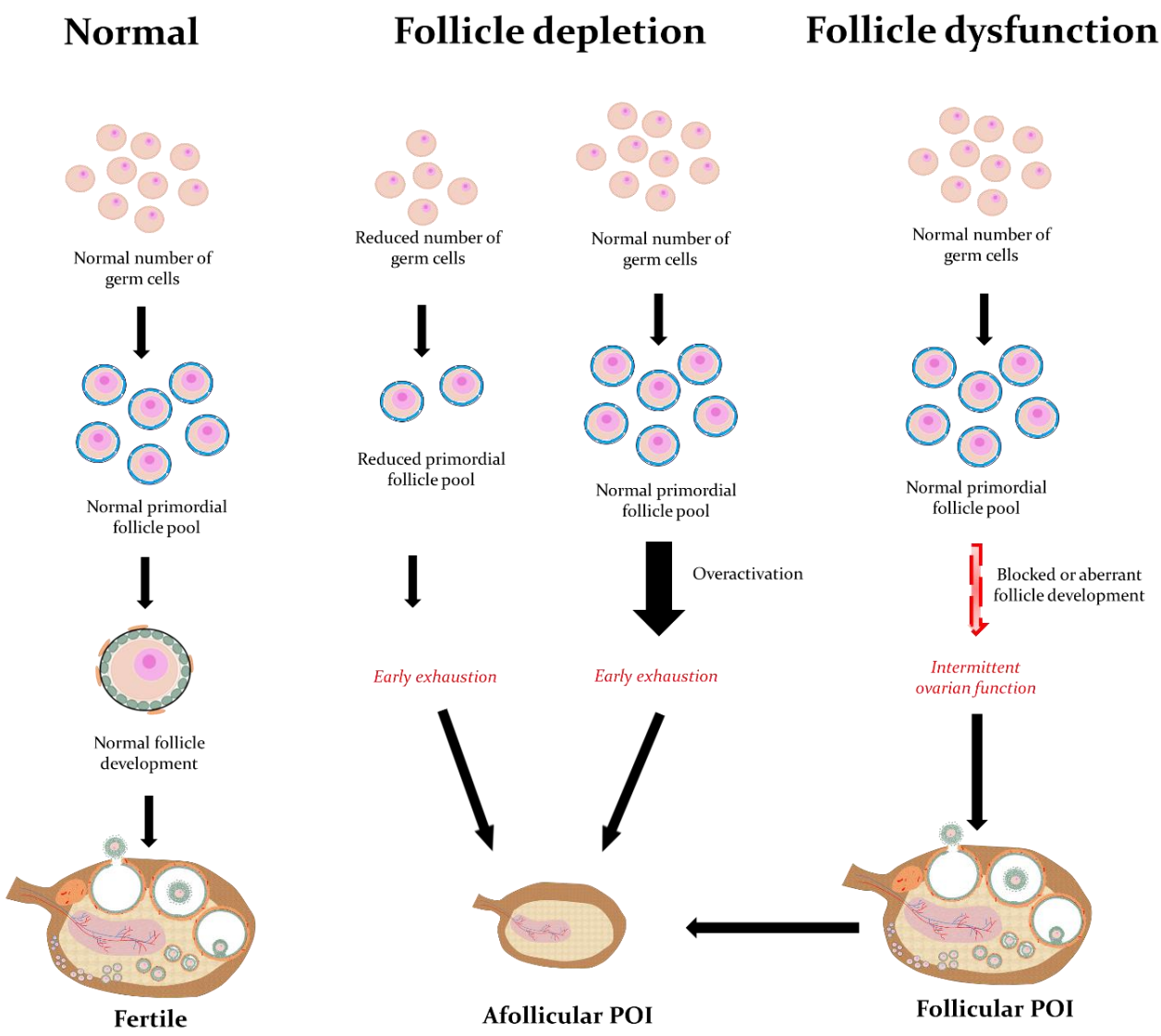



**Figure 1. 7 Mechanisms underlying afollicular and follicular POI.** In women with normal ovarian function (Normal), primordial germ cells develop into primordial follicles that form the primordial follicle pool established by birth. Follicle development can occur normally resulting in generation of pre-ovulatory follicles and fertilisable oocytes (Fertile). In POI, ovarian function can be compromised due to Follicle depletion or Follicle dysfunction. Follicle depletion can be attributed to developmental reduction in the initial follicle pool (Reduced primordial follicle pool) or due to overactivation of primordial follicles (Normal primordial follicle pool) resulting in early exhaustion and afollicular POI (Afollicular POI). In follicle dysfunction, while a normal number of primordial follicles are established by birth (Normal primordial follicle pool), follicle development can be blocked or aberrant resulting in intermittent ovarian function and thus, follicular POI (Follicular POI). Follicular POI ultimately results in afollicular POI, an irreversible state of ovarian function in POI.

#### 1.3.3.1 Follicle depletion

Follicle depletion occurs due to 1) a significant reduction of the initial primordial follicle pool (due to a reduced number of oogonia during embryonic development) , or 2) overactivation of the primordial follicle pool, resulting in a diminished ovarian reserve (Figure 1. 7).

Overactivation of the primordial follicle pool can be explained by the 'burn-out theory' (Roness et al. 2013). This theory has been used to describe the effect of chemotherapy on fertility as an iatrogenic cause of POI. In the absence of growing follicles, which are destroyed by chemotherapeutic agents, inhibitory paracrine factors (i.e. AMH) are reduced. This loss of inhibitory signals causes accelerated primordial follicle activation resulting in follicle depletion. Moreover, ovaries in Pten and Foxo3 knock-out mice were devoid of follicles due to overactivation of primordial follicles induced by inactivation of PTEN and FOXO3 which inhibit primordial follicle activation in wild type ovaries in mice (Reddy et al. 2008; Castrillon et al. 2003).

#### 1.3.3.2 Follicle dysfunction

In follicle dysfunction, follicle maturation is prevented due to a pathological process. Manifestations of this condition vary; in some cases only primordial follicles are present, while in others, follicles at different stages of development including preovulatory follicles (though not able to ovulate) can be observed (Reynaud et al. 2004; Guzel et al. 2017; Nelson et al. 2014) (Figure 1. 7).

An inactivating FSHR mutation, known as a genetic cause of POI in a small population of women (Loutradis et al. 2006) and in a mouse model (Dierich et al. 1998), results in

blocking of follicle development before the antral stage. The follicles in the FSHR mutant mouse ovaries are unable to respond to FSH and therefore, do not mature into preovulatory follicles or ovulate. In the GDF-9 mouse model of follicular POI, follicle development is disrupted at the primary stage (Dong et al. 1996), whilst folliculogenesis in the aromatase knockout mouse model is disrupted and ovulation fails (Britt et al. 2000).

In the double-mutant (DM) mouse (Williams et al. 2011), an oocyte-specific deletion of glycosyltransferase genes, *C1galt1* (also known as T-syn) and *Mgat1* results in aberrant glycosylation, a form of post-translational modification. Glycoproteins, have many roles, including key roles in female reproduction and include hormones such as FSH, LH (Jiang et al. 2014) and AMH (Pankhurst et al. 2013), as well as oocyte-secreted BMP-15 and GDF-9 (Hayashi et al. 1999), and are involved in essential functions in follicle development such as ZP formation (Williams et al. 2007), GC function and follicle selection (Williams et al. 2008) in the mouse.

In contrast to follicular POI mouse models discussed above, which are never fertile, DM female mice are fertile before the onset of POI (Williams et al. 2011; Grasa et al. 2012). At 3 weeks of age (prepubertal), females have normal ovaries and contain follicles at all stages of development (Williams et al. 2011). At 6-weeks of age (puberty), these females are subfertile and produce a smaller litter than control mice (Williams et al. 2011; Grasa et al. 2012). By 9-weeks of age (adult), DM females are infertile, and after 3-months POI occurs (Williams et al. 2011; Grasa et al. 2012). Also, in the infertile 3-month-old DM

females, gonadotropins are elevated whilst sex steroids are decreased (Williams et al. 2011); this endocrine profile is also a feature of POI in women as discussed (Section 1.3).

### 1.3.4 Available treatments for women and young girls diagnosed with POI

According to the European Society of Human Reproduction and Embryology (ESHRE) guidelines, there are no known treatments that consistently improve ovarian activity, ovulation or conception rate for patients with POI (Society, European and Human Reproduction 2015). Oestrogen treatment may increase ovulation rates in women with less advanced POI and improve IVF outcomes, however, large scale studies providing robust evidence are lacking (Webber et al. 2016; Van Kasteren et al. 1999) What is more, ESHRE states that there are no intervention methods to date that reliably increase natural conception rates (5% to 10%) or ovarian activity in POI patients (Webber et al. 2016; Van Kasteren et al. 1999). Oocyte donation is suggested as the only successful treatment for women diagnosed with POI (Webber et al. 2016).

*Ovarian tissue cryopreservation*

Ovarian tissue cryopreservation is the only available fertility preservation option for pre-pubertal patients undergoing chemotherapy that are at a high risk of developing POI post-treatment (Van DerVen et al. 2016; Lakhoo et al. 2019; Poirot et al. 2019; The Practice Committee of the American Society for Reproductive Medicine 2014). Despite the potential of ovarian tissue cryopreservation to preserve fertility in girls at risk of suffering follicle depletion (i.e. Turner Syndrome) (Birgit et al. 2009; Hreinsson et al. 2002), ovarian tissue cryopreservation is not widely used as a fertility option for patients diagnosed with non-iatrogenic POI (Condorelli et al. 2019) and it is not considered as a

standard option for fertility preservation in POI patients (Webber et al. 2016). In Suzuki et al., among 37 women aged 28-48 years diagnosed with POI (amenorrhoea for <4 months, age <40 years and elevated serum FSH levels) two live births were reported (Suzuki et al. 2015). After ovarian tissue cryopreservation, *in vitro* activation (IVA) of follicles (discussed below) was performed followed by auto-transplantation (Suzuki et al. 2015). After IVF and embryo transfer, three pregnancies were detected followed by one miscarriage and two successful deliveries (Suzuki et al. 2015).

*Oocyte/embryo cryopreservation*

Embryo cryopreservation is a well-established method for fertility preservation and has been used for over 30 years (El Grynberg et al. 2016). Oocyte cryopreservation is no longer considered experimental and is used as an established method for patients wishing to preserve their fertility (The Practice Committee of the American Society for Reproductive Medicine 2013).

*In vitro* maturation (IVM) of immature oocytes is used primarily for patients with polycystic ovarian syndrome (PCOS) prior to *in vitro* fertilisation (IVF) to avoid ovarian hyperstimulation (OHSS) (Revel et al. 2011). To avoid introducing malignant cells into the patient's body through ovarian tissue auto-transplantation, IVM is also used for cancer survivors that were given the option to cryopreserve ovarian tissue prepuberty (Shirasawa et al. 2017; Revel et al. 2009).

*In vitro activation*

*In vitro* activation (IVA) of primordial follicles is another emerging method in the field aiming at rescuing the residual ovarian reserve (primordial follicles) in women at risk of

developing POI (follicle depletion). This process involves both dissection of the tissue, activating the Hippo pathway, and the use of Akt stimulators or PTEN inhibitors (factors known to have key roles in primordial follicle activation). Live births have been reported in women after IVA of residual follicles followed by auto-transplantation of ovarian tissue and egg retrieval for IVF (Kawamura et al. 2013; Suzuki et al. 2015). Despite some promising results (Suzuki et al. 2015; Lee et al. 2019) IVA may not be beneficial for POI patients with follicle dysfunction. Even if the primordial follicles remaining in the ovary of POI patients with follicle dysfunction are activated *in vitro* (IVA) further follicle development would still be abnormal, and IVF or auto-transplantation success rates would not be improved using this approach. In a study by Zhai et al. (Zhai et al. 2016), follicle development was achieved through IVA in POI patients, however, premature luteinisation was observed, which is an indicator of follicle dysfunction in POI (Nelson et al. 2014). This observation confirmed our hypothesis that IVA might not be an effective method to rescue follicle development in cases of follicle dysfunction and POI.

*Oogonia stem cells*

Investigation into the potential of putative oogonia stem cells (OSCs) has challenged the consensus of the fixed follicle pool in the mammalian ovary. A number of reports showed that isolation of putative OSCs from mouse ovaries or human ovarian cortex using the germ cell-specific marker Dead box helicase 4 (DDX4) was achieved with fluorescence-activated cell sorting (FACS) (discussed in detail in Chapter 5) (Grieve et al. 2015); DDX4 is expressed in germ cells from PGCs through to oocytes in antral follicles (Castrillon et al. 2000). Human DDX4 positive cells appeared to be able to form oocyte-like structures when placed in an ovarian somatic-cell environment (Clarkson et al. 2018;

White et al. 2012). The existence of OSCs could contribute to fertility preservation (FP) especially in cases of follicle depletion, where early exhaustion of the follicular reserve would be overcome. However, the isolation of putative OSCs using the DDX4 germ cell marker has been controversial due to concerns regarding the specificity of the antibody used to detect the C-terminus in the DDX4 protein (discussed in Chapter 5). To date, there is insufficient data to support the existence of OSCs in the mammalian ovary.

#### 1.3.4.1 Considerations

Cryopreservation of the ovarian cortex could potentially preserve fertility in POI patients at risk of follicle depletion (if diagnosed early enough). However, this method might be ineffective in the case of follicle dysfunction, where even though follicles are present in the ovaries, follicle development is disrupted. What is more, in follicle dysfunction, aberrant follicle development might also be a limiting factor in IVM used prior to oocyte retrieval for cryopreservation. Therefore, oocyte cryopreservation might not be effective for post- and pre-pubertal patients with follicle dysfunction desiring to restore ovarian function and preserve fertility. IVA might not be effective in follicle dysfunction either, as follicle development could potentially be abnormal.

There is clearly a need for fertility preservation/ovarian function restoration for POI patients especially in pre-pubertal girls with follicle dysfunction for whom other fertility preservation methods are unavailable (Table 1. 2).

**Table 1. 2 Options for pre- and post-pubertal POI patients to restore ovarian function in the case of follicle depletion or follicle dysfunction.**

| | Pre-pubertal | | Post-pubertal | |
|---|---|---|---|---|
| | Follicle depletion | Follicle dysfunction | Follicle depletion | Follicle dysfunction |
| Oocyte Cryopreservation (following IVA/IVM) | Potentially (if diagnosed early enough) | No | Potentially (success rate is low) | Potentially (success rate is low) |
| Embryo Cryopreservation | NA | NA | | |
| Ovarian cortical tissue cryopreservation/ reimplantation | Potentially (if diagnosed early enough) | No | Yes | No |

### 1.3.5 The Reaggregated Ovary method as a potential technique to restore follicle development for dysfunctional ovaries

Promising results from studies investigating follicular POI using the DM mouse model in our laboratory (discussed below) have revealed the potential of using the Reaggregated Ovary (RO) method to restore follicle development in POI (follicle dysfunction) (unpublished data).

The RO was first established by Eppig and Wigglesworth in 2000 (Eppig et al. 2000). Williams was the first to establish the RO method in the UK and since then, it has been routinely used in our laboratory to investigate ovarian function in mice (Lo et al. 2019). The RO method allows for the formation of chimeric ovaries that support follicle development (discussed in detail in Chapter 6). Eppig et al. showed that in chimeric ROs containing mouse oocytes and rat somatic cells, fertilisable mouse eggs were generated by chimeric follicles and resulted in the birth of one healthy female mouse pup. This animal later produced 83 normal offspring (Eppig et al. 2000).

Previous work in our laboratory (unpublished data), has shown that follicle development in the DM mouse model of POI (follicle dysfunction) can be re-established when replacing the dysfunctional DM somatic cells with neonatal wild type somatic cells *in vivo* in the RO. Using this method to generate human eggs could potentially enable us to explore the mechanisms underlying POI (follicle dysfunction) and contribute to developing a method to restore follicle dysfunction in patients diagnosed with POI especially pre-pubertal young girls.

More information about the RO method is provided in detail in Chapter 6.

## 1.4. Aims

The long-term goal for the work in this thesis was to develop a method that could potentially restore follicle development for patients diagnosed with follicular POI, or follicle dysfunction using the RO method. The main aim of this thesis was to develop the RO method for use with human ovarian cells. The aims of this thesis were:

- To explore the dissociation of human ovarian tissue (Chapter 3)
- To establish an effective method to dissociate human frozen/thawed ovarian cortex into viable single cells (Chapter 4)
- To develop a method to detect human ovarian oocytes for future isolation (Chapter 5)
- To explore an alternative source of human somatic cells that can support follicle development *in vitro* using the RO method (Chapter 6)

# CHAPTER 2

# *General materials and methods*

## 2.1. Human ovarian tissue samples

### 2.1.1. Sourcing tissue from the Oxford Cell and Tissue Biobank

Ovarian tissue cryopreservation is available for children and young women who are at a high risk of premature infertility due to treatment and for whom standard hormone stimulation and egg collection and storage is not appropriate. At the time of consent for the procurement and storage of tissue, patients were given the option of donating material to research. Donated material included remnant ovarian tissue (that would otherwise be discarded) or stored/cryopreserved ovarian tissue if over 50 cortical strips were collected and cryopreserved per patient; a maximum of 10 strips could be allocated to research provided no fewer than 50 strips remained in storage per patient. Patients undergoing oophorectomy for pathological reasons or gender reassignment

wishing not to store ovarian tissue, were also given the option to donate ovaries to research (that would otherwise be discarded).

Donated ovarian tissue was used in several investigations presented in this thesis. Informed consent was obtained from all patients by the Oxford Cell and Tissue Biobank (OCTB) located at the John Radcliffe Hospital, Oxford, UK prior to collection of ovarian tissue. The study was approved by the Oxford University Hospitals, NHS Foundation Trust (Ethics Reference Number: 14/SC/0041, R&D Reference: 8825).

### 2.1.2. Information on patient characteristics

Non-identifying information was collected for patients whose tissue was used in this thesis. Information was obtained from the OCTB and included patient age, pubertal status (pre- or post-pubertal), diagnosed disease or disorder (if the OCTB was informed) and treatment prior to procurement.

### 2.1.3. Inclusion and exclusion criteria

To be included in this thesis, ovarian tissue had to be donated by patients who, or their parents/carers, had consented to the use of tissue (whole ovaries, remnants, stored cortical strips) for research. Tissue was not included in this study if donors were diagnosed with ovarian disease (i.e. ovarian cancer). Detailed inclusion and exclusion criteria are presented in the relevant chapters.

### 2.1.4. Collection and cryopreservation of ovarian tissue

All tissue was collected by laparoscopic oophorectomy of the ovaries at the John Radcliffe Hospital Oxford, and cryopreservation was performed by the OCTB. The

protocols used by the OCTB for medium preparation, tissue processing, cryoprotection, and cryopreservation of ovarian tissue are based on those used in the well-established programme at Hadassah Hebrew University Hospital (Revel et al. 2003; Gosden 2000). The cryopreservation protocol used at the OCTB is that established at the Hadassah Hebrew University Hospital (Revel et al. 2003) which is based on the protocol published by Gosden (Gosden 2000). Live births following auto-transplantation of tissue cryopreserved using this protocol have been reported however the cryoprotective agent used was dimethyl sulfoxide (DMSO) and sucrose (Revel et al. 2009, 2011). The protocol established by Gosden (Gosden 2000) utilises a specialised cryoprotectant combined with sucrose which is not commercially available.

Following surgical removal, the ovary or ovarian tissue was transported immediately to the tissue processing centre in chilled Leibovitz's L-15 medium (L5520; Sigma-Aldrich, Dorset, UK). Dissection of the ovarian tissue was performed by OCTB technicians on ice blocks under aseptic conditions as soon as possible after procurement; if the process was not performed immediately after surgery was completed, the tissue was stored at 4°C overnight. The ovary was hemisected using a scalpel, and the medulla was removed leaving a thin layer of ovarian cortex. The cortex was cut into smaller pieces as required to achieve a suitable depth of 1-2 mm and then cut into pieces of approximately 1x2x5 mm in size.

The cryoprotective medium is prepared by the OCTB (1.5 M ethylene glycol (Merck Chemicals Ltd, Hull Yorkshire, UK), 0.1 M sucrose (Sigma Aldrich), 10% v/v serum substitute supplement (Irvine Scientific, Newtown Wicklow, Ireland) in L-15 medium).

Up to 6 cortical strips were placed into a single cryovial (2 ml, internal thread; Nunc, Rochester, New York, USA) containing 1 ml of cryoprotectant medium and incubated for 1 hour at 4°C before being frozen using the Sy-Lab Ice Cube controlled rate freezer (Sy-Lab, Neupurkersdorf, Austria). Cryovials were loaded into the pre-cooled 0°C controlled rate freezer and set to cool at -2°C/min until the chamber reached -9°C, after which each tube was manually seeded to enable controlled ice crystal formation. After seeding, the cryovials were cooled to -40°C at a rate of -0.3°C per min, and finally to -140°C at -10°C per min. Following cryopreservation, the vials were stored in vapour phase liquid nitrogen (-196°C).

## 2.2. Obtaining human ovarian tissue samples

### 2.2.1. Fresh ovarian cortex from whole ovaries

Fresh tissue was made available on the day of procurement or, if the surgery was completed out of hours, the next day. Whole ovaries were stored in Leibovitz's L-15 medium (L5520) at 4$^{o}$C until use. On the day of experiment, ovaries were dissected, the medulla was removed and the whole cortex was used (detailed in Chapter 3).

### 2.2.2. Ovarian remnant tissue after cortical tissue dissection prior to cryopreservation

Ovarian remnant tissue was collected after ovary dissection by the OCTB team was completed and kept in Leibovitz's L-15 medium (L5520) at 4$^{o}$C until use. Remnants contained medullary tissue, and debris and single cells that were released during tissue dissection. Remnant tissue is generated every time ovarian tissue is processed for cryopreservation and is discarded if not donated for research.

### 2.2.3. Frozen/stored ovarian cortical tissue

Cryovials were collected from the OCTB and immediately placed in a small tank of liquid nitrogen (-196°C) to be transported to our laboratory.

## 2.3. Thawing of human ovarian cortical strips

Prior to removing the cryovials from liquid nitrogen, thawing solutions (10 ml of a solution (constituents from Sigma Aldrich) per cryovial) were made and sterile filtered into 15 ml Falcon tubes (Table 2. 1).

The composition of thawing Solution 1, 2 and 3 and the protocol used to thaw tissue is the same as that used by the OCTB with the exception that human serum albumin (HSA) is used in place of the serum substitute supplement used by the OCTB. HSA has been demonstrated to yield comparable rates of follicle survival to those observed using a human serum substitute (Hreinsson et al. 2003). HSA was used at 3 mg/ml consistent with that used for transporting fresh tissue prior to culture (Telfer et al. 2008).

**Table 2. 1 Thawing solution components.**

| | Solution 1 | Solution 2 | Solution 3 |
|---|---|---|---|
| **Ethylene glycol** | 1 M | 0.5 M | 0 M |
| **Sucrose in sterile $H_2O$** | 1 M | 1 M | 1 M |
| **Human Serum Albumin** | 3 mg/ml | 3 mg/ml | 3 mg/ml |
| **Leibovitz's L-15 medium** | yes | yes | yes |

To thaw stored cortical strips, cryovials were removed from liquid nitrogen, held at room temperature for ≤30 sec then immersed in a 30°C water bath until tissue thawed (≤3 min). After thawing, the cortical strips were transferred to the Falcon tube

containing Solution 1 under sterile conditions and inverted by hand for 5 min at room temperature. This was repeated for Solution 2 and 3.

## 2.4. Calculating net weight of human ovarian cortical strips

Prior to weighing cortical tissue (fresh or frozen/thawed strips), bijou tubes (VWR International Ltd) were labelled, filled with 1 ml of chilled Leibovitz's medium L-15 (L5520) and weighed. Cortical strips were placed in the bijou tubes and weighed to calculate the gross weight of tissue (weight of tissue plus weight of bijou tubes filled with media). Net weight of cortical strips was calculated by subtracting the weight of the bijou tube from the weight of the bijou tube containing the tissue. Weight was expressed as grams of tissue (g) and used to calculate the number of cells isolated using tissue dissociation methods.

## 2.5. Mouse Colonies

### 2.5.1 Ethical Approval

All experiments using mice were carried out with permission from the Local Ethical Review Panel at the University of Oxford in accordance with the UK Animals (Scientific Procedures) Act 1986, under a project license held by Prof. Williams (30/3352).

### 2.5.2 Mouse colony management system

The management systems used to track the mouse colonies were excel sheets generated by Prof Williams and the Sanger system used by the Home Office. The excel sheets were updated weekly and were used to plan experiments, track breeding cage productivity, and allocate newborn mice. The Sanger system was used to track the

procedures performed, breeding productivity, setting up breeding cages and culling requests.

### 2.5.3 Mouse breeding maintenance

Breeding cages were set up as pairs (one male and female) or trios (one male and two females) when mice reached the age of 6 weeks. With a gestation time of 19-21 days, mice were able to give litters every 3 weeks due to post-partum oestrus, where females enter oestrus and are receptive to mating just after littering down. Mice were maintained on a 12:12 hour light: dark cycle and had water and food *ad libitum.*

Female and male mice were weaned at 3 weeks of age.

### 2.5.4 Tail tipping, ear clipping and weaning

The ROSA*LacZ* mouse colony contained mice with a C57BL/6 background which ubiquitously expressed the *LacZ* gene. Male breeders expressed *LacZ* (*LacZ*$^{+}$) while females did not (*LacZ*$^{-}$) thus producing *LacZ*$^{+}$ or *LacZ*$^{-}$ offspring, both of which were required for experiments.

The F1 CD1xC57BL6 mouse colony contained CD1 female mice and C57BL6 male mice; this colony was used because these F1 hybrids gave bigger litters in comparison to the ROSA*LacZ* mouse colony.

Tail tipping was performed on neonatal mice up to 7 days old (P7) to collect tissue for genotyping. Ethyl chloride-based cryogenic fine spray (Acorus Therapeutics Ltd., Chester, UK) was used to numb the tail to prevent any pain during the process. A small piece of the tail, ≤1 mm in length was removed with a scalpel blade when the tail

became pale in appearance (pale colour indicated the local anaesthesia was sufficient). All tail tipping procedures were performed by Dr Belinda Lo and Dr Xi Wei.

Ear clipping was performed for identification and genotyping purposes. When setting up the CD1xC57BL6 colony, breeders were ear clipped for identification. For ROSA*LacZ* newborn mice that had not been tail tipped, ear clipping was performed at the age of 12-14 days (P12-P14) for both identification and genotyping purposes. The ear clip was collected using an ear biopsy tool (Vet-tech, Congleton, UK) and placed in a 96-well plate using blind forceps.

### 2.5.5 β-galactosidase genotyping

To determine the genotype of ROSA*LacZ* mice, X-gal staining was used to detect the product of *LacZ*, β-galactosidase. Tissue samples (ear clips and tail tips) were incubated in X-gal (components from Sigma-Aldrich) staining solution (Table 2. 2) at 37˚C for at least one hour and the tissue expressing *LacZ* turned blue. Positive and negative controls were included in all *LacZ* genotype procedures.

**Table 2. 2 Components of the X-gal staining solution.**

| Reagent | Volume per 1 ml of solution |
|---|---|
| 50 mg/ml X-gal | 20 µl |
| 250 mL potassium ferricyanide | 20 µl |
| 250 mL potassium ferrocyanide | 20 µl |
| 1M $MgCl_2$ | 2 µl |
| 1% sodium deoxycholate | 10 µl |
| 1% NP-40 | 20 µl |
| 1M Tris (pH 7.3) | 20 µl |
| 0.1M PBS (pH 7.3) | 888 µl |

## 2.6. The Reaggregated Ovary Technique

### 2.6.1. Generation of Reaggregated Ovaries

The generation of Reaggregated Ovaries (ROs) was based on Eppig and Wigglesworth 2000 (Eppig et al. 2000) with modifications. Mouse ovaries from 3-8-day-old mice were collected into warmed Dulbecco's PBS (DPBS, Sigma, Gillingham, UK) supplemented with 1 mg/ml bovine serum albumin (BSA, Factor V Heat Shock Treated; Fisher Scientific, Loughborough, UK). Bursa and fat were removed using fine forceps (Dumont #5; Fine Science Tools, Heidelberg, Germany) and micro-scissors (Fine Science Tools). The ovaries were washed twice in DPBS/BSA.

To dissociate the ovaries into a single cell suspension, 0.05% trypsin and 0.53mM Ethylenediamine tetraacetic acid (EDTA) (Gibco, ThermoFisher Scientific, Paisley, UK) supplemented with 0.02% DNase-I (Sigma) were used to digest the ovaries at 37°C for 30 minutes. To enhance dissociation, tissue in the enzymatic solution was gently agitated using a pipette three times during incubation (at 15 minutes and then every 5 minutes). To stop the enzymatic reaction, 1ml of warm, gassed M199/FBS medium: Medium 199 (M199; Gibco, ThermoFisher Scientific) supplemented with 10% (v/v) foetal bovine serum (FBS; Labtech, Uckfield, UK), 31.3 mM sodium DL-lactate (Sigma) and 10 mg/ml penicillin-streptomycin (P0781; Sigma) was added. The cell suspension was transferred into a 15 ml falcon tube and the petri dish was rinsed with 2 ml of warm, gassed M199/FBS to collect any remaining cells. The cell suspension was centrifuged at 660 x g for 5 min to pellet cells and the supernatant was discarded. Cells were resuspended in 3 ml of M199/FBS.

Germ and somatic cells were separated using differential adhesion (Figure 2. 1). To achieve this, the cell suspension was transferred to a tissue culture dish and cultured overnight at 37°C in an atmosphere of 5% CO2 and 95% air. After overnight culture, the somatic cell population had adhered to the culture dish whereas the germ cell population remained unattached (including oocytes, non-viable somatic cells, red blood cells). The differential adhesion step was repeated to obtain clean cell populations. For this, the floating germ cell population was carefully collected without dislodging the attached cells and transferred into a new culture dish with 1 ml of warm, gassed M199/FBS. The adhered somatic cells were vigorously rinsed with warm DPBS/BSA three times to remove any loosely adhered or unattached cells. To collect the adhered somatic cells, they were incubated with 2 ml of trypsin/EDTA at 37°C for 5 minutes. Dislodged cells were then transferred into a 15 ml falcon tube with 2ml of warm, gassed M199/FBS and centrifuged at 660 x g for 5 minutes to form a pellet. The supernatant was discarded, and the cell pellet was resuspended in 3 ml of warm, gassed M199/FBS and transferred to a new tissue culture petri dish. The germ and somatic cell suspensions were then incubated for 6 hours (Figure 2. 1). After 6 hours of incubation, the germ and somatic cell populations were collected as described previously and each centrifuged (660 x g) to pellet cells which were resuspended in 200 µl of warm, gassed M199/FBS.

### 2.6.2. Cell viability assessment

To assess cell viability 10 µl of the mouse (or human) ovarian single cell suspension was mixed with 10 µl of trypan blue solution (T8154; Sigma). Trypan blue dye is soluble in water and permeable to cells with compromised membranes (dead cells) which are stained blue allowing for differentiation of viable (non-stained) cells. Cells were loaded

to a Neubauer Improved haemocytometer and cells in the 4 big squares (1 big square: 16 smaller squares) were counted and averaged.

After cell viability was assessed (see the formula below), the number of live cells remaining in the 190 µl of cell suspension was calculated using the following formula:

Cells/190 µl = Average number of cells in big 4 big squares
x
10,000 (Volume factor for the hemocytometer)
x
2 (Dilution factor due to 1:1 dilution with trypan blue)
x
0.2 (because cells were resuspended in 200 µl)
x
0.95 (because 10 µl were taken for cell viability assessment)

To form the RO, germ and somatic cells were combined using 1/3 of germ cells and all somatic cells (Figure 2. 1). This ratio is routinely used for neonatal ROs (Eppig et al. 2000).

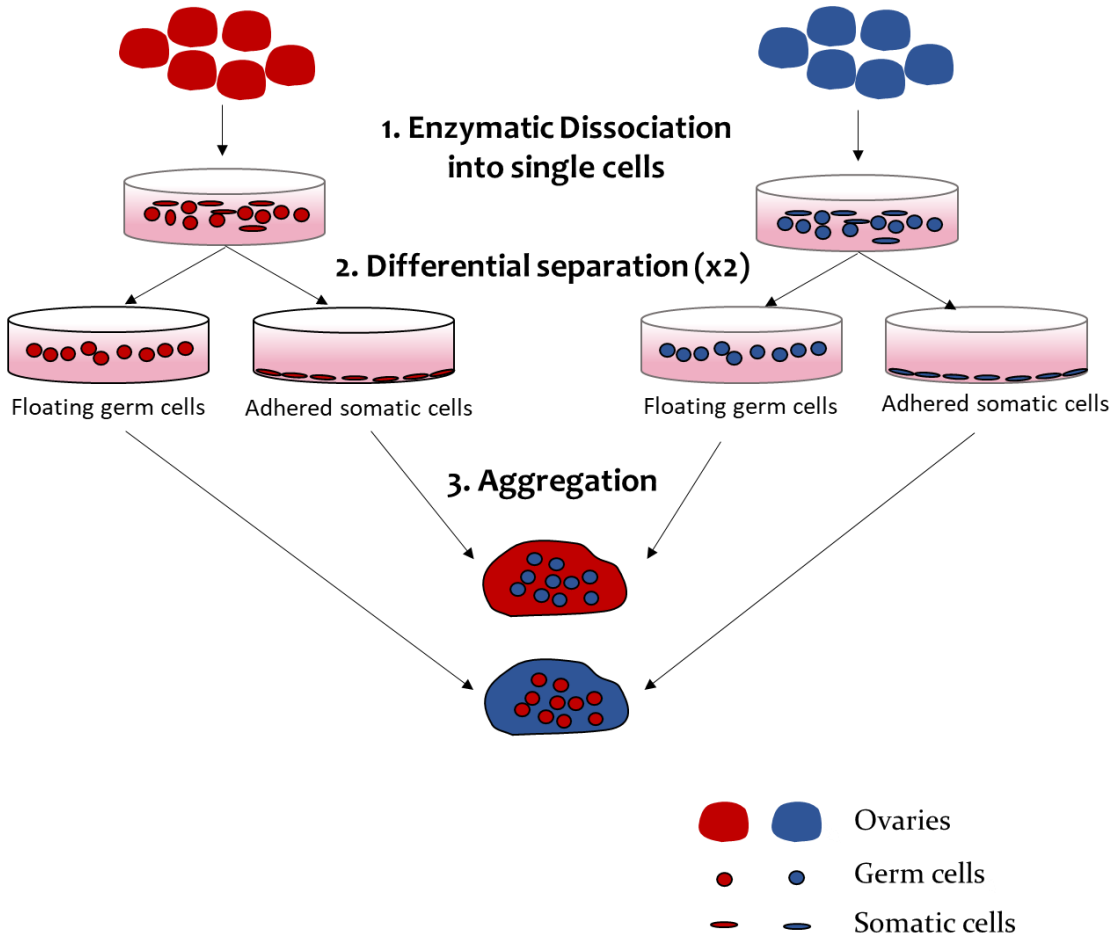



**Figure 2. 1 Generation of Reaggregated Ovaries**. (1) Ovaries were enzymatically digested into a single cell suspension. (2) Germ and somatic cell populations were separated using differential adhesion; somatic cells adhere to the bottom of tissue-treated culture dishes while germ cells remain unattached. The differential separation step was repeated to obtain clean cell populations. (3) Germ (floating) and somatic (adhered) cell populations from different ovaries were re-aggregated to form a pellet, the Reaggregated Ovary (RO).

To enhance germ and somatic cell cohesion, 6µl of Phytohemagglutinin (PHA-P; Sigma) at 5 mg/ml was added into 190 µl of the combined cells. The cell suspension was then centrifuged at 10,000 x g for 1 minute to form a 'pellet', referred to from now on as a reaggregated ovary (RO). The RO was transferred onto a polycarbonate Transwell membrane (6.5 mm diameter, 0.4 µm pore; Corning, New York, USA) in a 24-well tissue culture-treated plate (Corning Costar) with Waymouth MB752/1 media (Sigma) supplemented with 10% (v/v) FBS and cultured overnight. The membrane was prepared

two hours before the RO was transferred, by adding 250 µl of Waymouth/FBS medium above and below the membrane followed by an incubation at 37°C for at least two hours. When the RO was transferred onto the membrane, it was placed at the edge of the membrane to assist rounding. The excess media was removed, and the culture plate was incubated overnight at 37°C in 5% CO2 and 95% air.

### 2.6.3. Reaggregated Ovary culture

ROs were cultured in Waymouth-based culture media: Waymouth medium supplemented with 5% (v/v) FBS, 1% (v/v) insulin-transferrin-selenium (ITS; Life Technologies), 100 IU/ml penicillin and 0.1 mg/ml streptomycin (Sigma), 2.5 IU/10µl recombinant FSH (Gonal-F; Merck-Serono, Middlesex, UK) and 25 µg/ml ascorbic acid (Fisher), both suspended in alpha minimal essential media (MEM alpha; Fisher Scientific) supplemented with 10 µg/ml BSA (Factor V heat shock treated; Fisher). After overnight culture (Section 2.6.1), the membrane holding the rounded RO was picked up by hand and transferred into a new well containing 300 µl of fresh, warm, gassed media, and this was considered day 0 of culture (Figure 2. 2). Every two days, the culture media was replaced and the RO was gently moved to prevent tight adherence to the membrane using excess culture media that was removed after the RO was replaced in the centre of the membrane so that only a thin layer of media covered the RO (Figure 2. 2). RO culture was performed at 37°C in 5% CO2 and 95% air for 7 or 14 days.

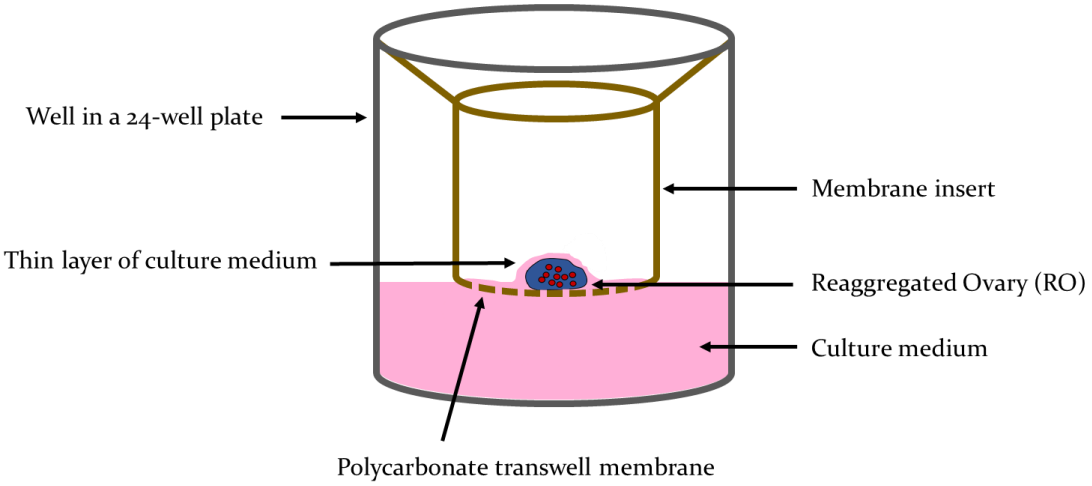



**Figure 2. 2 Reaggregated Ovary on a transwell membrane.** The RO was placed in the centre of the transwell membrane. Culture medium was added below the membrane in the well that was used to culture the RO. The volume of culture medium above the membrane was adjusted to a minimum so that the RO was covered with a thin film of culture medium. ROs were cultured for 7 or 14 days and culture medium was replaced every two days.

## 2.7. Tissue processing

### 2.7.1. Tissue collection and fixation methods

ROs were collected on day 7 or 14 of culture. The RO was gently removed from the membrane using excess culture media and transferred into the fixative solution. If the RO contained LacZ expressing cells, the fixative solution used was 25% (v/v) glutaraldehyde (Sigma-Aldrich) in 0.1 M PBS supplemented with 1 M $MgCl_2$. ROs were fixed for 1 hour and then washed 3 times for 15 minutes in a detergent rinse (Table 2. 3). ROs were then incubated overnight at 37°C in X-gal solution (Table 2. 3) and then washed in detergent rinse three times for 15 minutes each (Table 2. 3). Fixed ROs were then stored in PBS at 4°C for a maximum of 3 weeks before embedding. ROs without LacZ expressing cells were fixed in 10% buffered formalin for 6 hours. Fixed ROs were then transferred into 70% ethanol and stored at 4°C until embedding.

**Table 2. 3 Components of the X-gal staining method.**

| Steps | Reagent | Volume (µl) per 1 ml of solution |
|---|---|---|
| Fixative | 25% Gluteraldehyde | 8 |
| | 1M $MgCl_2$ | 2 |
| | 0.1M PBS (pH 7.3) | 990 |
| Detergent | 1M $MgCl_2$ | 2 |
| | 1% sodium deoxycholate | 10 |
| | 1% NP-40 | 20 |
| | 0.1M PBS (pH 7.3) | 968 |
| X-gal staining | 50 mg/ml X-gal | 20 |
| | 250 mL potassium ferricyanide | 20 |
| | 250 mL potassium ferrocyanide | 20 |
| | 1M $MgCl_2$ | 2 |
| | 1% sodium deoxycholate | 10 |
| | 1% NP-40 | 20 |
| | 1M Tris (pH 7.3) | 20 |
| | 0.1M PBS (pH 7.3) | 888 |

## 2.7.2. Embedding process

Before starting the embedding process, cassettes, moulds, and tubes containing paraffin wax were placed in the oven at 62°C. If the tissue was too small to visualise clearly in the dehydration (ethanol) and clearing (xylene) solutions, it was stained in a 1:10 eosin (Sigma-Aldrich) to 50% ethanol solution (if the tissue was stored in PBS) or a 1:10 eosin to 70% ethanol solution (if the tissue was stored in 70% ethanol) for 30 minutes prior to staining and embedding.

### 2.7.2.1. Dehydration

The tissue was dehydrated in increasing concentrations of ethanol followed by clearing in xylene (Table 2. 4). For the dehydration steps, if a 96-well plate was used, then 200 µl

of each solution was used per well (one well per RO), or if a 24-well plate was used then 500 µl of each solution was used per well. If tissue was stored in 70% ethanol, then the 50% EtOH solution was omitted. Tissue was transferred from well to well using blunt forceps or a wide bore 200 µl pipette (depending on the size of the tissue) to avoid damage. For xylene washes, xylene was replaced for each step using a glass Pasteur pipette. All procedures using xylene were performed using glass embryo dishes. One ml of xylene was used for each step per dish (Table 2. 4).

**Table 2. 4 Dehydration solutions and incubation times for tissue prior to embedding.**

| Solution | Time |
|---|---|
| 50% EtOH | 15 min |
| 70% EtOH | 15 min |
| 80% EtOH | 15 min |
| 95% EtOH | 15 min |
| 100% EtOH I | 15 min |
| 100% EtOH II | 15 min |
| 100% EtOH III | 15 min |
| Xylene I | 20 min |
| Xylene II | 20 min |
| Xylene III | 20 min |

### 2.7.2.2. Embedding

Paraffin wax was placed into the warm moulds kept in the oven. After dehydration, the tissue was transferred into the centre of plastic moulds containing melted paraffin wax (Fisher Scientific, Loughborough, UK) and incubated for 2 hours at 62°C. After 2 hours, a labelled cassette lid was placed gently on top of the mould so as not to move the pellet. If needed, additional melted wax was added on top of the cassette lid to ensure it would be secure, the oven was turned off and the moulds were left in the oven

overnight to cool slowly. The next day, cassettes were stored at 4°C until sectioning (Figure 2. 3).

#### 2.7.2.3. Sectioning

Blocks (Figure 2. 3) were sectioned at 5 µm using a microtome (Leica, Nussloch, Germany) and mounted on positively charged microscope slides (Superfrost® Plus, VWR International, Leuven, Belgium). The number of sections per slide depended on the staining process and downstream analysis of the tissue (usually 5 sections per slide). Slides were baked at 62°C for an hour and kept in slide boxes.

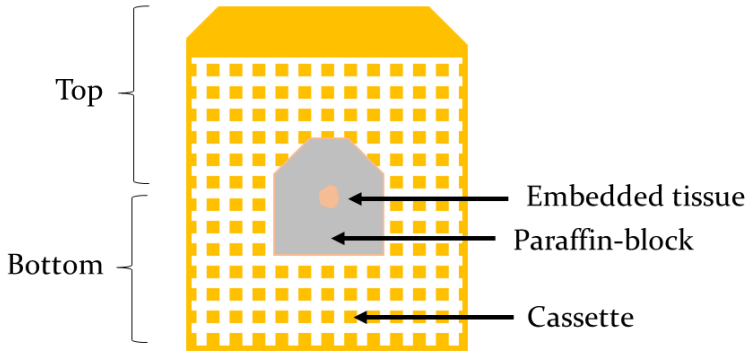



**Figure 2. 3 Schematic of embedded ovarian tissue in paraffin wax.** Tissue (pink) was embedded using paraffin wax (grey) on an embedding cassette (yellow). The top left and right corners of the block were trimmed (e.g. ''house-shape'') to maintain the same orientation of paraffin-embedded tissue during sectioning.

## 2.8. Histological process

### 2.8.1. Haematoxylin and Eosin staining

For histological analysis, tissue was stained with Haematoxylin & Eosin using a regressive protocol (Table 2. 5). To stain the cell nucleus, slides were immersed in haematoxylin (Shandon Gill 2 Haematoxylin; Fisher Scientific). Cytoplasmic staining was performed

using eosin (Sigma-Aldrich). The stained slides were then cover-slipped using Dibutylphthalate polystyrene xylene (DPX) moutant medium (Sigma-Aldrich) and left to dry overnight.

**Table 2. 5 Haematoxylin and Eosin staining process.**

| STEP | REAGENT | TIMING |
|---|---|---|
| **Dewax** | Xylene I | 8 min |
| | Xylene II | 4 min |
| | Xylene III | 4 min |
| **Rehydrate** | 100% EtOH I | 3 min |
| | 100% EtOH II | 3 min |
| | 90% EtOH | 2 min |
| | 70% EtOH | 2 min |
| | 50% EtOH | 3 min |
| | $ddH_2O$ | 3 min |
| **Stain** | Harris haematoxylin | 2 min |
| | Wash in running water | 5 min |
| | Destain in acid alcohol (1% HCl in 70% EtOH) | 5 sec |
| | Wash in running water | 5 min |
| | Running tap water | 5 min |
| | 80% EtOH | 5 min |
| | Eosin alcoholic | 1 min |
| **Dehydrate** | 95 % EtOH | 30 sec |
| | 100% EtOH I | 45 sec |
| | 100% EtOH II | 1 min |
| | 100% EtOH III | 2 min |
| | Xylene I | 8 min |
| | Xylene III | 8 min |

## 2.9. Assessment of follicle development in ROs

Follicle development in ROs was assessed by analysis of images obtained using a DM2500 microscope (Microscope services Ltd, Woodstock, UK) and a MicroPublisher

5.0 RTV camera (Qimaging, Microscope services Ltd). Follicles with a healthy nucleus (not pyknotic) and healthy cytoplasm were categorised into follicle stages (Figure 2. 4) according to Pedersen and Peters criteria established in 1968 (Pedersen et al. 1968).

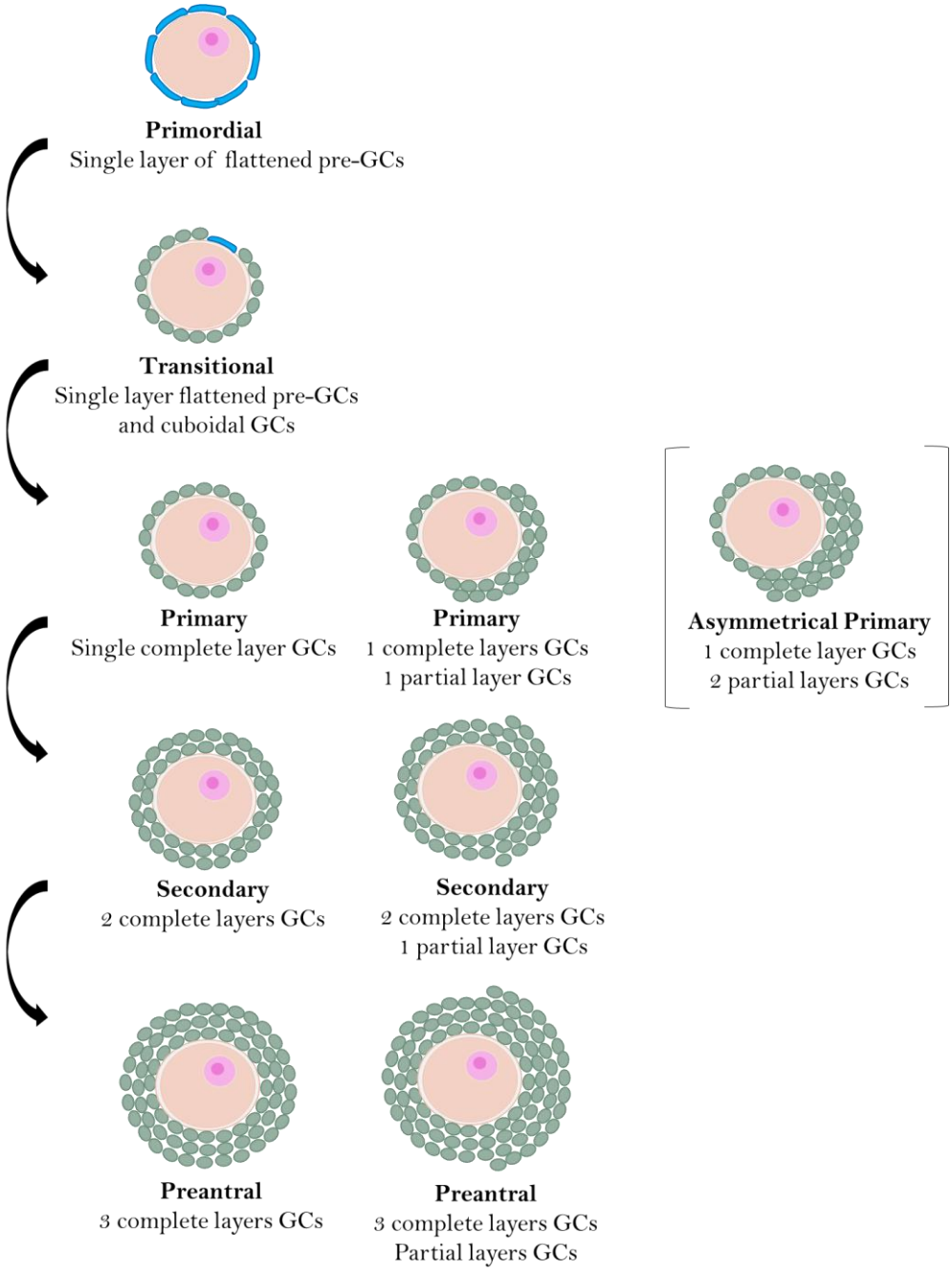



**Figure 2. 4 Stages of follicle development in ROs.** Follicles analysed in this thesis were categorised into stages of follicle development according to the type (flattened pre-GCs or cuboidal GCs) and number of GCs surrounding the oocyte. The size of the follicle gradually increases as it continues to develop (not accurately illustrated). Oocyte in pink, flattened pre-GCs in blue, cuboidal GCs in green. GCs: granulosa cells. NB Theca cells are not shown.

# CHAPTER 3

# *Investigation into dissociation of human ovarian tissue*

## 3.1 Introduction

### 3.1.1 Overview

The current methods available for fertility preservation are egg and embryo cryopreservation or ovarian cortical tissue cryopreservation followed by reimplantation (Dolmans et al. 2018). However, as discussed in Chapter 1, POI patients with follicle dysfunction do not benefit from the above methods of fertility preservation, because normal follicle development does not occur in these patients. The long-term aim of my thesis was to adapt the mouse RO technique and establish a RO method using human ovarian tissue to restore follicle development for POI patients with follicle dysfunction. This method aims to rescue germ cells by replacing the dysfunctional somatic cells with an alternative source of cells and placing the resulting RO in an environment that supports follicle development.

### 3.1.2 Background

In the mouse RO model, to isolate germ cells, ovaries are dissociated in an enzymatic solution of Trypsin (protease), ethylenediaminetetraacetic acid (EDTA), a chelating agent that inhibits cation-dependent cell binding (Duguay et al. 2003; Zhang et al. 2012) and DNase I (nuclease that cleave DNA). Trypsin is characterised by many as an "aggressive" protease, and digests proteins at the C-termini of arginine and lysine with high cleavage specificity (Olsen et al. 2004; Kirkpatrick et al. 1985). Trypsin enzymatic solution is very effective for mouse ovarian tissue and digests neonatal (Lo et al. 2019) or adult (unpublished work) mouse ovaries into a single cell suspension within 30 min of incubation. However, long term incubation of tissue with trypsin can lead to the digestion of cell membranes (Kirkpatrick et al. 1985) and cell death.

Many studies have shown that collagens are the most abundant fibrous protein in the mouse and human extracellular matrix (ECM) with focus on Collagen type I, III, IV, VI, laminin and fibronectin (Heeren,et al. 2015; Davidson et al. 2015; Lind et al. 2006; MacDonald et al. 2019; Berkholtz et al. 2006; Ouni et al. 2019). However, the human ovarian cortex is a highly fibrous, dense and stiff region (Hornick et al. 2012; Chiti et al. 2018) with inhomogeneous structure characterized by interlaced collagen fibers of comparable thickness (Chiti et al. 2018), as opposed to the mouse ovarian cortex which is none of these at any age. Work in our laboratory using assays to stain collagen fibers (i.e. Masson's Trichrome stain) showed that the human ovarian cortex contained more collagen compared to mouse ovaries based on qualitative analysis (unpublished data). Therefore, due to higher density and stiffness of human ovarian tissue, trypsin might

not be as effective for the dissociation of human ovaries into single cells as for mouse ovaries.

### 3.1.3 Commercially available enzymes

Isolation of follicles from human ovarian tissue has been performed using enzymes such as collagenase, liberase, and dispase (Table 3. 1). Prior to enzymatic dissociation, human ovarian tissue is typically dissected into small pieces, which increases the surface area that the enzymes can act on.

**Table 3. 1 Human ECM target proteins of collagenase, dispase and liberase.**

| | Collagenase | Dispase | Liberase |
|---|---|---|---|
| **Collagen type I** | ✓ | ✓ | ✓ |
| **Collagen type III** | ✓ | | ✓ |
| **Collagen type IV** | ✓ | ✓ | ✓ |
| **Collagen type VI** | ✓ | | ✓ |
| **Fibronectin** | | ✓ | |

*Collagenase*

There are several commercially available enzyme blends that target collagens. Collagenase (Table 3. 1) is a crude mixture of enzymes, that belong to the matrix metalloproteinases (MMP) family, and are produced by certain bacteria of the genus *Clostridium* (Davidson et al. 2015). These proteolytic enzymes digest collagen or gelatin (the denatured form of collagen (Jennison 1945)), and have been used in Phosphate Buffered Saline (PBS) (Lierman et al. 2015; Dolmans et al. 2006; Zver et al. 2017; Nakamura et al. 1994; Stenn et al. 1989) or Leibovitz's L-15 (Martinez-Madrid et al. 2004; Asiabi et al. 2019; Peek et al. 2019) to isolate follicles (Hovatta et al. 1999; Oktay et al. 1997; Vanacker et al. 2011; Peek et al. 2019; Martinez-Madrid et al. 2004; Fauque et al.

2007; Mouloungui et al. 2018; Dolmans et al. 2006) from human ovarian cortex. However, there is very limited information on the dissociation of human fresh ovarian cortical tissue (Asiabi et al. 2019) or frozen/thawed ovarian cortical tissue (discussed below) into single cells. Some studies have also incorporated mechanical dissociation (shaker (Wagner et al. 2020; Nakamura et al. 1994)), gentle agitation and/or pipetting (Zver et al. 2017; Vanacker et al. 2011) for up to 3 hours at 37$^{o}$C or overnight at 4$^{o}$C (Fan et al. 2019).

*Dispase*

Dispase (Table 3. 1) is a neutral protease produced by bacteria *Bacillus polymyxa* and specifically cleaves collagen type IV and fibronectin and to a lesser extent collagen type I (Stenn et al. 1989). In the few experiments carried out, dispase was used in combination with collagenase (Kristensen et al. 2011; Lierman et al. 2015) or alone (Lierman et al. 2015) to isolate human ovarian follicles from fresh medulla (Kristensen et al. 2011) or frozen/thawed cortex (Lierman et al. 2015).

*Liberase*

Liberase (Table 3. 1) is a commercially produced blend that contains highly purified clostridial collagenases, to enrich collagen specificity, combined with high-specific-activity neutral proteases in optimal ratios to enhance tissue dissociation. More specifically, liberase contains Collagenase type I (high collagenase activity) and II (moderate collagenase activity), as well as high or low concentrations of dispase as a neutral protease (Liberase Dispase High; DH or Dispase Low; DL). Also, the level of endotoxins (bacterial by-products) are significantly reduced in liberase products compared to crude collagenases. Thus, liberase products may be more effective at

isolating high numbers of viable cells from human ovarian tissue due to increased reproducibility of tissue dissociation compared to crude collagenase products, and low endotoxin levels (Jahr et al. 1999). Liberase can be used to incubate tissue in L-15 (Schmidt et al. 2018a, 2018b) or PBS (Dolmans et al. 2006; Nakamura et al. 1994; Stenn et al. 1989; Chiti et al. 2017) with the addition of shaking (Schmidt et al. 2018a, 2018b) or gentle agitation (Dolmans et al. 2006; Lierman et al. 2015; Vanacker et al. 2011) for 75 min at 37$^{o}$C. Liberase has also been used in combination with collagenase to isolate human ovarian follicles (Lierman et al. 2015).

Liberase has been explored as an alternative to collagenase for isolation of human ovarian follicles due to collagenase batch-to-batch variation problems and higher endotoxin levels. Vanacker et al. evaluated the efficacy of enzymatic methods to isolate human follicles from fresh ovarian cortex and demonstrated no difference in follicle yield or viability when comparing collagenase (type I) with liberase$^{DH}$ (Vanacker et al. 2011). In contrast, Dolmans et al. showed that more follicles but with lower viability were yielded using collagenase (type I) as compared to liberase$^{DH}$ using fresh human ovarian cortex (Dolmans et al. 2006).

#### 3.1.3.1. Considerations

The long-term aim of this thesis was to adapt the RO method for human ovarian tissue and restore follicle development for POI patients who do not benefit from fertility preservation methods available (e.g. pre-pubertal patients with follicle dysfunction). However, cryopreservation of ovarian cortical tissue is the only option available for pre-pubertal patients to preserve their fertility (discussed in Chapter 1) and thus, frozen/stored ovarian cortex may be the only source of ovarian tissue for some patients.

Additionally, to generate a RO, isolation of viable ovarian single cells is required. Hence, developing a method to dissociate human frozen/thawed ovarian cortex into viable single cells is required in this study.

Cryopreservation of ovarian cortical tissue has been widely used as a fertility preservation method, and has been shown to preserve primordial follicles effectively (Kim et al. 2018). There are studies indicating that primordial follicles are resistant to damage associated with freezing and thawing (Hovatta et al. 1996; Qu et al. 2000). Hovatta et al. observed that despite the 27% and 19% of follicles exhibiting signs of atresia observed in human fresh and frozen/thawed ovarian cortical tissue, respectively, the cryopreservation process did not affect the number of morphologically normal follicles and oocytes in human frozen/thawed ovarian cortex compared to fresh tissue (Hovatta et al. 1996). In alignment with these results, Qu et al. showed that the population of normal primordial follicles and stromal cells in frozen/thawed ovarian cortex, analysed using histological analysis, wasn't significantly different to fresh tissue implying that freezing and thawing did not affect viability in human ovarian cells (Qu et al. 2000). In contrast to these findings, Gook et al. reported that the survival rate of oocytes and granulosa cells was compromised in human frozen/thawed ovarian cortical tissue compared to fresh after histological evaluation of a follicular population where primordial follicles were dominant (Gook et al. 1999). In another study, Hreinsson et al. using histology, showed that viability of follicles and oocytes was significantly reduced after freezing and thawing as compared to fresh tissue where 99.3% of the follicles observed were viable (Hreinsson et al. 2003). Considering the potential effect of freezing

and/or thawing on cell viability, optimisation of a method to dissociate human frozen/thawed ovarian cortical tissue is necessary to achieve better results.

Studies investigating the isolation of human follicles from frozen/thawed ovarian cortical tissue comparing the efficacy of different enzymes have shown variation. Lierman et al. showed that fewer viable follicles were isolated using collagenase (type IV) compared to liberase or liberase™ (with medium thermolysin concentration) combined with collagenase (type IV) (Lierman et al. 2015). In another study, Schmidt et al. showed that the viability of follicles from fresh or frozen/thawed ovarian cortical tissue was significantly lower when isolated with liberase™ compared to Tumor Dissociation Enzyme (TDE), a cocktail of highly purified collagenase (secured composition due to patent) developed to effectively isolate tumour cells (Schmidt et al. 2018b).

To our knowledge, at the time of writing there were only 3 publications where human frozen/thawed ovarian cortex was dissociated into single cells for downstream analysis with FACS (Wagner et al. 2020; White et al. 2012; Clarkson et al. 2018). In Wagner et al., thawed ovarian cortex was enzymatically digested in collagenase (type I) in combination with liberase in a shaking 37 °C water bath (Wagner et al. 2020). White et al. dissociated frozen/thawed ovarian cortex in collagenase (type IV) followed incubation in trypsin (White et al. 2012). However, to our knowledge, there is only one study where the efficacy of different methods to dissociate human frozen/thawed ovarian cortex into single cells was explored (Zver et al. 2017). In Zver et al., human fresh or frozen/thawed ovarian cortex were dissociated into single cells using 2 different methods; a method

developed by Zver et al. using collagenase type I combined with DNase I, and a commercially available dissociation kit utilising a cocktail of 3 enzymes (proprietary) (Zver et al. 2017). Zver et al. demonstrated that live-cell yield retained from fresh or frozen/thawed cortex using the 2 protocols was not different, but cell viability was significantly lower using the laboratory protocol (Zver et al. 2017). However, information regarding the efficacy of these 2 methods to yield viable ovarian cells from frozen/thawed ovarian cortex was not available since fresh and frozen/thawed samples were combined in this analysis (Zver et al. 2017).

Investigation into the dissociation of human frozen/thawed ovarian cortex was required in this thesis to determine the most effective method to yield highest number of viable ovarian single cells.

### 3.1.4 Anti-apoptotic factors

Rho-associated coiled-coil containing kinase (ROCK) inhibitor can reduce enzymatic dissociation-induced apoptosis and promote cell survival in human embryonic stem cells (Watanabe et al. 2007; Rungsiwiwut et al. 2013). ROCKs are kinases involved in actomyosin cytoskeleton contractility downstream of Rho GTPase or Caspase 3 activation resulting in plasma membrane blebbing and thus, cell apoptosis. ROCK inhibitors specifically inhibit ROCKs through binding to the Rho-kinase adenosine triphosphate (ATP) binding pocket in an ATP-competitive manner (Julian et al. 2014; Coleman et al. 2002). These inhibitors may be useful to retain cell viability during ovarian cortical tissue dissociation, as it was shown that anti-apoptotic factors can improve the survival and development of cultured follicles (Abdollahi et al. 2018).

## 3.2 Aims

The primary objective of this study was to optimise and develop a method for human frozen/thawed ovarian cortical tissue dissociation. To help explore and test various tissue dissociation protocols, different types of ovarian tissue from the OCTB were used. This included fresh cortex from whole ovaries, fresh ovarian remnants, and frozen/thawed ovarian cortical tissue. The aims of this chapter were:

- To compare the efficacy of trypsin (routinely used in the mouse RO method) with collagenase (preferred for human ovarian tissue dissociation) to dissociate human fresh ovarian cortex.
- To compare the efficacy of collagenase with liberase to dissociate human frozen/thawed ovarian cortical tissue.
- To test the efficacy of using a shaker to aid in the mechanical dissociation of human fresh ovarian cortex.
- To explore human fresh ovarian remnant tissue dissociation.

## 3.3 Materials & Methods

### 3.3.1 Ovarian tissue source

Human ovarian tissue was obtained from the Oxford Cell and Tissue Biobank (OCTB), as described (Chapter 2).

#### 3.3.1.1. Types of human ovarian tissue used

*Fresh ovarian cortical tissue from whole ovaries*

Fresh cortical tissue can be obtained from whole ovaries (removed due to pathological conditions). Because the whole cortex of the organ was available for research, it was possible to test many variables in this preliminary analysis before using the limited frozen/stored ovarian cortex.

*Fresh ovarian remnant tissue generated after cortex was dissected prior to tissue cryopreservation*

The main advantage to using remnants in tissue dissociation is that this tissue is routinely available from patients of all ages. It is also fresh, and therefore, not affected by cryopreservation. Thus, using of remnant tissue in this study was an alternative source of fresh ovarian tissue to explore human ovarian tissue dissociation.

*Frozen/stored ovarian tissue*

As the long-term aim of this thesis was to develop a method that could potentially be used for fertility preservation, it was important to use human frozen/thawed ovarian cortical tissue in this study.

### 3.3.2 Exclusion criteria for tissue donors

The exclusion criterion for remnant tissue and frozen/stored cortex was patients older than 35 years. For fresh cortical tissue from whole ovaries, patients over 50 years were excluded. Patients with ovarian diseases (e.g. ovarian cancer) were also excluded from this study.

### 3.3.3 Overview of the methodology applied to dissociate human ovarian tissue

To explore the dissociation of human ovarian tissue into a single cell suspension, multiple experiments were carried out using fresh cortex (obtained from whole ovaries), fresh remnants or frozen/thawed cortical strips (Figure 3. 1). Modified methodologies were applied to dissociate fresh cortex, fresh ovarian remnant tissue and frozen/thawed cortex. Preliminary observations obtained from experiments presented here informed investigations presented in Chapter 4.

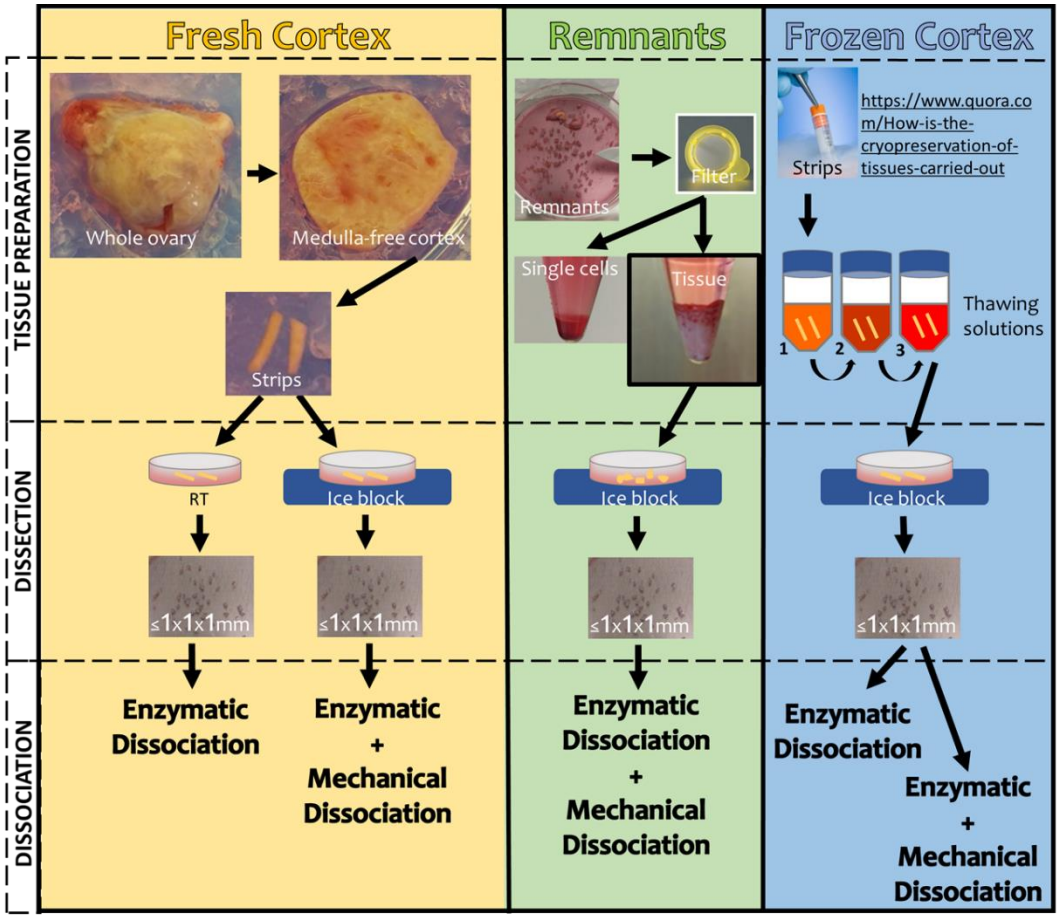



**Figure 3. 1 Overview of methodology to dissociate human ovarian tissue.** Whole ovaries, remnants and frozen/stored cortical tissue were acquired from the OCTB.

## 3.3.4 Human fresh ovarian cortical tissue dissociation

### 3.3.4.1 Variables tested to investigate the dissociation of fresh cortex

Protocol A and B were used to dissociate fresh ovarian cortical strips (Figure 3. 2).

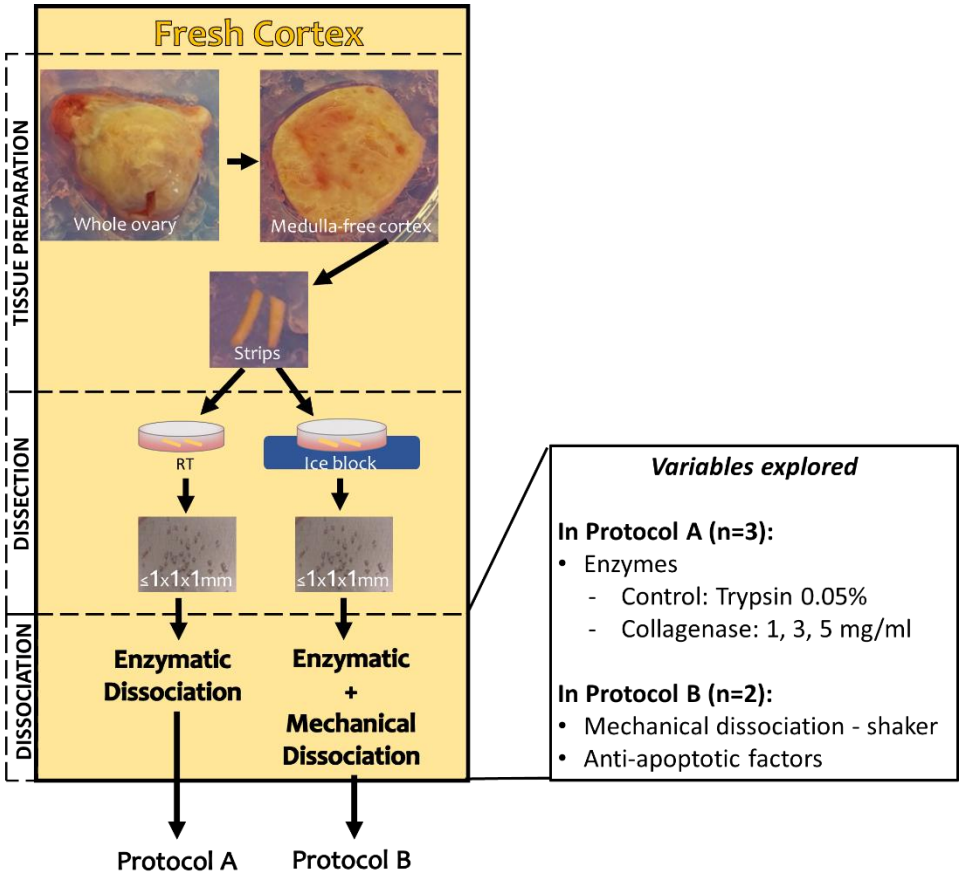



**Figure 3. 2 Variables explored to dissociate human fresh ovarian cortical tissue.** Whole ovaries were acquired from the OCTB. RT: room temperature.

In the first set of experiments using fresh cortex (see Section 3.3.4.2), the efficacy of trypsin was compared to collagenase (Protocol A); here, the enzymatic solution used in the RO method (Chapter 2) was used as a starting point (control Trypsin).

In the second set of experiments using fresh cortex (see Section 3.3.4.3), mechanical dissociation of fresh cortical tissue was explored. Differences between the two set of experiments using fresh cortex are highlighted in Table 3. 2, including dissection media and temperature, digestion time, media used to dissolve enzymes, and media used to inhibit the enzymatic reaction.

**Table 3. 2 Differences between Protocol A and B used to dissociate human fresh ovarian cortical tissue.** Whole ovaries were obtained from the OCTB. L-15: Leibovitz's L-15 medium; M199: medium 199; RT: room temperature; PBS: phosphate buffered saline; FBS: fetal bovine serum.

| | FRESH CORTEX | |
|---|---|---|
| | **Enzyme focused (Protocol A)** | **Mechanical dissociation using shaker (Protocol B)** |
| **Dissection media** | L-15 with L-glutamine | L-15/10% FBS |
| **Dissection temperature** | RT | ice block |
| **Dissociation** | Enzymatic | Enzymatic plus mechanical |
| **Enzymatic solution** | Trypin: 0.05%<br>Collagenase 1 mg/ml in PBS<br>Collagenase 3 mg/ml in PBS<br>Collagenase 5 mg/ml in PBS | Collagenase 3mg/ml in L15 |
| **Digestion time** | 30 min | 40 min |
| **Media to inhibit enzymatic reaction** | M199 supplemented | L-15/10% FBS |

### 3.3.4.2 Methodology applied to explore the efficacy of trypsin and collagenase to dissociate fresh cortical tissue (Protocol A)

Tissue was obtained from a 24-year-old patient undergoing gender reassignment, who had her ovaries removed, and from a 48- and 49-year-old patient, who had her ovaries removed for pathological reasons (unknown). Whole ovaries were processed on the day of procurement (fresh), and/or kept overnight at 4°C to be processed next day following procurement (O/N). Under sterile conditions, ovaries were cut into quartiles in Leibovitz's medium (L-15) with L-glutamine (11415049; Gibco, ThermoFisher Scientific, Paisley, UK) using sterile spring scissors, micro scissors, and blades. The medulla was removed and the medulla-free cortex (1mm thickness) was cut into strips of 1x1x5 mm in L-15 with L-glutamine. Cortical strips were weighed, and net tissue weight was

calculated as described (Chapter 2). Cortical strips were further cut into pieces ≤ 1mm$^3$ in L-15 with L-glutamine using the tissue chopper and scalpel blades. Tissue was digested in Trypsin-EDTA (0.53 mM) 0.05% (25300054; Gibco, ThermoFisher Scientific, Paisley, UK) with 0.02% DNase I (DN25; Sigma-Aldrich, Dorset, UK) or collagenase type I [1, 3 and 5 mg/ml] (C0130; Sigma-Aldrich, Dorset, UK) with 0.078 mg/ml DNase I. The concentration of Trypsin-EDTA was the same as the mouse RO method. Tissue was digested at 37°C in an atmosphere of 5% $CO_2$ and 95% air for 30 min. Tissue was mixed by gentle pipetting at 15 min, 20 min, 25 min and 30 min of incubation.

The enzymatic reactions were inhibited by the addition of warm, equilibrated medium (supplemented M199) routinely used in the mouse RO method (Medium 199 (31150022) supplemented with 10% FBS (Labtech), 10 mg/ml penicillin-streptomycin (P0781; Sigma-Aldrich, Dorset, UK) and 31.3 mM sodium DL-lactate (Sigma)). Samples were centrifuged at 650 x g for 5 min. The supernatant was discarded, and cells resuspended in 3 ml of supplemented M199 and then filtered through a 100 µm strainer to remove any undigested tissue. Finally, the single cell suspension was centrifuged at 650 x g for 5 min, the supernatant was discarded, and cells resuspended in 3 ml of supplemented M199. Viability was assessed as described (Chapter 2).

### 3.3.4.3 Methodology to explore the efficacy of mechanical dissociation using a shaker to dissociate fresh cortical tissue (Protocol B)

Tissue was obtained from a 29-year-old and 47-year-old patient, who both had their ovaries removed. Because the morphology of the ovaries from the 47-year-old patient looked abnormal (harsh and wrinkled surface, some parts of the medulla were black), the 'abnormal' part was excluded. One whole ovary from the 47-year-old was processed on the day of procurement (fresh) and the other kept overnight at 4°C (O/N) and processed the following day. Tissue from the 29-year-old was kept overnight at 4°C (O/N) and processed the following day.

Under sterile conditions ovaries were cut into quartiles in L-15 without L-glutamine (L5520; Sigma-Aldrich, Dorset, UK) supplemented with 10% v/v FBS on ice block and dissected into strips as described above. Cortical strips were then cut further into pieces ≤ 1mm$^3$ on ice block using blades only. To digest the tissue, chopped tissue was transferred into a sterile tube with 4 ml of L-15 without L-glutamine containing 3 mg/ml of collagenase I and 0.078 mg/ml DNase I. Tissue was digested at 37°C using a shaker (200 rpm) for 40 min. To aid dissociation, every 15 min the tube was vigorously shaken by hand for a few seconds. The enzymatic reaction was inhibited by the addition of L-15 without L-glutamine supplemented with 10% v/v FBS. The digestion mixture was centrifuged at 650 x g for 5 min, the supernatant was discarded, and the pellet was resuspended in 4 ml of Leibovitz's medium L-15/10% v/v FBS and filtered through a 100 µm strainer to remove any undigested tissue. Cells were centrifuged at 650 x g for 5 min, the supernatant was discarded, and the pellet was resuspended in 1 ml of L-15/10% v/v FBS. Cell viability was assessed as described (Chapter 2).

#### 3.3.4.4 Methodology to explore the efficacy of anti-apoptotic factors to improve dissociation of human fresh ovarian cortical tissue using Protocol B

To investigate if dissociation of fresh cortex using Protocol B could be improved, the effect of anti-apoptotic factors on cell viability was explored. Dissection and dissociation of the tissue was performed as described in Section 3.3.4.3. Additionally, anti-apoptotic factors (RevitaCell Supplement; A2644501; Gibco, Life Technologies, Paisley, UK) were added in both the dissection media and enzymatic solution, or in the dissection media only. Viability was assessed as described (Chapter 2).

### 3.3.5 Human ovarian remnant tissue dissociation

Remnant ovarian tissue (generated by tissue processing), consisting of medulla (primarily), cortex and cells (Figure 3. 3), was filtered through a 100 µm strainer. Remnants collected on top of the filter were chopped and dissociated enzymatically (see Section 3.3.5.2).

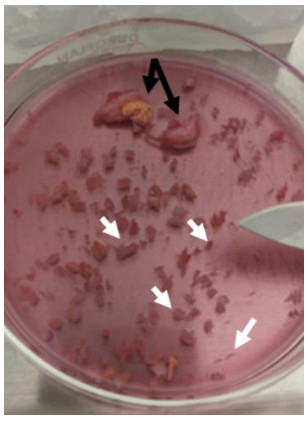


**Figure 3. 3 Representative image of human fresh ovarian remnant tissue sample.** Remnants were collected in Leibovitz's L-15 medium at 4°C. Samples contained big pieces of medulla (black arrows), smaller pieces of medulla or cortex of dissimilar sizes (white arrows).

### 3.3.5.1. Variables tested to investigate the dissociation of human fresh ovarian remnant tissue

Mechanical dissociation using a shaker was explored to dissociate human fresh ovarian remnant tissue was (Figure 3. 4).

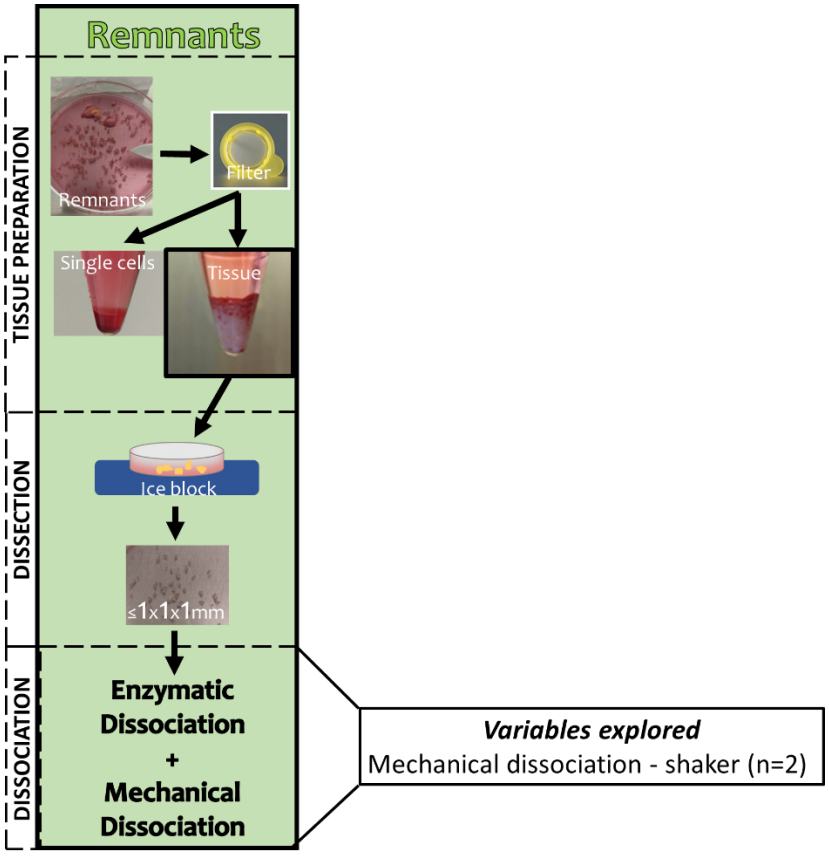



**Figure 3. 4 Variables explored to dissociate human fresh ovarian remnant tissue.** Remnant tissue was acquired from the OCTB.

### 3.3.5.2. Methodology used to dissociate human fresh ovarian remnant tissue (Protocol C)

Ovarian remnant tissue was obtained from a 6-year-old and 11-year-old patient. An overview of the method used to dissociate human ovarian remnant tissue is presented in Table 3. 3. The remnants collected on the strainer were dissected into smaller pieces prior to dissociation in the same way as previously the OCTB processed the tissue prior

to cryopreservation (i.e. in L-15 without L-glutamine and on ice blocks). To digest the tissue, chopped tissue was transferred into a tube containing 3 mg/ml collagenase I in 4 ml of L-15 medium without L-glutamine, with 0.078 mg/ml DNase I. Tissue was digested at 37°C using a shaker (200 rpm) for 40 min as previously described (Protocol B).

The enzymatic reaction was inhibited by the addition of 4 ml of L-15 without L-glutamine supplemented with 0.3% (w/v) HSA (A1653; Sigma-Aldrich, Dorset, UK). Cells were centrifuged at 650 x g for 5 min, the supernatant was discarded, the cell pellet was resuspended in 4 ml of L-15 without L-glutamine supplemented with 0.3% (w/v) HSA and filtered through a 100 µm strainer to remove any undigested tissue. The single cell suspension was centrifuged at 650 x g for 5 min, the supernatant was discarded, and the cell pellet was resuspended in 1 ml of L-15 without L-glutamine supplemented with 0.3% (w/v) HSA. Viability was assessed as described (Chapter 2).

**Table 3. 3 Variables tested to dissociate human fresh ovarian remnant tissue using Protocol C.** Remnant tissue was obtained from the OCTB. L-15: Leibovitz's L-15 medium; HSA: human serum albumin.

| | FRESH REMNANTS |
|---|---|
| | Mechanical dissociation using shaker (Protocol C) |
| **Dissection media** | L-15 |
| **Dissection temperature** | ice block |
| **Dissociation** | Enzymatic plus mechanical |
| **Enzymatic solution** | Collagenase 3mg/ml in L15 |
| **Digestion time** | 40 min |
| **Media to inhibit enzymatic reaction** | L15/0.3%HSA |

### 3.3.6 Methodology used to dissociate human frozen/thawed ovarian cortical tissue (Protocol D)

Frozen/thawed ovarian cortical strips were obtained from a 13-year-old patient. The method used to dissociate frozen/thawed cortical tissue is briefly described in Figure 3. 5. Variables explored to digest human frozen/thawed ovarian tissue were enzymes (collagenase or liberase), media used to digest the tissue (L-15 or PBS), enzymatic dissociation plus mechanical dissociation (using a shaker) and dissociation time (40 min for mechanical dissociation or 75 min for enzymatic dissociation without mechanical dissociation) (Figure 3. 5).

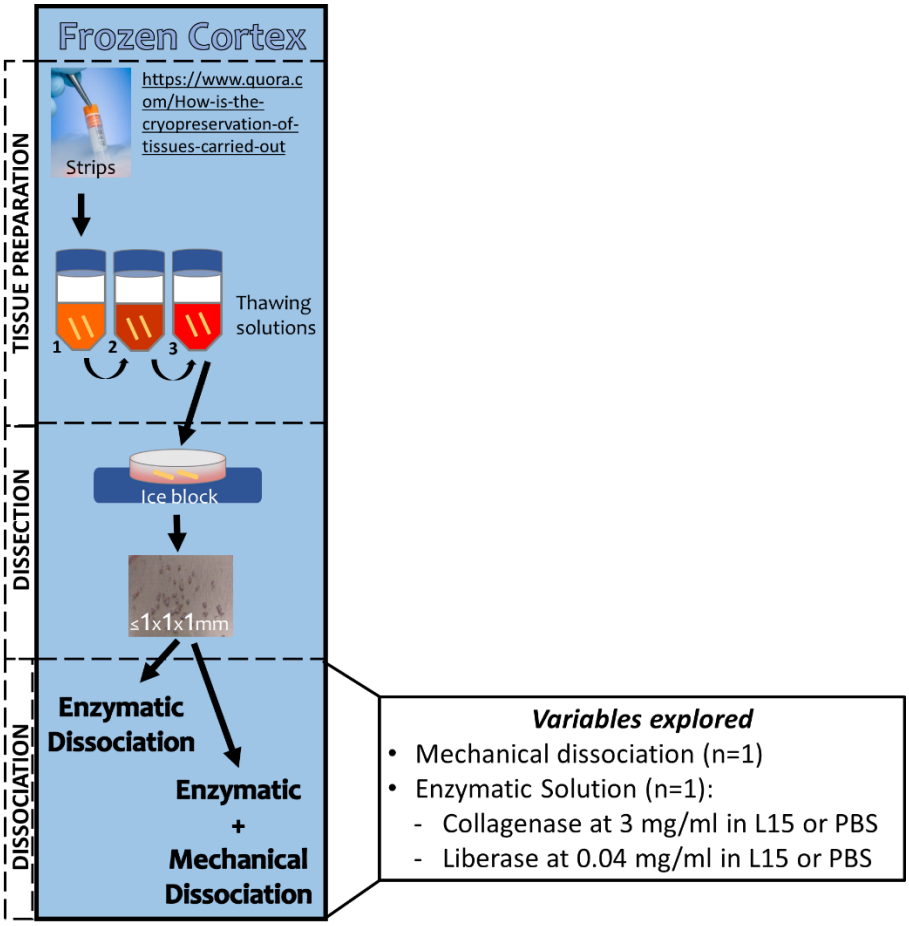



**Figure 3. 5 Variables explored to dissociate human frozen/stored ovarian cortical tissue.** Frozen cortical strips were acquired from the OCTB. L-15: Leibovitz's L-15 medium; PBS: phosphate buffered saline.

Frozen ovarian cortical strips were thawed (Chapter 2) and chopped as described (Protocol C). Chopped tissue was dissociated in 4 ml of either L-15 (without L-glutamine) or PBS containing either collagenase I at 3 mg/ml or Liberase$^{DH}$ at 0.04 mg/ml (Research Grade; 5401054001; Sigma-Aldrich, Dorset, UK). To aid digestion, the enzymatic mixture was mixed every 15 min by gentle pipetting. For methods using a shaker, tubes were shaken by hand as described (Protocol B). Enzymatic reaction was inhibited by adding 4 ml of L-15 or PBS supplemented with 0.3% HSA. Cells were centrifuged at 650 x g for 5 min, supernatant was discarded, the pellet was resuspended in 4 ml of media (L-15 or PBS supplemented with 0.3% HSA) and filtered through a 100 µm strainer to remove any remaining undigested tissue. The single cell suspension was centrifuged at 650 x g for 5 min, the supernatant was discarded, and the cell pellet was resuspended in 1 ml of L-15 without L-glutamine supplemented with 0.3% (w/v) HSA. Viability was assessed as described (Chapter 2).

An overview of the variables tested in Protocol A (fresh cortex), B (fresh cortex) , C (fresh remnants), and D (frozen/thawed cortex) are highlighted in Table 3. 4.

**Table 3. 4 Differences between Protocol A, B, C and D used to dissociate human ovarian tissue.**

| | FRESH CORTEX | | FRESH REMNANTS | FROZEN THAWED CORTEX |
|---|---|---|---|---|
| | Enzyme focused (Protocol A) | Mechanical dissociation using shaker (Protocol B) | Mechanical dissociation using shaker (Protocol C) | Optimisation (Protocol D) |
| **Dissection media** | L-15 with L-glutamine | L-15/10% FBS | L-15 | L-15 |
| **Dissection temperature** | RT | ice block | ice block | ice block |
| **Dissociation** | Enzymatic | Enzymatic plus mechanical | Enzymatic plus mechanical | Enzymatic<br>Enzymatic plus mechanical |
| **Enzymatic solution** | Control Trypin: 0.05%<br>Collagenase 1 mg/ml in PBS<br>Collagenase 3 mg/ml in PBS<br>Collagenase 5 mg/ml in PBS | Collagenase 3mg/ml in L15 | Collagenase 3mg/ml in L15 | Collagenase 3mg/ml in L15<br>Collagenase 3mg/ml in PBS<br>Liberase 0.04mg/ml in L15<br>Liberase 0.04mg/ml in PBS |
| **Digestion time** | 30 min | 40 min | 40 min | 75 min (enzymatic)<br>40 min (enzymatic+mechanical) |
| **Media to inhibit enzymatic reaction** | M199 supplemented | L-15/10% FBS | L15/0.3%HSA | L15/0.3%HSA |

### 3.3.7 Normalisation of cell numbers

Cortical tissue used in this study was cut into strips by hand, and therefore there was small variation in the final size of strips. Cell numbers were calculated per gram of tissue (when applicable) using the formula below:

***Step 1 - to calculate the total number of cells isolated:***

$$\underline{\text{Total number}} \text{ of cells yielded} = Number\ of\ Viable\ cells + Number\ of\ Dead\ cells$$

***Step 2 - to calculate the number of viable cells per gram of tissue:***

$$\text{Number of live cells yielded } \underline{\textbf{per gram of tissue}} = \frac{Total\ Number\ of\ viable\ cells}{Tissue\ weight\ (grams)}$$

***Step 3 - to calculate the total number of cells isolated per gram of tissue*:**

$$\text{Number of cells yielded } \underline{\textbf{per gram of tissue}} = \frac{Total\ number\ of\ cells\ yielded}{Tissue\ weight\ (grams)}$$

### 3.3.8 Statistical analysis

GraphPad Prism version 8.2.1 (GraphPad Software, La Jolla, California, USA) was used to perform statistical analysis. The number and percentage of viable cells/g isolated from fresh ovarian cortex using dissociation Protocol A was calculated, data was matched, tested for normality using Shapiro-Wilk test. Cell viability, and live-cell yield/g, was compared across the enzymatic conditions used: control trypsin versus collagenase 1 mg/ml versus collagenase 3 mg/ml versus collagenase 5 mg/ml., and analysed using a One-Way ANOVA Friedman test with Dunn's multiple comparisons tests (data wasn't normally distributed). Data was matched across enzymatic conditions. Results are presented as mean±SD, with $P \leq 0.05$ considered significant.

## 3.4 Results

### 3.4.1 Age and characteristics of the patients included

Whole ovaries were obtained from 5 patients with an age of 39±12 years (mean±SD) (Table 3. 5). Remnant tissue was obtained from 2 patients (mean age of 9 years) (Table 3. 6), and cryopreserved cortical tissue from a 13-year-old patient (Table 3. 7).

**Table 3. 5 Detailed list of patients who donated whole ovaries for research investigations including in Chapter 3.**

| FRESH OVARIAN CORTICAL TISSUE | | | | | |
|---|---|---|---|---|---|
| **Protocol used to dissociate tissue** | **Patient no.** | **Age** | **Pubertal status** | **Condition** | **Chemotherapy treatment** |
| Protocol A | Patient 1 | 24 | Post-pubertal | Gender reassignment | No |
| | Patient 2 | 49 | Post-pubertal | Unknown | No |
| | Patient 3 | 48 | Post-pubertal | Unknown | No |
| Protocol B | Patient 4 | 47 | Post-pubertal | Unknown | No |
| | Patient 5 | 29 | Post-pubertal | Unknown | No |

**Table 3. 6 Detailed list of patients who donated ovarian remnant tissue for research investigations including in Chapter 3.**

| FRESH REMNANT OVARIAN TISSUE | | | | | |
|---|---|---|---|---|---|
| **Protocol used to dissociate tissue** | **Patient no.** | **Age** | **Pubertal status** | **Condition** | **Chemotherapy treatment** |
| Protocol C | Patient 6 | 11 | Pre-pubertal | Unknown | No |
| | Patient 7 | 6 | Pre-pubertal | Wilms tumour | Yes |

**Table 3. 7 Detailed information about a patient who donated frozen/stored ovarian cortical tissue for research investigations including in Chapter 3.**

| FROZEN OVARIAN CORTICAL TISSUE | | | | | |
|---|---|---|---|---|---|
| **Protocol used to dissociate tissue** | **Patient no.** | **Age** | **Pubertal status** | **Condition** | **Chemotherapy treatment** |
| Protocol D | Patient 8 | 13 | Post-pubertal | Ewing's Sarcoma | No |

### 3.4.2 Efficacy of control trypsin compared with collagenase to dissociate human fresh ovarian cortex (Protocol A)

To explore if the enzymatic solution routinely used in the RO method to dissociate mouse ovaries (Lo et al. 2019) was effective for human ovarian cortex, the efficacy of control trypsin to dissociate human fresh ovarian cortical tissue from 3 patients aged 24- to 49-years was compared using collagenase at 3 concentrations: 1, 3 and 5 mg/ml.

The percentage of viable cells isolated using trypsin was similar to collagenase at any concentration (Figure 3. 6A). The highest number of viable cells was obtained when using 3 mg/ml of collagenase, however this was not significantly different to any of the conditions tested here (Figure 3. 6B).

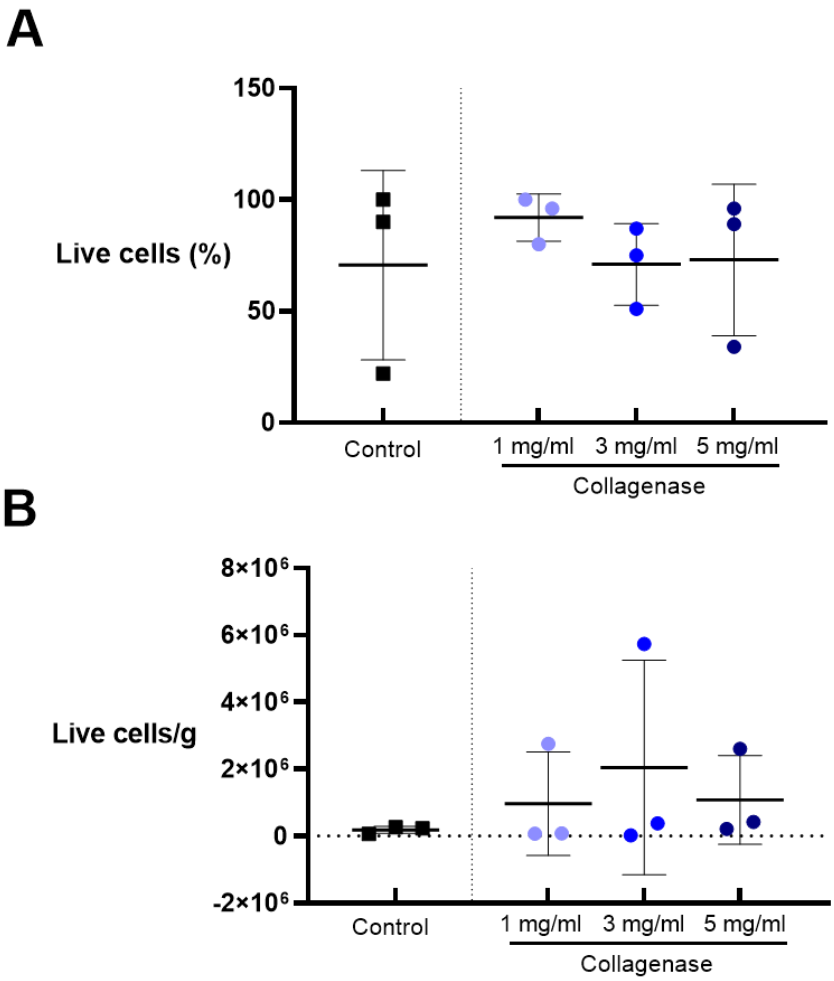



**Figure 3. 6 Analysis of cell viability after dissociation of human fresh ovarian cortical tissue using trypsin or collagenase.** Cortical tissue from a 24-year-old (patient 1), 49-year-old (patient 2), and 48-year-old (patient 3) was dissociated using control trypsin (control, black), and collagenase (blue) at 1, 3 or 5 mg/ml. Viability was expressed as a percentage (A) and number (B) of viable cells/g. Results are expressed as mean±SD. P>0.05. N=3.

Collagenase at the moderate concentration tested (3 mg/ml) was selected to dissociate fresh human ovarian cortical tissue in the next set of experiments (Figure 3. 7).

From Protocol A, it was also evident that many chunks of tissue had not been completely digested. Therefore, the next experiment also investigated implementing mechanical dissociation using a shaker.

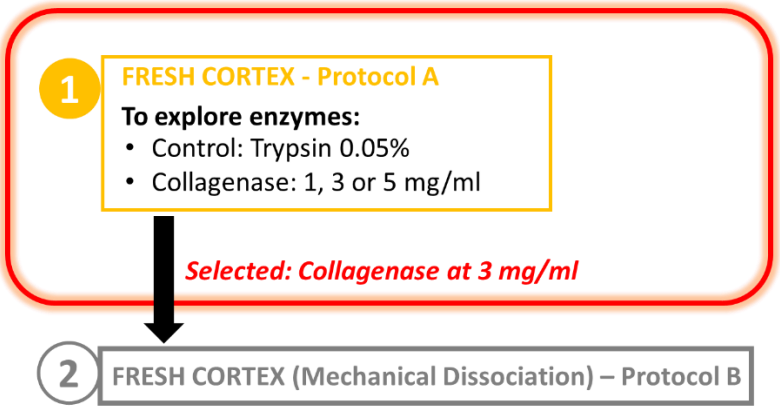



**Figure 3. 7 Overview of experimental flow – part 1**. Collagenase 3 mg/ml was used in the next investigations to explore mechanical dissociation to dissociate fresh ovarian cortical tissue.

### 3.4.3 Enzymatic digestion combined with mechanical dissociation for fresh ovarian cortex (Protocol B)

A mechanical dissociation method using a shaker, in addition to enzymes, was used to dissociate human fresh ovarian cortex from a 47-year-old patient. The effect of anti-apoptotic factors on dissociation was also tested here. In this preliminary analysis, the percentage of viable cells in a 47-year-old patient was low (30%), and anti-apoptotic factors added in the dissection media did not seem to improve viability (Figure 3. 8).

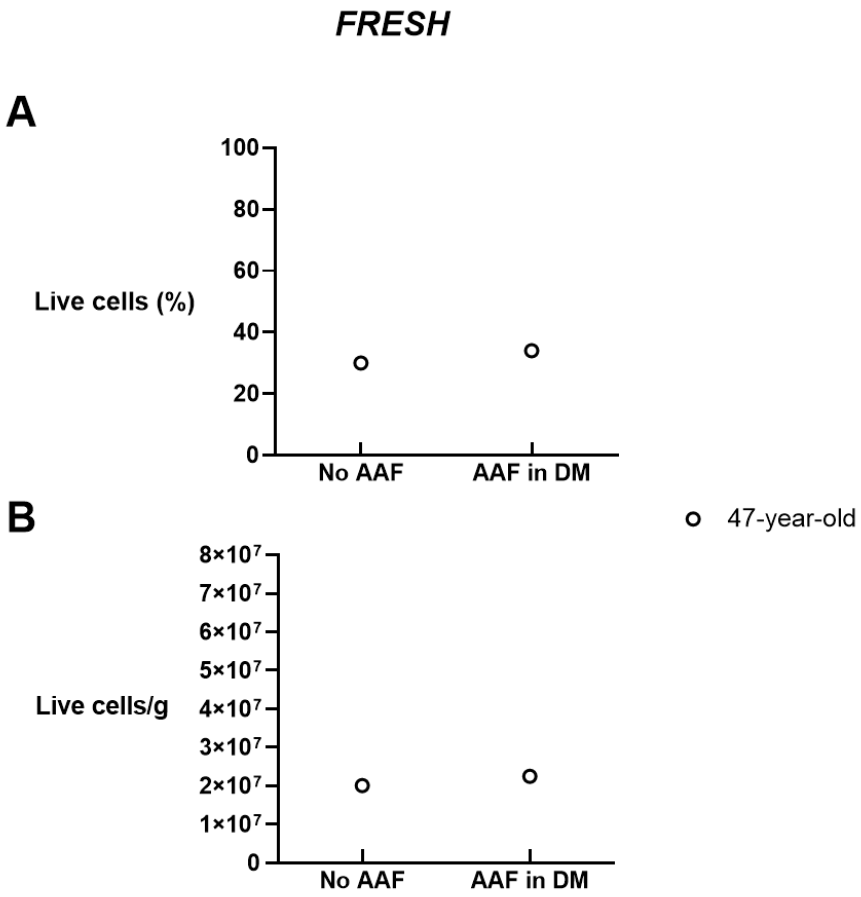



**Figure 3. 8 Analysis of the effect of anti-apoptotic factors to dissociate fresh ovarian cortex using a shaker.** Tissue obtained from a 47-year-old patient (patient 4) was dissociated using Protocol B. Results are expressed as a percentage (A) and number (B) of viable cells/g. No statistical analysis was performed. AAF: anti-apoptotic factors; DM: dissection media.

Although no improvement in cell viability was observed with the addition of anti-apoptotic factors (AAF), this experiment used samples from only one patient. Therefore, the effect of anti-apoptotic factors in the enzymatic solution and/or dissection media was further explored with samples from one more patient (a 29-year old (patient 5) in addition to the 47-year-old (patient 4), who was also included in the previous experiment (Figure 3. 8)).

As discussed in the introduction, ovarian tissue is processed for cryopreservation by the OCTB team either immediately after procurement or the next day following

procurement (O/N); here, the tissue was processed on the next day following procurement (Figure 3. 9).

Cell viability didn't seem to improve with the addition of the AAF (Figure 3. 9). Furthermore, there was large variability in the percentage and number of viable cells between the two patients (Figure 3. 9).

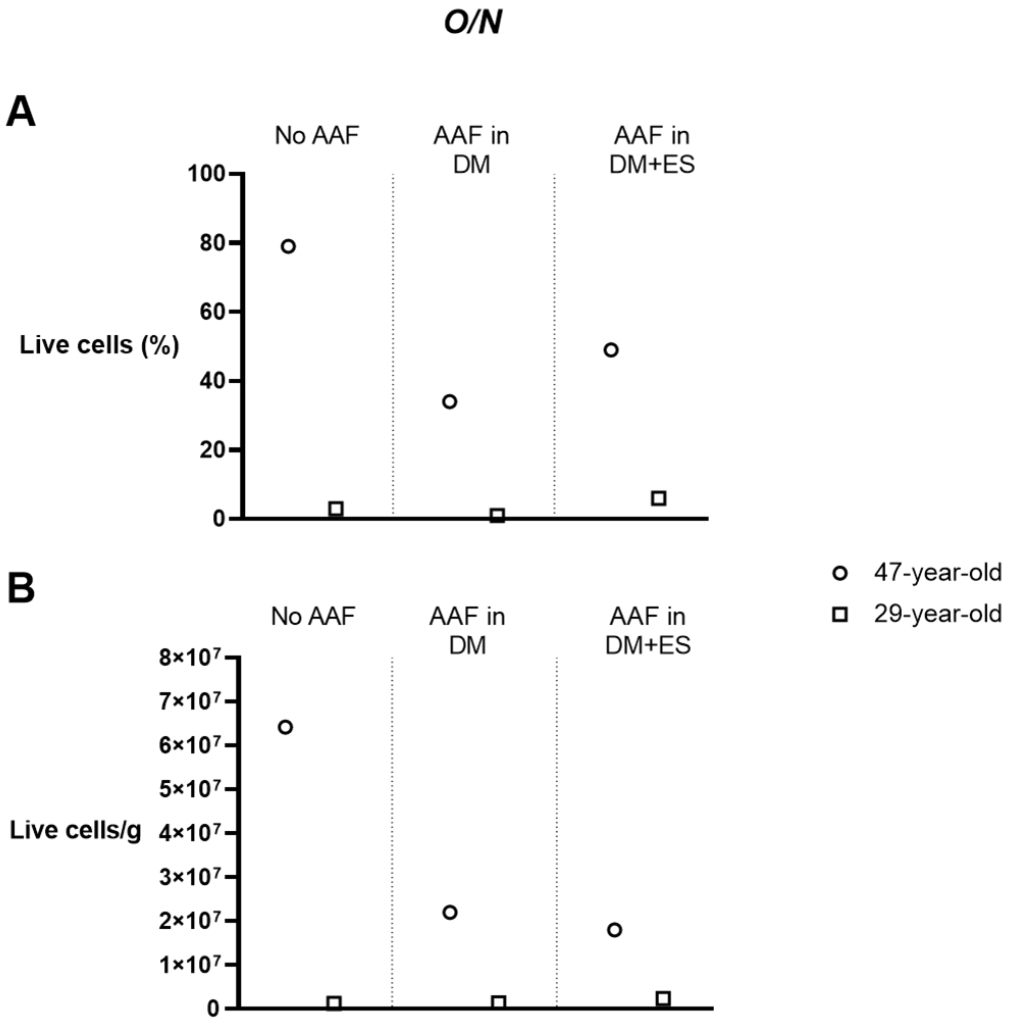



**Figure 3. 9 Analysis of the efficacy of anti-apoptotic factors (AAF) to dissociate human fresh ovarian cortex.** Tissue obtained from a 47-year-old (patient 4, blue) and a 29-year-old (patient 5, green) was dissociated using Protocol B. Anti-apoptotic factors (AAF) were added into the dissection media (AAF in DM) or in both the dissection and enzymatic solution (AAF in DM+ES). The effect of dissociation on cell viability was compared with control (No AAF). Results are expressed as a percentage (A) and number (B) of viable cells/g. No statistical analysis was performed. O/N; tissue was kept overnight at 4°C.

The above preliminary analysis showed that using human fresh ovarian cortical tissue from whole ovaries results in high heterogeneity not only between patients (Figure 3. 9) but also within the same ovary (Figure 3. 9 and Figure 3. 8). Due to the large variability in data generated from using the fresh cortical tissue, and other limitations, such as low availability and tissue 'abnormalities', an alternative source of tissue was investigated; human fresh ovarian remnants (Figure 3. 10).

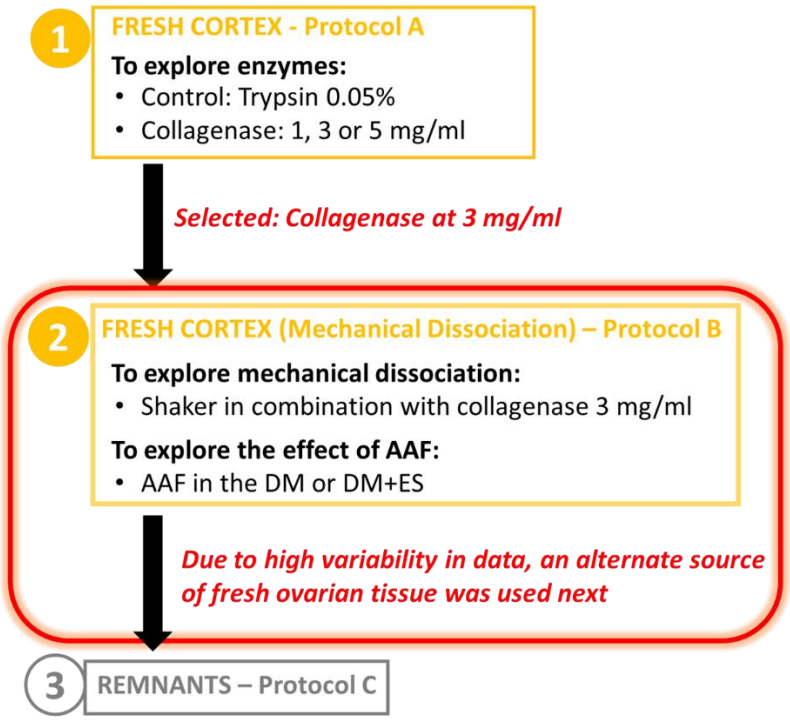



**Figure 3. 10 Overview of experimental flow – part 2.** Mechanical dissociation using a shaker was explored to investigate the dissociation of fresh human ovarian cortex and other variables. L-15; Leibovitz's L-15 medium, FBS; fetal bovine serum.

### 3.4.4 Enzymatic digestion combined with mechanical dissociation for human fresh ovarian remnant tissue (Protocol C)

To explore if mechanical dissociation (shaker) would improve enzymatic dissociation of ovarian tissue, fresh ovarian remnants from an 11-year-old and 6-year-old patient were dissociated in collagenase 3 mg/ml in L-15 (without L-glutamine) using a shaker for 40 min at 37°C.

Similar to fresh ovarian cortex, this preliminary data varied between the two patients included in this study with 87% of viable cells in the 11-year-old patient and 39% in the 6-year-old patient (Figure 3. 11A). Live-cell yield also varied considerably; ~$37x10^6$ cells and ~$5x10^6$ cells in the 11- and 6-year-old patient, respectively (Figure 3. 11B).

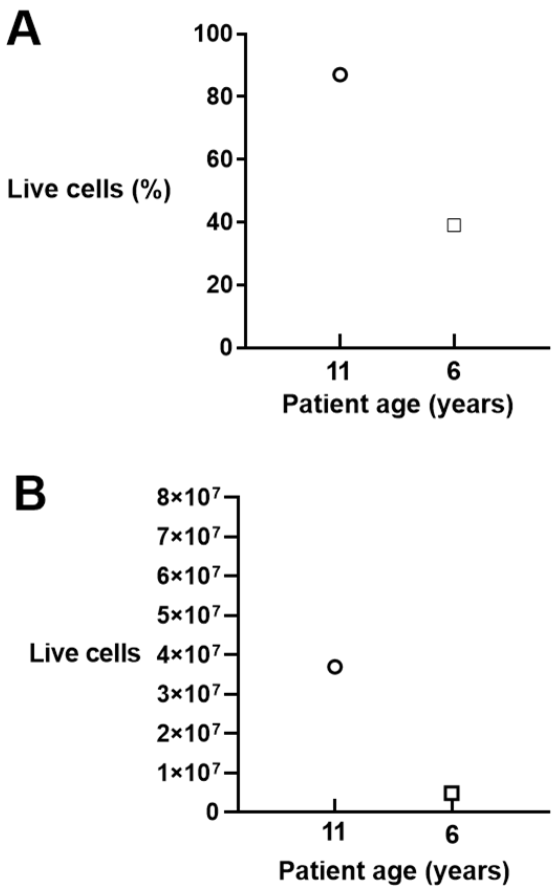



**Figure 3. 11 Cell viability after dissociation of human fresh remnant tissue using enzymatic and mechanical dissociation.** Fresh ovarian remnants obtained from an 11-year-old (patient 6, red) and a 6-year-old (patient 7, blue) was dissociated using Protocol C. Results are expressed as a percentage (A) and number (B) of viable cells per patient. No statistical analysis was performed.

Due to the high variability between the two patients included in this preliminary study and the small number of patients (n=2), which did not allow for statistical testing, we were not able to draw any conclusions. Therefore, samples from more patients were obtained to investigate the dissociation of fresh ovarian remnants (Chapter 4).

As the main aim of this study was to dissociate human frozen/thawed ovarian cortex effectively, considering that human frozen/stored ovarian samples are limited, it was

important to determine an effective dissociation method for frozen/thawed cortex before using more samples for testing (Figure 3. 12).

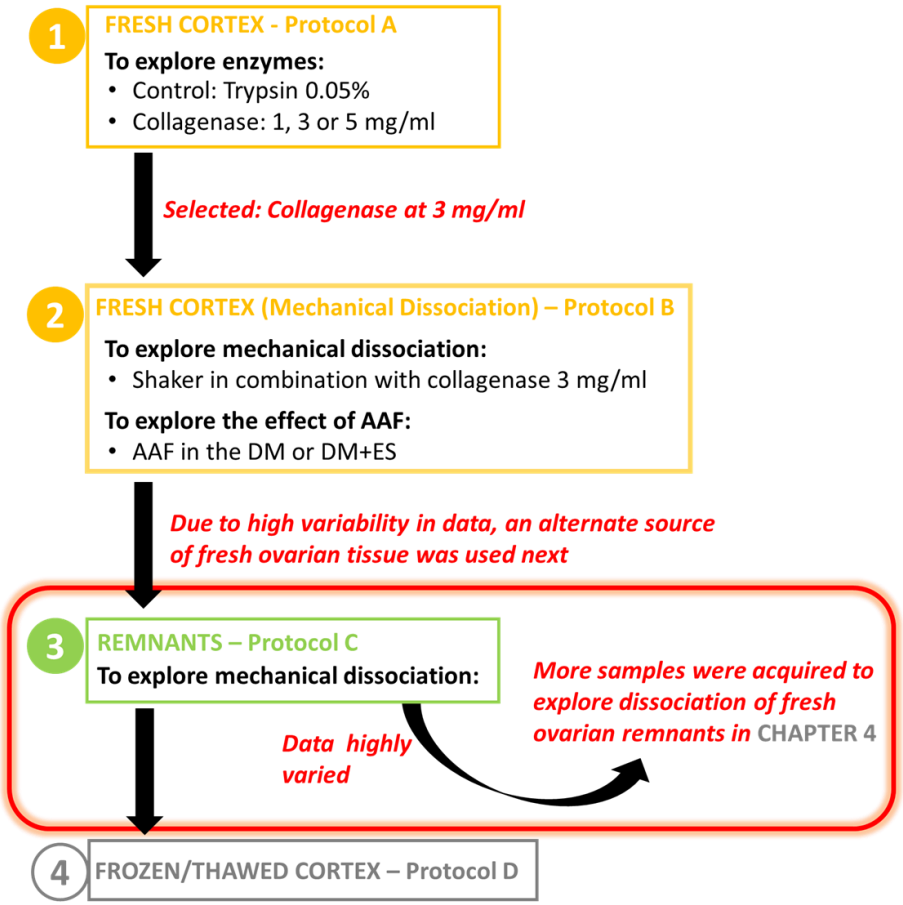



**Figure 3. 12 Overview of experimental flow – part 3.** A dissociation method used in previous experiments to dissociate human ovarian remnant tissue (Protocol C) was used to dissociate human frozen/thawed ovarian cortical tissue and compared with other methods (Protocol D). L-15; Leibovitz's L-15 medium, PBS; phosphate buffered saline, FBS; fetal bovine serum, HSA; human serum albumin.

### 3.4.5 Exploring a method to dissociate human frozen/thawed ovarian cortex

To explore the dissociation of frozen/thawed ovarian cortex, the method described above for ovarian remnant tissue was applied for frozen/thawed cortex from a 21-year-old patient. However, it seemed that using of mechanical dissociation (shaker) to aid enzymatic digestion of frozen/thawed cortex was too vigorous as only 12% of cells

isolated were viable. Therefore, using tissue obtained from a 13-year-old patient (Table 3. 8), the efficacy of shaker to dissociate frozen/thawed ovarian cortex in combination with enzymes was further explored (Dissociation method 1, Table 3. 8) and compared with another 7 dissociation methods before using more frozen/thawed ovarian cortical tissue samples.

**Table 3. 8 Dissociation methods used for frozen/thawed ovarian cortical tissue sample from a 13-year-old patient.**

| Dissociation methods | Collagenase 3 mg/ml | | Liberase 0.04 mg/ml | | Mechanical dissociation (shaker) | Dissociation time | |
|---|---|---|---|---|---|---|---|
| | L15 | PBS | L15 | PBS | | 40 min | 75 min |
| 1 | ✓ | | | | ✓ | ✓ | |
| 2 | | ✓ | | | ✓ | ✓ | |
| 3 | ✓ | | | | | | ✓ |
| 4 | | ✓ | | | | | ✓ |
| 5 | | | ✓ | | ✓ | ✓ | |
| 6 | | | | ✓ | ✓ | ✓ | |
| 7 | | | ✓ | | | | ✓ |
| 8 | | | | ✓ | | | ✓ |

Preliminary data from a 13-year-old patient showed that cell viability was higher in the liberase groups dissociated enzymatically without mechanical dissociation (75 min) compared to the collagenase groups (Figure 3. 13). In contrast, collagenase appeared more effective if combined with mechanical dissociation (40 min sh) compared with liberase (40 min sh) (Figure 3. 13). Collagenase was also more effective, compared with liberase, if combined with mechanical dissociation than without (40min sh L15 versus 75min L15, and 40min sh PBS versus 75min PBS) (Figure 3. 13).

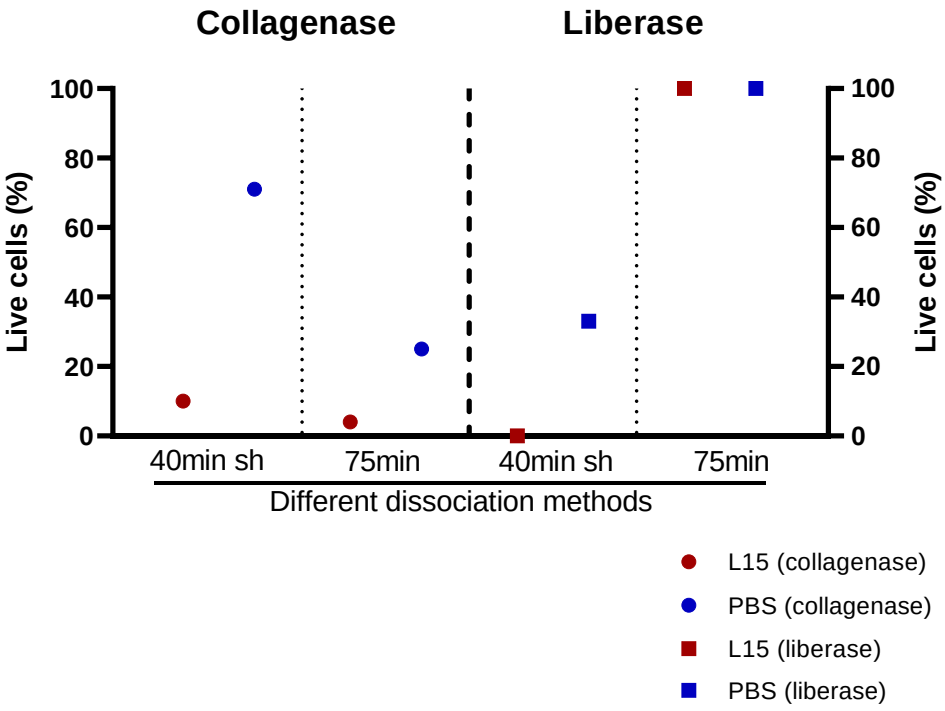



**Figure 3. 13 Comparison of the efficacy of dissociation methods using collagenase or liberase to dissociate human frozen/thawed ovarian cortex.** Tissue from a 13-year-old (patient 8) was acquired from the OCTB. Collagenase 3 mg/ml or liberase 0.04 mg/ml in Leibovitz's L-15 medium; L-15 (red), or Dulbecco's Phosphate-Buffered Saline; PBS (blue) and used to dissociate frozen/thawed cortex enzymatically for 75min (''75min'') and/or mechanically for 40 min using shaker (''40min sh''). Results are expressed as a percentage of total cells. No statistical analysis was performed.

According to preliminary results, although viability was higher in the liberase groups compared with collagenase, the total cell yield was lower in liberase (Figure 3. 14).

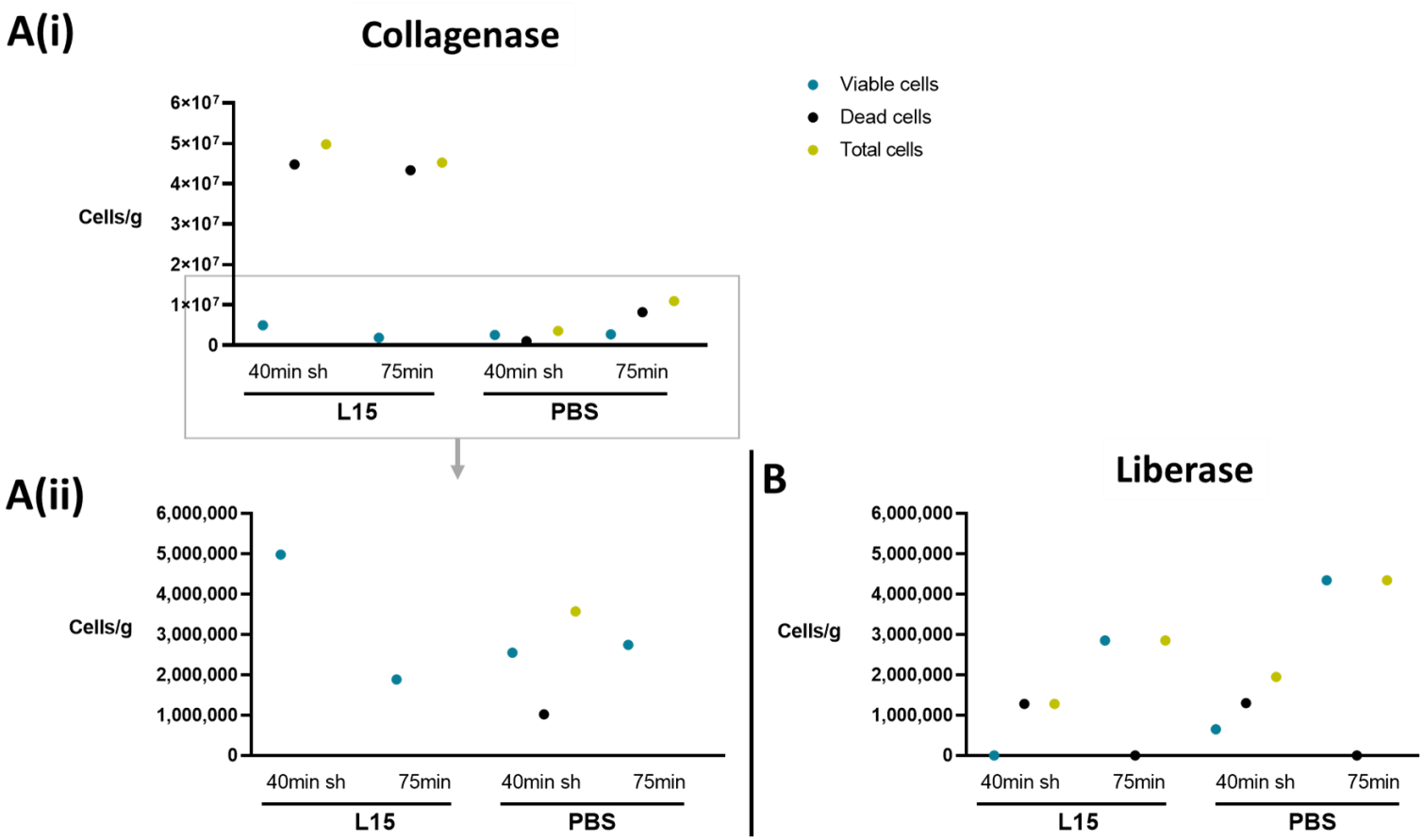



**Figure 3. 14 Cell yield using collagenase or liberase to dissociate frozen/thawed ovarian cortical tissue.** Tissue from a 13-year-old (patient 8) was acquired from the OCTB. Collagenase 3 mg/ml (A(i), A(ii)), or liberase 0.04 mg/ml (B), in L15 or PBS, was used to dissociate frozen/thawed cortex enzymatically for 75min (''75min''), or enzymatically combined with mechanical dissociation for 40 min using shaker (''40min sh''). Results are expressed as a number of viable cells/g (blue), dead cells/g (black) or total cells/g (yellow). No statistical analysis was performed. L15: Leibovitz's L-15 medium; PBS: Dulbecco's Phosphate-Buffered Saline.

Here, the ultimate objective was to determine a dissociation method that would yield the highest possible number of viable cells/g to use for downstream analysis. Based on the above preliminary observations, 2 out of 4 conditions in collagenase groups yielded a higher number of viable cells/g compared to liberase groups. Therefore, to determine an effective dissociation method, we decided to select the dissociation methods tested here that yielded the highest number of total cells/g, as the total number of cells/g seemed to be higher in all collagenase groups compared to liberase, aiming to optimise these methods in Chapter 4 in order to improve viability and live-cell yield. The selected methods were: 'collagenase L15 40min sh', 'collagenase L15 75min' and 'collagenase PBS 75min'.

Experiments on optimisation of human frozen/thawed ovarian cortex are discussed in Chapter 4 (Figure 3. 15).

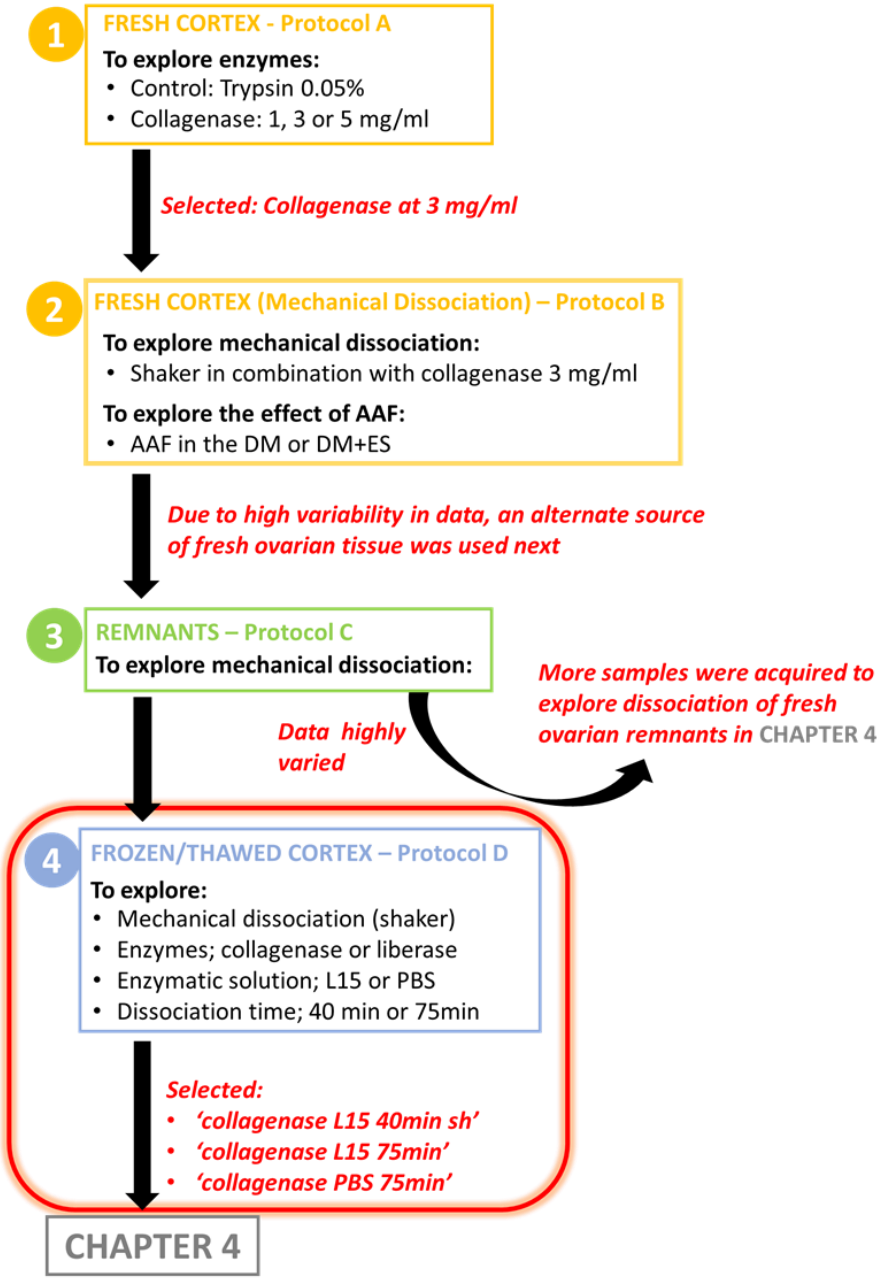



**Figure 3. 15 Overview of experimental flow – part 4.** Based on preliminary observations from exploring different methods (Protocol D) to dissociate human frozen/thawed ovarian cortex from a 13-year-old patient (patient 8), three methods were selected for subsequent studies: 'collagenase L15 40min sh', 'collagenase L15 75min' and 'collagenase PBS 75min. L-15: Leibovitz's L-15 medium; PBS: phosphate buffered saline; FBS: fetal bovine serum; HAS: human serum albumin.

## 3.5 Discussion

The aim of the preliminary investigations presented in this chapter was to explore methods to dissociate human frozen/thawed ovarian cortex into single cells. Experiments were carried out based on tissue availability and published literature.

### 3.5.1 Human fresh ovarian cortical tissue

This preliminary work began by using tissue from whole ovaries. The whole cortex of the organ was available to use which allowed testing of many variables. Using the Reaggregated Ovary (RO) dissociation method as a starting point, parameters including enzymatic solutions, mechanical dissociation to aid enzymatic digestion, use of anti-apoptotic factors in the digestion and/or dissection media were also explored using fresh cortical tissue.

The efficacy of control trypsin (routinely used in the mouse RO method) to dissociate fresh cortex, was compared with collagenase 1, 3 and 5 mg/ml. Based on this preliminary data, cell viability was similar between the two enzymes used (collagenase at all concentrations and control trypsin). Live-cell yield was not different in collagenase groups compared to control trypsin. Collagenase at the moderate concentration tested (3 mg/ml) was selected for the next experiments. What is more, the ovarian cortex was not digested completely, and therefore, to aid enzymatic dissociation, mechanical dissociation was also used in the next experiments. The early observations from this study revealed a huge variation in results. High heterogeneity between individuals should be considered as a limiting factor in similar studies (Schmidt et al. 2003). In addition, since the cortical tissue used was obtained from ovaries removed for

pathological reasons, this might indicate that the tissue was abnormal, even though the 'abnormal' part of the organ was removed. These data led us to conclude that fresh cortex obtained from whole ovaries might not be ideal for optimisation experiments studying viability. It was therefore decided to continue the preliminary work using ovarian tissue from younger patients: fresh remnants.

### 3.5.2 Human fresh ovarian remnant tissue

The ready availability of remnant tissue makes it a suitable source of tissue for exploration into the effects of dissociation on cell viability; remnants are generated from all ovarian samples that are processed for cryopreservation at the OCTB and are routinely discarded.

The use of mechanical dissociation to enhance enzymatic digestion of fresh ovarian remnant tissue was explored. Preliminary analysis showed variation in viability and live-cell yield between the two patients included. Patient-age difference appeared to have an impact on the number of cells obtained; the younger the patient, the smaller the ovary and therefore, less remnants to use, resulting in different live-cell yield between patients. What is more, the younger patient used here had undergone chemotherapy prior to ovarian tissue cryopreservation, and therefore, it is likely that viability in this sample was compromised by chemotherapy and deteriorated after tissue dissociation.

Overall, for fresh remnants, no conclusions were drawn due to large variation and the small number of patients included. Therefore, samples from more patients were acquired to investigate dissociation of fresh ovarian remnants in Chapter 4.

### 3.5.3 Human frozen/thawed ovarian cortical tissue

As the overall objective of this thesis was to further techniques for fertility preservation, and a source of tissue to restore fertility for patients is cryopreserved ovarian cortex, it was important to explore the effect of dissociation of frozen/thawed ovarian cortical tissue on cell viability.

The method developed in the previous experiments using a shaker was applied to frozen/thawed cortical tissue from a 21-year-old patient. However, viability was very low, only 12%, indicating that using shaker to dissociate frozen/thawed cortex might be too vigorous. To obtain better viability for frozen/thawed cortex, using of a shaker was compared with gentle pipetting as an alternative mechanical dissociation method. Collagenase and liberase in L-15, or PBS, were also compared.

As discussed previously, to our knowledge, there are no published methods comparing the efficacy of collagenase and liberase to isolate single cells from human ovarian tissue. Our preliminary data showed that the total-cell yield was very low in liberase groups, however, viability (%) was higher in liberase compared to collagenase groups. These data, even though obtained from one patient, were consistent with other studies where viability of follicles isolated from human ovarian cortex, though fresh tissue, using collagenase or liberase was compared (Dolmans et al. 2006). Dolmans et al. indicated that viability of human follicles isolated from fresh ovarian cortex after liberase treatment was significantly higher compared to collagenase (99% and 74%, respectively), but the number of follicles yielded was lower in liberase compared to collagenase (Dolmans et al. 2006). In another study, Schmidt et al. used liberase in L15 to isolate follicles from human fresh and frozen/thawed ovarian cortex and cell viability

was assessed with flow cytometry analysis (Schmidt et al. 2018a). They showed that the percentage of viable cells reached 91% in fresh group and 87% in frozen/thawed group (not statistically significant) (Schmidt et al. 2018a). However, Dolmans and Schmidt studied the efficacy of collagenase and liberase to isolate follicles but not dissociation of tissue into single cells, which was the aim of this chapter; however, there are no such studies to help us to assess data generated in this study.

Because the purpose of this study was to develop a method to isolate the highest possible number of viable cells, it was considered important to focus on the conditions with the highest total-cell yield aiming to optimise the dissociation methods in order to increase viability in future studies (Chapter 4). The 3 conditions identified as the most promising methods with the potential to improve live-cell yield and viability were:

1) enzymatic plus mechanical dissociation (shaker) in collagenase/L-15 for 40 min
2) enzymatic dissociation in collagenase/L-15 for 75 min
3) enzymatic dissociation in collagenase/PBS for 75 min

## 3.6 Conclusions

In this chapter, the dissociation of human ovarian tissue was explored. To develop a method to dissociate human ovarian tissue, three different types of ovarian tissue available (fresh cortex, fresh remnants, and frozen/thawed cortex) were utilised. Fresh cortical tissue, obtained from whole ovaries removed from patients for pathological reasons, made us consider that these ovaries might not be the ideal tissue to explore the effect of different dissociation methods on cell viability. However, because the whole cortex of the organ was available, it was possible to explore many variables before using fresh remnants and frozen/stored cortical tissue. Fresh remnant tissue was

obtained from younger patients who stored ovarian cortex for fertility preservation. Due to the small number of patients (n=2) and high variability, no conclusions were drawn regarding fresh remnant dissociation before obtaining samples from more patients to investigate dissociation of fresh ovarian remnants (Chapter 4). Regarding frozen/thawed cortex dissociation, early data were not promising as viability was low and therefore, more methods were explored to study dissociation of frozen/thawed cortex. From the preliminary data in this chapter, three frozen/thawed cortex dissociation methods were identified for further exploration presented in Chapter 4.

# CHAPTER 4

# *Dissociation of human fresh ovarian remnants and human frozen/thawed ovarian cortex*

## 4.1 Introduction

### 4.1.1 Overview

Since there is limited information regarding dissociation protocols for human ovarian tissue, completion of a series of preliminary experiments (Chapter 3) investigating the dissociation of human fresh and frozen/thawed ovarian cortex, as well as human fresh ovarian remnants was essential. Observations in Chapter 3, though preliminary, helped determine the most promising dissociation methods to test here with obtaining more patient samples. The present chapter extends the findings of Chapter 3 and focuses on the establishment of a dissociation method for human fresh ovarian remnant tissue and optimisation/establishment of a method to dissociate human frozen/thawed ovarian cortical tissue.

### 4.1.2 Ovarian age

Ovarian structure changes with age. In young girls the cortex is populated by follicles which, with age, are largely replaced by collagen fibres due to ovulation and follicle atresia (Faddy 2000). Briley et al. found that there was a correlation between the amount of collagen in mouse ovaries and age (Briley et al. 2016). Furthermore, Manuel et al. demonstrated collagen concentration changes in the human ovarian cortex with age (Manuel et al. 2019). They showed that collagen fibres gradually increased from onset of puberty until fibrosis occurred in patients over 51 years. Therefore, an age-induced increase in collagen deposition in the ovarian cortex may affect the dissociation of human ovarian cortical tissue.

## 4.2 Aims

This study addresses the optimisation of methods to dissociate human fresh ovarian remnant tissue and human frozen/thawed ovarian cortical tissue. The aims of this chapter were to:

- To test the dissociation method used previously to dissociate human fresh ovarian remnant tissue using more samples.
- Optimise and establish an effective method to dissociate human frozen/thawed ovarian cortical tissue.
- Investigate the effect of age on dissociation of human frozen/thawed ovarian cortical tissue.

## 4.3 Materials & Methods

### 4.3.1. Ovarian tissue source and exclusion criteria

Fresh ovarian remnants and frozen ovarian cortical tissue were acquired from the OCTB, as described (Chapter 2). Donors older than 35 years of age and/or with ovarian diseases and/or having undergone chemotherapy (or radiotherapy) treatment prior to ovarian tissue cryopreservation were excluded from this study.

### 4.3.2. Human fresh ovarian remnant tissue

#### 4.3.2.1. Process of ovarian remnants and cell debris prior to tissue dissociation

Ovarian remnants were comprised of tissue and cell debris collected in the dissection media when processed by the OCTB; Leibovitz l-15; L-15 medium (L5520; Sigma) at 4°C. To isolate chunks of tissue, remnants were filtered through a 100 µm strainer. The tissue remaining on the strainer was dissected into pieces ≤ 1mm$^3$ in L-15 medium (L5520; Sigma) at 4°C using sterile blades and micro scissors to dissociate (see below), and the cells that passed through the strainer were centrifuged for 5 min at 650 x g. Single cells were resuspended in L-15 (L5520; Sigma) supplemented with 0.3% Human Serum Albumin (HSA; A1653; Sigma-Aldrich) at 4°C.

#### 4.3.2.2. Dissociation of ovarian remnant tissues

Dissected remnant tissues were dissociated in an enzymatic solution; collagenase I 3 mg/ml (C0130; Sigma-Aldrich) dissolved in L-15 with 0.078 mg/ml DNase I (DN25; Sigma-Aldrich) for 40min at 37°C using a shaker at 200 rpm. To aid dissociation, the tube

(430053; Scientific Laboratory Supplies) containing the digestion mixture was taken out of the shaker and shaken by hand for a few seconds every 15 min.

The enzymatic reaction was inhibited by adding L-15/0.3% HSA into the digestion mixture, centrifuged for 5 min at 650 x g, washed with L-15/0.3% HSA, and filtered through a 100 µm strainer to remove any undigested tissue. The single cell suspension was centrifuged for 5 min at 650 x g to pellet cells. Cell viability was assessed as described (Chapter 2).

## 4.3.3. Human frozen/thawed ovarian cortical tissue

### 4.3.3.1. Dissection of frozen/thawed ovarian cortical tissue

Frozen/thawed ovarian cortical strips were thawed as described (Chapter 2) and cut into pieces ≤ 1mm$^3$ in L-15 (L5520; Sigma) on ice blocks (~4°C) using sterile micro-scissors and blades.

### 4.3.3.2. Dissociation of frozen/thawed ovarian cortical tissue

To dissociate chopped frozen/thawed ovarian cortex, 3 methods were used as developed and described in Chapter 3 (Table 4. 1).

**Table 4. 1 The three methods used to dissociate human frozen/thawed ovarian cortical tissue: Shaker L15, L15 and PBS.** Collagenase I was used at 3 mg/ml. DNase I was used at 0.078 mg/ml. L-15 Leibovitz's medium (L5520; Sigma); PBS: Dulbecco's PBS (D8662; Sigma).

| Dissociation methods as named in Chapter 3 | Dissociation methods in Chapter 4 | Enzymes | Media in enzymatic solutions | Digestion time | Digestion environment |
|---|---|---|---|---|---|
| 'Collagenase L15 40min sh' | 'Shaker L15' | Collagenase I Dnase I | Leibovitz's L-15 | 40 min | 37°C shaker |
| 'Collagenase L15 75min' | 'L15' | | | 60 min | 37°C |
| 'Collagenase PBS 75min' | 'PBS' | | Dulbecco's PBS | | |

Collagenase I was used at 3 mg/ml with 0.078 mg/ml of DNase I (DN25; Sigma) dissolved in L-15 (L5520; Sigma). Tissue was digested for 40 min (Shaker L15) or 60 min (L15 and PBS) at 37°C; 60 min was selected for L15 and PBS as a moderate digestion time tested previously for dissociation methods used (Chapter 3). To aid enzymatic dissociation, tissue was mixed by gentle pipetting (L15 and PBS) every 15 min. For Shaker L15, the tube containing the digestion mixture was taken out of the shaker and shaken by hand for a few seconds. To minimise cell exposure to enzymes and thus, improve live-cell yield, single cells isolated from the digested tissue were collected from the dissociation mixture every 15 min for L15 and PBS method, but not Shaker L15. The same volume was replaced with enzymatic solution for the remainder of the digestion time. Isolated cells were centrifuged for 5 min at 650 x g, the supernatant was discarded, and the cell pellet was resuspended in 1 ml of media (L15 or PBS supplemented with 0.3% (v/v) HSA) lacking enzymes and kept on ice.

At the end of the digestion period, the enzymatic reaction was inhibited by adding an equal volume of media; L-15 (for 'Shaker L15' and 'L15') or PBS (for 'PBS') supplemented

with 0.3% HSA. The dissociated mixture was centrifuged for 5 min at 650 x g, washed with media (L-15 or PBS) supplemented with 0.3% HSA, and filtered through a 100 µm strainer to remove any undigested tissue. The single cell suspension was centrifuged for 5 min at 650 x g to pellet cells. Cell viability was assessed as described (Chapter 2).

### 4.3.4. Cell numbers

The number of viable cells isolated from frozen/thawed ovarian cortex was calculated per gram of tissue as described (Chapter 3). Since the remnant tissue obtained was dissected into pieces of dissimilar sizes (Chapter 3Figure 3. 3) and could not be weighed accurately under sterile conditions, the number of cells isolated per gram of tissue from remnants was not calculated.

### 4.3.5. Exploring the efficacy of different dissociation methods in younger and older patients

Patients aged 13-33 years were categorised into age groups. To determine how to divide them, I used the median split approach. The median of age was calculated using GraphPad Prism version 8.2.1 (GraphPad Software, La Jolla, California, USA) and patients were categorised into the Younger group (<median) and Older group (>median). Additionally, an analytical method to determine ovarian biological age differences was developed in this thesis (Appendix I). In this analytical study, the difference in live-cell yield between different dissociation methods (Shaker L15, L15 and PBS) used per patient was calculated and expressed as percentage (%). Results were interpreted as high (≥50%) or low variation (<50%) (Appendix I).

### 4.3.6. Exploring the effect of age on the dissociation of frozen/thawed ovarian cortex

The effect of dissociation (L15 method) on cell viability and live-cell yield was analysed across different age groups: pre-pubertal versus post-pubertal versus adult group. Pre-pubertal (n=4) and post-pubertal (n=4) frozen/thawed cortical tissue samples were dissociated using L15, as described (Section 4.3.3). These data were combined with the data obtained previously (Section 4.3.5), and analysed post-hoc. More specifically, data obtained from post-pubertal samples (n=5), which were analysed in Section 4.3.5 namely 'L15 Younger group', was combined with data obtained from the 4 additional post-pubertal frozen/thawed cortical tissue samples (n=4), which were introduced here, and analysed as the post-pubertal group (n=9). The percentage and number of viable cells/g were compared across the pre-pubertal (n=4) versus post-pubertal (n=9) versus Older (adult) group; the Older group, which was previously analysed in Section 4.3.5 namely 'L15 Older group', was also included in this post-hoc analysis.

It should be highlighted that the data obtained from the post-pubertal patients (L15 Younger group and additional post-pubertal samples) were acquired from 2 experiments. Therefore, even though the same methodology was used in both experiments, we considered it wise to test for data distribution and statistical differences before combining these data.

### 4.3.7. Statistical analysis

GraphPad Prism version 8.2.1 (GraphPad Software, La Jolla, California, USA) was used to perform statistical analysis. Data was tested for normality using Shapiro-Wilk test. Results are presented as mean±standard deviation, with $P \leq 0.05$ considered significant.

*Remnant tissue groups*

For remnant tissue samples, the percentage of viable cells was compared between pre- and post-pubertal patients using unpaired t-test with Welch's correction (data was normally distributed).

*Frozen/thawed cortical tissue groups*

For frozen/thawed ovarian cortical tissue samples, the total number of cells/g, the number of live cells/g, and the percentage of live cells were compared across the three dissociation methods used: Shaker L15 versus L15 versus PBS. Data was matched and analysed using One-Way ANOVA and Tukey's multiple comparisons test (if data was normally distributed), or One-Way ANOVA Friedman test with Dunn's multiple comparisons tests (if data wasn't normally distributed).

*Post-hoc analysis*

An unpaired t-test with Welch's correction (data was normally distributed) was used to compare the percentage and number of live cells/g isolated from the frozen/thawed ovarian cortex using L15 in the 2 sub-groups of post-pubertal samples before combining these data. In this analysis, the number and percentage of live cells/g isolated from frozen/thawed cortical tissue samples using L15 were compared across the three age groups (pre-pubertal versus post-pubertal versus Older group). Here, data was analysed using Brown-Forsythe and Welch's One-Way ANOVA (data was normally distributed and not matched).

## 4.4 Results

### 4.4.1. Patient age and characteristics

Human fresh ovarian remnant tissue was obtained from 6 patients (3 pre-pubertal and 3 post-pubertal) (Table 4. 2).

**Table 4. 2 Patients who donated human fresh ovarian remnant tissue for research.**

| FRESH OVARIAN REMNANT TISSUE | | | | |
|---|---|---|---|---|
| **Patient no.** | **Age** | **Pubertal status** | **Condition** | **Chemotherapy treatment** |
| Patient 9 | 2 | Pre-pubertal | Wilms tumour | No |
| Patient 10 | 3 | Pre-pubertal | GATA deficiency | No |
| Patient 11 | 12 | Pre-pubertal | Immunodeficiency | No |
| Patient 12 | 15 | Post-pubertal | Ewing's Sarcoma | No |
| Patient 13 | 18 | Post-pubertal | Sickle Cell Disease | No |
| Patient 14 | 18 | Post-pubertal | Osteosarcoma | No |

Frozen/stored ovarian cortical tissue was obtained from 18 patients (Table 4. 3). Tissue obtained from patients 15-24 (pink/orange) was used to optimise and establish a method to dissociate frozen/thawed ovarian cortex. Data acquired using tissue obtained from patients 15-24, was combined with data obtained from dissociation of tissue obtained from patients 25-32 in a post-hoc analysis, to investigate the effect of age on the dissociation of frozen/thawed ovarian cortex.

**Table 4. 3 Patients who donated frozen/stored ovarian cortical tissue for research.**

| FROZEN/THAWED OVARIAN CORTICAL TISSUE | | | | |
|---|---|---|---|---|
| **Patient no.** | **Age** | **Pubertal status** | **Condition** | **Chemotherapy treatment** |
| Patient 15 | 13 | Post-pubertal | Ewing's Sarcoma | No |
| Patient 16 | 13 | Post-pubertal | Ewing's Sarcoma | No |
| Patient 17 | 14 | Post-pubertal | Osteosarcoma | No |
| Patient 18 | 15 | Post-pubertal | Ewing's Sarcoma | No |
| Patient 19 | 15 | Post-pubertal | Ewing's Sarcoma | No |
| Patient 20 | 18 | Post-pubertal | Stage IV Neuroblastoma | No |
| Patient 21 | 22 | Post-pubertal | Atypical teratoid rhabdoid tumor | No |
| Patient 22 | 28 | Post-pubertal | Hodgkins Disease | No |
| Patient 23 | 29 | Post-pubertal | Glioblastoma multiforme | No |
| Patient 24 | 33 | Post-pubertal | Ewing's Sarcoma | No |
| Patient 25 | 5 | Pre-pubertal | Beta Thalassaemia | No |
| Patient 26 | 5 | Pre-pubertal | Embryonal rhabdomyosarcoma | No |
| Patient 27 | 8 | Pre-pubertal | Beta Thalassaemia | No |
| Patient 28 | 8 | Pre-pubertal | Adenosine Deaminase 2 Deficiency (ADA2) | No |
| Patient 29 | 13 | Post-pubertal | Ewings Sarcoma | No |
| Patient 30 | 13 | Post-pubertal | Ewings Sarcoma R Ilium | No |
| Patient 31 | 15 | Post-pubertal | Ewings Sarcoma | No |
| Patient 32 | 15 | Post-pubertal | Sickle Cell Disease | No |

### 4.4.2. Cell viability was maintained after dissociation of human fresh ovarian remnants

To establish a dissociation method for human fresh ovarian remnants, tissue from 3 pre-pubertal and 3 post-pubertal patients was used. A mean total of $6.2x10^7 \pm 7.6 \times 10^6$ viable cells was collected (n=6). The proportion of viable cells exceeded 75% in both pre-pubertal and post-pubertal patients and there was no difference (p=0.0973) between the two groups (Figure 4. 1).

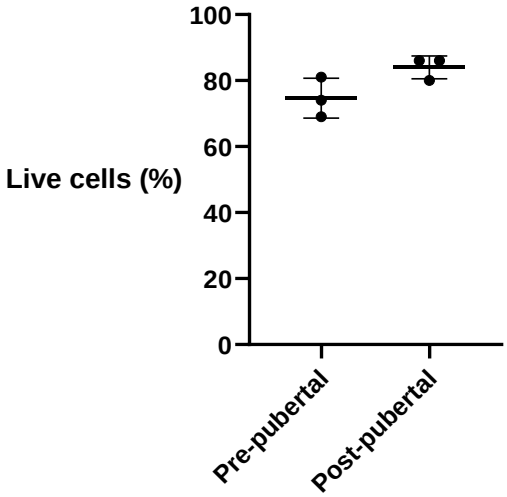



**Figure 4. 1 Cell viability after dissociation of human fresh ovarian remnant tissue.** Tissue from pre-pubertal (n=3) and post-pubertal (n=3) patients aged 2-18 years (n=6) was dissociated into a single cell suspension using collagenase I/L15 and mechanical shaking for 40 min at 37°C. Cell viability was expressed as a percentage of total cells. There was no significant difference between groups ($p>0.05$). Results are expressed as mean±SD.

There was an increase in the number of viable cells obtained in the post-pubertal group compared to pre-pubertal group ($1.15x10^8 \pm 0.8x10^8$ cells versus $9x10^6 \pm 7x10^6$ cells), but this difference was not significant ($p=0.1$).

This analysis showed that dissociation of human fresh ovarian remnant tissue using enzymatic (collagenase 3 mg/ml) and mechanical dissociation (shaker) at 37°C for 40 min maintains a high cell viability for both pre- and post-pubertal samples.

### 4.4.3. Comparison of three methods to dissociate human frozen/thawed ovarian cortex: 'Shaker L15', 'L15' and 'PBS'

To determine an effective method to dissociate human frozen/thawed ovarian cortex, three methods ('Shaker L15'; 'Sh.L15', 'L15' and 'PBS') were compared for tissue obtained from 10 patients; 5 post-pubertal (13-15 years) and 5 adult (18-33 years). At the end of the dissociation procedure, it was evident that some of the larger pieces of tissue, despite being visibly reduced in size, were not completely dissociated. However, all three methods produced a population of single cells that were analysed.

The total cell yield observed in PBS was lower compared to Sh.L15 (p=0.0417), and L15 (p=0.0110) (Figure 4. 2). There was no difference in the total number of cells yielded between Sh.L15 and L15 (Figure 4. 2).

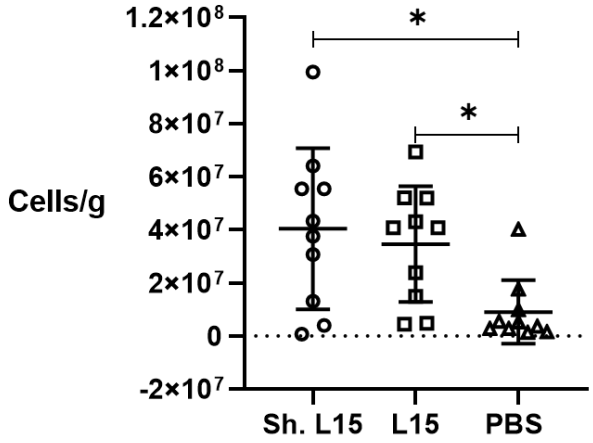



**Figure 4. 2 Total cell yield in different methods used to dissociate human frozen/thawed ovarian cortex.** Tissue from patients aged 13-33 years (patients 15-24, n=10) was dissociated using Shaker L15; Sh.L15, L15 or PBS and total cell yield per gram of tissue was analysed. Results are expressed as mean±SD. *P≤0.05

Analysis of live-cell yield in the three dissociation methods showed that viability ranged from 19%±21% (Sh.L15) to 52%±17% (PBS). The percentage of viable cells observed in Sh.L15 was significantly lower compared with PBS (p=0.0052) (Figure 4. 3A). No other significant differences were observed between groups. The number of viable cells isolated per gram of tissue showed no difference between groups (Figure 4. 3B). Analysis of the number of dead cells isolated per gram of tissue showed that viability was compromised in Sh.L15 compared to PBS since the number of dead cells was significantly higher in Sh.L15 (p=0.0219) (Figure 4. 3B), as also showed by analysis of cell viability (Figure 4. 3A).

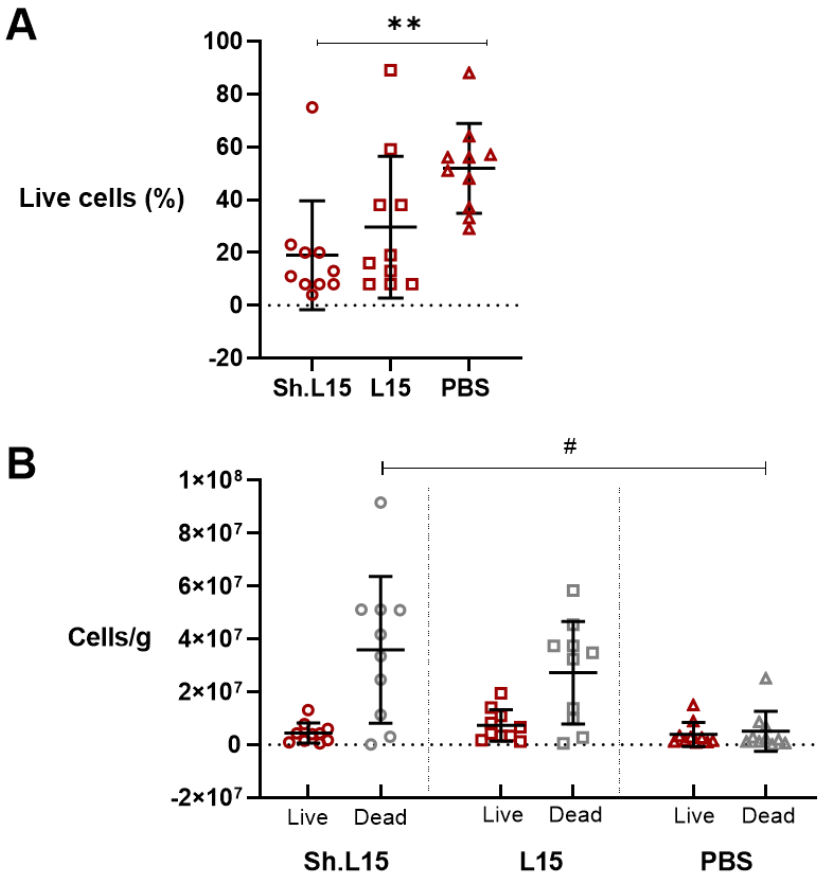



**Figure 4. 3 Comparison of cell viability from three methods used to dissociate human frozen/thawed ovarian cortex.** Tissue from patients aged 13-33 years (patients 15-24, n=10) was dissociated using Shaker L15; Sh.L15, L15 or PBS. Cell viability was expressed as a percentage (A) of total cells, number of viable (red) and dead (grey) cells per gram of tissue (B). Results are expressed as mean±SD. **P≤0.01 for live cells, #P≤0.05 for dead cells. L: live cells/g; D: dead cells/g.

### 4.4.4. Comparing the efficacy of 'Sh.L15', 'L15', and 'PBS' to dissociate human frozen/thawed ovarian cortex from younger and older patients

To explore the effect of dissociation on cell viability and live-cell yield, tissue from ten patients aged 13 (2x), 14, 15 (2x), 18, 22, 28, 29 and 33 years was used in this study. To determine age groups, the median of these ages was calculated; 16.5 years was the median of ages used in this study. Patients younger than 16.5 years were put into the Younger group and patients older than 16.5 years were included into the Older group. Additionally, an analytical method used to explore age differences based on the variation in live-cell yield per patient, showed that per cent variation was similar in patients aged 18-33 years (≤50%), reflecting the Older group (Appendix I).

Total cell-yield and cell viability in the Younger and Older group was analysed to determine the most effective dissociation method for each group. The Younger group included patients aged 13-15 years (n=5), and the Older group included patients aged 18-33 years (n=5).

Analysis of the total number of cells/g showed that, in the Younger group, the total number of isolated cells was significantly higher in L15 ($p=0.0390$) compared to PBS (Figure 4. 4). No differences were found in the Older group (Figure 4. 4).




**Figure 4. 4 Total cell yield from frozen/thawed ovarian cortex in Younger and Older patients.** Frozen/thawed ovarian cortex from patients aged 13-15 years (Younger group, patients 15-19, n=5) and 18-33 years (Older group, patients 20-24, n=5) was dissociated using Shaker L15, L15 and PBS. The number of total cells isolated per gram of tissue was calculated. Results are expressed as mean±SD. *P≤0.05

Analysis of cell viability in the Younger and Older groups revealed that PBS was more effective, compared to Shaker L15, for Older patients as the percentage of viable cells in PBS (48%±13%) was significantly higher (p=0.0427) compared to Shaker L15 (13%±8%) (Figure 4. 5A). In the Younger group, no significant difference was observed between Shaker L15, L15 and PBS (Figure 4. 5A). Moreover, the number of isolated viable cells/g was higher in L15 ($9.9x10^6±6.8x10^6$ cells/g, p=0.0342) compared to PBS ($1.8x10^6±0.9x10^6$ cells/g) in the Younger group (Figure 4. 5B), but no difference was found in the Older group (Figure 4. 5B).

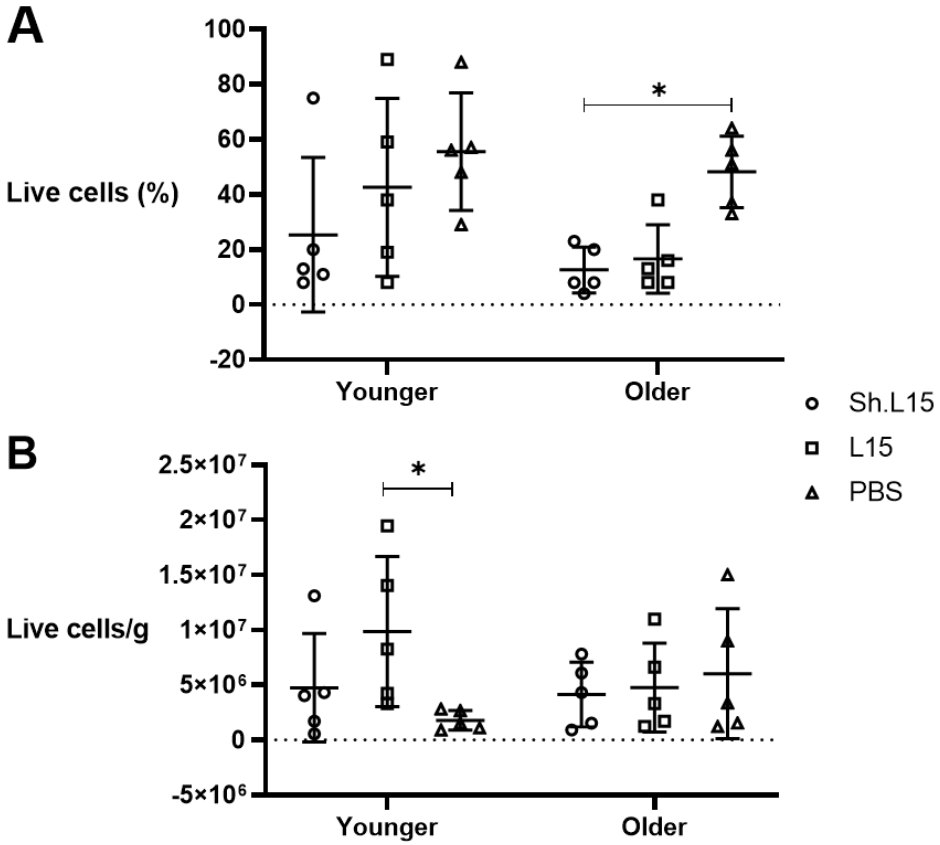



**Figure 4. 5 Cell viability in the Younger and Older groups after dissociation of frozen/thawed ovarian cortex.** Tissue from patients aged 13-15 years (Younger group, patients 15-19, n=5) and 18-33 years (Older group, patients 20-24, n=5) was dissociated using Shaker L15, L15 and PBS. Viability was expressed as a percentage (A) and number (B) of viable cells per gram of tissue. Results are expressed as mean±SD. *P≤0.05.

Overall, L15 showed higher efficacy as a method to isolate viable cells from frozen/thawed ovarian cortical tissue from patients aged <18 years compared to PBS, but there was no difference in the efficacy of Shaker L15 versus L15, or Shaker L15 versus PBS; no difference was found in the efficacy of the three dissociation methods in older patients (≥18 years). Despite the lack of evidence suggesting that Shaker L15 was too vigorous compared to L15 in any of the groups tested here, to minimise cell death, we decided not use mechanical dissociation in further investigations; therefore, L15 was

determined as an effective method to dissociate human frozen/thawed ovarian cortical tissue into single viable cells in our study.

### 4.4.5. The efficacy of dissociation across different ages

To explore the effect of age on the dissociation of frozen/thawed ovarian cortex, samples were obtained from pre-pubertal (aged 5-8, n=4) and post-pubertal (aged 13-15, n=4) patients. Statistical analysis showed no difference in the percentage (p=0.3162) or number (p=0.3118) of live cells/g isolated between the 2 sub-groups of post-pubertal patients, thus allowing for further analysis. Data from the post-pubertal group (n=4) was combined with data from the L15 Younger group (Figure 4. 4 page 130 and Figure 4. 5 page 131) forming the post-pubertal group (n=9). The percentage and number of live cells/g isolated using L15 from the frozen/thawed cortical tissue samples were compared across the pre-pubertal, post-pubertal and Older group (Figure 4. 6).

Cell viability was compromised in the Older group compared to the post-pubertal group; the percentage of viable cells isolated in the Older group was significantly lower (p=0.0178) compared to the post-pubertal group (17%±12% and 50%±25%, respectively) (Figure 4. 6A). No difference was found in cell viability between the pre-pubertal and post-pubertal group, or between the pre-pubertal and Older group (p=0.0961) (Figure 4. 6A). What is more, the efficacy of dissociation was affected by age as the number of live cells/g isolated in the post-pubertal group was significantly higher (p=0.0425) compared to pre-pubertal group ($8.3x10^6±5.3x10^6$ and $2.9x10^6±0.8x10^6$ cells/g, respectively) (Figure 4. 6B), but no difference was found between the Older and pre- or post-pubertal group (Figure 4. 6B).

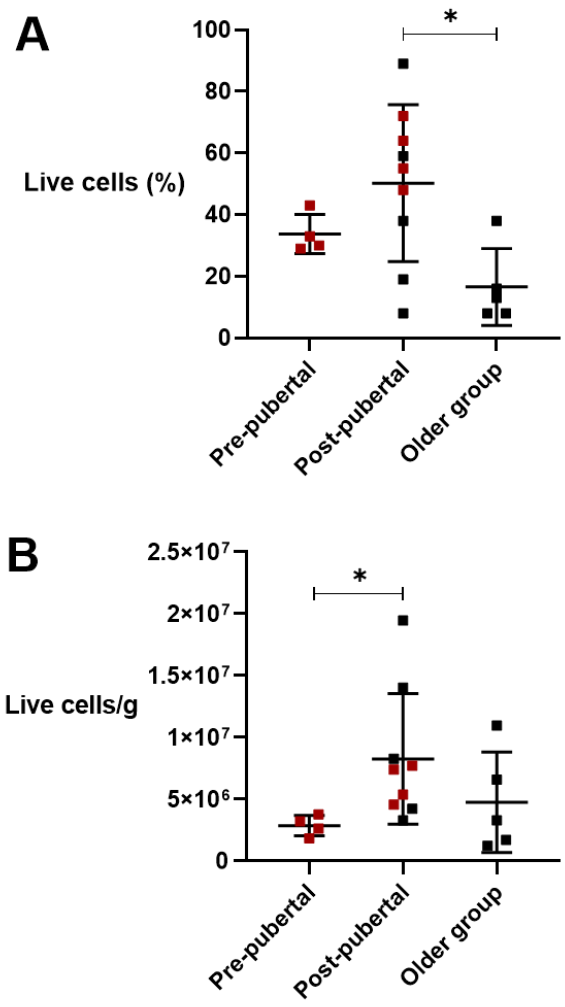



**Figure 4. 6 Cell viability in pre-pubertal, post-pubertal and adult patients after dissociation of frozen/thawed cortex using L15 method.** Frozen/thawed ovarian cortical tissue from pre-pubertal patients aged 5-8 years (patients 25-28, n=4, red), post-pubertal patients aged 13-15 years (n=9: L15 Younger post-pubertal samples, patients 15-19, n=5, black; post-pubertal samples, patients 29-32, n=4, red), and Older group (patients aged 18-33 years, patients 20-24, n=5, black) was dissociated using L15. Cell viability was expressed as a percentage (A) and number of viable cells per gram of tissue (B). Results are expressed as mean±SD. *P≤0.05.

Nevertheless, it was possible to isolate viable cells from both fresh ovarian remnant tissue (Figure 4. 1 page 126) and frozen/thawed ovarian tissue (Figure 4. 6 page 133) obtained from both pre- and post-pubertal samples, enabling downstream analysis.

## 4.5 Discussion

### 4.5.1. Overview

One of the objectives in this chapter was to obtain high numbers of viable cells after dissociation of human fresh ovarian remnant tissue and human frozen/thawed ovarian cortical tissue. Fresh ovarian remnants are available every time ovarian cortical tissue is processed for cryopreservation. Hence, this type of tissue was an invaluable source of ovarian tissue as fresh ovarian remnant samples were used in a series of experiments before using the limited cryopreserved ovarian cortical tissue.

While a protocol for dissociation of fresh ovarian remnant tissue with a high yield of viable cells was established, remnant tissue is not an ideal cell source for developing methods that could potentially be used for fertility preservation. Thus, informed by findings from investigation into the dissociation of human fresh ovarian remnant tissue, optimisation of a method to dissociate human frozen/thawed ovarian cortex was carried out; L15 was determined as an effective method to dissociate human frozen/thawed ovarian cortex as a significantly higher number of viable cells/g was isolated, and cell viability was not compromised in patients aged <18 years using L15 compared to PBS; cell viability and live-cell yield was not compromised using L15 in adult patients either.

### 4.5.2. Factors that may affect dissociation of human frozen/thawed ovarian cortex

*Cryoprotectants and thawing solutions*

Ovarian tissue cryopreservation is the only current option for pre-pubertal patients to preserve fertility and its success regarding primordial follicle maintenance is well

established (Kim et al. 2018). However, little attention has been given to optimise cryopreservation and thawing methods to improve stromal health as opposed to primordial follicle health. The effect of cryopreservation on the ovarian stroma is of great importance too, especially in cases where the cryopreserved tissue is transplanted back to the patient to restore fertility. It has been shown that cryoprotectants and thawing solutions used in slow freezing cryopreservation and tissue thawing procedures can have a deleterious effect on stromal health (Perdrix et al. 2010; Marsella et al. 2008; Faustino et al. 2010; Oskam et al. 2010). This is a very important note, since the stromal cell population comprises a large proportion of the total ovarian cell populations that can be isolated from the ovary.

It is likely that cryopreservation and thawing affected the ovarian cells, and thus, enzymatic dissociation caused additional damage, deteriorating cell viability in this study.

*Collagen increase due to freezing*

Cryopreservation-induced fibrosis may have affected dissociation of frozen/thawed cortex. It has been reported that slow freezing significantly increases the proportion of collagen deposition in cryopreserved-xenografted human ovarian cortex compared to fresh cortical tissue (Gallardo et al. 2018). Therefore, it is possible that the efficacy of dissociation of frozen/thawed tissue was compromised in our study due to the presence of fibrotic areas that were rich in collagen, formed due to freezing, and thus dissociation of the tissue into a viable single cell suspension was not as effective.

*Donors medical condition*

Two of the 4 pre-pubertal patients included in this study had been diagnosed with β-thalassemia. B-thalassemia is a hereditary disease where ineffective production and replacement of hematopoietic cells into the body is due to increased nitric-oxide-mediated apoptosis caused by accumulated unmatched alpha-haemoglobins (Kheansaard et al. 2011). What is more, regular blood transfusions are necessary for some patients in order to avoid anaemia (Roussou et al. 2013). However, frequent blood transfusions result in accumulated iron in many organs, including the ovary, causing high oxidative stress (Roussou et al. 2013; Kheansaard et al. 2011). It is possible that the unmatched toxic alpha-haemoglobins reaching the ovarian tissue induced apoptosis in the ovarian cells. Thus, ovarian tissue in these patients might be more susceptible to cell death stimuli; this may explain the reduced number of live cells/g in the pre-pubertal group compared to post-pubertal frozen/thawed ovarian cortex (Figure 4. 6).

### 4.5.3. The effect of age on the dissociation of human frozen/thawed ovarian cortical tissue

Alterations in the synthesis and structure of the mouse (MacDonald et al. 2019) and human ovary (Heeren et al. 2015) regarding ECM proteins (e.g. collagens) have been reported during foetal development and adolescence. However, studies have focused on changes in the ovarian ECM occurring in early stages of human ovarian development and menopause whereas there is limited information with regard to the components of the ovarian ECM from early childhood until early twenties. In fact, at the time of writing, there had been only one study exploring this scientific question namely Manuel et al. (Manuel et al. 2019). To our knowledge, our study is the first to examine the efficacy of

different dissociation methods to isolate viable single cells from frozen/thawed ovarian cortex, and the effect of age on the dissociation of frozen/thawed ovarian cortex.

Different results were observed between the Younger and Older group of patients regarding viability and total-cell yield. The L15 method was more effective for the Younger group, compared to PBS, as a significantly higher number of cells (total- and live-cell yield) were isolated, while cell viability was not affected; in the Older group, no difference was found in live-cell yield across the three dissociation methods, but cell viability was compromised in Shaker L15 compared to PBS. Additionally, we conducted a post-hoc analysis to test the effect of age on dissociation using 2 additional samples (pre- and post-pubertal). We found that age affected cell viability as the percentage of viable cells/g was compromised in the Older group compared to post-pubertal. Also, age affected the efficacy of dissociation as a lower number of viable cells/g was isolated in the pre-pubertal group compared to post-pubertal.

Briley et al. found a correlation between collagen increasing in the ovary and reproductive age leading to fibrosis in two mouse models (Briley et al. 2016). Manuel et al. investigated the changes in the amount of collagen in the ovaries of 60 individuals from 1.8-58 years of age and demonstrated that structural changes occur in the human ovary (Manuel et al. 2019). Such changes might reflect the functionality of the ovary according to reproductive age and pubertal status of the individual. It was shown that collagen was reduced between the patients aged 1.8-10 years and 11-20 years, suggesting that a decrease in collagen at this age might be related to the onset of puberty (Manuel et al. 2019). Moreover, collagen was increased in patients aged over

51 years compared to those aged 11-20 years, an observation probably reflecting age-induced fibrosis (Zhou et al. 2017). This provides evidence that the ECM in human ovarian cortical tissue goes through key changes that are likely to affect the dissociation of the human ovarian cortex. Collagen deposition during aging as demonstrated in Manuel et al. (Manuel et al. 2019) might affect the dissociation of the cortex.

Increased collagen between patients aged 1.8-10 years and 11-20 years (Manuel et al. 2019) might have prevented effective dissociation of ECM in the cortical tissue in our study, where a lower number of live cells/g were isolated in the pre-pubertal group (aged 5-8 years) compared to post-pubertal (aged 13-15 years). What is more, the efficacy of the three methods used was equivalent in the Older group, and live-cell yield/g was not affected by age in the Older group. Manuel et al. demonstrated increased collagen deposition in patients over 51 years (Manuel et al. 2019), which is likely to affect the efficacy of dissociation. However, in our study, patients were ≤51 years; hence why live-cell yield was not affected by age, or dissociation method, in the Older group in our study. However, compromised cell viability in the Older group, compared to post-pubertal, indicated that older tissue might be more susceptible to enzymatic-dissociation-induced cell death compared to post-pubertal tissue according to our post-hoc analysis.

Due to alterations in the composition of the ECM in the ovary (Briley et al. 2016), including fluctuations in the concentration of collagen during lifespan, the use of more enzymes may be helpful. This mixture should contain collagenases and other enzymes based on the ovarian ECM components, and this may need to be altered with age.

Collagen IV is well characterised in the human ovary (Lind et al. 2006; Yamada et al. 1999; Heeren et al. 2015), but the most abundant type of collagen in the human ovarian cortex is Collagen VI (Ouni et al. 2019). Collagenase products are a mixture of enzymes (mainly collagenases, tryptic-like enzymes, and neutral proteases). There are several products commercially available that differ in the ratio of enzymes they contain. I used collagenase type I to dissociate fresh ovarian remnant and human frozen/thawed ovarian cortical tissue, which is characterised by a normal balanced ratio of enzymatic activity and targets a range of collagens including collagen IV and VI. Future studies could investigate other collagenase products to determine their effect on the age-related synthesis of the ECM in the human ovarian cortex and whether these result in a higher live-cell yield.

### 4.5.4. Conclusions

In this chapter, methods to dissociate human fresh ovarian remnant tissue and human frozen/thawed ovarian cortical tissue were established. Additionally, it was revealed that age affects the efficacy of dissociation of human frozen/thawed ovarian cortex. This study suggests that changes occurring in the synthesis of the human ovarian cortex with age could affect ovarian tissue dissociation and therefore, the age of the patient should be considered when developing ovarian tissue dissociation methods.

# CHAPTER 5

# *Developing a method to detect human germ cells using flow cytometry*

## 5.1. Introduction

The overall objective of present thesis was to develop a method to restore follicle development for patients with premature ovarian insufficiency (POI), and follicle dysfunction (idiopathic) using the Reaggregated Ovary (RO) technique (Chapter 2). The RO method is established in our laboratory using mouse ovaries and we have demonstrated this both *in vitro* and *in vivo* (Lo et al. 2019). Adapting the RO method for human ovarian samples required significant experimental development as outlined in Chapter 3 and Chapter 4.

In the RO method, isolation of germ cells is achieved using enzymatic dissociation of mouse ovaries into a single cell suspension and subsequent cell culture to allow for differential separation via somatic cell only adhesion (Chapter 2). Investigation into

dissociation of human ovarian tissues was explored and discussed in Chapters 3 and 4 with new methods established to obtain viable cells from fresh human ovarian remnants or frozen/thawed human ovarian cortical tissue. Prior to developing a method to isolate the germ cell population for generation of a human RO it is important to analyse the human ovarian single cell suspension obtained after dissociation. What is more, preliminary experiments on human ovarian single cell culture revealed that human cells did not behave as mouse ovarian cells as they did not adhere sufficiently (data not shown). To this end, flow cytometry (FC) was selected as a useful tool to investigate the cells obtained after ovarian dissociation.

FC can facilitate cell phenotyping by using multiple cell markers which could enable us to identify ovarian cell populations isolated from human fresh ovarian remnant tissue and human frozen/thawed ovarian cortex after tissue dissociation. What is more, this method enables us to identify single viable cells, which is a prerequisite to making a functional RO. Furthermore, a specialised type of FC, Fluorescence-Activated Cell Sorting (FACS), enables isolation of viable cell populations for downstream analysis. Using FACS, cells are sorted and separated into different populations based on fluorescent labelling (Adan et al. 2017).

Therefore, the main aim was to develop a FC method to detect human germ cells obtained from frozen/thawed ovarian cortex after tissue dissociation.

### 5.1.1. Basic principles of flow cytometry

FC is a state-of-the-art technique widely used in the field of biology including, but not limited to molecular biology, immunology, and cancer biology. FC is a laser-based tool

that allows for complex analysis of cell populations by measuring single cell features (Mckinnon 2018). Cell features analysed by FC can be cell size and granularity or specific markers (cell surface or intracellular) identified with immunolabelling (Mckinnon 2018).

#### 5.1.1.1. Flow cytometer instrument components

A flow cytometer is comprised of a fluidics system, an optical system and an electronic/data processing system (Mckinnon 2018; Adan et al. 2017)(Figure 5. 1).

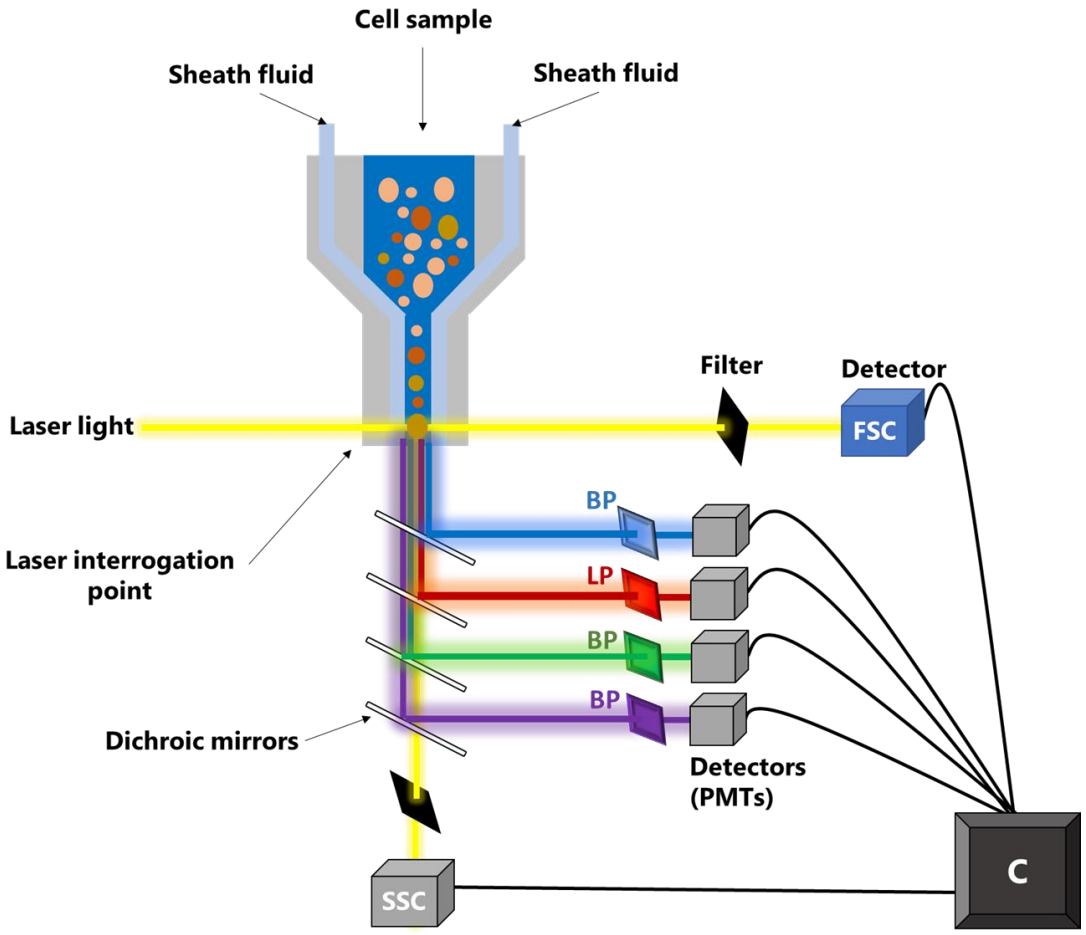



**Figure 5. 1 Components of a flow cytometer.** The fluidics, optical and processing system. Single cells pass through the laser light at the interrogation point where the light scattered from the cells is detected in a forward direction (FSC) and in a 90° direction (SSC). Fluorescence detectors measure the fluorescence emitted from the labelled cells as they go through the laser beam. Using dichroic mirrors at a 90° direction, the light is directed into long pass (LP) and band pass (BP) filters which capture a range of a specific wavelengths. Different channels are used for fluorochromes emitting different wavelengths of light. Wavelength of light is analysed by the electronic system and data interpreted into information regarding cell features using specialised software. FSC: Forward Scatter; SSC Side Scatter; BP: bandpass; LP: longpass; C: Computer.

*The fluidics system*

FC requires a single cell suspension which can be obtained from solid tissue (human ovarian tissue was used in this study) after enzymatic and mechanical dissociation. The single cell sample and a diluent (sheath fluid) is channelled into the instrument (Figure 5. 1). The sheath fluid pressure is lower than the sample pressure and thus, due to this pressure difference, the sample becomes the central core of the flow. This phenomenon, known as hydrodynamic focusing, accounts for a single file flow through the instrument allowing for single cell analysis (Adan et al. 2017), which is crucial to acquire robust data on cell populations; cell aggregates can produce inaccurate results regarding cell size, granularity or fluorescence, leading to false conclusions.

*The optical system*

Excitation optics (lasers) and collection optics (dichroic mirrors and filters) are used to acquire data on cell size, granularity and fluorescence (Figure 5. 1). Single cells are exposed to light (generated by a laser beam) at the interrogation point (Figure 5. 1). Cells that autofluoresce or are bound to fluorescent antibodies emit fluorescence after being exposed to light (discussed below). This light is captured by photodetectors as light scattering and fluorescence. Light scattering is captured by photodetectors in a forward direction (Forward Scatter or FSC) which can indicate information about cell size, and in a $90^{o}$ direction (Side Scatter or SSC) which can reveal information about cell granularity (Mckinnon 2018; Reggeti et al. 2011).

*Signal detection and processing*

The light signal generated by single cells is converted into an electrical current by photomultiplier tubes (PMTs). The electrical current is then converted into a voltage

pulse (analog signal) and amplified by a logarithmic and a linear amplifier. This analog signal is converted into a digital signal by an analog-to-digital converter and further processed using a computer and specialised software (Adan et al. 2017) (Figure 5. 1).

#### 5.1.1.2. Fluorochromes and fluorescence principles in flow cytometry

Fluorescent molecules (e.g. R-phycoerythrin; RPE) are used in FC to label cell surface or intracellular proteins (e.g. DDX4) covalently, as well as for the detection of nucleic acids or reporter molecules. Different types of fluorescent compounds absorb light energy at a range of specific wavelengths (i.e. for RPE the absorption wavelength ranges from 488 to 561nm with a maxima at 496nm). The absorption wavelength is also known as excitation wavelength. When light is absorbed by the fluorescent compound, an electron is excited and rises from the ground energy state to a higher state (excited state). The excited electron returns to its ground state and the excess energy is emitted as a photon of light at a range of a specific wavelength within the visible electromagnetic spectrum (emission wavelength or spectrum); the excitation spectrum is always larger than the emission spectrum (Adan et al. 2017). The range of the emission wavelength varies between different fluorochromes. The change in energy from the excited state to the ground state, known as fluorescence, is detected by photodetectors as light signal and is perceived by detectors as a positive signal compared to a negative background (Adan et al. 2017).

#### 5.1.1.3. Monoclonal antibodies in flow cytometry

In FC, antibodies are used to detect cell-specific proteins to investigate cell features. Monoclonal antibodies (mAbs) are preferentially used over polyclonal antibodies (pAbs)

(Nelson et al. 2000). A monoclonal antibody can bind to a single epitope whereas polyclonal antibodies are a pool of different immunoglobulins (e.g. immunoglobulin IgG1) and can bind to different epitopes of a protein (Nelson et al. 2000). Therefore, use of mAbs allows for applying the correct isotype controls. Moreover, mAbs have higher specificity and affinity as they recognise a single epitope on a protein (Nelson et al. 2000). pAbs, on the other hand, recognise multiple epitopes on the same protein and there can be variation from batch-to-batch (Nelson et al. 2000). Antibodies can be unconjugated or conjugated to a fluorophore of interest. Unconjugated antibodies can be used in conjunction with a fluorescently labelled secondary antibody and this is typically referred to as indirect staining.

#### 5.1.1.4. Viability assessment by flow cytometry

In FC, viability can be measured using fluorescent viability dyes which permeate dead cells due to compromised membranes and are hence excluded from live cells (Mckinnon 2018; Zhang et al. 2017). These dyes emit fluorescence when excited at a specific wavelength and therefore, live/dead cell discrimination can be performed by exclusion of dyes. Viability dyes are molecules that can bind either to DNA in the nucleus of a dead cell or to amine groups in the cytoplasm of dead cells (e.g. Zombie Aqua™) (Mckinnon 2018). Amine-binding viability dyes can produce background fluorescence as amine groups can also be found on the surface of an intact membrane. However, the signal generated by a dead cell would be stronger compared to a live cell allowing for live/dead cell discrimination. What is more, amine-binding viability dyes are fixable whereas DNA-binding dyes are not, and therefore, should be used if downstream analysis is required (Mckinnon 2018).

#### 5.1.1.5. Flow cytometry analysis

In FC analysis, data are recorded as events and typically displayed using histograms or two parameter plots. In this study, two parameter density dot plots were used. A density plot displays the distribution of events in a given cell population, and the colours illustrate cell frequency; the highest density is shown in red and lowest density in darker blue (Figure 5. 2).

Analysis is performed by first selecting the cells of interest displayed as events on a two-parameter density dot plot. This process is known as gating and is carried out by drawing a region (gate) around the cells of interest (Mckinnon 2018; Adan et al. 2017) (Figure 5. 2). Gating enables the user to identify a main cell population, detect specific characteristics of cell populations such as expression of specific markers, exclude dead cells and identify doublets or debris (Figure 5. 2). Debris is fragmented remains of dead cells, cell membranes or tissue and are displayed on the bottom left on a two parameter density plot using forward scatter area (FSC-A) on the x-axis and side scatter area (SSC-A) on the y-axis (Figure 5. 2). It is crucial to exclude debris from the analysis as antibodies can bind non-specifically to cell debris, resulting in high background or false positives. A drawn gate for a given cell population can be applied to another cell population allowing for the investigation of multiple parameters in complex data analysis.

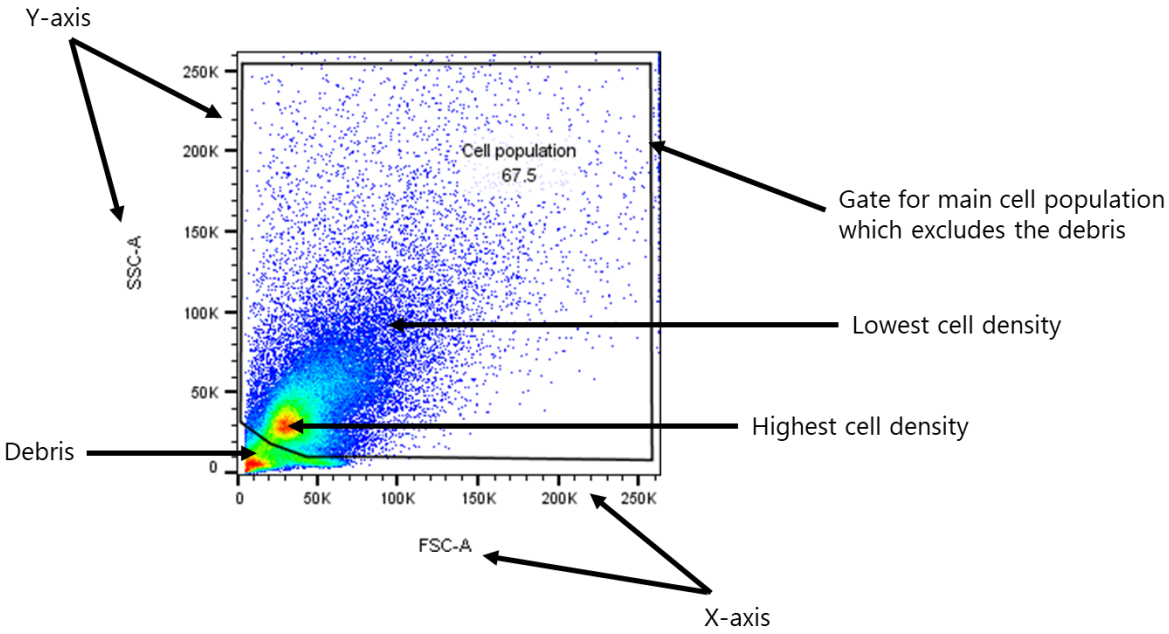



**Figure 5. 2 Representative figure of a FC two parameter density plot.** Two parameter side scatter (SSC-A) versus forward scatter (FSC-A) dot plot whereby each cell is represented as a dot. The main cell population is indicated within a drawn region (gate). Events excluded from the main cell population are displayed at the bottom left of the scatter plot and represent debris. The highest cell density is displayed in red while the lowest in blue. FSC-A: forward scatter area; SSC-A: side scatter area.

### 5.1.2. DEAD-box helicase 4 germ line regulator

DEAD-box family proteins are ATP-dependent helicases, highly conserved between species and involved in regulation processes for the translation of a large number of mRNAs (Linder and Jankowsky 2011). DEAD-box helicase 4 (DDX4), also known as VASA (as commonly used for mouse DDX4), has been identified in many species including *Drosophila melanogaster, Caenorhabditis Elegans, Xenopus*, sea urchin, spider, zebrafish, mouse, rat, chicken and human (Lasko 2013).

DDX4 is characterised as a germline specific protein and is implicated in the maintenance of germ cell cysts and oocyte differentiation (Styhler et al. 1998). Studies exploring the effect of DDX4 mutants in many species have provided information on the

implication of DDX4 in germ cell development and fertility. In *Drosophila melanogaster*, VASA is required for the completion of oogenesis and further germ cell development (Styhler et al. 1998). VASA is expressed in both male and female drosophila, however only female VASA-mutated embryos lack primordial germ cells (and are sterile), whereas male VASA-mutants are fertile (Schupbach et al. 1989; Gustafson et al.2010). In contrast, female VASA-mutant mice are fertile and their ovaries look histologically similar to wild type mice, whereas males have atrophied testes, germ cell depletion and are infertile (Tanaka et al. 2000). In humans, low levels of DDX4 expression is associated with idiopathic azoospermia or severe oligozoospermia (Sugimoto et al. 2009), but little is known about the effect of DDX4 mutations in the ovary or testes, and to our knowledge, there are no studies exploring DDX4 mutations in human ovaries/testes.

#### 5.1.2.1. DDX4 localisation

It is well established that DDX4 can be found in the cytoplasm of oocytes and is involved in gametogenesis (Castrillon et al. 2000; White et al. 2012; Lasko 2013; Zarate-Garcia et al. 2016; R. A. Anderson et al. 2007; Stimpfel et al. 2013). In the human ovary, DDX4 is initially expressed in foetal primordial germ cells (PGCs) (Anderson et al. 2007). Expression continues through childhood and puberty to adulthood (Anderson et al. 2007), and it is found in both the non-growing (primordial follicles) and growing oocyte (from transitional to antral follicle stage) (Castrillon et al. 2000). VASA was first identified *in Drosophila* (Schupbach et al. 1989; Tanaka et al. 2000), and since then researchers have been using DDX4 as a cytoplasmic germ cell marker.

#### 5.1.2.1.1. Studies supporting the hypothesis that DDX4 can be a transmembrane protein

Recently, evidence supporting the existence of oogonial stem cells (OSCs) in the human adult ovary suggested that DDX4 can function as a transmembrane protein whereby the N-terminus is intracellular and the C-terminus extracellular, which is internalised in primordial follicles (White et al. 2012; Stimpfel et al. 2013; Silvestris et al. 2018; Clarkson et al. 2018) (Figure 5. 3).

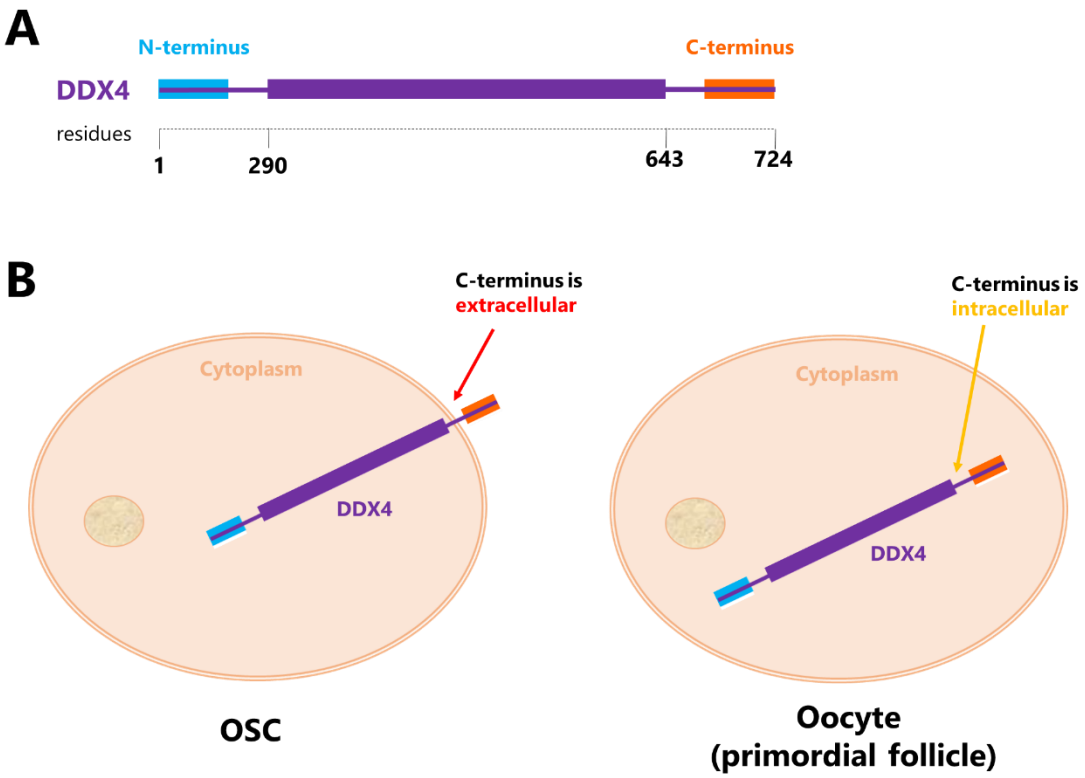



**Figure 5. 3 DDX4 protein in putative OSCs and the oocyte.** (A) DDX4 protein is comprised of 724 residues including the N-terminus and C-terminus (Zarate-Garcia et al. 2016). (B) In putative OSCs, DDX4 is considered to function as a transmembrane protein with the C-terminus bound to the cell surface and N-terminus cytoplasmic, whereas in the oocyte both the N- and C-terminus are intracellular. OSC: oogonial stem cell.

Scientists have sorted putative OSCs from adult human ovarian cortex by first dissociating the tissue into a single cell suspension and then detecting the C-terminus of

DDX4 in non-permeabilised cells using a polyclonal antibody (ab13840; Abcam) and FACS (White et al. 2012; Clarkson et al. 2018) or immunomagnetic cell-sorting (Silvestris et al. 2018). Isolated putative OSCs had a diameter of about 8 µm, and when aggregated with human foetal somatic cells they formed follicle-like structures after 10 days *in vitro* (Clarkson et al. 2018). In these follicle-like structures, DDX4 was detected in the cytoplasm of the oocyte-like structure indicating that some germ cell characteristics may have developed from putative OSCs *in vitro* (Clarkson et al. 2018).

White et al. isolated viable mouse and adult human ovarian DDX4-positive putative OSCs using the same polyclonal antibody (ab13840; Abcam) and FACS. They showed the putative OSCs could be maintained *in vitro* and generate oocyte-like cells as determined by morphology, gene expression and haploid (1n) status (White et al. 2012). Furthermore, the FACS-isolated mouse DDX4-positive cells were engineered to express GFP using retroviral transduction and were transplanted into ovaries of adult female mice. In these ovaries follicles developed containing GFP-positive oocytes along with host follicles containing GFP-negative oocytes (White et al. 2012). GFP-expressing oocytes developed into mature follicles, were fertilised *in vitro* and successfully produced embryos, demonstrating that isolation of oocytes that can develop into mature and fertilisable eggs is achievable (White et al. 2012). In the same study, human FACS-isolated DDX4-positive putative OSCs were transduced with a GFP expressing vector and either injected into adult human ovarian cortex which was xenografted into mice or reaggregated with dispersed adult human ovarian cortical tissue and cultured *in vitro* (White et al. 2012). Immature follicle-like structures and small aggregates with GFP-positive oocytes and GFP-negative surrounding cells were observed in xenografts

and reaggregated tissue, respectively (White et al. 2012). Immunofluorescence-based detection for GFP and YBX2 (a diplotene-stage oocyte-specific marker) or LHX8 (an oocyte-specific transcription factor) revealed many GFP-YBX2 and GFP-LHX8 double-positive cells in the xenografts that were injected with GFP-expressing human putative OSCs isolated with FACS (White et al. 2012).

Silvestris et al. isolated DDX4-positive viable cells from ovarian cortical tissue using the same polyclonal anti-DDX4 antibody (ab13840) obtained from non-menopausal and menopausal women using immunomagnetic cell sorting supporting the existence of extracellular DDX4 (Silvestris et al. 2018). Positive and negative sorted cells were then cultured separately *in vitro* and after 21 days, oocyte-like structures of 80 to 90 µm in diameter and smaller immature cells were observed in the DDX4-positive cell culture (Silvestris et al. 2018). Analysis revealed that two advanced-stage oocyte differentiation markers (GDF-9 and SYCP3) were expressed only in large mature oocyte-like structures and not in small immature OSCs (Silvestris et al. 2018). Also, chromosomal analyses showed that large mature oocyte-like cells had only one X chromosome (Silvestris et al. 2018).

#### 5.1.2.1.2. Debate over the specificity of an antibody commonly used to detect extracellular DDX4

Studies using the extracellular C-terminus of the DDX4 protein to isolate viable ovarian cells, as described above, support the idea that viable putative OSCs isolated from mice or humans have the potential to grow into mature oocytes (White et al. 2012; Stimpfel et al. 2013; Silvestris et al. 2018; Clarkson et al. 2018). Not all researchers agree with these findings and there is debate as to whether the DDX4 protein is purely cytoplasmic

at all stages of follicle development and therefore, isolation methods using a C-terminus anti-DDX4 antibody do not produce a pure ovarian OSCs population. Whilst some researchers do not necessarily reject the existence of OSCs in the adult human ovary (Hashimoto et al. 2008; Kim et al. 2014) they question the specificity of the ab13840 polyclonal antibody to recognise an epitope in the C-terminus region of DDX4 in putative OSCs.

Zarate-Garcia et al. used the polyclonal anti-DDX4 C-terminus-binding antibody (ab13840) and FACS to demonstrate DDX4 positive labelling in non-permeabilised ovarian cells. They also showed positive DDX4 labelling in permeabilised epithelial cells from oviductal tissue sections (Zarate-Garcia et al. 2016). However, using RT-PCR, no DDX4 mRNA was detected in either the sorted DDX4-positive non-permeabilised cells or in permeabilised oviductal cells therefore raising significant doubt over the specificity of the ab13840 DDX4 antibody (Zarate-Garcia et al. 2016). In addition, Zarate-Garcia et al. also used an alternative antibody (produced by ProteinTech,) that recognises a longer epitope in the C-terminus region of the DDX4 protein. The alternative C-terminus-binding antibody was used on permeabilised putative OSCs previously isolated using the ab13840 C-terminus-binding antibody with FACS, and permeabilised epithelial cells from oviductal tissue sections alongside permeabilised ovarian tissue sections (Zarate-Garcia et al. 2016). Intracellular DDX4 was not observed in either permeabilised putative OSCs previously isolated using the ab13840 C-terminus-binding antibody or permeabilised epithelial oviductal cells, whereas oocytes in mouse adult ovarian tissue were positive (Zarate-Garcia et al. 2016).

Wagner et al. investigated the existence of OSCs by exploring the surface bound C-terminus of DDX4 and expression of DDX4 protein in non-permeabilised cells obtained from the adult human ovary using transcriptomic analysis (Wagner et al. 2020). Wagner demonstrated that non-permeabilised ovarian cells sorted by FACS using the ab13840 C-terminus-binding DDX4 antibody were neither putative OSCs nor oocytes, since DDX4 expression was not detected using single-cell RNA sequencing, but showed that these cells were actually perivascular cells expressing markers of pericytes and smooth muscle cells (Wagner et al. 2020). Furthermore, using two separate polyclonal anti-DDX4 antibodies (produced by different manufacturers; Sigma-Aldrich and Abgent), non-permeabilised ovarian cells from adult human ovaries were DDX4 negative. This data therefore suggests that ovarian cells do not express transmembrane DDX4 and the C-terminus of the DDX4 protein is intracellular in the adult human ovary (Wagner et al. 2020).

It is important to highlight again that despite its wide application in the field (White et al. 2012; Stimpfel et al. 2013; Silvestris et al. 2018; Clarkson et al. 2018; R. A. Anderson et al. 2007; Feng et al. 2014; Venn et al. 2001; Z. Pan et al. 2015; Cao et al. 2012; Cen et al. 2020; Zou et al. 2011), the ab13840 C-terminus-binding antibody is polyclonal and hence potentially less specific than mAb. The advantages of mAbs over pAbs in FC have been highlighted (Section 5.1.1.3).

The main aim of this chapter was to detect germ cells in the ovarian single cell population isolated from fresh remnant tissue or frozen/thawed cortex. To our knowledge, DDX4 is the most well characterised germ cell marker. To this end, a

monoclonal antibody produced against human DDX4 in mouse was used (clone 2F9H5, Sigma-Aldrich, UK); this antibody binds to residue 1 to 160 in the N-terminus region of DDX4 (Figure 5. 4A) and FC. The N-terminus is localised in the cytoplasm of the oocyte and thus enabling investigation of intracellular DDX4. However, even if DDX4 is a transmembrane protein (i.e. OSCs), by using an N-terminus binding antibody, the methodology of detecting an intracellular epitope would still be valid since the N-terminus is considered to be located in the cytoplasm of putative OSCs (according to evidence supporting this theory) as well as the oocyte (Figure 5. 4B). Furthermore, by using a monoclonal antibody, it was possible to use a respective isotype control antibody.

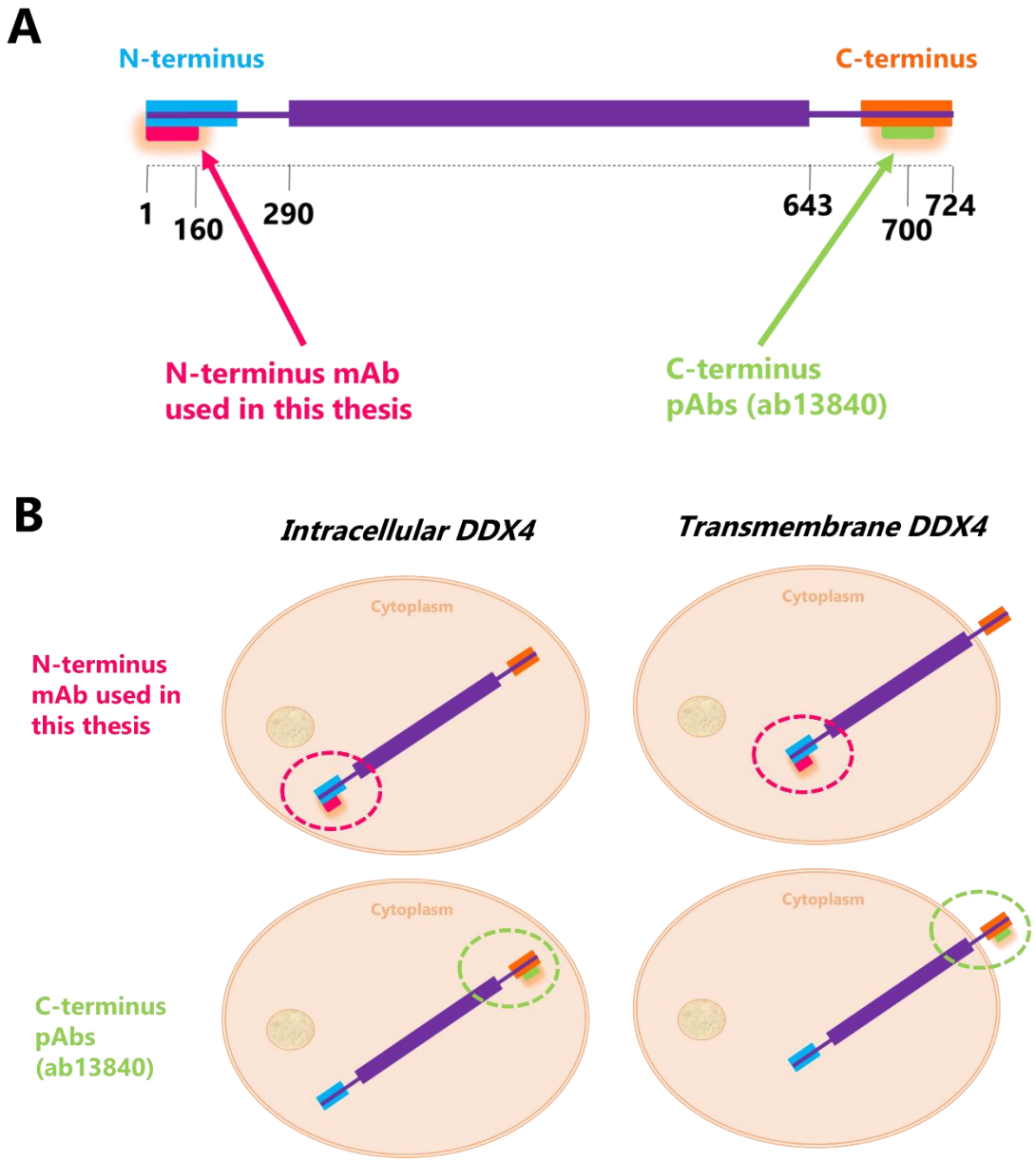



**Figure 5. 4 The monoclonal N-terminus-binding anti-DDX4 antibody and polyclonal C-terminus-binding anti-DDX4 antibody.** (A) The monoclonal anti-DDX4 antibody (raised against human DDX4, clone 2F9H5) used in this study can recognise residues 1 to 160 in the N-terminus region on the DDX4 protein, and the ab13840 polyclonal anti-DDX4 antibody recognises the C-terminus by binding to the residue 700 region (proprietary). (B) Detection of the intracellular or transmembrane DDX4 protein using the monoclonal N-terminus-binding (pink) or the polyclonal C-terminus-binding (green) anti-DDX4 antibody in a germ cell.

### 5.1.3. The role of HeLa cells and human ovarian remnant tissue in this chapter

Studies presented in this chapter were carried out to establish a method to detect intracellular DDX4 in cells isolated from human frozen/thawed ovarian cortical tissue. As frozen/thawed ovarian cortical tissue is of limited supply, HeLa cells (kindly provided by Dr Rebecca Dragovic) were utilised as a positive control in order to develop FC methodology for the detection of intracellular DDX4.

HeLa cells are an immortal cell line initially obtained from a cervical cancer patient (Scherer et al. 1953). Non-transfected HeLa cells are used by anti-DDX4 antibody manufacturers to test their products by detecting DDX4 protein using western blotting (personal correspondence with manufacturers). DDX4 is involved in rapid cell proliferation which is a cancer cell feature (Hashimoto et al. 2008; Kim et al. 2014). Hence, the implication of DDX4 in cell proliferation may justify why HeLa cell lysates are positive for DDX4.

To determine if the method used to detect intracellular DDX4 in HeLa cells would be effective for human ovarian cells, the same technique was applied to cells isolated from fresh human ovarian remnant tissue. Although remnants contain primarily medullary tissue (Chapter 2) and may not be the ideal ovarian tissue source to develop a fertility preservation method, remnants are readily available and provide a source of material to test many experimental variables.

## 5.2. Aims

The main objective of this chapter was to establish a method to detect intracellular DDX4 in ovarian cells isolated from human frozen/thawed ovarian cortical tissue. As the supply of this tissue is limited, optimisation experiments to test several variables were carried out using HeLa cells and human fresh ovarian remnant tissue. This also aided in development of a gating strategy to detect DDX4-positive cells using FC. The aims addressed in this chapter were:

***(Part 1)***

- To test the efficacy of:
  - a live/dead viability stain (HeLa cells)
  - a fixation/permeabilisation kit (HeLa cells)
  - a DDX4 monoclonal antibody (HeLa cells)
- To develop a FC gating strategy to detect intracellular DDX4-positive cells (HeLa cells)

***(Part 2)***

- To detect:
  - viable ovarian single cells by FC (human fresh ovarian remnant tissue)
  - viable ovarian single cells positive for intracellular DDX4 by FC (human fresh ovarian remnant tissue)

***(Part 3)***

- To detect:
  - viable ovarian single cells obtained from human frozen/thawed ovarian cortex by FC
  - viable ovarian single cells obtained from human frozen/thawed ovarian cortex that were positive for intracellular DDX4 by FC

## 5.3. Materials and Methods

### 5.3.1. HeLa cell viability analysis using flow cytometry

Live/dead cell discrimination (cell viability) was assessed using Zombie Aqua™ (ZA; 423101, BioLegend, London, UK) and FC. ZA is an amine reactive green fluorescent dye that only enters cells with compromised membranes. The dye is excited at 405 nm (violet laser) and has emission maxima at 516 nm.

HeLa cells stored in liquid nitrogen were thawed, washed free of Dimethyl sulfoxide (DMSO) and cultured in medium (Table 5. 1) in a 75cm$^2$ flask.

**Table 5. 1 Culture medium and supplements used for HeLa cell culture.**

| | Concentration | Product information |
|---|---|---|
| **Dulbecco's Modified Eagle's Medium (DMEM)/ Nutrient Mixture F-12 Ham** | N/A | D6424; Sigma, Dorset, UK |
| **L-glutamine** | 2 mM/L | 25030-054; Gibco, ThermoFisher Scientific, Paisley, UK |
| **Penicillin/Streptomycin** | 50 IU/ml | P4333; Sigma, Dorset, UK |
| **FBS** | 10% (v/v) | Labtech, Uckfield, UK |

Upon confluency, culture medium from HeLa cells was discarded and cells were washed twice with DPBS (D8537; Sigma). Cells were harvested using 10 ml of Trypsin-EDTA with 0.02% DNase I and the reaction was stopped by adding 10 ml of culture media. To create a positive control for ZA, cell death was induced; half of the cell sample was put in a water bath at 60°C for 1 hour and 30 min. Cells were centrifuged for 3 min at 1820 x g and the supernatant discarded. The cell pellet was washed in DPBS and cells were centrifuged at 1820 x g, twice, and incubated with 100 µl of 0.1% (v/v) ZA™ solution for 15 min at room temperature (RT) in the dark. Cells were washed twice in DPBS

supplemented with 1% (v/v) FBS and centrifuged for 3 min at 1820 x g. The supernatant was discarded, and the cell pellet was fixed and permeabilised (Fixation/Permeabilization Solution Kit; 554714; BD Biosciences, Berkshire, UK) for 20 min on ice in the dark. Cells were washed with BD Perm/Wash buffer (Fixation/Permeabilization Solution Kit; 554714; BD Biosciences, Berkshire, UK) and centrifuged at 1820 x g for 3 min, twice. The supernatant was discarded, and the cell pellet was resuspended in 500 µl of PBS/1% FBS.

### 5.3.2. Immunolabelling of intracellular cytokeratin 13 in HeLa cells

To test the efficacy of the fixation/permeabilisation method used, cells were labelled with an intracellular protein; cytokeratin 13. Cells were stained with ZA and fixed/permeabilised as described above (Section 5.3.1) and incubated with an unconjugated mouse monoclonal anti-cytokeratin 13 (NBP2-37468; NovusBiologicas, UK) at 5 µg/ml for 30 min on ice in the dark. Cells were washed in BD Perm/Wash buffer and centrifuged for 2 min at 1820 x g, twice. The supernatant was discarded, cells were resuspended in PBS/1% (v/v) FBS and mixed by vortex. Cells were incubated with a goat anti-mouse secondary antibody conjugated to R-Phycoerythrin (RPE) (R0480; Dako, Agilent, UK) at a concentration of 3.3 µg/ml for 30 min on ice in the dark. Cells were washed with BD Perm/Wash buffer and centrifuged at 1820 x g for 2 min, twice. The supernatant was discarded, cells were resuspended in PBS/1% FBS, mixed by vortex and analysed with FC. An equal number of cells were incubated with ZA, unconjugated mouse IgG1, k (401401; BioLegend, London, UK) at 5 µg/ml, goat anti-mouse secondary antibody conjugated to R-Phycoerythrin at 3.3 µg/ml, unconjugated mouse monoclonal

anti-cytokeratin 13 at 5 µg/ml, isotype control mouse IgG1, k at 5 µg/ml and mouse monoclonal anti-cytokeratin 13 at 5 µg/ml according to Table 5. 2.

**Table 5. 2 HeLa cell samples analysed to detect viable cells positive for intracellular cytokeratin 13 with FC.** ZA: zombie aqua; IgG1: primary isotype control; Cyt13: primary antibody cytokeratin 13; RPE: secondary antibody conjugated to R-Phycoerythrin.

| Sample | Label | | | |
|---|---|---|---|---|
| | ZA | IgG1 | Cyt13 | RPE |
| 'ZA' | ✓ | | | |
| 'IgG1 only' | ✓ | ✓ | | |
| 'Cyt13 only' | ✓ | | ✓ | |
| 'RPE only' | ✓ | | | ✓ |
| 'IgG1 + RPE' | ✓ | ✓ | | ✓ |
| 'Cyt13 + RPE' | ✓ | | ✓ | ✓ |

### 5.3.3. Immunolabelling of intracellular DDX4 in HeLa cells

Cells were labelled with ZA and fixed/permeabilised as described previously (Section 5.3.1). To label DDX4, cells were incubated with an unconjugated mouse monoclonal anti-DDX4 primary antibody (clone 2F9H5; SAB5300115; Sigma-Aldrich, Dorset, UK) at 5 µg/ml by adapting the method used previously to label cytokeratin 13 (Section 5.3.2). In addition, an equal number of cells were used that did not undergo fixation/permeabilisation to test if the DDX4 antibody specifically labels intracellular DDX4. Cells were labelled with ZA, unconjugated mouse IgG1, k (401401; BioLegend, London, UK) at 5 µg/ml, goat anti-mouse secondary antibody conjugated to R-Phycoerythrin at 3.3 µg/ml, unconjugated mouse monoclonal anti-cytokeratin 13 at 5 µg/ml, isotype control mouse IgG1, k at 5 µg/ml and unconjugated mouse monoclonal anti-DDX4 at 5 µg/ml according to Table 5. 3.

**Table 5. 3 HeLa cell samples analysed to detect viable cells positive for intracellular DDX4 with FC.** ZA: zombie aqua; IgG1: primary isotype control; DDX4: primary antibody DDX4; RPE: secondary antibody conjugated to R-Phycoerythrin.

| Sample | Label | | | |
|---|---|---|---|---|
| | ZA | IgG1 | DDX4 | RPE |
| 'ZA' | ✓ | | | |
| 'IgG1 only' | ✓ | ✓ | | |
| 'DDX4 only' | ✓ | | ✓ | |
| 'RPE only' | ✓ | | | ✓ |
| 'IgG1 + RPE' | ✓ | ✓ | | ✓ |
| 'DDX4 + RPE' | ✓ | | ✓ | ✓ |

### 5.3.4. Ovarian tissue source and exclusion criteria

Cells used in this study were obtained from fresh human ovarian remnants or human frozen/thawed ovarian cortex after dissociation of tissue into a single cell suspension, as described in Chapter 4 (Section 4.3.4 page 121 and Section 4.3.5 page 121). Fresh ovarian remnants (leftover ovarian tissue after the ovary has been processed for cortical tissue cryopreservation) and cryopreserved cortical strips were acquired from women who had given informed consent from the Oxford OCTB. Women older than 35 years of age and/or with ovarian diseases and/or had undergone chemotherapy (or radiotherapy) treatment prior to ovarian tissue cryopreservation were excluded from this study.

### 5.3.5. Patient age and characteristics

Detailed information on the characteristics of the patients included in this study are described in Chapter 4 (Table 4. 2 page 124 and Table 4. 3 page 125). To briefly summarise, fresh remnant ovarian tissue was obtained from six patients (patient 9-14) with an age of 11.3±7.2 (mean±SD) (Table 4. 2), and frozen ovarian cortical tissue was

obtained from eight patients (patient 25-32) with an age of 15.7±7.9 (mean±SD) (Table 4. 3).

### 5.3.6. Ovarian single cell suspension obtained from human fresh ovarian remnant tissue

Dissociation of remnant tissue into single cells has been described in detail in Chapter 4. In brief, the suspension was filtered to separate cells released during ovary dissection (referred to as Not Digested; ND) and pieces of remnant tissue. Pieces of remnant tissue were dissected as previously described (Section 4.3.4 page 121). Chopped tissue was dissociated enzymatically (collagenase solution) and mechanically (shaker) using the dissociation method 'Shaker L15' as described previously for remnant tissue (Section 4.3.4 page 121) and a single cell suspension was collected (referred to as Digested; D group). Cell viability of the ND group and D group was assessed manually with a Trypan Blue assay as described previously in Chapter 2 (Section 2.6.2 page 62).

### 5.3.7. Red-blood-cell lysis of cells from human fresh remnant tissue

To minimise red blood cell (RBC) contamination from both the ND group and D group cell pellets, these were treated with RBC Lysis Buffer (420301; BioLegend, London, UK). Cell pellets were resuspended in 1 ml of L-15 and topped up with 9 ml of 1 X RBC lysis buffer. Cells were briefly vortexed and incubated for 10 min at RT in the dark. After lysis, cells were centrifuged for 5 min at 185 x g and washed twice in L-15 supplemented with 0.3% HSA. Finally, cells were centrifuged for 5 min at 500 x g and the supernatant discarded. Cell pellets were resuspended in 1 ml of L-15/0.3% HSA, viability was

assessed manually using a Trypan Blue assay (Chapter 2), and cells were stored on ice in preparation for live/dead cell discrimination with FC (discussed below).

### 5.3.8. Ovarian single cell suspension from human frozen/thawed ovarian cortical tissue

Cryopreserved ovarian cortical tissue donated for research was thawed, dissected and dissociated enzymatically (collagenase solution) into single cells using dissociation method 'L15' as described in Chapter 4 for frozen/thawed ovarian cortical tissue (Section 4.3.5 page 121). Cell viability was assessed using a Trypan Blue assay (Chapter 2), and cells were stored on ice in preparation for live/dead cell discrimination (see below).

### 5.3.9. Live/Dead cell discrimination for flow cytometry analysis

To exclude dead cells, the fluorescent dye Zombie Aqua™ (ZA) was used. Cells isolated from the remnant (ND, D) group after RBC lysis, or frozen/thawed ovarian cortex were washed in DPBS (D8537; Sigma) and centrifuged at 1820 x g for 3 min, twice. Supernatant was discarded, the cell pellet was resuspended in and incubated with 100 µl of 0.1% (v/v) ZA solution for 15 min at RT in the dark. Cells were washed in DPBS supplemented with 1% (v/v) FBS and centrifuged for 3 min at 1820 x g, twice before fixation and permeabilisation.

### 5.3.10. Fixation and permeabilisation for flow cytometry analysis

To detect intracellular DDX4, cells were fixed and permeabilised using a Fixation/Permeabilization Solution Kit (BD Biosciences, UK) as used for HeLa cells (Section 5.3.1). For ovarian remnant (ND, D) and frozen/thawed ovarian cortex groups,

cells were incubated with 250 µl of Fixation/Permeabilization solution for 20 min on ice in the dark. Cells were washed in 1 ml of 1X BD Perm/Wash buffer and centrifuged at 1820 x g for 3 min, twice. The supernatant was discarded, and cells were resuspended in 100 µl of antibody solution for immunolabelling (see below).

### 5.3.11. Immunolabelling of cytoplasmic DDX4 in human ovarian cells using flow cytometry

To detect intracellular DDX4, a mouse monoclonal antibody raised against human DDX4 (amino acids 1 to 160, clone 2F9H5, Sigma-Aldrich, UK) was used. Cells obtained from remnants (ND, D) or frozen/thawed cortex were incubated with 5 µg/ml of anti-DDX4 or respective isotype control IgG1 (BioLegend UK) at 5 µg/ml for 30 min on ice in the dark. Following incubation, cells were washed with 1 mL of BD Perm/Wash buffer and centrifuged at 1820 x g for 3 min, twice. The supernatant was discarded, and cells were incubated with a goat anti-mouse secondary antibody conjugated to R-Phycoerythrin at 3.3 µg/ml for 30 min on ice in the dark. Cells were washed with 1 ml of BD Perm/Wash buffer and centrifuged for 3 min at 1820 x g, twice. Finally, the supernatant was discarded, and cell pellets were resuspended in PBS/1% (v/v) FBS for FC analysis.

For cells from **ovarian remnant tissue (ND and D)**, a total of 4 samples were analysed for each patient used (Table 5. 4).

**Table 5. 4 Human remnant ovarian cell samples analysed to detect viable cells positive for intracellular DDX4 with FC.** ZA: zombie aqua; IgG1: primary isotype control; DDX4: primary antibody DDX4; RPE: secondary antibody conjugated to R-Phycoerythrin.

| Sample | Label | | | |
|---|---|---|---|---|
| | ZA | IgG1 | DDX4 | RPE |
| 'Unlabelled' | | | | |
| 'ZA' | ✓ | | | |
| 'IgG1 + RPE' | ✓ | ✓ | | ✓ |
| 'DDX4 + RPE' | ✓ | | ✓ | ✓ |

For cells from **frozen/thawed ovarian cortical tissue**, a total of 3 samples were analysed for each patient used (Table 5. 5).

**Table 5. 5 Human frozen/thawed ovarian cell samples analysed to detect viable cells positive for intracellular DDX4 with FC.** ZA: zombie aqua; IgG1: primary isotype control; DDX4: primary antibody DDX4; RPE: secondary antibody conjugated to R-Phycoerythrin.

| Sample | Label | | | |
|---|---|---|---|---|
| | ZA | IgG1 | DDX4 | RPE |
| 'Unlabelled' | | | | |
| 'IgG1 + RPE' | ✓ | ✓ | | ✓ |
| 'DDX4 + RPE' | ✓ | | ✓ | ✓ |

### 5.3.12. Flow cytometry analysis

FC was performed using a BD LSRII Flow Cytometer (BD Biosciences, UK) equiped with a 405 nm violet laser, 488 nm blue laser and 633 nm red laser. A total of 3,000 - 670,000 events were recorded for each sample in the ND and 30,000 - 1,000,000 events for the D group. A total of 17,000 - 100,000 events were recorded for each frozen/thawed

ovarian cortical tissue sample. It should be noted here, that even though the absolute number of cells was not calculated per sample, the whole amount of each ovarian remnant sample and frozen/thawed ovarian cortex sample available (500 µl) was analysed leaving the minimum amount (~5 µl) to avoid air passing through the system. A total of 20,000 events were recorded for each HeLa cell sample using BDFACSDiva 8.0 software (BD Biosciences, UK). FC gating and analysis of viable DDX4 positive cells was performed using FlowJo-V10.5.3 software (Ashland Oregon, USA).

### 5.3.13. Statistical analysis

Statistical analysis was performed using GraphPad Prism version 8.2.1 (GraphPad Software, La Jolla, California, USA). Data was tested for normality using a Shapiro-Wilk test. The percentage of viable single cells, and the percentage of viable single DDX4-positive cells, as detected with FC, was compared between the pre- and post-pubertal group using unpaired t-test with Welch's correction (if data was normally distributed), or a Mann-Whitney unpaired t-test (if data was not normally distributed). Results are presented as mean±standard deviation, with $P \leq 0.05$ considered significant.

## 5.4. Results

### 5.4.1. Part 1 - HeLa cells

#### 5.4.1.1. Live/dead cell discrimination using HeLa cells

To explore the efficacy of ZA to bind to dead cells, cell death was induced in HeLa cells and analysed by FC. A gate was drawn around the main cell population, excluding debris from the analysis (Figure 5. 5A). Gated cells were then displayed on a FSC-Height (FSC-H) versus FSC-Area (FSC-A) plot to gate single cells and eliminate doublets (Figure 5. 5B). Exclusion of doublets is performed based on the cytometer electronics using the peak of the fluorescence signal versus the overall fluorescence signal per event (i.e. FSC-H or FSC-W versus FSC-A, SSC-H or SSC-W versus SSC-A)(Snow 2004). No dead cells were detected in the population of HeLa cells without induced cell death (Figure 5. 5C), whereas when cell death was induced viable single live cells were effectively discriminated from dead cells (a ZA-negative population (70%) which represented live cells and a ZA-positive cell population representing dead cells; Figure 5. 5D). This analysis demonstrated that ZA can bind to dead HeLa cells and therefore, enabled live/dead cell discrimination using FC analysis.

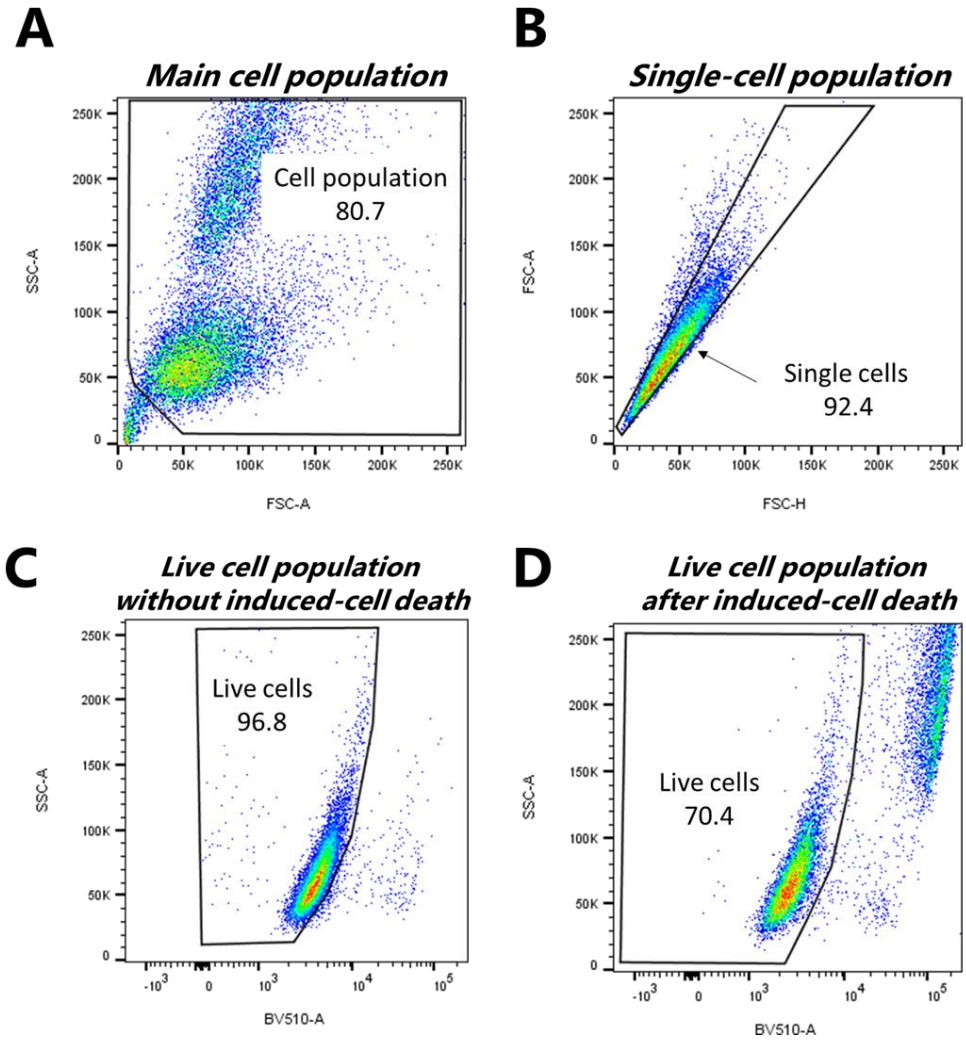



**Figure 5. 5 Analysis of cell viability of HeLa cell population without or after induced cell death using ZA and FC.** HeLa cells were stained with ZA (detected in the BV-510 channel) to allow for live/dead cell discrimination. Data shows the percentage of HeLa cells in the main population (A), single cells (B), HeLa cells without induced-cell death (C) and HeLa cells with induced cell death (D). ZA: zombie aqua; SSC-A: side scatter area; FSC-A: forward scatter area; FSC-H: forward scatter height; BV510-A: brilliant violet 510 area.

This gating strategy to detect viable single cells (as described above) was applied to test the efficacy of the fixation/permeabilisation method and detection of intracellular DDX4 using HeLa cells.

#### 5.4.1.2. Efficacy of fixation/permeabilisation using HeLa cells

To determine if the fixation/permeabilisation method was effective, detection of the intracellular marker cytokeratin 13 was explored using HeLa cells. Cytokeratin 13 has been previously detected in fixed/permeabilised HeLa cells (Novus Biologicals) and was therefore, used as a positive control.

To define the viable single cells that were labelled positive for intracellular cytokeratin 13, data was first obtained from the isotype control (IgG1 + RPE; IgG1 as primary antibody, and secondary antibody conjugated to RPE). This was necessary to set a gate to exclude ~99% of viable unstained-for-cytokeratin 13 HeLa cells which was then applied to the sample of interest (Cyt13 +RPE) in order to discriminate the cytokeratin 13-positive from negative HeLa cells (Figure 5. 6).

Results showed that 99.5% of viable single cells were cytokeratin 13-positive (Figure 5. 6). This finding showed that HeLa cells were effectively fixed and permeabilised allowing for detection of cytoplasmic markers.

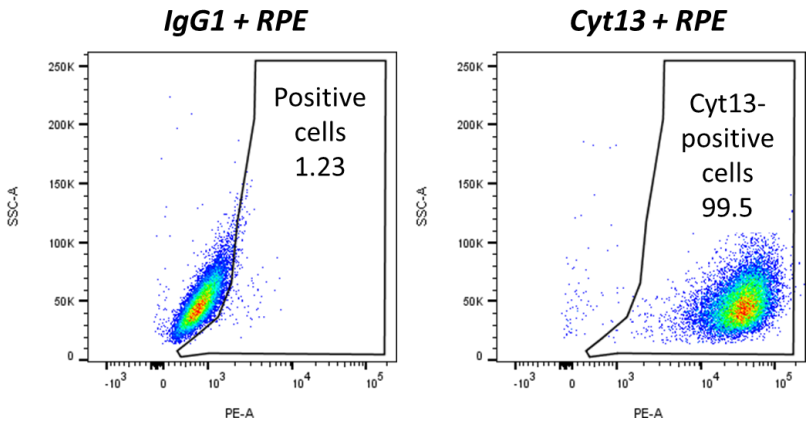



**Figure 5. 6 FC analysis of intracellular cytokeratin 13 in HeLa cells.** HeLa cells were labelled with the isotype control (IgG1 + RPE) or anti-cytokeratin 13 (Cyt13 + RPE). Data shows the percentage of positive cells. SSC-A: side scatter area; RPE: secondary antibody conjugated to R-Phycoerythrin; PE-A: R-Phycoerythrin area.

Having demonstrated intracellular staining of cytokeratin 13 using HeLa cells, the same methodology was applied for the detection of intracellular DDX4.

#### 5.4.1.3. Flow cytometry gating strategy to detect intracellular DDX4 using HeLa cells

Fixed/permeabilised HeLa cells stained with ZA were labelled to detect intracellular DDX4. Cells were labelled as described in Table 5. 3 (page 161). To detect a viable single cell population cells were gated as described previously (Figure 5. 5). Viable single cells in the controls were displayed on a SSC-A versus fluorescence (PE-A) density scatter plot. A gate was drawn to include ~1% of the population which excluded 99% of live unstained cells (Figure 5. 7A). This gating was then applied to the sample of interest ('DDX4 + RPE'; cells stained with ZA (Figure 5. 7B) and labelled with anti-DDX4 and the RPE secondary antibody) to detect the viable intracellular DDX4-positive cells (Figure 5. 7C).

Data obtained from this investigation showed that 99.6% of fixed/permeabilised viable single HeLa cells were positive for intracellular DDX4, indicating that the

fixation/permeabilisation and immunolabelling method developed to detect intracellular DDX4 in HeLa cells was successful.

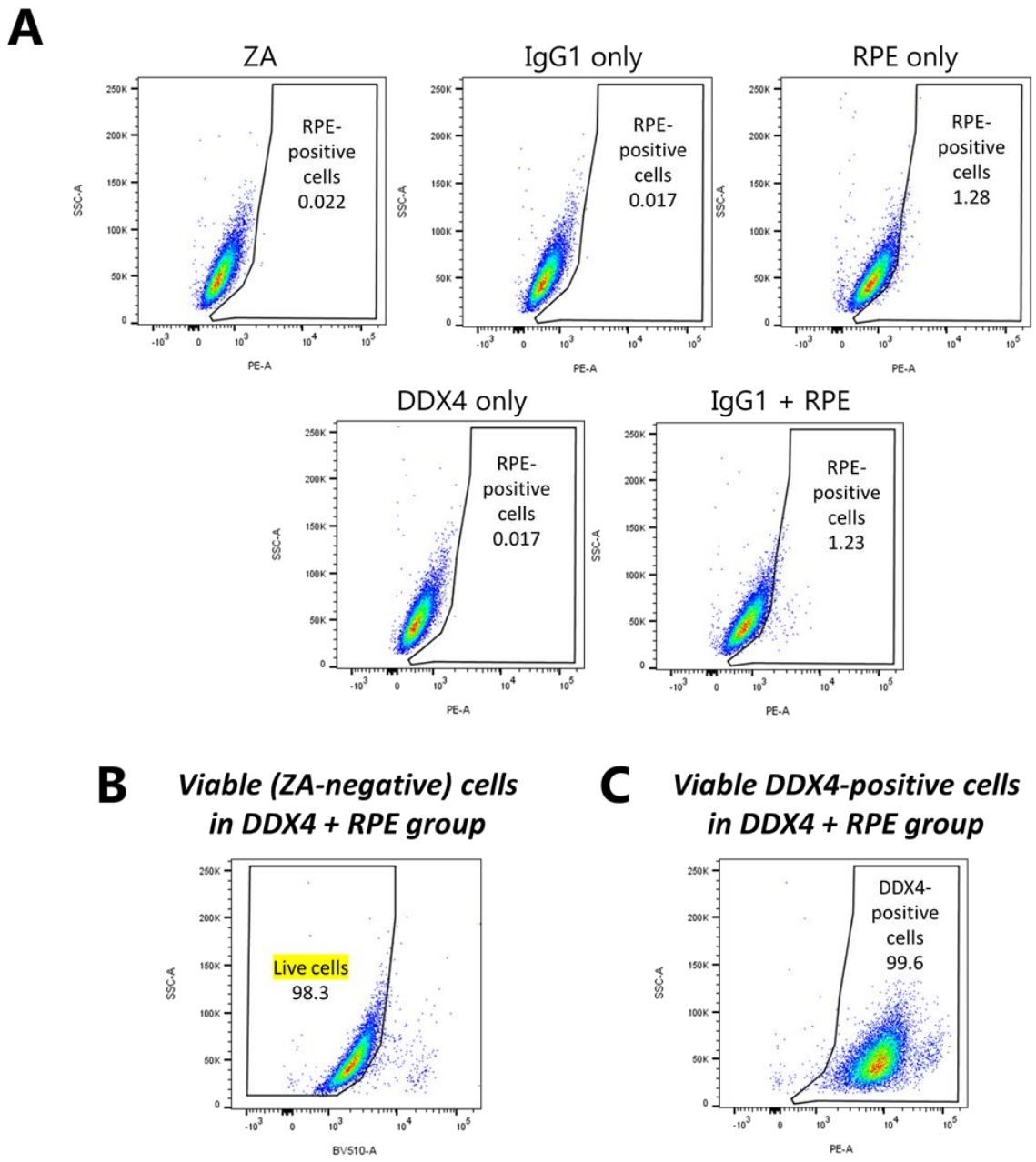



**Figure 5. 7 FC gating to identify intracellular DDX4-positive HeLa cells.** (A) Controls were used to set a gate at ~1% of cells; ZA, IgG1 only, RPE only, DDX4 only, or IgG1 + RPE. (B) The gate set using the controls was applied to viable single cells in the sample of interest (DDX4 + RPE) to detect cells positive for intracellular DDX4. Data shows the percentage of IgG1-RPE-positive cells (A), live cells (B) or DDX4-positive cells (C). SSC-A: side scatter area; BV510-A: brilliant violet 510 area; RPE: secondary antibody conjugated to R-Phycoerythrin; PE-A: R-Phycoerythrin area.

### 5.4.1.4. Detection of intracellular DDX4 in HeLa cells

To investigate whether the positive DDX4 labelling in HeLa cells was specific to intracellular DDX4, the anti-DDX4 antibody was used to detect any membrane bound DDX4 by using non-fixed and non-permeabilised cells. The FC gating strategy described in Section 5.4.1.3 was applied. Fixed and permeabilised cells (fixed/permeabilised) were 99.6% positive for intracellular DDX4 (Figure 5. 8A), whereas only 6.25% of non-fixed and non-permeabilised cells (non-fixed/non-permeabilised) were DDX4 positive (Figure 5. 8B), reflecting very low levels of membrane bound DDX4. This result demonstrated that the anti-DDX4 antibody was able to efficiently bind to intracellular DDX4 in fixed/permeabilised HeLa cells and the technique could be transferred to use with ovarian cells.

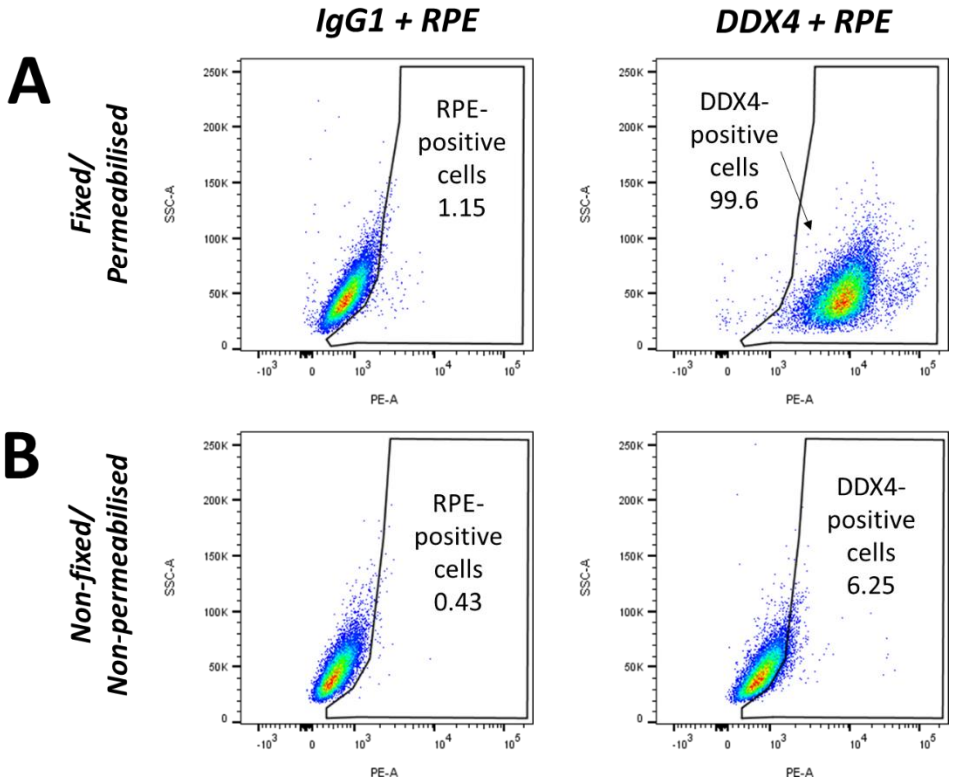



**Figure 5. 8 Analysis of intracellular and surface bound DDX4 in HeLa cells using FC.** (A) Fixed/Permeabilised HeLa cells labelled with the isotype control (IgG1 + RPE) or anti-DDX4 (DDX4 + RPE). (B) Non-Fixed/Non-permeabilised HeLa cells labelled with the isotype control (IgG1 + RPE) or anti-DDX4 (DDX4 + RPE). Data shows the percentage of positive cells. SSC-A: side scatter area; PE-A: R-Phycoerythrin area; RPE: secondary antibody conjugated to R-Phycoerythrin.

## 5.4.2. Part 2 – Human fresh ovarian remnant tissue

### 5.4.2.1. Flow cytometry gating strategy to identify viable cells from human fresh ovarian remnant tissue

The FC method and gating strategy used to detect intracellular DDX4 in HeLa cells (Figure 5. 7 page 171) was applied to ovarian single cells derived from human fresh ovarian remnant tissue obtained from pre- and post-pubertal patients. First, data was displayed using a SSC-A versus FSC-A dot plot and a gate was drawn to exclude cell debris. Gated cells were then displayed on a SSC-A versus SSC-H or SSC-W dot plot to eliminate doublets. To exclude dead cells, ZA (detected in channel BV-510) was plotted against SSC-A and gating was based on the 'Unlabelled' control sample (Figure 5. 9A). This gating strategy was then applied to samples (Table 5. 4, page 165): 'ZA' (Figure 5. 9B), 'IgG1 + RPE' (Figure 5. 9C) and 'DDX4 + RPE' (Figure 5. 9D).

Figure 5. 9 shows representative data of live/dead cell discrimination of a ND remnant sample obtained from a 12-year-old patient (patient 11, Table 4. 2 page 124).

FC gating of the main cell population and single cells for all patients is presented in Appendix IIa (Supplementary Figure 3 and Supplementary Figure 4).

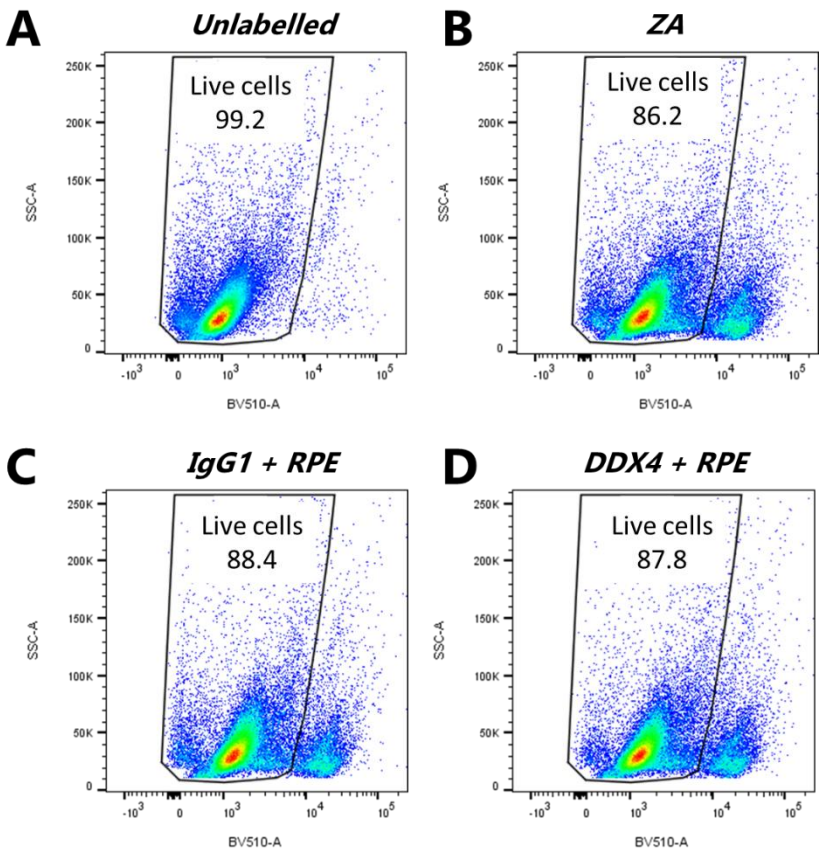



**Figure 5. 9 FC gating strategy to exclude dead cells in human fresh ovarian remnant tissue.** ND cells from a 12-year-old pre-pubertal patient were incubated with ZA and displayed on SSC-A versus ZA (BV510-A) density scatter plot. Viable (ZA-negative) cells were gated using the Unlabelled control sample (A). The same gate was then applied to (B) ZA control (C) IgG1 + RPE and (D) DDX4 + RPE to identify and exclude dead cells (ZA-positive cells). Data shows the percentage of viable cells (live cells). ZA: zombie aqua; SSC-A: side scatter area; BV510-A: brilliant violet 510 area; RPE: secondary antibody conjugated to R-Phycoerythrin; ND: not digested.

This analysis showed that the percentage of live cells across all samples was consistent ('ZA'; 86.2%, 'IgG1 + RPE'; 88.4% and 'DDX4 + RPE'; 87.8%).

### 5.4.2.2. Detection of viable cells from human ovarian remnants

Having established that the method developed was effective for human ovarian remnant samples, it was then applied for multiple patients (patients 9-14, Table 4. 2, page 124). Dead cells were identified and excluded using the FC gating strategy presented above (Figure 5. 9). Live and dead cells derived from fresh remnant tissue

were observed in the Not Digested (ND) group (Figure 5. 10A(i), B(i)) and Digested group (D) (Figure 5. 10A(ii), B(ii)). In 4 of the 6 samples analysed in the ND (A(i) and B(i)) group (12-, 15, 18- and 18-year old patient), two distinct cell populations (live and dead cells) were observed. Fewer total cells were analysed in the 2- and 3-year old patients (ND group), therefore making it difficult to observe a distinct dead cell population (Figure 5. 10A(i)).

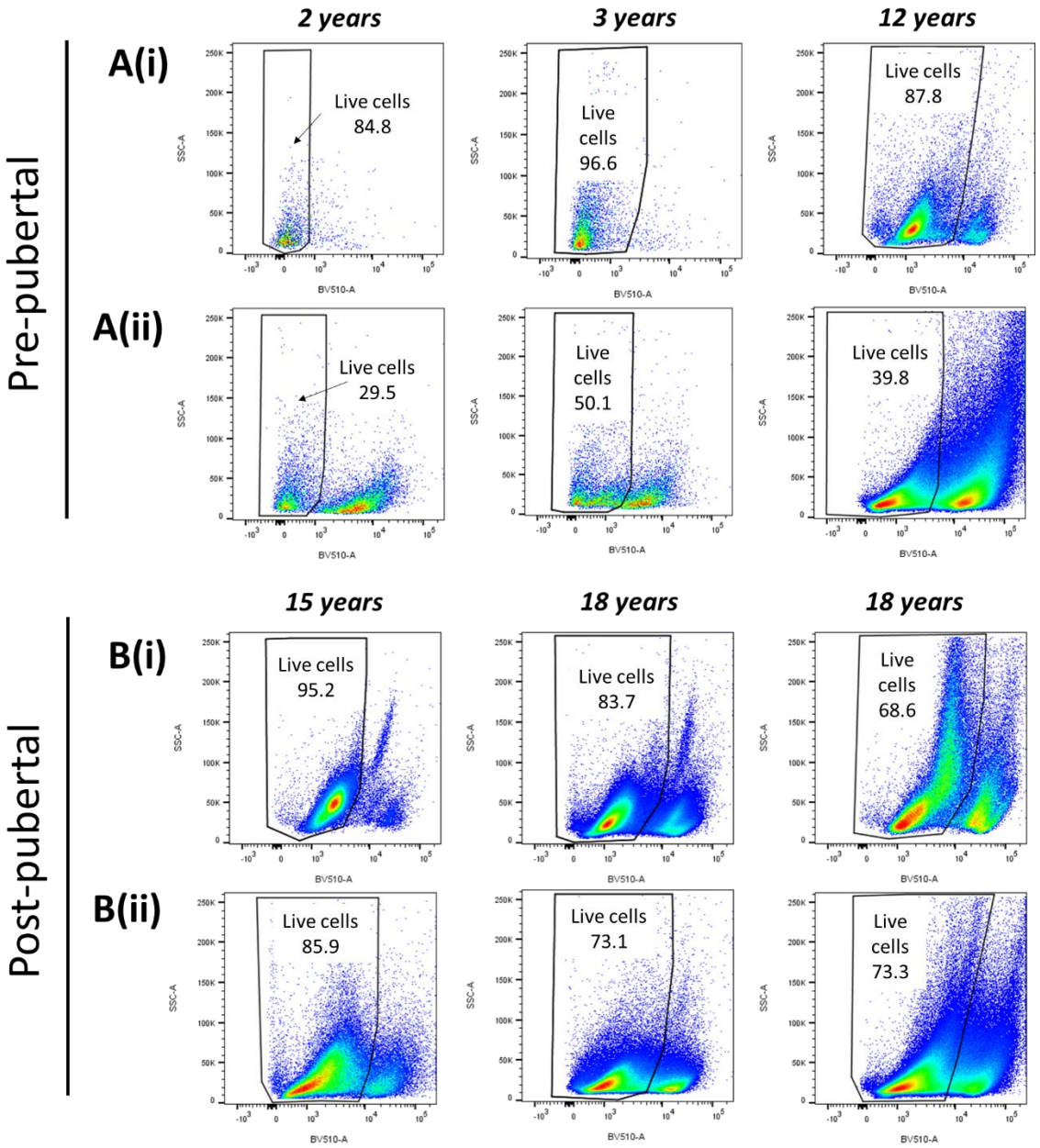



**Figure 5. 10 Viability of cells from human ovarian remnant tissue measured by FC.** Cells from pre-pubertal (A(i); ND-group and A(ii); D group) and post-pubertal (B(i); ND-group and B(ii); D-group) patients were incubated with ZA and displayed on SSC-A versus ZA (BV-510-A) density scatter plots. Live cells were gated based on the exclusion of ZA. Data shows the percentage of viable cells (live cells) for each patient. ND: not digested; D: digested; SSC-A: side scatter area; BV510-A: brilliant violet 510 area.

The number of total cells varied and was dependant on the amount of remnant tissue available for a given patient. As the ovary is larger in older patients compared to younger patients, more remnant tissue was available. As a result, smaller cell populations were

observed in the ND and D group of patients aged 2 and 3 years compared to the older patients (12- to 18-years old).

Cell viability expressed as the number of viable cells and percentage (%) of viable cells analysed for each patient sample is presented in Table 5. 6. The total number of single cells analysed is also shown in Table 5. 6, however this is not an absolute counting of cells (Brando et al. 2000) as this was not determined.

**Table 5. 6 Cell viability in ND and D groups from human fresh ovarian remnant tissue .** Cells from Pre-pubertal and Post-pubertal ND and D remnant samples were incubated with ZA and viability was assessed using FC. Viable cells were determined by excluding dead cells as measured by FC. Data shows the percentage (%) and number of viable cells (blue) as well as the number of total single cells analysed for each patient. ND: not digested; D: digested.

| | | **Pre-pubertal** | | |
|---|---|---|---|---|
| | | **2-years** (Patient 9) | **3-years** (Patient 10) | **12-years** (Patient 11) |
| **ND** | **% of VIABLE single cells** | 84.8 | 96.6 | 87.8 |
| | **Number of VIABLE single cells** | 1,532 | 5,482 | 46,216 |
| | **Number of TOTAL single cells** | 1,807 | 5,674 | 52,652 |
| **D** | **% of VIABLE single cells** | 29.5 | 50.1 | 39.8 |
| | **Number of VIABLE single cells** | 3,999 | 6,458 | 146,291 |
| | **Number of TOTAL single cells** | 13,544 | 12,892 | 367,106 |
| | | **Post-pubertal** | | |
| | | **15-years** (Patient 12) | **18-years** (Patient 13) | **18-years** (Patient 14) |
| **ND** | **% of VIABLE single cells** | 95.1 | 83.7 | 68.6 |
| | **Number of VIABLE single cells** | 102,317 | 339,853 | 73,267 |
| | **Number of TOTAL single cells** | 107,501 | 399,271 | 106,807 |
| **D** | **% of VIABLE single cells** | 85.9 | 73.1 | 73.3 |
| | **Number of VIABLE single cells** | 88,695 | 204,825 | 427,005 |
| | **Number of TOTAL single cells** | 103,278 | 280,086 | 582,262 |

The percentage of viable cells was compared in pre- and post-pubertal patients. No significant difference (p=0.48) was found in the yield of live cells (%) between pre-pubertal (67%±27%) and post-pubertal (76%±14%) patients (Figure 5. 11).

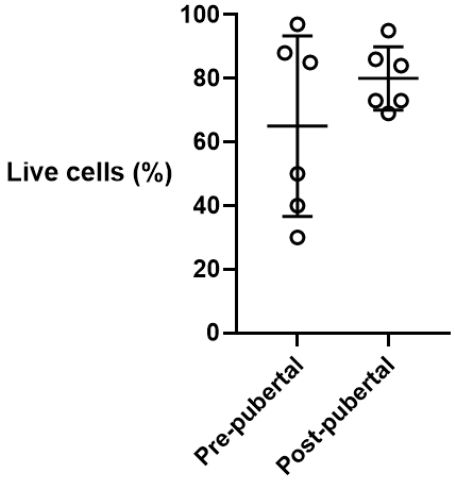



**Figure 5. 11 Viability of cells from pre-pubertal and post-pubertal fresh ovarian remnant tissue measured by FC.** Dissociated cells were incubated with ZA to exclude dead cells. Data shows the percentage (%) of live cells (mean±SD) analysed from 3 pre-pubertal (n=6: 3 ND samples and 3 D samples) and 3 post-pubertal patients (n=6: 3 ND samples and 3 D samples). No statistical difference was found. P>0.05.

### 5.4.2.3. Detection of DDX4-positive cells from human fresh ovarian remnant tissue

The gating strategy shown previously for HeLa cells (Figure 5. 7 page 171) was used to detect intracellular DDX4 in ovarian cells from fresh ovarian remnant tissue. Data was displayed on a SSC-A versus FSC-A density plot to identify the main cell population and remove any doublets. Using the 'Unlabelled' control, a gate was drawn for the live cell population which was then applied to the 'IgG1 + RPE' (Figure 5. 12A) and 'DDX4 + RPE' sample (Figure 5. 12B). Viable cells in the 'IgG1 + RPE' were displayed on a SSC-A versus IgG1-PE density dot plot and a gate was drawn to include ~1% of the population (Figure

5. 12C). This gate was applied to viable single cells in the 'DDX4 + RPE' sample to detect DDX4-positive cells (Figure 5. 12D). Figure 5. 12 shows representative data of a ND remnant sample obtained from a 12-year-old patient (patient 11, Table 4. 2 page 124) whereby 94% of viable single cells isolated from fresh ovarian remnant tissue was labelled positive for the intracellular marker DDX4.

FC gating for the isotype control ('IgG1 + RPE') for all patients is presented in Appendix IIa (Supplementary Figure 5).

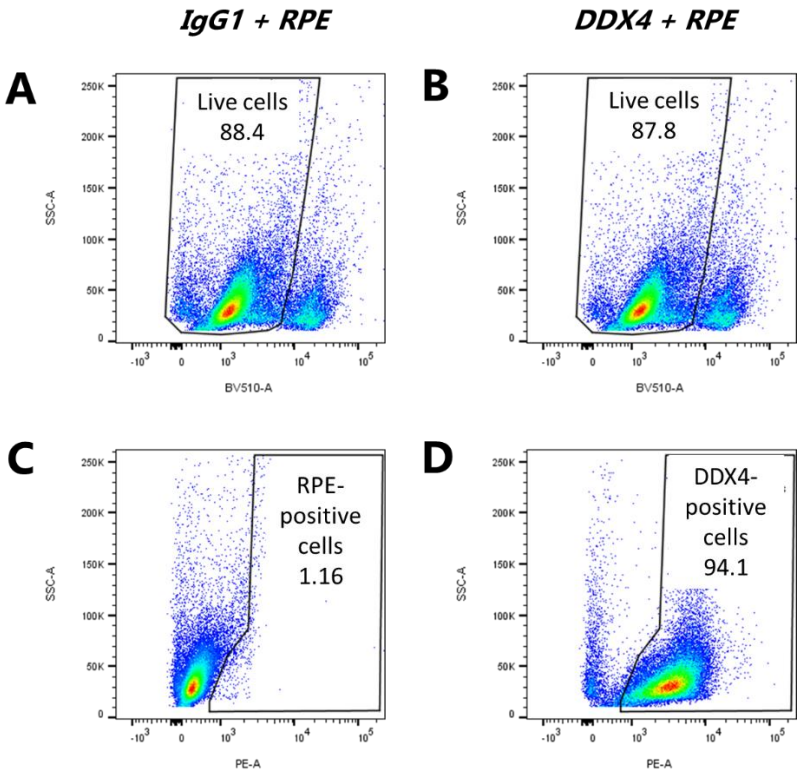



**Figure 5. 12 FC gating strategy to detect DDX4-positive cells from human fresh ovarian remnant tissue.** ND cells from a 12-year old pre-pubertal patient (patient 11) were incubated with ZA and labelled with anti-IgG1 ('lgG1 + RPE') or anti-DDX4 ('DDX4 + RPE'). (A) 'IgG1 + RPE' gated viable single cells. (B) 'DDX4 + RPE' gated viable single cells. (C) A gate was drawn to include ~1% of the population in the 'IgG1-RPE' sample. (D) This gate was applied to the 'DDX4 + RPE' sample to determine the percentage of DDX4-positive cells. Data shows the percentage of live cells or positive cells. ZA: zombie aqua; SSC-A: side scatter area; PE-A: R-Phycoerythrin area; RPE: secondary antibody conjugated to R-Phycoerythrin.

The described gating strategy was used to detect intracellular DDX4-positive cells in all patient samples (Figure 5. 13). DDX4-positive cells were detectable in 5 of 6 patients analysed; DDX4-positive cells were not detected in the 2-year-old patient for both the ND (Figure 5. 13A(i)) and D group (Figure 5. 13A(ii)). Less than 2% of cells labelled positive for DDX4 in the 3-year old patient for the ND group (Figure 5. 13A(i)), most likely due to the low number of cells analysed.

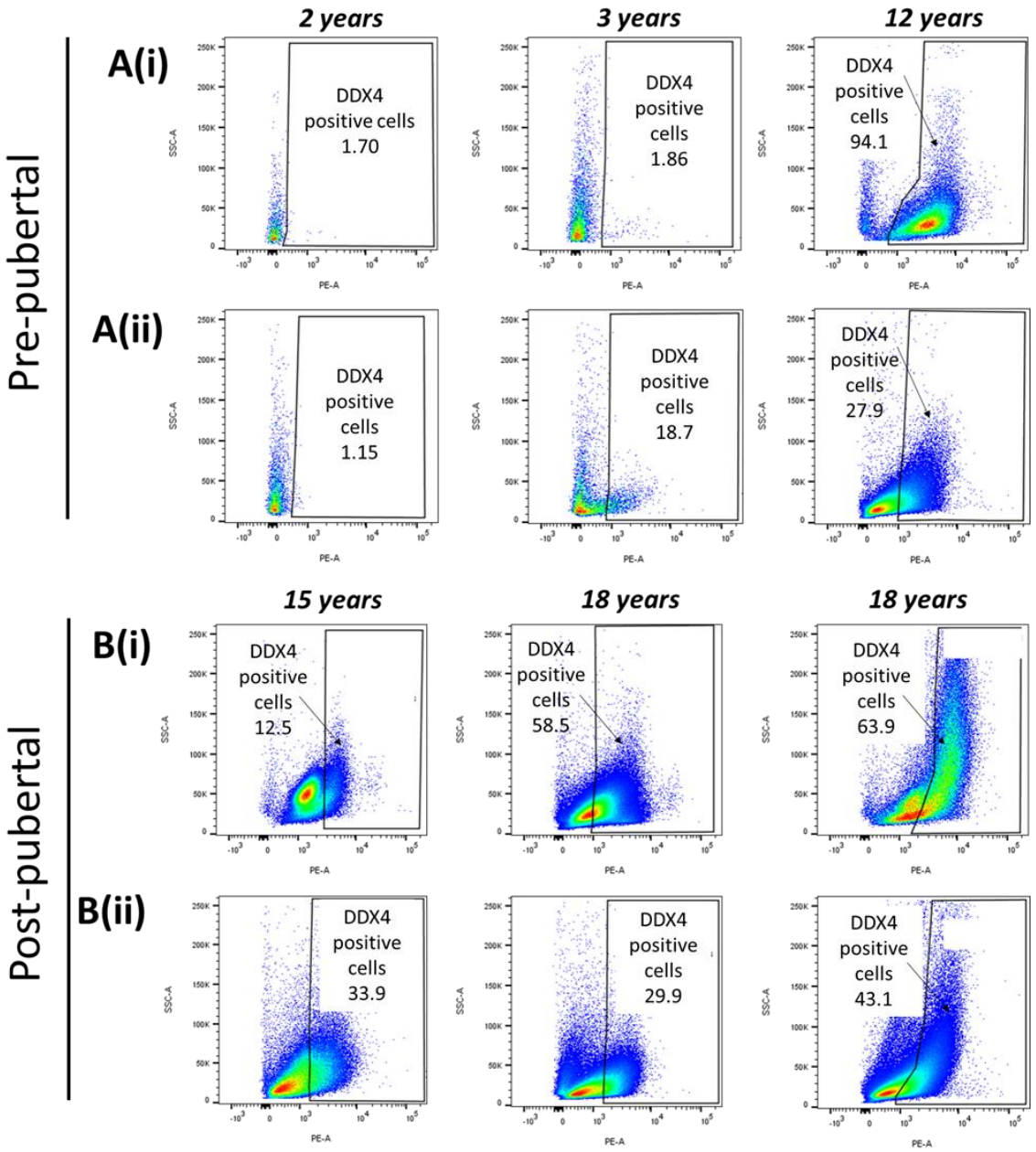



**Figure 5. 13 Percentage of DDX4-positive cells from human fresh ovarian remnant tissue measured by FC.** Cells obtained from pre-pubertal (A(i); ND-group and A(ii); D group) and post-pubertal (B(i); ND-group and B(ii); D-group) patients were labelled with anti-DDX4 and displayed on SSC-A versus DDX4-PE (PE-A) density plots. DDX4-positive cells were gated based on the isotype control 'IgG1 + RPE'. Data shows the percentage of DDX4-positive cells for each patient. SSC-A: side scatter area; RPE: secondary antibody conjugated to R-Phycoerythrin; PE-A: R-Phycoerythrin area.

The percentage of DDX4-positive cells varied between the 6 patient samples analysed (Table 5. 7). In the ND group, the percentage of DDX4-positive cells was lower in the pre-pubertal group compared to the post-pubertal except for the 12-year-old patient

which was higher. In the D group, the percentage of DDX4 positive cells was higher in the post-pubertal group compared to pre-pubertal (Table 5. 7).

**Table 5. 7 DDX4-positive cells from human fresh ovarian remnant tissue measured by FC.** Dissociated cells from pre-pubertal (A(i); ND-group and A(ii); D group) and post-pubertal (B(i); ND-group and B(ii); D-group) patients were labelled with anti-DDX4 and analysed with FC. DDX4-positive cells were detected based on the isotype control 'IgG1 + RPE'. Data show the percentage (%) and number of DDX4-positive cells (pink/orange) as well as the number of viable single cells (blue) analysed for each patient. ND: not digested; D: digested.

| | | Pre-pubertal | | |
|---|---|---|---|---|
| | | **2-years** (Patient 9) | **3-years** (Patient 10) | **12-years** (Patient 11) |
| **ND** | **% of DDX4-positive cells** | 1.7 | 1.86 | 94.1 |
| | **Number of DDX4-positive cells** | 26 | 102 | 43,499 |
| | **Number of VIABLE single cells** | 1,532 | 5,482 | 46,216 |
| **D** | **% of DDX4-positive cells** | 1.15 | 18.7 | 27.9 |
| | **Number of DDX4-positive cells** | 46 | 1,207 | 40,786 |
| | **Number of VIABLE single cells** | 3,999 | 6,458 | 146,291 |
| | | **Post-pubertal** | | |
| | | **15-years** (Patient 12) | **18-years** (Patient 13) | **18-years** (Patient 14) |
| **ND** | **% of DDX4-positive cells** | 12.5 | 58.5 | 63.9 |
| | **Number of DDX4-positive cells** | 12,790 | 195,614 | 46,830 |
| | **Number of VIABLE single cells** | 102,317 | 339,853 | 73,267 |
| **D** | **% of DDX4-positive cells** | 33.9 | 29.9 | 43.1 |
| | **Number of DDX4-positive cells** | 30,087 | 61,312 | 184,127 |
| | **Number of VIABLE single cells** | 88,695 | 204,825 | 427,005 |

The percentage of DDX4-positive cells in the pre-pubertal group was compared to the post-pubertal group and showed no significant difference (Figure 5. 14).

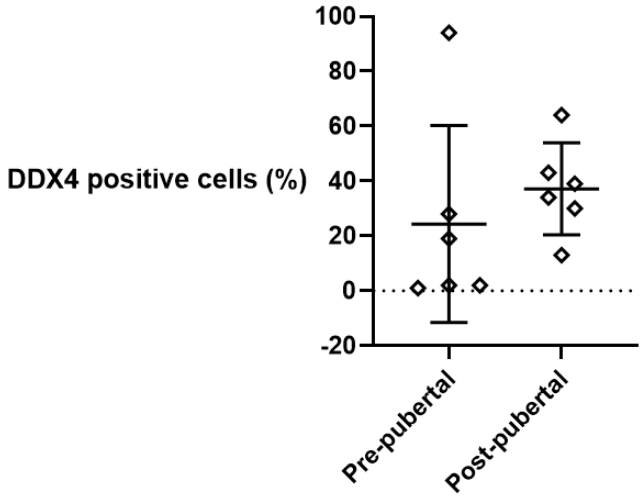



**Figure 5. 14 Analysis of the effect of pubertal status on DDX4-positive cells from human fresh ovarian remnant tissue.** Cells were labelled with anti-DDX4 to detect intracellular DDX4. Data shows the percentage (%) of viable single cells that were positive for intracellular DDX4 (mean±SD) in 3 pre-pubertal (n=6: 3 ND samples and 3 D samples) and 3 post-pubertal patients (n=6: 3 ND samples and 3 D samples). No statistical difference was found. P>0.05.

Using human fresh ovarian remnant tissue, a dissociation method was established to obtain a viable single cell suspension (Chapter 4) and here, a FC method to detect intracellular DDX4 in pre- and post-pubertal ovarian remnants. Next, this same method was tested using the cryopreserved ovarian cortical tissue.

## 5.4.3. Part 3 – Human frozen/thawed ovarian cortical tissue

### 5.4.3.1. Flow cytometry gating strategy to identify viable cells from human frozen/thawed ovarian cortical tissue

The FC gating strategy developed to detect viable single cells from ovarian remnant tissue samples (Figure 5. 9) was used to detect viable single cells in human frozen/thawed cortical tissue samples. A 'ZA' control (cells stained with ZA only) was not used in these experiments as it was previously shown for remnant tissue to be almost identical to the isotype control (see 'ZA' and 'IgG1+RPE' group in Figure 5. 9, page 174). Therefore, the controls used to investigate intracellular DDX4 using frozen/thawed ovarian cortex were the 'Unlabelled' and 'IgG1 + RPE' sample (Table 5. 5 page 165).

First, data were displayed using a SSC-A versus FSC-A dot plot and a gate was drawn to remove cell debris. The main cell population was then displayed on an SSC-A versus SSC-height (SSC-H) dot plot to eliminate doublets. To exclude dead cells, ZA was plotted against SSC-A and gating was based on the 'Unlabelled' control sample (Figure 5. 15A). This gating strategy was then applied to samples (Table 5. 5 page 165): 'IgG1 + RPE' (Figure 5. 15B) and 'DDX4 + RPE' sample (Figure 5. 15C) allowing for live/dead cell discrimination. Figure 5. 15 shows representative data of gating to detect viable cells from a 15-year-old pre-pubertal patient (patient 32, Table 4. 3 page 125).

Gating of the main cell population and single cells for all patients is presented in Appendix IIb (Supplementary Figure 6 and Supplementary Figure 7).

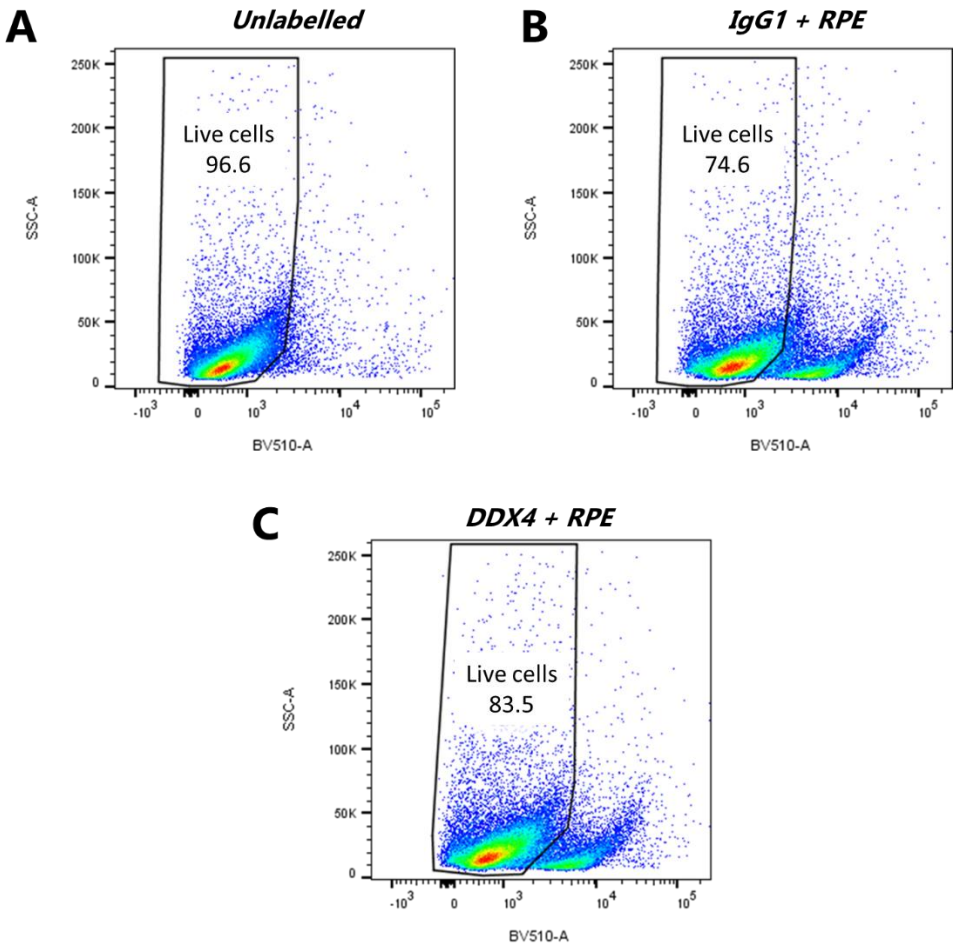



**Figure 5. 15 FC gating strategy to exclude dead cells from human frozen/thawed ovarian cortex.** Cells from a 15-year-old post-pubertal patient (patient 32) were incubated with ZA and displayed on SSC-A versus ZA (BV510-A) density scatter plot. (A) Viable (ZA-negative) cells were gated using the 'Unlabelled' control sample. The same gate was then applied to (B) isotype control 'IgG1 + RPE' and (C) 'DDX4 + RPE' sample to identify and exclude dead cells (ZA-positive cells). Data shows the percentage of viable cells (live cells) analysed. SSC-A: side scatter area; BV510-A: brilliant violet 510 area; RPE: secondary antibody conjugated to R-Phycoerythrin.

Data showed that the percentage of cells initially gated (main cell population, and single cell population) for the 15-year-old patient sample was consistent between controls ('Unlabelled', and 'IgG1 + RPE') and the sample of interest ('DDX4 + RPE'). This observation (which was also the case for remnant tissue) indicated that the gating strategy used was reproducible and was applied to all frozen/thawed ovarian cortical tissue samples.

### 5.4.3.2. Viable cells from human frozen/thawed ovarian cortical tissue

Dead cells were identified and excluded using the FC gating method described above for all patients. Live and dead cells were observed as two distinct populations derived from frozen/thawed cortical tissue in all pre-pubertal (Figure 5. 16A) and post-pubertal (Figure 5. 16B) patients analysed.

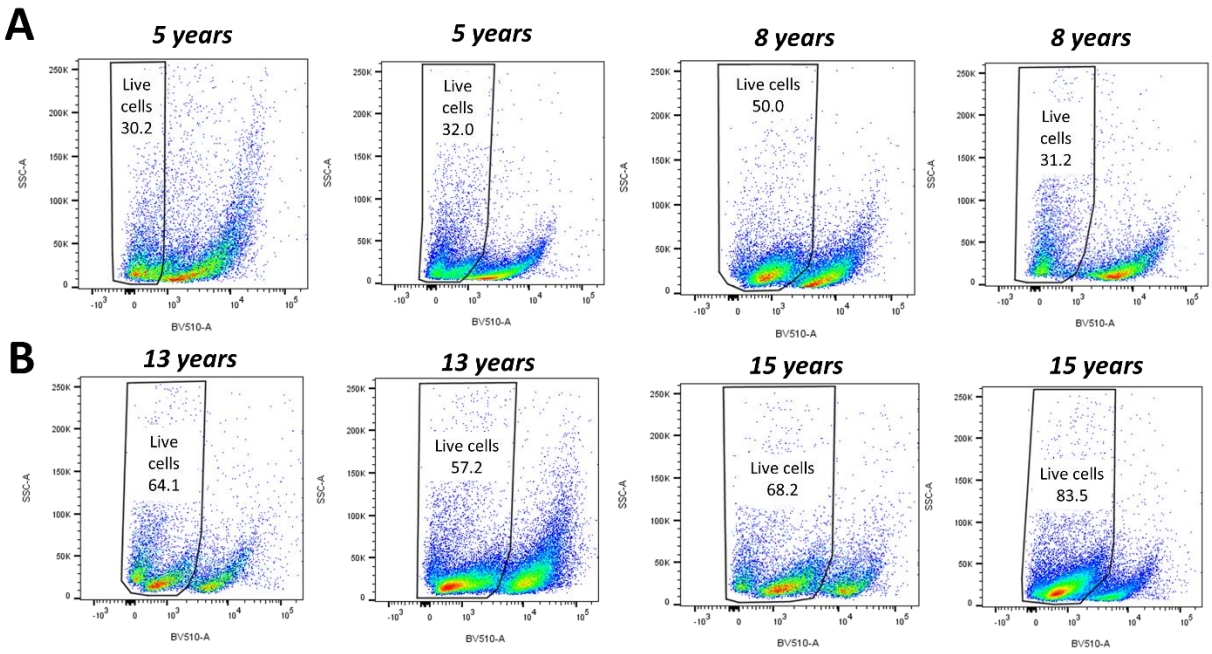



**Figure 5. 16 Viability of cells from human frozen/thawed ovarian cortical tissue measured by FC.** Dissociated cells from pre-pubertal (A) and post-pubertal (B) patients were incubated with ZA and displayed on SSC-A versus ZA (BV510-A) density plots. Live cells were gated based on the exclusion of ZA. Data shows the percentage of viable cells (live cells) for each patient. ZA: zombie aqua; SSC-A: side scatter area; BV510-A: brilliant violet 510 area.

Even though the same number of frozen/thawed cortical strips were used per patient (4 strips), the total number of single cells identified using FC varied from 11,000 to 47,000 single cells (Table 5. 8).

**Table 5. 8 Viability of cells from human frozen/thawed ovarian cortical tissue measured by FC.** Cells from Pre-pubertal and Post-pubertal patients were incubated with ZA and viable cells were determined by excluding dead cells as measured by FC. Data shows the precentage and number of viable (blue) as well as total single cells analysed for each patient. ZA: zombie aqua.

| | Pre-pubertal | | | |
|---|---|---|---|---|
| | **5-years** (Patient 25) | **5-years** (Patient 26) | **8-years** (Patient 27) | **8-years** (Patient 28) |
| **% of VIABLE single cells** | 30.2 | 32.0 | 50.0 | 31.2 |
| **Number of VIABLE single cells** | 4,679 | 8,140 | 12,552 | 3,989 |
| **Number of TOTAL single cells** | 15,493 | 25,444 | 25,103 | 12,791 |
| | **Post-pubertal** | | | |
| | **13-years** (Patient 29) | **13-years** (Patient 30) | **15-years** (Patient 31) | **15-years** (Patient 32) |
| **% of VIABLE single cells** | 64.1 | 57.2 | 68.2 | 83.5 |
| **Number of VIABLE single cells** | 6,832 | 25,267 | 9,997 | 39,148 |
| **Number of TOTAL single cells** | 10,662 | 44,154 | 14,661 | 46,887 |

To investigate if the difference in live-cell yield was significant, cell viability (%) in pre-pubertal patients was compared with post-pubertal patients. Cell viability was significantly compromised (p=0.005) in the pre-pubertal group (36±10%) compared to post-pubertal group (68±11%) (Figure 5. 17). This finding is in accordance with results in Chapter 4 where live-cell yield was assessed using a Trypan Blue assay and manual cell counts in frozen/thawed cortex from post-pubertal patients (Figure 4. 6B page 133).

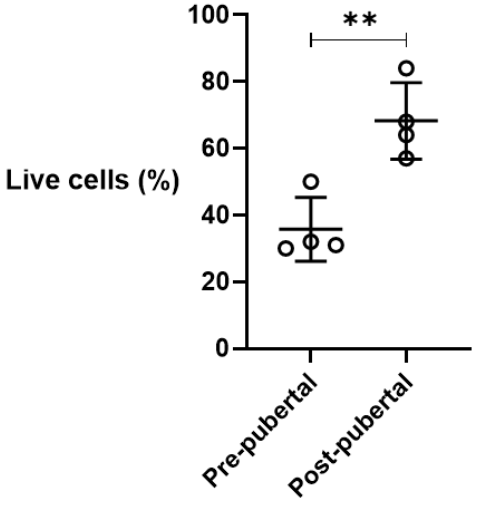



**Figure 5. 17 Viability of cells from pre-pubertal and post-pubertal frozen/thawed ovarian cortical tissue measured by FC.** Dissociated cells were incubated with ZA to exclude dead cells. Data shows the percentage (%) of live cells (mean±SD) in pre-pubertal (n=4) and post-pubertal patients (n=4). **P≤0.01.

This analysis demonstrated that despite the variation in the viable single cell population detected in frozen/thawed cortical tissue samples obtained from pre- and post-pubertal patients, a population of viable cells was isolated in which intracellular DDX4 could be explored.

### 5.4.3.3. Detection of DDX4-positive cells from human frozen/thawed ovarian cortical tissue

Having established a FC method to detect intracellular DDX4 in cells isolated from fresh human ovarian remnant tissue (Figure 5. 12 page 179), the same method was applied to cells from frozen/thawed ovarian cortex. Data was displayed on a SSC-A versus FSC-A density plot to identify the main cell population and remove any doublets. Using the 'Unlabelled' control, the ZA-negative cell population was gated, and this gate was then applied to the isotype control 'IgG1 + RPE' (Figure 5. 18A) and 'DDX4 + RPE' sample (Figure 5. 18B) to detect viable (ZA-negative) cells. Viable cells in the 'IgG1 + RPE' were

displayed on an SSC-A versus IgG1-PE dot plot and a gate was drawn to include ~1% of the population (Figure 5. 18C). This gate was then applied to the 'DDX4 + RPE' sample to detect viable DDX4-positive cells (Figure 5. 18D).

Figure 5. 18 shows representative data of a frozen/thawed cortical tissue sample obtained from an 8-year-old patient (patient 27, Table 4. 2 page 124) whereby 64.2% of viable single cells isolated from frozen/thawed ovarian cortical tissue was labelled positive for the intracellular marker DDX4.

Gating of the isotype control ('IgG1 + RPE') sample for all patients is presented in Appendix IIb (Supplementary Figure 8).

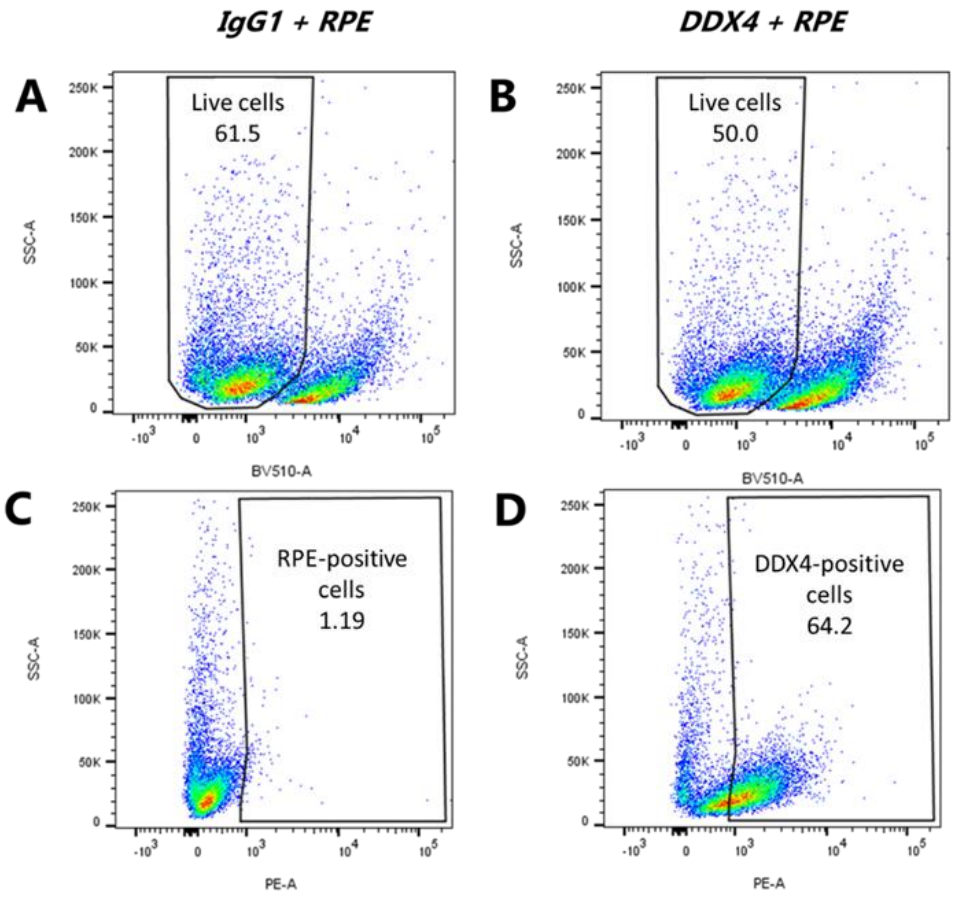



**Figure 5. 18 FC gating strategy to detect DDX4-positive cells from human frozen/thawed ovarian cortical tissue.** Cells from a post-pubertal patient (8-year-old, patient 27) were incubated with ZA and labelled with anti-IgG1 ('IgG1 + RPE') or anti-DDX4 ('DDX4 + RPE'). Viable single cells in the (A) 'IgG1 + RPE' and (B) 'DDX4 + RPE' sample were displayed on a SSC-A versus DDX4-PE (PE-A) density plot. Using the 'IgG1 + RPE', a gate was drawn to include ~1% of the population (C). The same gate was applied to the 'DDX4 + RPE' (D) sample to determine the percentage of DDX4-positive cells. Data shows the percentage of live cells or positive cells. ZA: zombie aqua; SSC-A: side scatter area; BV510-A: brilliant violet 510 area; PE-A: R-Phycoerythrin area; RPE: secondary antibody conjugated to R-Phycoerythrin.

The gating strategy described above was used to detect intracellular DDX4-positive cells in all patient samples (n=8). DDX4-positive cells were detected in both pre-pubertal and post-pubertal patients (Figure 5. 19). The percentage of DDX4-positive cells in one 8-year-old and one 15-year-old patient was very low (Figure 5. 19).

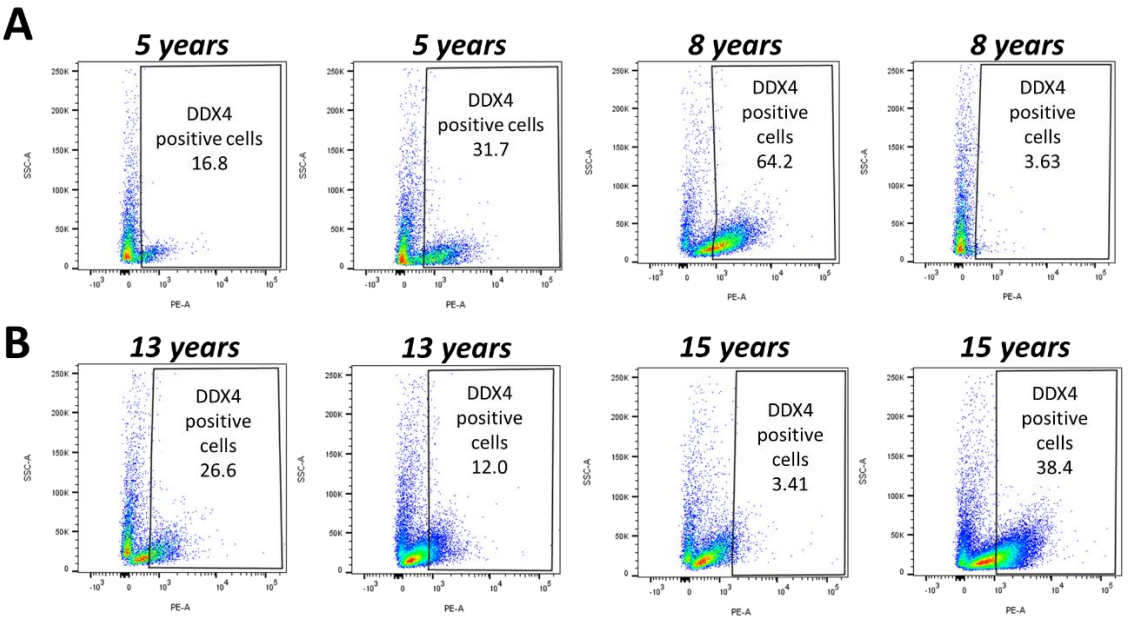



**Figure 5. 19 Percentage of DDX4-positive cells from frozen/thawed cortical tissue measured by FC.** Dissociated cells from pre-pubertal (A) and post-pubertal (B) patients were labelled with anti-DDX4 and displayed on SSC-A versus DDX4-PE (PE-A) density plots. DDX4-positive cells were gated based on the isotype control 'IgG1 + RPE'. Data shows the percentage of DDX4-positive cells analysed for each patient. SSC-A: side scatter area; PE-A: R-Phycoerythrin area; RPE: secondary antibody conjugated to R-Phycoerythrin.

The percentage of DDX4-positive cells identified across all samples was highly variable, ranging from 3.6-64.2% in the pre-pubertal group, and 3.4-38.4% in the post-pubertal group (Table 5. 9). The number of DDX4-positive cells also varied within the samples ranging from 145-8,063 in pre-pubertal patients and 341-15,029 in post-pubertal patients (Table 5. 9).

**Table 5. 9 DDX4-positive cells from human frozen/thawed ovarian cortical tissue measured by FC.** Dissociated cells from Pre-pubertal and Post-pubertal patients were labelled with anti-DDX4. DDX4-positive cells were detected based on the 'IgG1 + RPE' sample'. Data shows the percentage and number of DDX4-positive cells (pink/orange) as well as the number of viable single cells (blue) analysed for each patient.

| | Pre-pubertal | | | |
|---|---|---|---|---|
| | **5-years** (Patient 25) | **5-years** (Patient 26) | **8-years** (Patient 27) | **8-years** (Patient 28) |
| **% of DDX4-positive cells** | 16.8 | 31.7 | 64.2 | 3.63 |
| **Number of DDX4-positive cells** | 784 | 2,578 | 8,063 | 145 |
| **Number of VIABLE single cells** | 4,679 | 8,140 | 12,552 | 3,989 |
| | **Post-pubertal** | | | |
| | **13-years** (Patient 29) | **13-years** (Patient 30) | **15-years** (Patient 31) | **15-years** (Patient 32) |
| **% of DDX4-positive cells** | 26.6 | 12.0 | 3.41 | 38.4 |
| **Number of DDX4-positive cells** | 1,819 | 3,032 | 341 | 15,029 |
| **Number of VIABLE single cells** | 6,832 | 25,267 | 9,997 | 39,148 |

Further analysis was performed to investigate if pubertal status affected the percentage of DDX4-positive cells. There was no difference in the percentage of DDX4-positive cells in pre- and post-pubertal patients as measured using FC (Figure 5. 20).

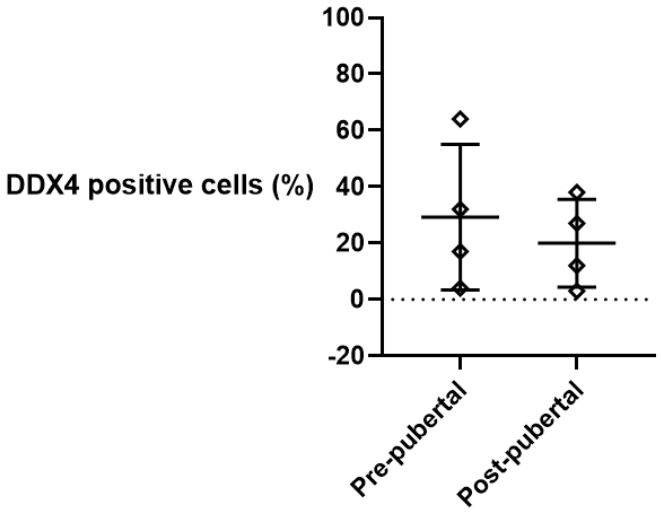



**Figure 5. 20 The effect of pubertal status on DDX4-positive cells from human frozen/thawed ovarian cortex as measured by FC.** Cells were labelled with anti-DDX4 to detect intracellular DDX4. Data shows the percentage of viable single cells that were positive for intracellular DDX4 (mean±SD) in pre-pubertal (n=4) and post-pubertal patients (n=4).

Overall, DDX4 positive cells were detected in viable cell populations in both the pre- and post-pubertal samples obtained from human fresh ovarian remnant tissue and human frozen/thawed ovarian cortex.

## 5.5. Discussion

### 5.5.1. Overview

In this chapter, a FC method was developed to label the cytoplasmic germ cell marker DDX4 in an ovarian single cell suspension obtained from human fresh ovarian remnants or frozen/thawed ovarian cortex after dissociation (Chapter 4). Detecting DDX4-positive cells (germ cells) in the ovarian single cell suspension would enable further development of methods to isolate this DDX4-positive cell population (germ cells) and generate a RO. Using HeLa cells, it was possible to explore many variables in order to develop an immunolabelling method and a FC gating strategy that was then applied to ovarian cells obtained from fresh remnant tissue. Although remnant tissue is not an ideal cell source for developing fertility preservation methods, it is readily available from young patients. What is more, because different cell types, such as HeLa and ovarian cells, might require different permeabilisation/fixation methods, testing of the permeabilisation/fixation method, which was previously used for HeLa cells, on ovarian cells was critical for this study. Therefore, fresh ovarian remnant tissue was useful to develop a FC method for detection of intracellular DDX4, which was then used to analyse the frozen/thawed ovarian cortical tissue in pre- and post-pubertal samples.

### 5.5.2. Establishment of a flow cytometry gating strategy to detect the intracellular germ cell marker DDX4

There has been much controversy over the effectiveness and specificity of a polyclonal DDX4 antibody commonly used by several groups to detect cell surface DDX4 on putative OSCs (White et al. 2012; Stimpfel et al. 2013; Silvestris et al. 2018; Clarkson et al. 2018). Commercial availability and use of anti-DDX4 antibodies have been thoroughly

discussed (Section 5.1.1.3 and 5.1.2.1). Observations from these studies suggest that this polyclonal antibody is non-specific in relation to the intended target protein (DDX4). What is more, as discussed, in comparison to polyclonal antibodies, monoclonal antibodies only recognise a single epitope per antigen and thus, they are less likely to cross-react with other proteins. For the above reasons, it was decided not to use the ab13840 polyclonal antibody, and instead used a mouse monoclonal antibody that was raised against the N-terminus region of the human DDX4 protein. To our knowledge, this is the first time this antibody has been used for the detection of intracellular DDX4 from human ovarian tissue samples using FC. Despite the controversial localisation (intracellular or cell surface) of the C-terminus region in the DDX4 protein in putative OSCs in the human adult ovary, it is well established that DDX4 is a cytoplasmic protein expressed in oocytes at all stages of follicle development in many species including mouse (Toyooka et al. 2000) and human (Castrillon et al. 2000). Therefore, regardless of the existence of a germ cell-surface DDX4 epitope in the young and/or adult human ovarian cells, in this study, the monoclonal anti-DDX4 antibody was used to detect primarily oocytes and not OSCs; though, should there be any OSCs, the antibody would likely detect them too.

To our knowledge, there is no published method for intracellular DDX4 labelling of cells from human frozen/thawed ovarian cortical tissue samples. Therefore, it was crucial to develop and optimise labelling of cytoplasmic DDX4 and a FC gating strategy. HeLa cells were identified as an ideal positive control and were used to first demonstrate that dead cells can be identified using the fluorescent dye ZA. Furthermore, the fixation/permeabilisation method was effective at labelling both cytoplasmic

cytokeratin 13 and DDX4 in fixed/permeabilised HeLa cells. DDX4 detection was negligible on non-permeabilised HeLa cells, therefore demonstrating that DDX4 was cytoplasmic specific in these cells.

Viable DDX4 populations were detected in human ovarian remnant tissue samples by applying the methodology developed using HeLa cells to label intracellular DDX4. Despite the low number of total cells analysed in some remnant samples (Not Digested), a population of viable cells that labelled positive for intracellular DDX4 was detected in pre- and post-pubertal patients. Using the same FC gating strategy, a viable cell population positive for intracellular DDX4, was also detected in frozen/thawed cortical tissue samples from pre- and post-pubertal patients.

Differences in the number of viable cells and the number of DDX4-positive cells between remnant tissue samples might be due to differences in the patient age; the older the patients the bigger the ovary and thus, potentially more tissue available. For frozen/thawed ovarian cortical tissue samples, even though the same number of strips were used, tissue weight was slightly variable (data not shown). This may explain the difference in the number of total cells isolated per patient and the high variation of viable DDX4 positive cells observed between patients. Furthermore, inter-patient variation and heterogeneity within human ovarian tissue (Schmidt et al. 2003; Walker et al. 2019) should also be considered as a variation factor in this investigation.

### 5.5.3. Verification of the specificity of the monoclonal anti-DDX4 antibody used

The monoclonal anti-DDX4 antibody was first validated in our laboratory on human ovarian cortical tissue sections using immunohistochemistry. Colleagues in the laboratory, demonstrated that the anti-DDX4 antibody was oocyte-specific (data not shown). However, since this antibody had not been used before to detect germ cells using FC, further investigation should be undertaken to validate the specificity of this antibody and thus, confirm the existence of oocytes positive for cytoplasmic DDX4 in the ovarian single cell suspension as well as the existence of cytoplasmic DDX4 in HeLa cells.

Mass spectrometry (MS) in combination with immunoprecipitation (IP) would be a useful method to help determine whether the anti-DDX4 antibody is specific for the intended target protein. After cell lysis of human ovarian and HeLa cells, and immunolabelling using the antibody of interest (in this case anti-DDX4), IP would be used to enrich antibody-target antigen complexes in the precipitate and prepared for MS analysis (Patel et al. 2016). MS allows for the verification of an antibody target, and in contrast to other applications commonly used for antibody validation such as Western Blot (WB), MS can also identify isoforms, post-translational modifications, and target-associated proteins present within a sample using proteomic analysis (Dunham et al. 2012; Angel et al. 2012). What is more, quantitative assessment of the binding specificity can be performed with MS by calculating the fold-enrichment of targets and off-targets (Patel et al. 2016); this method could provide valuable information on the effectiveness of the antibody to detect intracellular DDX4 in a given cell sample.

To validate the specificity of the antibody with two-dimensional sodium dodecyl sulphate polyacrylamide gel electrophoresis (2D SDS PAGE) and MS, cell lysates from human ovarian cells and HeLa cells would be separated according to their isoelectric point (Pearson et al. 1980) (first dimension) and molecular mass (Weiland et al. 2014) (second dimension) (Kendrick et al. 2019). After protein separation, WB using the antibody of interest (in this case anti-DDX4) can be performed. Bands formed on the WB membrane indicative of the identified proteins can be excised and further analysed with MS (Kendrick et al. 2019; Luque-Garcia et al. 2009) as described above.

The specificity of this antibody for FC can be validated by transfecting the DDX4 protein into human cells known not to express this protein. Having confirmed anti-DDX4 antibody specificity in relation to the intended target protein (DDX4) as discussed above, the DDX4 protein could be isolated from HeLa cells. Following this, the DDX4 protein can then be transfected into human dermal fibroblasts or human kidney cells (HEK 293 cells), which do not express the endogenous DDX4. Detection of the DDX4-positive transfected cells with FC could validate this antibody for FC.

### 5.5.4. Further assessment of the DDX4-positive cell population

While it is well established that human DDX4 is localised in the cytoplasm of the oocyte, there is evidence that DDX4 is also implicated in rapid cell cycle in ovarian cancer and blood-derived cancer cells as discussed. However, donors with ovarian diseases and/or blood-derived cancer were excluded from this study, and therefore it is unlikely that the DDX4-positive cells detected in this study were implicated in ovarian and blood cancer.

Van den Brink et al. reported that DDX4 was also expressed in embryonic somatic cells in response to tissue damage and wound healing as a cell cycle regulator in urchin (Yajima et al. 2015). Also, it has been shown that enzymatic dissociation of tissues affects the transcriptome by up-regulating genes including heat-shock proteins (HSPs) and immediate-early gene products (IEGs) (van den Brink et al. 2017). These findings suggest that dissociation can trigger changes to the cell transcriptome, and therefore, dissociation of human ovarian remnant or frozen/thawed ovarian cortical tissue may trigger DDX4 expression in some non-germ ovarian cells.

In addition to the above information, it is critical to confirm that the monoclonal anti-DDX4 antibody used in this thesis is specific to oocyte DDX4. This could be addressed by FC using oocyte and somatic cell-specific markers informed by Wagner et al. who performed single cell transcriptomic analysis of human frozen/thawed ovarian cortex (Wagner et al. 2020). They showed that 6 clusters of ovarian cell types were identified in the single cell suspension; stroma/theca cells, perivascular, endothelial, granulosa, immune cells and oocytes (Wagner et al. 2020). In these clusters, signature genes were identified with high expression for each cell cluster; *GDF9* and *FIGLA* in oocytes, *CD69* and *ITGB2* in immune cells, *AMH* and *FOXl2* in granulosa cells, *CD34* and *VWF* in endothelial cells, *MYH11* and *MCAM* in perivascular (pericyte) cells, *PDGFRA* and *DCN* in stroma/theca cells (Wagner et al. 2020). Using the above markers in FC analysis we could explore cell populations (e.g. stroma, granulosa, perivascular etc.) and more specifically if an oocyte population can be identified in the ovarian single cell suspension obtained from human remnant tissue and human frozen/thawed ovarian cortex.

Additionally, using of the monoclonal DDX4 antibody alongside these markers, we could explore if the DDX4 population detected in this study is a pure oocyte population.

Despite the valuable contribution of single cell transcriptome analysis, isolation of viable oocytes for downstream analysis, as required for generation of the RO, cannot be achieved with this technique. One such method to enable the isolation of viable oocytes is FACS analysis (Adan et al. 2017) using cell surface markers. FACS is a specialised form of FC that allows for sorting of the cell populations of interest identified using either intracellular or cell surface markers. Labelling of cell surface markers does not require fixation/permeabilisation and thus allows for downstream culture (a prerequisite for RO generation) of viable cell populations in contrast to intracellular markers whereby cells are permeabilised. The antibody used in this study, DDX4, is an intracellular marker and therefore oocyte-specific surface markers need to be identified. Specific surface markers would enable the identification and sorting of oocytes using FACS which could then be used for generating a RO. Identification of cell surface markers could be addressed by performing single cell RNA-sequencing and transcriptomic analysis of the ovarian cell suspension, obtained from human ovarian remnants or human frozen/thawed ovarian cortex, to identify genes differentially expressed in each cell population as discussed above (Wagner et al. 2020). This way, we could identify potential cell surface markers informed by human membrane-related proteins databases (Fagerberg et al. 2010; Apweiler et al. 2009; Saier et al. 2019). Additionally, to explore if these potential surface markers are differentially expressed in cell clusters identified in the ovarian single cell suspension, FC analysis could be used to identify co-expression of these potential cell surface markers and intracellular signature markers

such as DDX4. Thus, we could confirm if these cell-surface specific proteins are expressed in the oocyte population and other cell clusters within the ovarian single cell suspension to allow for future sorting of positive populations using FACS (Adan et al. 2017), and downstream analysis for generating a RO.

#### 5.5.4.1. Perivascular cells in the ovarian cell suspensions analysed

In this analysis, the percentage of DDX4-positive cells detected in the fresh ovarian remnant samples and frozen/thawed ovarian cortical tissue samples was higher than the oocyte population detected by Wagner using single-cell transcriptomic analysis for human frozen/thawed ovarian cortical tissue samples (Wagner et al. 2020). Despite the age difference in patients included in this study (mean age of patients was 11.3±7.2 years for remnant groups and 15.7±7.9 for frozen/thawed cortex) compared to those in Wagner et al. (mean age of 34 years) (Wagner et al. 2020), validation of the specificity of the anti-DDX4 antibody used is required as discussed. Wagner et al. demonstrated that the ab13840 polyclonal antibody is not specific to oocytes and can bind to non-permeabilised perivascular cells, specifically pericytes and smooth muscle cells (Wagner et al. 2020). Smooth muscle cells surround large vessels such as arteries and veins and pericytes surround endothelial cells in capillaries, venules and arterioles (Avolio et al. 2017). Therefore, since the medulla of the human ovary is a highly vascularised area, it is likely that the ovarian cell suspensions obtained from fresh remnant tissue samples in this study contained perivascular cells. Thus, to test if the monoclonal antibody used in this thesis also labels perivascular cells, immunolabelling of perivascular cell lines (e.g. pericytes) could be performed using both anti-DDX4 antibodies (monoclonal anti-DDX4 and polyclonal (ab13840) anti-DDX4) and the data compared.

### 5.5.5. Pubertal status did not affect DDX4 labelling

DDX4-positive cells were observed in pre- and post-pubertal patients and there was no difference in the percentage of viable DDX4 cells between the two groups for both fresh remnants and frozen/thawed cortex. These findings are not aligned with the consensus that the number of germ cells declines with age and thus, a larger DDX4 cell population is expected in the pre-pubertal group.

There was a large degree of variation in DDX4-positive cells and total cell numbers, in the current study. Interpatient variation and heterogeneity within patients have been demonstrated using frozen/thawed ovarian cortex (Schmidt et al. 2003; Walker et al. 2019). However, the main objective of this study was to establish a FC method to detect DDX4-positive cells from frozen/thawed ovarian cortical tissue samples. This aim was achieved using a small cohort of patients (n=8).

### 5.5.6. Barriers to this study

In this thesis, although a FC method to detect viable DDX4-positive cells was successfully developed, there are some restricting factors that should be considered for future studies. Since all individuals who donated tissue to this study had a medical condition this might have biased the results in some way, for example by affecting cell viability. However, availability of healthy ovarian tissue is often limited in research and tissue from patients undergoing fertility preservation is the only source of ovarian tissue. Furthermore, the incomplete dissociation of follicles was not examined and thus, it is possible that follicles remained within the cell suspension. Future work could include examining the cell suspension isolated after tissue dissociation. This could be addressed by performing immunocytochemistry of an ovarian cell suspension to detect oocyte and

granulosa cell-specific markers (i.e. GDF-9 for oocytes and AMH for granulosa cells) as well as transzonal projections (i.e. actin). Moreover, using permeabilised and non-permeabilised HeLa cells, it was confirmed that immunolabelling of the cytoplasmic DDX4 was successful; this was not tested in ovarian cells as only permeabilised cells were used in this study due to small number of cells. This should also be examined in future investigations.

### 5.5.7. Conclusions

In this chapter, I developed a FC method to detect intracellular DDX4 in cells from ovarian tissue samples. Despite the high variability in the number and percentage of DDX4-positive cells observed in human ovarian remnants and human frozen/thawed ovarian cortex between patients, DDX4-positive cell populations were detected in both pre- and post-pubertal samples. Findings from this chapter, will feed into future studies towards developing a method to isolate viable human germ cells using FACS to generate a RO. Furthermore, this chapter will contribute to deepening our understanding of the number and features of germ cells that can be detected in a human ovarian single cell suspension obtained from pre- and post-pubertal remnant or frozen/thawed cortical tissue samples in future.

# CHAPTER 6

# *Exploring an alternative source of human somatic cells to support germ cell development in vitro*

## 6.1. Introduction

### 6.1.1 Background

Although many causes for POI have been identified (i.e. genetic factors, autoimmune or iatrogenic causes and infections), the aetiology of the majority of the cases remains unknown (idiopathic POI) as discussed in Chapter 1. In idiopathic POI with follicle dysfunction (follicular POI) follicles at different stages of development are present in the ovaries but are unable to complete development due to a pathological process leading to premature infertility, before the age of 40 years (Suzuki et al. 2015; Jewelewicz et al. 1986; Nelson et al. 1994; Meskhi et al. 2006).

Our group previously investigated the mechanisms of POI using a mouse model of POI; the DM (discussed in Chapter 1). Colleagues found that follicle development was blocked at the primary stage in DM ovaries, as indicated by an increased number of

abnormal primary follicles (Kaune et al. 2017). Interestingly, follicle development was enabled *in vivo* if the dysfunctional somatic cells obtained from infertile DM mice (9-week-old) were replaced with wild type (WT) neonatal somatic cells using the Reaggregated Ovary (RO) method (unpublished data) (Figure 6. 1A). These data suggest that the germ cells in a POI mouse model maintain their ability to develop and that follicle development can occur if the dysfunctional somatic cells are replaced *in vitro* using the RO technique.

In addition to the usefulness of the RO method to explore follicle dysfunction in the DM ovaries, this technique has been used in our laboratory to explore follicle development *in vitro* as well as *in vivo* (Lo et al. 2019). In a neonatal WT RO (comprised of wild type germ and somatic cells), follicles reached the preantral stage after 14 days in culture and the antral stage after 21 days *in vivo* (Lo et al. 2019) (Figure 6. 1B). Moreover, follicle development was also demonstrated in WT ROs *in vivo* (unpublished data) where either the germ cells or the somatic cells were obtained from neonatal mice (i.e. adult WT germ cells aggregated with neonatal WT somatic cells and vice versa) (Figure 6. 1C).

In previous chapters, investigations were presented with the aim of isolating human germ cells. Here, the potential of an alternative source of human somatic cells to replace granulosa and theca cells was investigated, that can be obtained straightforwardly compared to invasive methods, and are capable of differentiating (human dermal fibroblasts (HDFs); rationale described below), to support follicle formation and development *in vitro* using the RO method (Figure 6. 1).

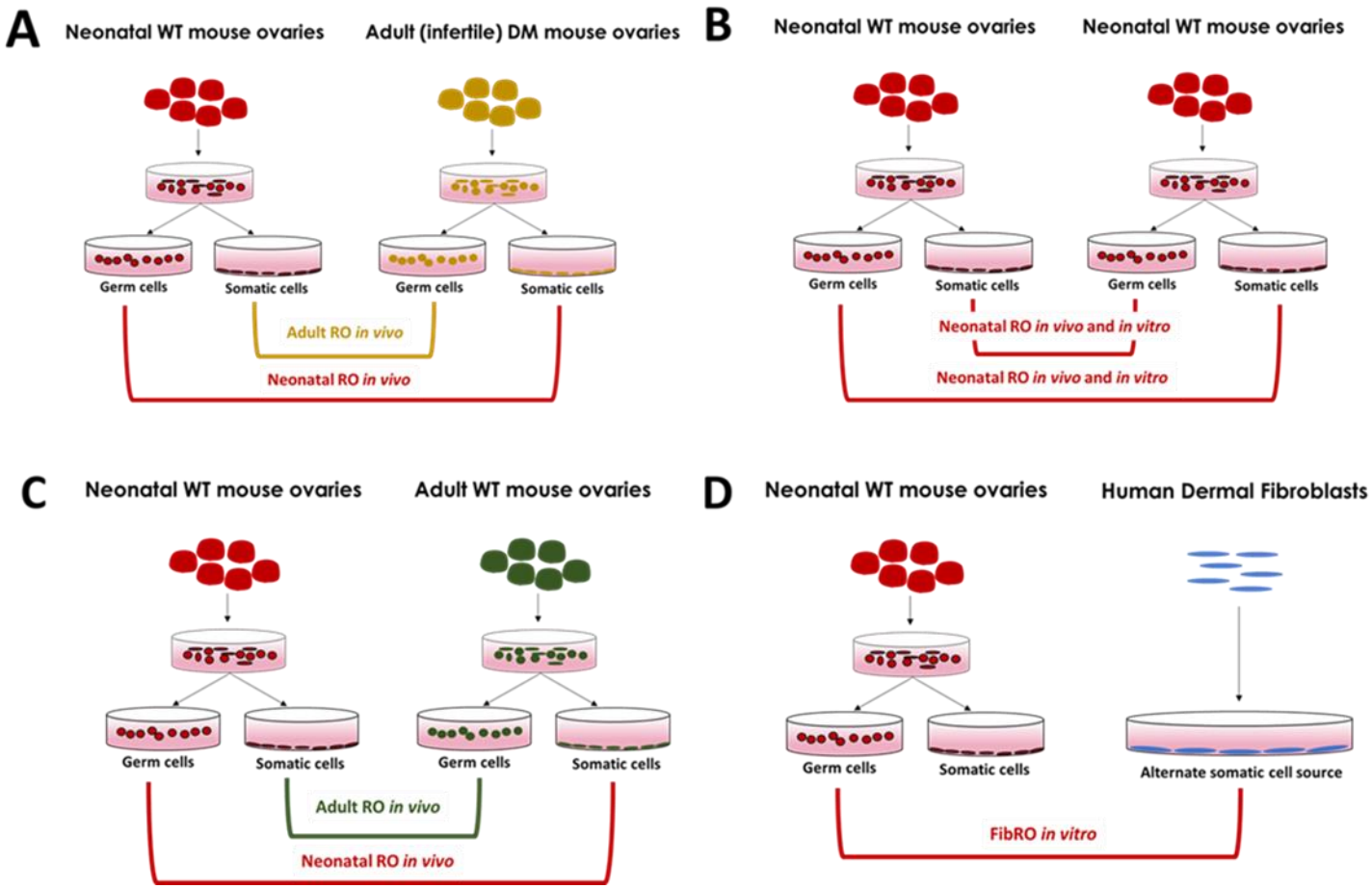



**Figure 6. 1 Overview of different types of RO used in our laboratory.** (A) Neonatal WT mouse germ cells were aggregated with adult DM mouse germ cells and vice versa to generate DM ROs *in vivo*. (B) Neonatal WT mouse germ cells were aggregated with neonatal WT mouse somatic cells and vice versa to generate ROs *in vivo* and *in vitro*. (C) Neonatal WT mouse germ cells were aggregated with adult WT mouse somatic cells and vice versa to generate ROs *in vivo.* (D) Neonatal WT mouse germ cell were aggregated with human dermal fibroblasts to generate FibROs *in vitro.*

### 6.1.2 The 'artificial ovary'

The 'artificial ovary' could be characterised as an umbrella term as it is used to cover a broad category of methodologies, such as the Reaggregated Ovary (RO), Reconstituted Ovaries and 3-dimensional (3D) scaffolds (encapsulated ovarian follicles in biomaterials; these are discussed below.

*Reaggregated Ovary (RO) and Reconstituted Ovary (rOvary)*

The RO, as discussed previously (Section 6.1.1 and 6.1.2), refers to the generation of xenogeneic or allogenic follicles comprised of ovarian cells (e.g. granulosa, theca cells, stroma cells, and germ cells) that had been separated before being recombined. Eppig et al. (2002), using the RO method, demonstrated that the oocyte orchestrates follicle development in mice (Eppig et al. 2002). Oocytes isolated from secondary follicles were aggregated with somatic cells from primordial follicles, the earliest stage of follicular development. These aggregates (ROs) were transplanted into immunocompromised and ovariectomised mice (Eppig et al. 2002). Differentiation of follicular somatic cells and accelerated follicle development was observed in these ROs, and the oocytes were developmentally competent and underwent fertilisation and embryonic development (Eppig et al. 2002). The RO method as described by Eppig et al. (Eppig et al. 2000) has been used by others to investigate follicle development (Park et al. 2006; Gittens et al. 2005).

In another study, Matoba et al. using the RO method showed that primordial germ cells can give rise to developmentally competent oocytes *in vitro* in a RO (Matoba et al. 2011). Gonadal ridges isolated from mouse embryos were dissociated into single cell suspensions (primordial germ cells and gonadal somatic cells) that were then

recombined to form reaggregated ovaries (ROs) (Matoba et al. 2011). These aggregates were transplanted under the kidney capsule in ovariectomised female mice (Matoba et al. 2011). Ovary-like structures were formed within 4 weeks *in vivo* and contained antral follicles (Matoba et al. 2011). These antral follicles generated developmentally competent oocytes and after IVM and ICSI, embryos were generated and transplanted into recipient mothers that gave birth to normal mice (Matoba et al. 2011).

Hikabe et al. reported successful oogenesis *in vitro* in a reconstituted ovary (rOvary) that was generated using mouse embryonic stem cells or induced pluripotent stem cells; iPSCs (to make germ cells) and somatic cells from the gonads of mouse embryos (Hikabe et al. 2016). These iPSCs were generated *in vitro* from mouse embryonic fibroblasts or mouse adult tail tip fibroblasts (Hikabe et al. 2016). Immature oocytes were generated in these rOvaries which were matured (IVM), fertilised (ICSI) and produced embryos *in vitro* (Hikabe et al. 2016). These embryos were transferred into female mice who delivered viable pups (Hikabe et al. 2016).

*Scaffolds*

Auto-transplantation of cryopreserved ovarian tissue is the only available fertility preservation method for pre-pubertal patients undergoing chemotherapy as discussed in Chapter 1. However, this approach has limitations with a potential risk of reintroducing malignant cells in patients who recovered from cancer (Dolmans et al. 2013). The 'artificial ovary' containing isolated follicles placed in a scaffold to provide 3D support could potentially facilitate transplanting in the human body (Cho et al. 2019). This approach could eliminate the risk of reintroducing cancerous cells (e.g. blood-derived cancer) into the patient as non-follicular ovarian cells would not be

transplanted. Using this method, not only would follicle development re-occur, but ovarian function could be restored (Cho et al. 2019). Xu et al. showed that secondary follicles from cancer patients could grow to antral follicles in a bio-engineered alginate culture system for 30 days (Xu et al. 2009). Follicles were steroidogenically active, and contained growing oocytes that were connected by transzonal projections with the somatic cells (Xu et al. 2009).

The above findings demonstrate the potential of the 'artificial ovary' in human reproduction. The 'artificial ovary' is a useful tool to explore follicle development and develop methods to preserve fertility for patients that do not benefit from current treatments. This chapter suggests developing the RO method using human ovarian tissue and an alternative source of human somatic cells (discussed below) to replace the dysfunctional ovarian somatic cells and restore follicle development in patients with POI, and follicle dysfunction.

### 6.1.3 Germ cell source

Eppig and Wigglesworth (2000) showed that female mouse germ cells (i.e. oocytes) developed into fertilisable eggs within xenogeneic follicles using the RO method (Eppig et al. 2000). Mouse germ cells and rat somatic cells were cleanly separated from ovaries using differential adhesion (routinely used in the RO method), and reaggregated to generate a chimeric RO, and vice versa. These ROs were transplanted into ovariectomised, immunocompromised mice to facilitate follicle development and chimeric follicles were formed with oocytes reaching the MII stage. In the chimeric ROs containing mouse oocytes and rat somatic cells, fertilisable mouse eggs were generated

within the chimeric follicles and resulted in the birth of one healthy female pup. This animal later produced 83 normal offspring (Eppig et al. 2000).

Other species have also been used to demonstrate follicle development in chimeric ROs. Ovarian cells from cats have been aggregated with mouse cells and follicle development occurred (personal correspondence between Prof Williams and Karen Wigglesworth). Moreover, work at our laboratory has resulted in follicle development in ROs containing bovine oocyte-like stem cells and mouse somatic cells.

No studies using human ovarian cells in a RO have been reported yet, likely due in part to challenges in separating the somatic and germ cell populations. Our group has observed insufficient differential adhesion of human somatic cells (data not shown) as opposed to mouse where effective differential adhesion of mouse somatic cells ensures a clean germ and somatic cell population. Therefore, to explore human somatic cells that can support follicle development *in vitro* in RO, it was decided to use mouse germ cells which have been demonstrated to be supported by other species and are a known entity, before using human germ cells. To this end, this study investigated the potential of human dermal fibroblasts (discussed below) to support mouse germ cell development *in vitro* using the RO method.

### 6.1.4 The potential of human dermal fibroblasts

To explore an alternative source of human somatic cells to support human germ cell development, there were two main considerations. Firstly, it was essential that cells were capable of differentiating, so they could potentially differentiate or de-differentiate into granulosa-like and theca-like cells. Secondly, obtaining the cells must

be straightforward and relatively easy in order to allow for eventual clinical application of this method. Human dermal fibroblasts (HDFs) met the above criteria; they are mesenchymal cells capable of differentiation and can be patient-derived using a primary cell culture obtained from a skin biopsy.

Dermal fibroblasts are localised in the dermis, the layer of the skin under the epidermis, that contains blood capillaries, sweat glands, hair follicles, nerve endings, etc. HDFs play a key role in the human body, whereby wound repair is the most well-known. In response to skin injury signals, secreted by the extracellular matrix (ECM), HDFs can migrate to the wound area and proliferate, produce collagen and/or differentiate into contractile myofibroblasts in order to aid rapid wound healing (Bainbridge 2013).

Despite the fact that it is the most abundant cell type in the human dermis, HDFs have not been defined as a completely differentiated somatic cell type due to lack of lineage-specific markers (Tracy et al. 2016). It is suggested that HDFs represent stromal cells that have not completely differentiated, and therefore, the fibroblast cell population is considered as a highly heterogenous and dynamic cell lineage (Tracy et al. 2016). Even within the dermis, fibroblast populations differ in their role and phenotype depending on the depth of dermis they are localised in. For instance, HDFs found in deeper layers of the dermis express less collagenase mRNA than those found closer to the epidermis (Tracy et al. 2016).

Aside from their well-known ability to differentiate into myofibroblasts, HDFs can be reprogrammed into induced pluripotent stem cells (iPSCs) *in vitro* (Takahashi et al. 2007). In Takahashi et al., iPSCs manifested similar characteristics with human

embryonic stem cells such as cell morphology, gene and cell surface antigen expression, as well as the capacity to form embryoid bodies and teratomas (Takahashi et al. 2007). Furthermore, these iPSCs could further differentiate into neural or cardiac somatic cells *in vitro* (Takahashi et al. 2007).

In a report by Hikabe et al. it was established that mouse embryonic or adult fibroblasts obtained from tail-tip biopsies are capable of de-differentiating into iPSCs *in vitro* (Hikabe et al. 2016). ROs (rOvaries) were generated by combining fibroblast-derived iPSCs with mouse embryonic somatic cells and cultured *in vitro*. Mature oocytes produced by dermal fibroblast-derived iPSC developed in the ROs indicating the RO culture is able to produce germ cells. After *in vitro* oocyte maturation and fertilisation, live pups were produced that were healthy and fertile (Hikabe et al. 2016).

This is evidence that dermal fibroblasts have the potential to de-differentiate and are able to produce other cell types *in vitro.* In this study, due to the ease of obtaining HDFs, this study explored whether HDFs aggregated with mouse germ cells were capable of forming follicle-like structures in response to oocyte signalling *in vitro* in a RO; hereafter, referred to as the fibroblast-RO (FibRO).

To determine if HDFs could function as granulosa-like cells in the FibRO and support follicle development, AMH was used as a marker to investigate if fibroblasts were able to acquire granulosa cell function such as expression of AMH *in vitro* in FibROs.

## 6.2. Aims

This chapter studied the potential of HDFs to support mouse germ cell development *in vitro* in a RO. As mentioned, because no studies using human germ cells existed, mouse germ cells were used, which have been well characterised in this method. Additionally, the RO method in mouse had been previously established in our laboratory. Mastery of the RO technique was first required demonstrating clean separation of germ and somatic cells as well as follicle development *in vitro* (Appendix III).

Therefore, the aims of this chapter were:

- To generate ROs using mouse germ cells and human dermal fibroblasts *in vitro*; fibroblast-ROs (FibROs)
- To investigate if follicle-like structures formed *in vitro* in FibROs
- To investigate if human dermal fibroblasts in a RO produce AMH

## 6.3. Materials and Methods

### 6.3.1. Source of cells to generate fibroblast-ROs

Mouse germ cells and HDFs were combined to make a FibRO *in vitro*. Mouse ovaries were obtained from C57xCD1 mice at postnatal day 7 and dissociated into single cells and the germ cells were isolated (Chapter 2).

HDFs (passage no. 13) from a 21-year-old male with no known condition were kindly provided by Janet Carver and Professor Joanna Poulton.

### 6.3.2. Human dermal fibroblast cell culture

HDFs were cultured in DMEM-High Glucose (D5796; Sigma) supplemented with 10% (v/v) FBS, 2 mM/L L-Glutamine (59202C; Sigma), 50 IU/ml Pen and 0.05 mg/ml Strep (P4458;Sigma) at 37°C in an atmosphere of 5% $CO_2$ with 95% air using T-25 culture filter flasks. Culture medium was replaced every 3 days. Cells at 80%-100% confluency were used to make a FibRO or split to maintain cell culture. To harvest cells the adhered cell monolayer was washed twice with Dulbecco's PBS (D8537; Sigma) supplemented with 1 mg/ml Bovine Serum Albumin (BSA), followed by incubation with 1 ml of trypsin 0.05%/EDTA (T4049; Sigma) for 1 min until all cells were dislodged off the bottom of the flask. To stop the trypsin-enzymatic reaction, 4 ml of medium M199 supplemented with 10% FBS was added and cells were centrifuged at 660 x g for 5 min as described (Chapter 2). The supernatant was discarded, and the cell pellet was resuspended in 200 µl of culture medium.

### 6.3.3. Generating Control-ROs and fibroblast-ROs *in vitro*

To generate a FibRO, germ cells were collected after dissociation of mouse ovaries obtained at postnatal day 7 and separated from somatic cells using differential adhesion as described (Chapter 2). Fibroblasts were harvested as described above (Section 6.3.2) and combined with mouse germ cells to form a pellet. Control ROs were generated using mouse germ cells reaggregated with mouse somatic cells (Chapter 2). To make a single Control-RO, a third of the germ cells obtained from 3 neonatal mouse ovaries were combined with all mouse somatic cells from 3 neonatal ovaries; this ratio is routinely used for neonatal ROs (Eppig et al. 2000). To make a single FibRO, a third of the germ cells obtained from 3 neonatal mouse ovaries were combined with 100,000 HDFs. The number of HDFs was determined based on previous work generating ROs in mice; the number of viable mouse somatic cells used per RO ranged from ~70,000 to ~300,000 (data not shown). Thus, it was decided to use an average of HDFs (100,000 cells/RO) to generate the FibRO.

To enhance cell cohesion, 6µl of Phytohemagglutinin (PHA-P; Sigma) at 5 mg/ml was added into 190 µl of the combined cells. The cell suspension was then centrifuged at 10,000 x g for 1 minute to form a 'pellet', the FibRO (or Control-RO). FibRO and Control-RO were transferred onto a polycarbonate transwell membrane (6.5 mm diameter, 0.4 µm pore; Corning, New York, USA) in a 24-well tissue culture treated plate (Corning Costar) as described (Chapter 2).

### 6.3.4. *In vitro* culture of Control-ROs and FibROs

To allow for follicle development, Control-ROs and FibROs were cultured *in vitro* for 7 or 14 days using the RO culture method (Chapter 2). Every 2 days, culture medium was replaced, and the Control-RO and FibRO were lifted off the membrane and re-centred on the membrane to facilitate the rounded structure.

### 6.3.5. Tissue fixation, Embedding and Sectioning

At the end of the culture period, Control-ROs and FibROs were collected, fixed in 10% neutral buffered formalin, embedded and serially sectioned (Chapter 2).

### 6.3.6. Histological analysis

FibROs and Control-ROs were processed for histological analysis using Haematoxylin only (Chapter 2).

Follicle formation was assessed in 7- and 14-day cultured FibROs on tissue sections analysed using imaging as described (Chapter 2). Follicle development was assessed in Control-ROs, follicles were counted, and follicle stage was determined as described (Chapter 2).

### 6.3.7. AMH detection using immunohistochemistry

Sections from FibROs and Control-ROs were used to detect AMH in follicle-like structures (FibROs) and follicles (Control-ROs). An indirect method of immunohistochemistry was used with the Avidin/Biotin-peroxidase Complex (ABC) to amplify the target antigen signal (Figure 6. 2). Sections of mouse ovary were used as a

positive control in these experiments. The reactivity of the AMH antibody with human granulosa cells was confirmed using human ovarian cortical tissue.

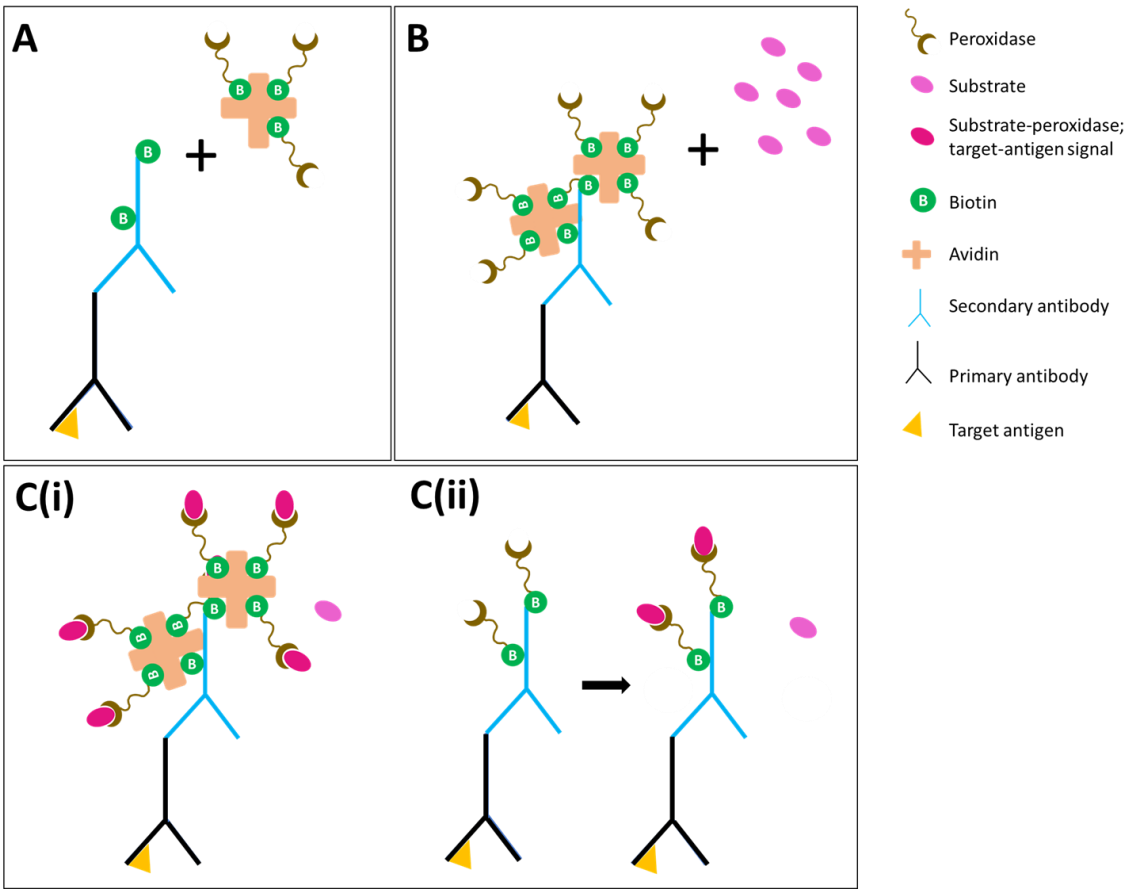



**Figure 6. 2 An illustration of the Avidin-Biotin-peroxidase Complex method of immunohistochemistry used to amplify the target antigen signal.** (A) Primary antibody (black) was bound to the target antigen (yellow), the primary antibody-target-antigen complex was conjugated to a biotinylated secondary antibody (blue), and the Avidin-Biotin-peroxidase complex (ABC) was added. (B) The ABC complex was bound to the biotinylated sites of the secondary antibody, and the peroxidase substrate; DAB solution (pink) was added. (C(i)) Peroxidase (Horseradish Peroxidase) catalyzes the substrate (3,3'-Diaminobenzidine; DAB) and a detectable signal (brown) was produced. If ABC is not used to amplify, then the target antigen can still be detected but the signal would be weak (C(ii)).

*Dewax and rehydration*

Sections were dewaxed in xylene solution and rehydrated in decreasing concentrations of ethanol (Table 6. 1) prior to immunolabelling.

**Table 6. 1 Solutions used to dewax and rehydrate tissue sections prior to immunohistochemistry.**

| Solution | Time |
|---|---|
| *Dewaxing* | |
| Xylene I | 4 min |
| Xylene II | 3 min |
| Xylene III | 3 min |
| *Rehydration* | |
| 100% EtOH I | 1 min |
| 100% EtOH II | 1 min |
| 90% EtOH | 1 min |
| 70% EtOH | 1 min |
| 50% EtOH | 1 min |
| $ddH_2O$ | 1 min x 3 |

For antigen retrieval, an antigen unmasking solution with high pH was used at 1:100 dilution (H-3301; Vector Labs). Tissue sections were placed in a coplin jar with the unmasking solution, warmed in a microwave for 10 min (1 min at high power and 9 min at low power), and left to cool for 20 min. Tissues were then washed in $ddH_2O$ (2 min x 2) and incubated with 3% of $H_2O_2$ (Fisher Scientific) diluted in PBS for 5 min at room temperature (RT) to block endogenous peroxidase in the tissues. Tissues were then washed in PBS (2 min x 2).

*Immunohistochemistry*

To reduce background staining due to non-specific binding, sections were incubated with blocking solution; 5% of Normal Goat Serum (NGS) diluted in PBS for 2 hours at RT in a humidifying chamber.

To detect the antigen of interest, a mouse monoclonal anti-human AMH antibody (MCA2246T; Bio-Rad) was used at 1:100 dilution in blocking solution. Sections were

incubated with primary antibody solution overnight at 4°C in a humidifying chamber. Blocking solution only (no primary antibody) was added to the negative control. After washing with PBS (3 min x 3), sections were incubated with the secondary antibody solution, a biotinylated goat anti-mouse IgG (BA-9200; Vector Labs) at 1:200 dilution in blocking solution, at RT for 1 hour in a humidifying chamber. Tissues were then washed with PBS (3 min x 3) and incubated with Vectastain ABC Elite kit reagents (Avidin-Biotin-Peroxidase Complex kit, Vector Labs) for 30 min at RT in a humidifying chamber to amplify the target antigen signal. Tissue sections were washed in PBS (5 min x 3) and a peroxidase substrate kit (Vectastain, Vector Labs) containing the substrate; 3,3'-Diaminobenzidine (DAB) was used. The DAB solution was prepared according to the manufacturer's instructions and the solution was added onto the tissue, and staining development was observed under the microscope. The positive control was exposed to DAB first, so that the exposure time was determined. When staining was adequate (usually after 45 to 180 seconds) the reaction was stopped by placing the slide into $ddH_2O$. All sections in each experiment were exposed to DAB staining solution for the same amount of time.

*Dehydration and Mounting*

Tissues were dehydrated in increasing concentrations of ethanol and xylene solutions (Table 6. 2) and covered with coverslips using DPX mountant. Slides were left to dry in a laminar flow cabinet before analysis.

**Table 6. 2 Dehydration method of tissues after immunohistochemistry.**

| Solution | Time |
|---|---|
| 50% EtOH | 1 min |
| 70% EtOH | 1 min |
| 90% EtOH | 1 min |
| 100% EtOH I | 1 min |
| 100% EtOH II | 1 min |
| Xylene I | 3 min |
| Xylene II | 3 min |
| Xylene III | 4 min |

### 6.3.8. Analysis of AMH in FibROs and Control-ROs

Expression of AMH was analysed using imaging as described (Chapter 2). At this stage of the current investigation, it was essential to explore if AMH was expressed in follicles observed in Control-ROs (not studied before) and in follicle-like structures observed in FibROs; human ovary was used as a positive control. To this end, AMH detection was analysed in 7- and 14-day cultured Control-ROs and FibROs in a qualitative manner; no quantitative analysis was performed.

### 6.3.9. Assessment of follicle development in Control-ROs and follicle-like structure formation in FibROs

Follicle development in Control-ROs was assessed as described (Chapter 2). Five sections were analysed out of 12 in a 7-day cultured Control-RO and 5 sections out of 39 in a 14-day cultured Control-RO. Analysis of follicle-like structures in the fibROs was carried out in 5 out of 85 sections in three 7-day cultured FibROs and 5 out of 108 in three 14-day cultured FibROs.

## 6.4. Results

### 6.4.1 Generation of fibroblast-RO *in vitro*

To investigate the potential of HDFs to support follicle development *in vitro* using the RO method, it was important to determine if HDFs (Figure 6. 3A) could form a pellet if aggregated with mouse germ cells (Figure 6. 3B) and if this pellet could maintain its structure and grow for up to 14 days *in vitro*.

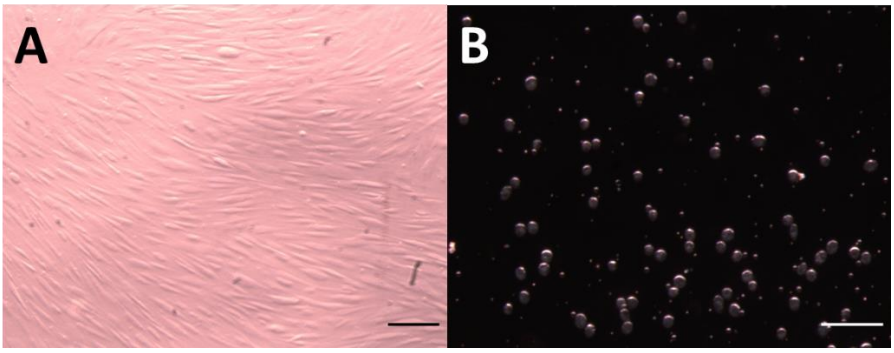



**Figure 6. 3 Representative images of human dermal fibroblasts (HDFs) and mouse germ cells used to generate a FibRO.** Neonatal mouse ovaries at postnatal day 7 (P7) were dissociated into single cells using the RO dissociation method. The mouse ovarian single cell suspension was incubated to allow separation of germ and somatic cells using differential adhesion. The germ cell population (B) was collected and aggregated with HDFs (A) derived from a 21-year-old male. HDF culture was split at 80% confluency in supplemented DMEM medium. Scale bar: 50 µm.

Our data showed that HDFs could form a rounded and fairly dense pellet when aggregated with mouse germ cells using the RO method. On day 0, these pellets were more rigid compared to Control-ROs (which had a more flattened shape and were more prone to break apart during manipulation). Pellets were cultured for 7 (Figure 6. 4A) or 14 days (Figure 6. 4B) *in vitro*; it was observed that pellets grew in size and appeared more dense on day 7 or 14 compared with a FibRO on day 0 or the Control-RO on day 7 or 14 (Figure 6. 4).

A tail-like structure was observed in all FibROs cultured for 14-days (Figure 6. 4B). This structure was developed on the contact point between the FibRO and culture membrane.

In Control-ROs (mouse germ cells aggregated with mouse somatic cells), the development of follicles was evident in culture as bubble-like structures (follicles) were observed (Figure 6. 4).

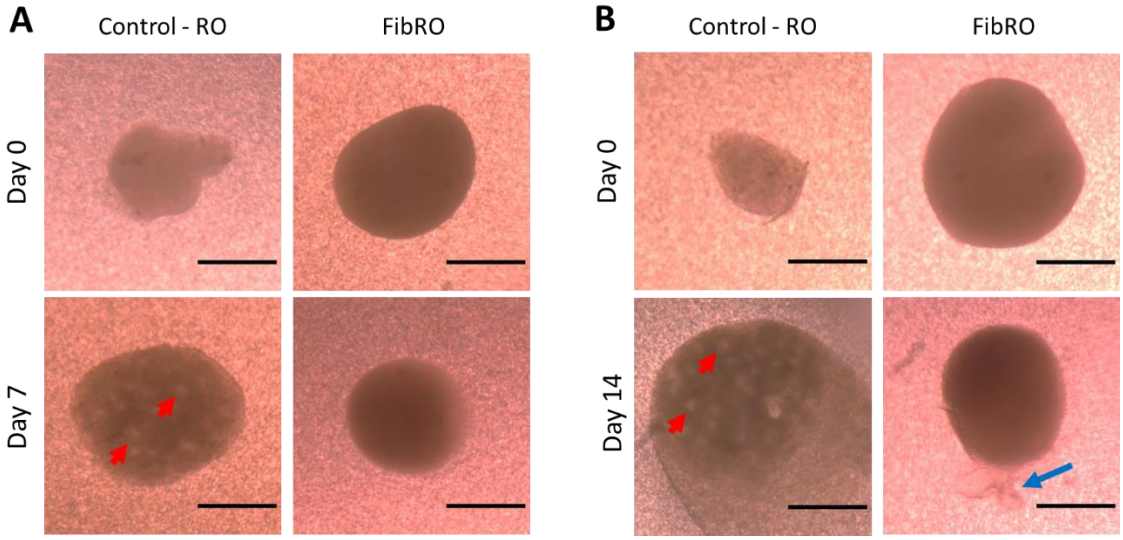



**Figure 6. 4 Representative images of FibROs and Control-ROs in 7- and 14-day culture *in vitro*.** Mouse germ cells obtained from neonatal mice at postnatal day 7 (P7) were aggregated with HDFs derived from skin biopsis obtained from a 21-year-old male to generate FibROs. As a control, mouse germ cells were reaggregated with mouse somatic cells to generate Control-ROs. FibROs and Control-ROs were cultured for 7- (A) or 14-days (B) in culture media on a polycarbonate membrane in a 24-well plate routinely used in the RO method. Red arrowheads indicate follicles. Blue arrow indicates tail-like structure. Scale bar: 50 µm.

Producing a FibRO using mouse germ cells and HDFs was achieved *in vitro*; a rounded pellet was formed that was similar in size and shape to the Control-ROs and maintained its structure for up to 14 days in culture. However, generation of follicles as bubble-like structures (at the surface of the RO) was not evident in FibROs (n=6) even though the existence of follicles was evident in the Control-ROs (n=2). Therefore, histological

analysis was carried out to investigate the development of follicle-like structures and potential follicle development in FibROs, and Control-ROs (see below).

### 6.4.2 Histological analysis revealed follicle-like structures in FibROs

FibROs and Control-ROs were analysed histologically to determine if follicle formation and development occurred *in vitro* in FibROs.

Growing follicles were observed in Control-ROs (n=2) confirming that the mouse cells used, and the culture conditions supported follicle development *in vitro* (Figure 6. 5). Sixteen follicles were observed in the Control-RO cultured for 7 days and 6 follicles in the Control-RO cultured for 14-days. In neither of the Control-ROs were there any primordial or antral follicles.

In the Control-RO cultured for 7 days, 12 out of 16 of the follicles reached the primary stage (Figure 6. 5B, C); 2 of them were characterised as asymmetric (Figure 6. 5D). Only 1 follicle reached the secondary stage (Figure 6. 5E), and 3 transitional follicles were also found (Figure 6. 5A). Theca cells were observed in 4 out of 12 primary follicles and in the secondary follicle observed in the Control-RO cultured for 7 days, though a complete layer of TCs was not seen.

In the 14-day Control-RO analysed, 3 out of 6 follicles reached the secondary stage (Figure 6. 5E), and there was 1 preantral follicle (Figure 6. 5F). There were also 2 asymmetric follicles found that contained 1 complete and 4-5 partial layers of GCs (Figure 6. 5G).

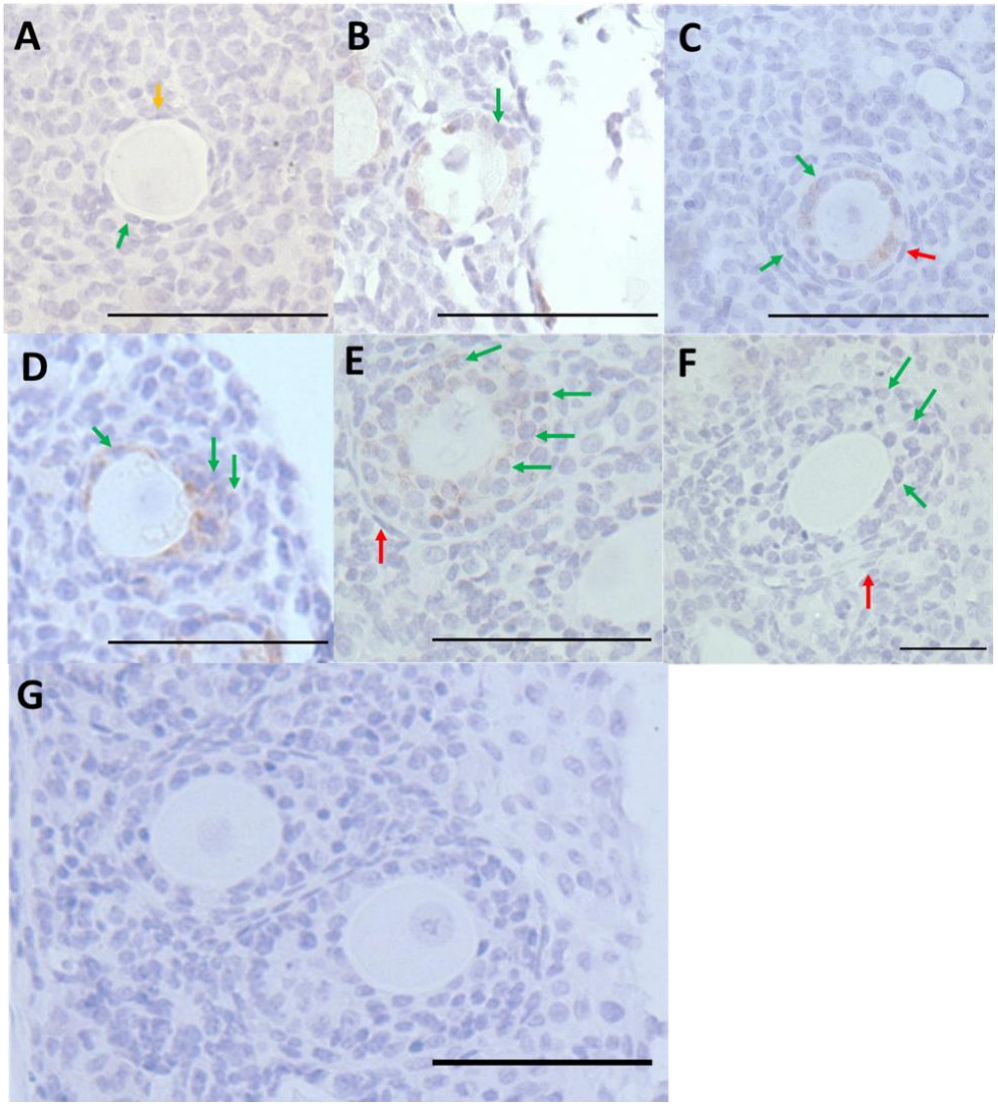



**Figure 6. 5 Representative images of follicle stages found in Control-ROs.** (A) Transitional follicles were characterised by a single layer of flattened pre-granulosa and cuboidal GCs surrounding the oocyte. Primary follicles contained an oocyte surrounded by 1 complete layer (B) or 1 complete and a partial second layer (C) of GCs. In asymmetric primary follicles there was 1 complete layer and partial layers of GCs attached to the oocyte (D, G), and in secondary follicles the oocyte was surrounded by 2 complete layers of GCs (E). (F) Preantral follicles had 3 complete layers of GCs attached to the oocyte. TCs were also observed in some primary (C), secondary (D) and preantral follicles (F). Arrows indicate flattened pre-granulosa cells (yellow), cuboidal GCs (green), and TCs (red). Scale bar: 100 µm. GCs: granulosa cells; TCs: theca cells.

Analysis of FibROs revealed that follicle-like structures were formed within 7- (Figure 6. 6C) and 14-days in culture (Figure 6. 6D). In these follicle-like structures, the oocyte (as observed morphologically) was surrounded by a heterogenous single incomplete layer

of flattened and cuboidal cells that seemed to be directly attached resembling pre-granulosa and granulosa cells, respectively (Figure 6. 6C(i), D(i)).

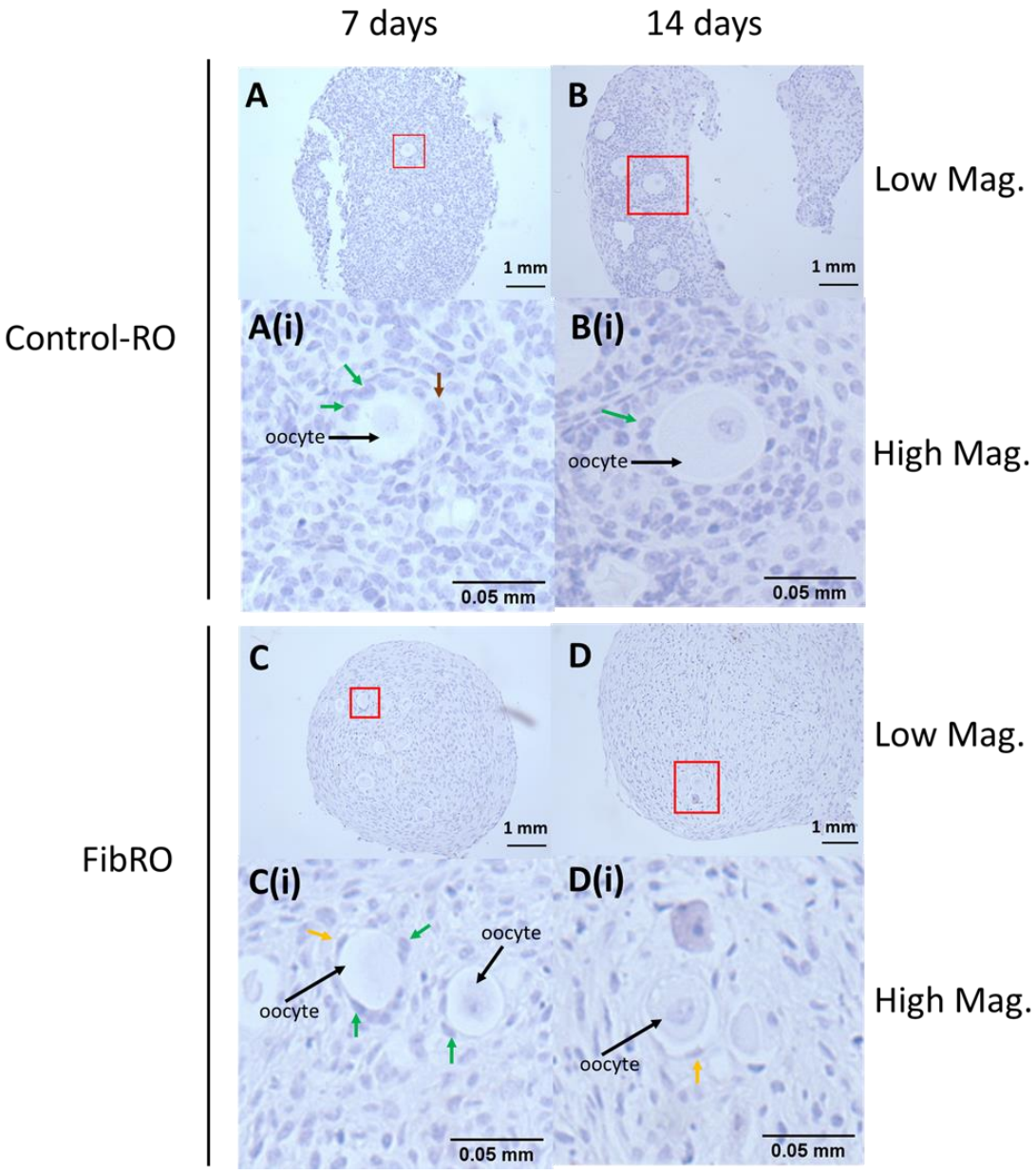



**Figure 6.** 6 **Representative images of Control-ROs and FibROs.** Mouse germ cells (obtained from postnatal day 7 mouse ovaries) were aggregated with mouse somatic cells (Control-RO) obtained from postnatal day 7 mouse ovaries or HDFs (FibRO) using the RO method to form a pellet (the RO or FibRO) that was cultured for 7 (A, A(i) and C, C(i)) or 14 days (B, B(i) and D, D(i)) on a polycarbonate membrane in a 24-well culture plate with culture media routinely used for the RO culture. Control-ROs and FibROs were harvested and processed for histological analysis using Haematoxylin stain. Follicles were analysed in the Control-ROs and follicle-like structures were observed in the FibROs. Black arrows; oocytes. Green arrows; cuboidal granulosa cells (first layer). Red arrow; cuboidal granulosa cells (second layer). Yellow arrows indivate flatenned pre-granulosa cells. HDFs: human dermal fibroblasts; Low/High Mag.: low/high magnification. Scale bar: 1 mm (A, B, C, and D) or 0.05 mm (A(i), B(i), C(i), and D(i)).

A total of 11 follicle-like structures were observed in 7-day cultured FibROs (n=3) while only 1 follicle-like structure was found in 14-day cultured FibROs (n=3). However, FibROs which were cultured for 14 days showed signs of necrosis in the centre of the tissue (data not shown).

This analysis revealed that follicle-like structures were formed in FibROs cultured for 7-days that were morphologically similar to transitional follicles found in the Control-ROs.

### 6.4.3 Analysis of AMH in Control-ROs and FibROs

To investigate if follicle-like structures observed *in vitro* in FibROs were follicles, the presence of AMH (a protein expressed in granulosa cells of follicles from the primary stage of development) was investigated. AMH was analysed in FibROs cultured for 7 or 14 days, as well as in Control-ROs; to our knowledge this was the first time AMH was investigated in the RO. As an AMH-positive control, tissue sections from a mouse ovary were used.

AMH-positive GCs were observed in the mouse positive control (Figure 6. 7A, A(i)) and human ovary control (Figure 6. 7B, B(i)) confirming AMH antibody immunoreactivity and specificity. AMH was detected in granulosa cells in all follicles in Control-ROs after 7- and 14-day *in vitro* culture (Figure 6. 7C, C(i)). AMH was detected in the cytoplasm of granulosa cells in all stages of follicle development in Control-ROs; transitional, primary, secondary and preantral. However, there was no positive staining in follicle-like structures found in FibROs (Figure 6. 7D, D(i)).

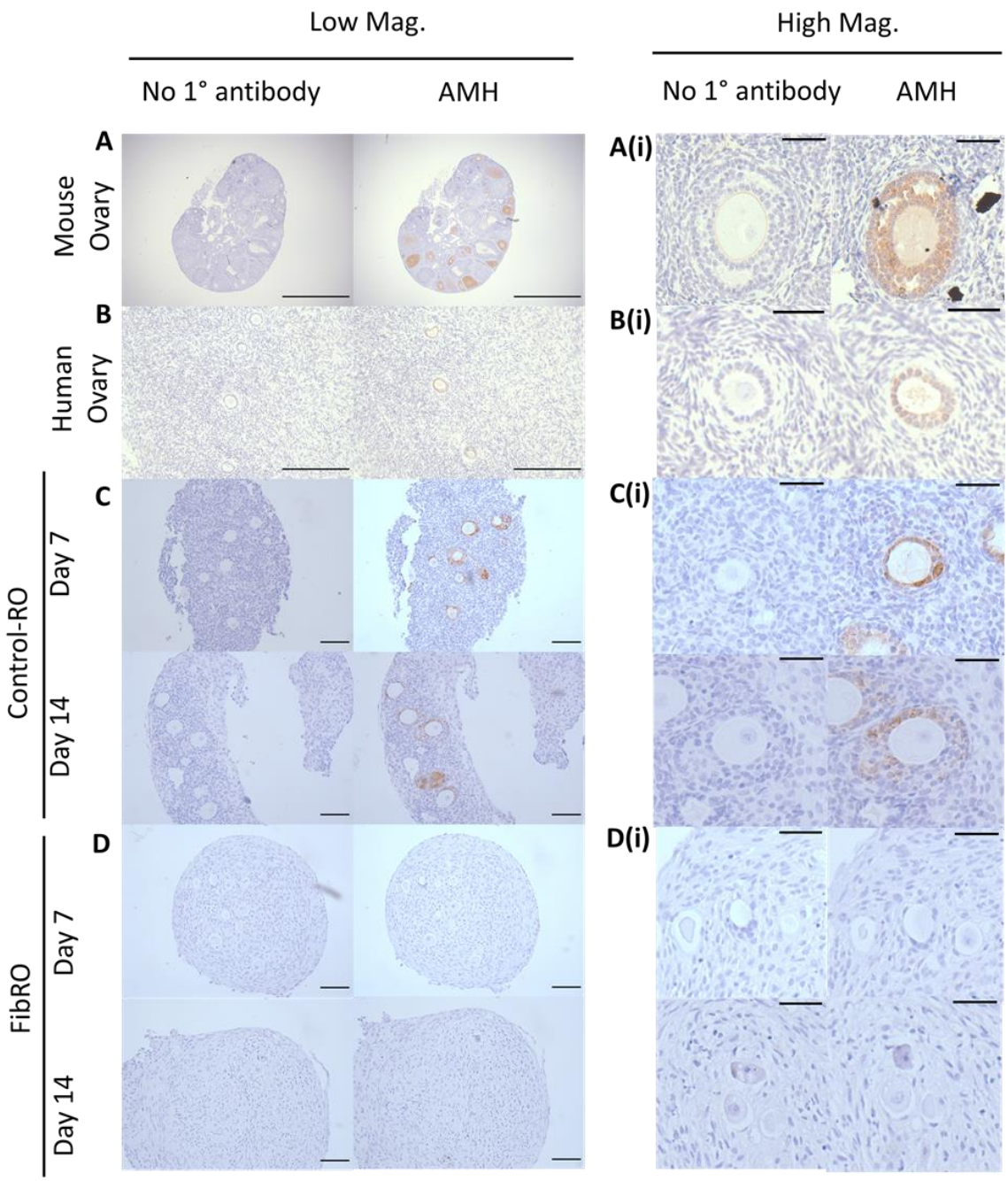



**Figure 6. 7 Analysis of AMH detection in Control-ROs and FibROs.** Control-ROs and FibROs were cultured for 7- or 14-days *in vitro*. Tissue was processed for histological analysis using Haematoxylin staining and further processed for immunohistochemistry. Mouse (A, A(i)) and human (B, B(i)) sections were used for positive control. AMH was analysed in follicles found in Control-ROs (C, C(i)) and follicle-like structures found in FibROs (D, D(i)). Granulosa cells in Control-ROs were positive for AMH but no signal was observed in follicle-like structures. Background staining was controlled using negative control sections (no primary antibody). Scale bars: 250 µm (A and B), 100 µm (C and D), and 50 µm (A(i), B(i), C(i), and D(i)).

## 6.5. Discussion

Dermal fibroblasts are mesenchymal cells that lack a specific somatic cell lineage identity and can differentiate into fully differentiated mesenchymal somatic cells in response to signalling secreted by the ECM (Tracy et al. 2016). The level of 'potency' HDFs manifest *in vivo* could be characterised as oligopotency, since there is no evidence that they can differentiate into non-mesenchymal cell types *in vivo* (multipotency). However, as discussed, it has been shown that HDFs can de-differentiate into induced pluripotent cells (iPSCs) *in vitro* if given the right signals. These iPSCs were similar to human Embryonic Stem Cells (hESCs) (Takahashi et al. 2007). In that study, iPSCs were also able to differentiate into neural or cardiac cells induced by lineage-directed differentiation methods routinely used for hESCs (Takahashi et al. 2007).

In another study, it was demonstrated that iPSCs from biopsy-derived dermal fibroblasts, could differentiate into germ cells and give rise to the complete germ cell lineage; primordial germ cell-like cells that developed to MII mature oocytes that were fertilisable *in vitro* (Hikabe et al. 2016). This indicates that dermal fibroblasts can acquire some capacity to differentiate if induced (i.e. directed differentiation methods) or in response to stimulus secreted in their environment (e.g. skin injury).

The key role of the oocyte as a coordinator in follicle development and maturation has been well established (Eppig et al. 2002). This study explored whether HDFs can differentiate into ovarian somatic cells and/or support germ cell development *in vitro* in FibROs in response to oocyte signalling using the RO, which has already been established

as a supportive environment for the generation of developed follicles (either homogenic or xenogeneic) (Lo et al. 2019; Eppig et al. 2000).

HDFs used in our study were obtained from biopsy-derived primary culture. Based on the literature, de-differentiation of HDFs into iPSCs *in vitro* prior to aggregation with mouse oocytes (to form the FibROs) might have been a more efficient method to achieve granulosa-like cells from HDFs. However, use of HDFs as an alternative for follicular somatic cells was more advantageous versus other cell sources such as iPSCs. HDFs are obtained from skin biopsies and therefore, is a patient-derived cell source. Also, acquiring a skin biopsy is relatively easy and considered simple compared to other invasive methods. What is more, due to iPSCs differentiation capacity, these may have been considered a more suitable choice for our study. However, tumorigenicity of iPSCs is a well-known side effect in the field of stem cell science (Knoepfler 2009). Thus, use of iPSCs in the RO method *in vitro* might introduce risks and problems regarding safety and efficacy for future clinical use. Another consideration of using iPSCs in the RO method is the uncontrolled generation of cell populations that inevitably derive during differentiation of iPSCs (Cohen et al. 2011). Random iPSCs-derived cell populations would contaminate the RO pellet and may compromise its function and efficacy.

### 6.5.1 Fibroblast-RO structure

This analysis showed that HDFs could form a pellet if combined with mouse germ cells: the FibRO. FibROs were morphologically similar to the Control-ROs (mouse germ cells combined with mouse somatic cells) and maintained their structure for up to 14 days *in vitro*.

FibROs and Control-ROs were rounded in shape and would adhere firmly to the culture membrane if not moved (every 2 days). What is more, FibROs on day 7 or 14 were bigger compared to day 0 in culture, indicating that fibroblasts were able to proliferate in the FibRO *in vitro*. A tail-like structure was observed in all FibROs cultured for 14-days. This structure was developed on the contact point between the FibRO and culture membrane, and it can also be seen in Control-ROs, though it is less common. This observation may indicate that HDFs had a higher tendency to proliferate on surfaces such as the culture membrane compared to mouse somatic cells in a Control-RO.

Overall, similarities were found between the FibRO and Control-RO regarding structure and growth dynamic in culture. This finding is encouraging that HDFs can sustain a RO-like structure within the RO culture system used.

### 6.5.2 Follicle-like structures in fibroblast-RO

Histological analysis revealed follicle-like structures in FibROs. These structures resembled transitional or primary follicles; with flattened and rounded cells that formed an incomplete single layer and were smaller in size compared to the oocyte.

To determine the species (human or mouse) of the fibroblast-derived somatic-like cells surrounded the oocyte in the follicle-like structures, immunohistochemistry could be performed using antibodies that detect human (or mouse) cells, such as anti-nuclei human antibodies.

A decreased number of follicle-like structures in 14-day cultured FibROs versus 7-day cultured FibROs indicated that culture conditions used in this study could not support

HDF survival for up to 14 day in FibRO. Follicles up to the preantral stage developed in Control-ROs at 14 days, but not in FibROs, therefore showing that culture conditions did not support development of xenogeneic follicles (containing mouse germ cells and HDFs). The RO culture method was established by Eppig and Wigglesworth (2000) using mouse and rat ovarian cells (Eppig et al. 2000), and generation of xenogeneic follicles using other cell sources have been reported as discussed, demonstrating that the RO culture is not restricted to supporting mouse ovarian cells only. Yet, human somatic cells (HDFs) may require different culture conditions. As discussed in previous chapters, adapting the RO method for human required the optimisation of many other aspects, including dissociation of human ovarian cortex and isolation of human germ cells from human somatic cells.

The use of different media in this study might have also contributed to insufficient development of follicle-like structures in FibROs. Dulbecco's Modified Eagle Media (DMEM), which contains a higher concentration of supplementary components including vitamins, amino acids and glucose compared to other Eagle's medium, is commonly used for the culture of HDFs (Takahashi et al. 2006; Takahashi et al. 2007). In this study, HDFs were derived and maintained in supplemented-DMEM, but the medium used in FibRO culture was supplemented-Medium 199 (as routinely used in the RO method (Lo et al. 2019)). The efficacy of these culture media regarding development of follicle-like structures in FibROs has not been investigated. Modifications in the RO culture may facilitate the generation of xenogeneic follicles containing HDFs and mouse germ cells, including culture medium, different concentration of components or additional factors in the media.

Rapid proliferation of HDFs when in the FibRO might have resulted in an increased size and density of FibROs resulting in insufficient penetration of elements contained in the culture medium for longer than 7 days *in vitro*. Thus, not only follicle-development but also cell survival might have been compromised in the centre of the FibRO, which morphologically seemed to have become necrotic after 7-days *in vitro*.

As discussed, 100,000 HDFs were used per FibRO. Assessment of the effect of different number of HDFs used per FibRO might reveal a threshold whereby follicle development can occur *in vitro* in FibRO. Due to time restrictions this was not carried out in this thesis, however future studies could include a dose response.

Inadequate formation of follicle-like structures in the 14-day cultured FibROs might be due to inability of HDFs to express ovary-specific receptors responsible for transmitting signals related to follicle development such as FSHR. Therefore, even though follicle-like structures were initially formed (7-day FibROs), development was not supported potentially, due to lack of such receptors; HDFs are unable to de-differentiate into follicular cells e.g. functional granulosa cells. Potential (endogenous) expression of such receptors in HDFs could be tested with immunohistochemistry or Western Blot. Additionally, stimulation of pathways resulting in expression of relevant receptors (i.e. BMP15-induced expression of FSHR through the Smad pathway (Shimizu et al. 2019)) could be performed to investigate whether HDFs are capable of expressing ovarian receptors. Furthermore, use of HDFs engineered to express key ovarian receptors in primordial follicle activation and granulosa cell proliferation (e.g. FSH receptor) could

be aggregated with mouse oocytes to generate FibROs to explore the ability of HDFs to form follicles in the presence of key factors.

In this study, generation of chimeric ROs (FibROs) containing mouse germ cells and HDFs as well as formation of follicle-like structures in FibROs was achieved *in vitro*. These chimeric ROs shared structural characteristics with Control-ROs. However, further optimisation of the FibRO culture system is required for the investigation of the development potential of these putative xenogeneic follicles.

### 6.5.3 No AMH detection in fibroblast-RO

To investigate if HDFs differentiated into granulosa-like cells in follicle-like structures observed *in vitro*, AMH was explored; a well-known granulosa cell marker. Previously, AMH had not been studied in the RO and therefore, mouse ovary and human ovarian cortical tissue were used as controls.

This data showed that AMH was immunolocalised to granulosa cells in all stages of follicles generated in the Control-ROs indicating that the culture conditions supported the development of functional follicles containing mouse germ and somatic cells. On the contrary, no AMH was detected in FibROs. This observation led us to three hypotheses; 1) HDFs do not differentiate into granulosa-like cells and therefore, do not express AMH, 2) HDFs responded to oocyte signalling only to some extent and surrounded the oocyte to form follicles but weren't able to function as ovarian somatic cells by expressing AMH and/or support further follicle development, or 3) HDFs can differentiate into granulosa-like cells and form follicle-like structures that were immature, but not capable of producing AMH. This could be tested by immunohistochemistry to detect granulosa cell

(GC) markers that are produced in earlier stages of follicle development; for example, tyrosine kinase receptor CD117 (Høyer et al. 2005; Tuck et al. 2015), and/or forkhead transcription factor FOXL2 (Duffin et al. 2009; Wagner et al. 2020).

Communication between the oocyte and somatic cells, and between somatic cell populations (granulosa and theca cells), is required for the development of mature follicles and developmentally competent oocytes. Therefore, it is critical to investigate whether transzonal projections, which facilitates communication between the oocyte and granulosa (or cumulus) cells (El-Hayek et al. 2018), can be formed in follicle-like structures in FibROs. What is more, the basal lamina, which is present in follicles from the primordial stage, is also necessary for follicle development (Heeren et al. 2015). To explore whether somatic-like cells in follicle-like structures were encapsulated by a basal lamina, immunohistochemistry or other staining assays (such as Periodic Acid-Schiff (PAS)) could be performed to detect basal lamina components such as laminin, fibronectin and collagen IV (Heeren et al. 2015).

Findings in this chapter demonstrated that the RO culture system supported the generation and development of homogenic follicles (containing mouse cells only), and the formation of xenogeneic follicle-like structures (containing mouse germ cells and another source of cells; HDFs in this case). However, it was not possible to demonstrate that somatic cells in follicle-like structures differentiated into GCs *in vitro* in FibROs. Nevertheless, the above observations are encouraging for future investigations into the fibroblast-RO function and potential.

### 6.5.4 The FibRO as a promising tool to restore follicle development for POI patients with follicle dysfunction

The RO, though still experimental, could potentially enable us to substitute the abnormal ovarian environment (follicle dysfunction) in idiopathic POI with an alternative source of human somatic cells. In the DM ovaries, as discussed, follicular somatic cells may block follicle development and maturation. Using the RO method, we could be able to investigate if follicle development is impaired in POI due to dysfunctional somatic cells by replacing these dysfunctional cells with cells that support follicle development to rescue germ cell development *in vitro*.

It has been shown that ECM (i.e. collagen I, III, etc.) affected the function of dermal fibroblasts and played a key role in the differentiation process into myofibroblasts *in vitro* (Tracy et al. 2016; Homcha et al. 2011; Lygoe et al. 2007; Volk et al. 2011). Use of ECM components in the culture medium and/or the FibRO pellet may affect the differentiation processes of HDFs *in vitro* in FibRO. What is more, transplantation of FibRO into immunocompromised mice might constitute a more supportive environment (*in vivo*) for follicle development compared to *in vitro* culture and therefore, enable us to explore the full potential of HDFs to differentiate into granulosa-like cells.

The potential of mouse dermal fibroblast (MDFs) to differentiate into mouse granulosa-like cells *in vitro* in RO was not explored. As it was discussed earlier, the generation of mature eggs in xenogeneic follicles containing ovarian cells from different species was demonstrated. However, in this study we combined mouse germ cells with adult non-ovarian cells from another species (human fibroblasts), which has not been practiced before. Thus, generation of ROs containing mouse oocytes and MDFs may reveal critical

information about the ability of dermal fibroblasts to support development in allogeneic and/or homogenic follicles (containing cells from the same species).

Using HDFs from one patient might be a potential disadvantage to this study as any unknown dysfunctions or mutations might have affected results. Further investigation into the FibRO using HDFs from more patients should be performed in future studies to explore the potential of HDFs to support follicle development *in vitro* in the FibRO.

### 6.5.5 Conclusions

To our knowledge, this is the first study investigating the potential of HDFs obtained from biopsy-derived primary cell culture to support oocyte development using the RO method. It was hypothesized that HDFs could support germ cell development by differentiating into granulosa-like cells and/or form follicle-like structures *in vitro* in response to oocyte signalling. This data revealed that HDFs could form pellets if combined with mouse oocytes (FibROs), which were similar to Control-RO pellets, and maintained their structure *in vitro*. Also, the formation of follicle-like structures in FibROs cultured for 7- or 14-days was evident. Findings in this chapter demonstrated that the FibRO could be considered as a potential tool to develop that could be used for fertility preservation for patients with follicle dysfunction. Further studies are required to bring the full potential of this method to light.

# CHAPTER 7

# *Future work and final remarks*

Despite its relatively high prevalence, the majority of POI cases remain idiopathic, and there is no established method in clinical practice to restore ovarian function in patients with POI. However, there is ongoing research to establish fertility preservation methods for POI patients. Ovarian tissue cryopreservation (OTC) is a promising method for fertility preservation that would benefit patients with follicle depletion; however, patients with POI, and follicle dysfunction, would not benefit due to aberrant follicle development. As discussed in detail in Chapter 1, *in vitro* activation (IVA) and/or *in vitro* maturation (IVM) are promising experimental methods to preserve fertility for POI patients with residual follicles present in the ovary (follicular POI); live births have been reported for young women with POI but, to our knowledge, not for pre-pubertal patients.

Findings from this thesis will contribute to the development of a method that could potentially restore follicle development in pre- and post-pubertal patients diagnosed

with POI by replacing the dysfunctional ovarian follicles with an alternative using the RO method.

## 7.1 Main findings from this thesis

There are many steps required towards the development of the RO method using human ovarian tissue. Investigations carried out in this thesis addressed critical requirements for such work.

Isolation of human germ cells for generating of a RO requires dissociation of human ovarian tissue into single cells whereby oocytes could then be separated from ovarian cells (e.g. granulosa, theca, stroma, perivascular, fibroblasts, immune cells). In Chapter 3 and 4, I explored various methods to dissociate human ovarian tissue into single cells and established a protocol to dissociate fresh ovarian remnant tissue and frozen/thawed ovarian cortical tissue from pre- and post-pubertal patients. This analysis could be applied to the dissociation of human ovarian tissue obtained from POI patients to facilitate isolation of viable human eggs and thus, generation of a RO to investigate POI in future studies. Furthermore, in Chapter 4 I demonstrated for the first time that age affects the efficacy of human ovarian tissue dissociation which may contribute to opening new horizons in developing personalised methods in fertility preservation.

Prior to isolating human oocytes from POI ovarian tissue, it is crucial to confirm the presence of oocytes in the ovarian single cell suspension retained after tissue dissociation. In Chapter 5, I established a method to detect human germ cells isolated from pre- and post-pubertal frozen/thawed ovarian cortex and fresh ovarian remnant tissue using the intracellular marker DDX4 and flow cytometry. A viable DDX4

population was detected in both pre- and post-pubertal samples. This data will feed into further investigation into the analysis of the DDX4 population.

Identifying an alternative source of human somatic cells that can support follicle development in a RO is crucial for this work, as one of the long-term aims of this study was to explore the capacity of human germ cells (obtained from POI or non-POI patients) to develop if the follicular somatic cells are replaced with an alternative. In Chapter 6, I explored the potential of human dermal fibroblasts to support mouse follicle development *in vitro* in a chimeric RO (the FibRO). Follicle-like structures were evident in the ROs resembling primordial/primary follicles. Moving forward, studying follicle dysfunction in POI patients using the RO method would provide meaningful information about POI oocytes to retain their ability to develop if the dysfunctional follicular environment (i.e. follicular somatic cells) is replaced, and potentially restore follicle development in POI patients.

The findings from this thesis has given rise to many more research questions and future ideas which will be discussed below.

## 7.2 Future work

Future studies will enable us to investigate the ability of human POI oocytes to develop into mature follicles, and to deepen our understanding of the mechanisms underlying POI using the RO.

*Investigation into the capacity of human oocytes to develop in a RO*

The ability of mouse ovarian cells to develop into mature follicles *in vitro* and *in vivo* in allogeneic and xenogeneic ROs has been previously demonstrated (discussed in Chapter 6). Mouse somatic cells could be used as a gold standard somatic cell source. Viable human germ cells would be aggregated with mouse neonatal somatic cells to generate a human:mouse RO; $H_E$:$M_{OS}$ (i.e. human eggs to mouse ovarian somatic cells) (Figure 7. 1). Follicle development could then be analysed in the $H_E$:$M_{OS}$ ROs after transplantation into immunocompromised mice, since the *in vivo* environment supports better follicle development in the RO (Lo et al. 2019). Other types of ROs would also be required to help us determine the optimum alternative follicular environment that could support follicle development of immature human oocytes.

Human dermal fibroblasts appeared to be a promising alternative to support follicle development in xenogeneic follicles as formation of follicle-like structures *in vitro* in FibROs (mouse oocytes + human dermal fibroblasts) was evident. To reveal the full potential of human dermal fibroblasts, future studies could involve xenotransplantation of the FibRO ($M_E$:$H_{HDFs}$ (i.e. mouse eggs to human dermal fibroblasts)) into immunocompromised mice as a more supportive environment for follicle development (Figure 7. 1).

As discussed above, mouse oocytes are a gold standard and therefore, using mouse oocytes in xenogeneic $M_E$:$H_{HDFs}$ ROs before generating the homogenic human:human $H_E$:$H_{HDFs}$ ROs will provide crucial information regarding the ability of human dermal fibroblasts to support follicle development. These fibroblasts would be obtained from

patients consent to donate fibroblasts for research in addition to the consent for ovarian tissue to allow for the generation of allogenic $H_E$:$H_{HDFs}$ ROs (Figure 7. 1).

Other alternative sources of human somatic cells should also be considered such as induced pluripotent stem cells (iPSCs) ($H_E$:$H_{iPSCs}$ (i.e. human eggs to human induced pluripotent stem cells)) (Figure 7. 1). However, caution should be taken as maintenance of these cells in culture is notoriously difficult due to instability of their undifferentiated state and sensitivity due to mechanical treatments (Konagaya et al. 2015; Steiner et al. 2010; Chen et al. 2017; Jager et al. 2017) and thus, could impair RO function as discussed in Chapter 6. Human embryonic somatic cells obtained from human foetuses after elective termination of pregnancy could also be used as an alternative ($H_E$:$H_{HESomCs}$ RO) (Figure 7. 1). Human fetal-derived somatic cells have been successfully used in other studies (Clarkson et al. 2018) to form follicle-like structures as an alternative to adult human ovarian somatic cells.

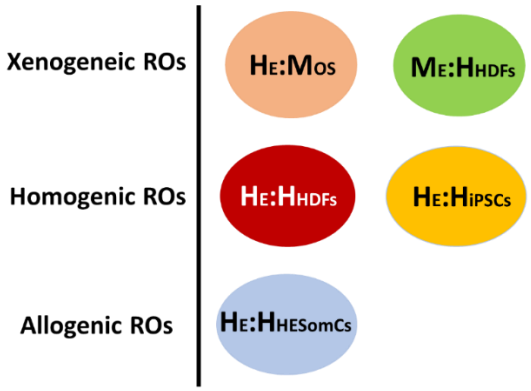



**Figure 7. 1 Xenogeneic, homogenic and allogeneic ROs.** RO: reaggregated ovary; H: human; M: mouse; E: eggs; OS: ovarian somatic cells; HDFs: human dermal fibroblasts; HESomCs: human embryonic somatic cells; iPSCs: induced pluripotent stem cells.

There are ethical issues to consider when using somatic cells from human foetuses for research purposes because their use is associated with abortion, which is unacceptable

to some. The use of human embryonic somatic cells in this investigation would entirely be restricted to the experimental stage, to explore if human oocytes can develop into mature follicles *in vitro* in the RO. On the contrary, use of iPSCs would avoid these ethical issues as they are derived from adult somatic cells; however, as discussed above, iPSCs have their limitations and the use of other cell lines might be required.

To develop the RO as a method to restore follicle development for follicular POI, it is critical to first demonstrate that 1) human oocytes from healthy (non-POI) donors can develop *in vivo* in the RO, and 2) alternative sources of human somatic cells can support human oocyte development into mature follicles *in vivo* in the RO. I present an experimental design that could address the above objectives (Table 7. 1). Conclusions based on the observations regarding follicle development in each type of RO would determine the experimental flow of this study (Table 7. 1)

**Table 7. 1 Experimental workflow to determine an alternative source of human somatic cells to support follicle development *in vivo* in the RO**. RO: reaggregated ovary; H: human, M: mouse; E: eggs; OS: ovarian somatic cells; HDFs: human dermal fibroblasts; HESomCs: human embryonic somatic cells; iPSCs: induced pluripotent stem cells.

| | Follicle development Yes ✓ or No ✗ | Conclusions | Next steps |
|---|---|---|---|
| Phase 1 | A He:Mos ✓ | Human oocytes can develop in a xenogeneic RO | If A + C / If B + C → He:HHDFs (To explore follicle development in homogenic ROs) |
| | B He:Mos ✗ | Human oocytes do not develop in a xenogeneic RO, or mouse somatic cells do not support human follicle development in RO | |
| | C Me:HHDFs ✓ | HDFs can support mouse follicle development in RO | If A + D / If B + D → He:HHESomCs (To explore follicle development in allogeneic ROs using an alternative source of human somatic cells) |
| | D Me:HHDFs ✗ | HDFs do not support mouse follicle development in RO | |
| Phase 2 | E He:HHDFs ✓ | HDFs can support human follicle development in RO | If E → RO *in vitro* |
| | F He:HHDFs ✗ | HDFs do not support human follicle development in RO | If F → He:HHESomCs (To explore follicle development in allogeneic ROs using an alternative source of human somatic cells) |
| Phase 3 | G He:HHESomCs ✓ | HESomCs can support human follicle development in RO | If G → RO *in vitro* |
| | H He:HHESomCs ✗ | HESomCs do not support human follicle development in RO | If H → He:HiPSCs (To explore follicle development in homogenic ROs using an alternative source of human somatic cells) |

To be able to use the RO as a fertility preservation method for POI patients in healthcare, establishment of this method *in vitro* is required since xenotransplantation of a chimeric RO (mix of two species) into human is forbidden (Bourret et al. 2016). What is more, the ROs described above (Figure 7. 1) have not been explored before and thus, health risk impositions to patients are unknown. Therefore, demonstrating follicle development *in vitro* in ROs is required to allow of the RO method for clinical practice in future.

In this thesis, the RO method is suggested as a tool to replace the dysfunctional ovarian tissue from POI patients and explore if the oocytes can develop and reach the early

antral stage where *in vitro* fertilisation of eggs could be successfully achieved (i.e. late antral follicles), and thus, fertility would be restored. To assess the developmental capacity of the oocyte in $M_E$:$H_{HDFs}$ ROs, which would indicate that human dermal fibroblasts can support follicle development in the RO, *in vitro* maturation (IVM) and fertilisation (IVF) of the mature oocytes obtained from these xenogeneic follicles could be performed.

To determine if oocytes from POI patients can retain their ability to develop into mature follicles *in vitro* in the RO, human oocytes from non-POI patients, should be used first to generate a RO. Furthermore, demonstrating these oocytes are fertilisable would be indicative of the RO being functional. This would show that POI primarily affects the ovarian somatic cells, as the oocytes would continue to develop if the dysfunctional somatic cells are replaced. Deepening our understanding of the mechanisms underlying non-idiopathic follicular POI (i.e. genetic causes) using the RO method may provide key information about idiopathic follicular POI. POI is associated with conditions such as Turner Syndrome or mutations such as FSHR, FOXL2 and INHA (genetic causes of POI) and could be included in future studies to investigate POI using the RO method. To test if the RO can restore follicle development for patients with idiopathic POI, young women ≥18 years with secondary amenorrhoea (no known cause) or young girls ≤18 years with primary amenorrhoea (no known cause) seeking fertility treatments could be included in future work.

*Investigation into follicle development in POI, and follicle dysfunction using the RO method*

In addition to the potential of the RO method as a fertility preservation method, this culture system would also enable us to explore follicle development in POI. Using a model of follicular POI, the double mutant (DM) mouse model, our group were able to reveal important features of follicular POI regarding follicular function (discussed in Chapter 1 and 6). We could investigate these same features (discussed below) using human ovarian tissue from POI patients to explore if these can be altered and thus restore follicle function using the RO method.

The zona pellucida and transzonal projections are necessary elements of follicle development and oocyte maturation. Also, the zona pellucida has a key role in follicle and oocyte development as well as fertilisation (Wassarman et al. 2012) while transzonal projections facilitate communication between the oocyte and granulosa (or cumulus) cells (El-Hayek et al. 2018). In the DM mouse model, analysis of the morphology of the zona pellucida revealed that DM follicles had a thinner zona, however, fertilisation and implantation proceeded (Shi et al. 2004). Abnormalities in the zona pellucida has been associated with POI in humans, too, such as in the case of autoimmune ovarian damage (Komorowska 2016). Studies using ovarian autoantibodies showed that ovarian autoimmunity can be directed to ovarian somatic cells (granulosa or theca cells), the oocyte, or zona pellucida (Forges et al. 2004). It would be interesting to explore if the removal of oocytes from POI patients with zona pellucida-directed ovarian autoimmunity, to an alternative follicular environment using the RO method enhances follicle development. Furthermore, we would also be able to explore 1) if the non-ovarian somatic cells used in the RO could form functional

transzonal projections, and 2) if these projections would enhance follicle formation in cases of autoimmune ovarian damage by re-establishing oocyte-somatic cell communication.

Formation of functional mature follicles in the mouse RO has been established (discussed in Chapter 6), however, we lack knowledge in the mechanisms underlying follicle formation in a RO. Cell tracing analysis using the RO method would help us to address this question. By using traceable somatic cells (i.e. granulosa or theca cells ubiquitously expressing the *LacZ* gene) in a neonatal mouse RO we would be able to trace these cells in a RO from day 0 up to the end of culture. We believe that there are three potential mechanisms: 1) somatic cell trans-differentiation and/or 2) somatic cell migration or 3) cell survival only if in the 'correct location'. In the case of trans-differentiation, the differentiated somatic cell population should trans-differentiate into another somatic cell population depending on either the new location acquired within the RO and/or germ cell signal-instructions. In the case of somatic cell migration, somatic cells should migrate to their original location depending on germ cell signal-instructions no matter what their new location in the RO. In the case of cell survival 'only if in the correct location', then only granulosa or theca cells that were symptomatically distributed within the granulosa cell layer, theca cell layer or between follicles, respectively, in the newborn ROs will survive. Findings from this analysis could contribute to further explore the potential of non-ovarian somatic cells to support follicle development either by de-differentiating into ovarian somatic cells (i.e. granulosa, cumulus, theca cells) or by altering their function in response to oocyte signalling.

Eppig et al. (Eppig et al. 2002) demonstrated that the oocyte orchestrates follicle development in the mouse RO (discussed in Chapter 6). Oocytes obtained from secondary follicles were aggregated with ovarian somatic cells obtained from primordial follicles and xenotransplanted into immunocompromised mice (Eppig et al. 2002). Analysis revealed that *in vivo* development of these follicles to the antral stage was accelerated, and was equal to the time required for secondary follicles to develop into the antral stage (~9 days) (Eppig et al. 2002). This study provided evidence that the oocyte can alter the rate of follicle development. Using the RO method, we could explore if age and/or puberty affects the rate of follicle development in human in the RO as was revealed in mice. Such analysis would help to optimise RO culture according to patient age and/or pubertal status. Additionally, it would be interesting to explore if the alternative sources of human somatic cells (i.e. human dermal fibroblasts) can respond to oocyte signalling in a similar manner as ovarian somatic cells do and support follicle development within different timeframes.

## 7.3 Final remarks

The inability to diagnose POI before clinical manifestation of the condition limits our ability to study the mechanisms underlying POI and therefore the development of fertility preservation methods. Also, the huge variation in the clinical manifestations of POI, the inter-patient variation and high heterogeneity between patients should be considered as limiting factors in the development of fertility preservation methods. Large-scale studies should be conducted to acquire robust data regarding POI to allow for the establishment of fertility preservation methods in healthcare. Ovarian tissue from patients with different conditions related to POI could be obtained to generate

ROs in order to analyse follicle dysfunction in each condition. Thus, we could compare the benefits or needs of the RO method for each case of follicular POI and develop personalised fertility preservation options for different cases of POI.

To our knowledge, the 'artificial' ovary (RO) is the only available method to date that could facilitate replacing dysfunctional ovarian tissue. The RO method could be considered as a novel method in fertility preservation to primarily benefit POI patients with idiopathic follicle dysfunction. Also, it can help to develop interventions and treatments to study POI. We suggest the generation of an alternative environment that can replace dysfunctional somatic cells and support premature oocytes from POI patients with follicle dysfunction to develop. In combination with current fertility treatments such as IVA and IVM, this method could potentially contribute to the generation of mature and developmentally competent oocytes that could be fertilised *in vitro* to produce embryos for pre-pubertal or adult POI patients with follicle dysfunction.

# List of figures and tables

## Figures

### CHAPTER 1

**Figure 1. 1 Follicle development in the human ovary. ..... 17**
**Figure 1. 2 Estimated timeline for follicle development in humans.. ..... 20**
**Figure 1. 3 The structure of the antral follicle. ..... 24**
**Figure 1. 4 The two cell-two gonadotropin theory for oestradiol production. . ..... 28**
**Figure 1. 5 Categories of causes of POI. ..... 34**
**Figure 1. 6 Categories of ovarian function in POI.. ..... 42**
**Figure 1. 7 Mechanisms underlying afollicular and follicular POI. ..... 43**

### CHAPTER 2

**Figure 2. 1 Generation of Reaggregated Ovaries..... 64**
**Figure 2. 2 Reaggregated Ovary on a transwell membrane..... 66**
**Figure 2. 3 Schematic of embedded ovarian tissue in paraffin wax..... 69**
**Figure 2. 4 Stages of follicle development in ROs. ..... 71**

### CHAPTER 3

**Figure 3. 1 Overview of methodology to dissociate human ovarian tissue. ..... 83**
**Figure 3. 2 Variables explored to dissociate human fresh ovarian cortical tissue..... 84**
**Figure 3. 3 Representative image of human fresh ovarian remnant tissue sample. ..... 88**
**Figure 3. 4 Variables explored to dissociate human fresh ovarian remnant tissue..... 89**
**Figure 3. 5 Variables explored to dissociate human frozen/stored ovarian cortical tissue. ..... 91**
**Figure 3. 6 Analysis of cell viability after dissociation of human fresh ovarian cortical tissue using trypsin or collagenase. ..... 97**
**Figure 3. 7 Overview of experimental flow – part 1. ..... 98**
**Figure 3. 8 Analysis of the effect of anti-apoptotic factors to dissociate fresh ovarian cortex using a shaker. ..... 99**
**Figure 3. 9 Analysis of the efficacy of anti-apoptotic factors (AAF) to dissociate human fresh ovarian cortex. ..... 100**
**Figure 3. 10 Overview of experimental flow – part 2. ..... 101**
**Figure 3. 11 Cell viability after dissociation of human fresh remnant tissue using enzymatic and mechanical dissociation. ..... 103**
**Figure 3. 12 Overview of experimental flow – part 3. ..... 104**
**Figure 3. 13 Comparison of the efficacy of dissociation methods using collagenase or liberase to dissociate human frozen/thawed ovarian cortex. ..... 106**
**Figure 3. 14 Cell yield using collagenase or liberase to dissociate frozen/thawed ovarian cortical tissue..... 107**
**Figure 3. 15 Overview of experimental flow – part 4. ..... 109**

### CHAPTER 4

**Figure 4. 1 Cell viability after dissociation of human fresh ovarian remnant tissue. ..... 126**
**Figure 4. 2 Total cell yield in different methods used to dissociate human frozen/thawed ovarian cortex. ..... 127**
**Figure 4. 3 Comparison of cell viability from three methods used to dissociate human frozen/thawed ovarian cortex. ..... 128**
**Figure 4. 4 Total cell yield from frozen/thawed ovarian cortex in Younger and Older patients..... 130**
**Figure 4. 5 Cell viability in the Younger and Older groups after dissociation of frozen/thawed ovarian cortex. ..... 131**

**Figure 4. 6 Cell viability in pre-pubertal, post-pubertal and adult patients after dissociation of frozen/thawed cortex using L15 method. ..... 133**

## CHAPTER 5

**Figure 5. 1 Components of a flow cytometer. ..... 142**
**Figure 5. 2 Representative figure of a FC two parameter density plot. ..... 147**
**Figure 5. 3 DDX4 protein in putative OSCs and the oocyte. ..... 149**
**Figure 5. 4 The monoclonal N-terminus-binding anti-DDX4 antibody and polyclonal C-terminus-binding anti-DDX4 antibody. ..... 155**
**Figure 5. 5 Analysis of cell viability of HeLa cell population without or after induced cell death using ZA and FC. ..... 168**
**Figure 5. 6 FC analysis of intracellular cytokeratin 13 in HeLa cells. ..... 170**
**Figure 5. 7 FC gating to identify intracellular DDX4-positive HeLa cells. ..... 171**
**Figure 5. 8 Analysis of intracellular and surface bound DDX4 in HeLa cells using FC. ..... 172**
**Figure 5. 9 FC gating strategy to exclude dead cells in human fresh ovarian remnant tissue. ..... 174**
**Figure 5. 10 Viability of cells from human ovarian remnant tissue measured by FC. ..... 176**
**Figure 5. 11 Viability of cells from pre-pubertal and post-pubertal fresh ovarian remnant tissue measured by FC. ..... 178**
**Figure 5. 12 FC gating strategy to detect DDX4-positive cells from human fresh ovarian remnant tissue. ..... 179**
**Figure 5. 13 Percentage of DDX4-positive cells from human fresh ovarian remnant tissue measured by FC. ..... 181**
**Figure 5. 14 Analysis of the effect of pubertal status on DDX4-positive cells from human fresh ovarian remnant tissue. ..... 183**
**Figure 5. 15 FC gating strategy to exclude dead cells from human frozen/thawed ovarian cortex. ..... 185**
**Figure 5. 16 Viability of cells from human frozen/thawed ovarian cortical tissue measured by FC. ..... 186**
**Figure 5. 17 Viability of cells from pre-pubertal and post-pubertal frozen/thawed ovarian cortical tissue measured by FC. ..... 188**
**Figure 5. 18 FC gating strategy to detect DDX4-positive cells from human frozen/thawed ovarian cortical tissue. ..... 190**
**Figure 5. 19 Percentage of DDX4-positive cells from frozen/thawed cortical tissue measured by FC. 191**
**Figure 5. 20 The effect of pubertal status on DDX4-positive cells from human frozen/thawed ovarian cortex as measured by FC. ..... 193**

## CHAPTER 6

**Figure 6. 1 Overview of different types of RO used in our laboratory. ..... 206**
**Figure 6. 2 An illustration of the Avidin-Biotin-peroxidase Complex method of immunohistochemistry used to amplify the target antigen signal. ..... 217**
**Figure 6. 3 Representative images of human dermal fibroblasts (HDFs) and mouse germ cells used to generate a FibRO. ..... 221**
**Figure 6. 4 Representative images of FibROs and Control-ROs in 7- and 14-day culture *in vitro*. ..... 222**
**Figure 6. 5 Representative images of follicle stages found in Control-ROs. ..... 224**
**Figure 6. 6 Representative images of Control-ROs and FibROs. ..... 225**
**Figure 6. 7 Analysis of AMH detection in Control-ROs and FibROs. ..... 227**

## CHAPTER 7

**Figure 7. 1 Xenogeneic, homogenic and allogeneic ROs. ..... 241**

# Tables

## CHAPTER 1

**Table 1. 1 Clinical states of POI according to FSH levels, fecundity and amenorrhoea (Welt 2008). .....40**
**Table 1. 2 Options for pre- and post-pubertal POI patients to restore ovarian function in the case of follicle depletion or follicle dysfunction. .....50**

## CHAPTER 2

**Table 2. 1 Thawing solution components. .....57**
**Table 2. 2 Components of the X-gal staining solution. .....60**
**Table 2. 3 Components of the X-gal staining method. .....67**
**Table 2. 4 Dehydration solutions and incubation times for tissue prior to embedding. .....68**
**Table 2. 5 Haematoxylin and Eosin staining process. .....70**

## CHAPTER 3

**Table 3. 1 Human ECM target proteins of collagenase, dispase and liberase. .....74**
**Table 3. 2 Differences between Protocol A and B used to dissociate human fresh ovarian cortical tissue.....85**
**Table 3. 3 Variables tested to dissociate human fresh ovarian remnant tissue using Protocol C.....90**
**Table 3. 4 Differences between Protocol A, B, C and D used to dissociate human ovarian tissue. .....93**
**Table 3. 5 Detailed list of patients who donated whole ovaries for research investigations including in Chapter 3.....95**
**Table 3. 6 Detailed list of patients who donated ovarian remnant tissue for research investigations including in Chapter 3.....95**
**Table 3. 7 Detailed information about a patient who donated frozen/stored ovarian cortical tissue for research investigations including in Chapter 3. .....95**
**Table 3. 8 Dissociation methods used for frozen/thawed ovarian cortical tissue sample from a 13-year-old patient. .....105**

## CHAPTER 4

**Table 4. 1 The three methods used to dissociate human frozen/thawed ovarian cortical tissue: Shaker L15, L15 and PBS.....120**
**Table 4. 2 Patients who donated human fresh ovarian remnant tissue for research. .....124**
**Table 4. 3 Patients who donated frozen/stored ovarian cortical tissue for research. .....125**

## CHAPTER 5

**Table 5. 1 Culture medium and supplements used for HeLa cell culture. .....158**
**Table 5. 2 HeLa cell samples analysed to detect viable cells positive for intracellular cytokeratin 13 with FC. .....160**
**Table 5. 3 HeLa cell samples analysed to detect viable cells positive for intracellular DDX4 with FC. 161**
**Table 5. 4 Human remnant ovarian cell samples analysed to detect viable cells positive for intracellular DDX4 with FC.....165**
**Table 5. 5 Human frozen/thawed ovarian cell samples analysed to detect viable cells positive for intracellular DDX4 with FC.....165**
**Table 5. 6 Cell viability in ND and D groups from human fresh ovarian remnant tissue. . .....177**
**Table 5. 7 DDX4-positive cells from human fresh ovarian remnant tissue measured by FC. .....182**
**Table 5. 8 Viability of cells from human frozen/thawed ovarian cortical tissue measured by FC. .....187**
**Table 5. 9 DDX4-positive cells from human frozen/thawed ovarian cortical tissue measured by FC. .192**

## CHAPTER 7

**Table 7. 1 Experimental workflow to determine an alternative source of human somatic cells to support follicle development *in vivo* in the RO. .....243**

# Bibliography


Aaltonen, Johanna, Mika P. Laitinen, Kaisa Vuojolainen, Risto Jaatinen, Nina Horelli-Kuitunen, Laura Seppä, Henna Louhio, et al. 1999. "Human Growth Differentiation Factor 9 (GDF-9) and Its Novel Homolog GDF-9B Are Expressed in Oocytes during Early Folliculogenesis 1." *The Journal of Clinical Endocrinology & Metabolism* 84 (8): 2744–50.

Abdollahi, Maasoume, Mojdeh Salehnia, Saghar Salehpour, and Shahram Pour-Beiranvand. 2018. "Analysis of Apoptosis in Cultured Human Vitrified Ovarian Tissue in the Presence of Leukemia Inhibitory Factor." *Journal of Reproduction and Infertility* 19 (4): 193–202.

Adan, Aysun, Günel Alizada, Yağmur Kiraz, Yusuf Baran, and Ayten Nalbant. 2017. "Flow Cytometry: Basic Principles and Applications." *Critical Reviews in Biotechnology* 37 (2): 163–76.

Aittomäki, Kristiina, JoséLuis Dieguez Lucena, Pirjo Pakarinen, Pertti Sistonen, Juha Tapanainen, Jörg Gromoll, Riitta Kaskikari, et al. 1995. "Mutation in the Follicle-Stimulating Hormone Receptor Gene Causes Hereditary Hypergonadotropic Ovarian Failure." *Cell* 82 (6): 959–68.

Aittomaki, Kristina, Riitta Herva, Ulf-Hakan Stenman, Kaisa Juntunen, Pekka Ylostalo, Outi Hovatta, and Albert Chapelle. 1996. "Clinical Features of Primary Ovarian Failure Caused by a Point Mutation in the Follicle-Stimulating Hormone Receptor Gene." *Journal of Clinical Endocrinology and Metabolism* 81 (10): 3722–26.

Albright, Fuller, Patricia H. Smith, and Russell Fraser. 1942. "A Syndrome Characterised by Primary Ovarian Insufficiency and Decreased Stature." *The American Journal of the Medical Sciences* 204 (5): 625–48.

Anderson, Everett, and David F Albertini. 1976. "Gap Junctions between the Oocyte and Companion Follicle Cells in the Mammalian Ovary." *The Journal of Cell Biology* 71: 680–86.

Anderson, Richard A, Norma Fulton, Gillian Cowan, Shona Coutts, and Philippa Tk Saunders. 2007. "Conserved and Divergent Patterns of Expression of DAZL, VASA and OCT4 in the Germ Cells of the Human Fetal Ovary and Testis." *BMC Developmental Biology* 7 (136).

Angel, Thomas E, Uma K Aryal, Shawna M Hengel, Erin S Baker, Ryan T Kelly, Errol W Robinson, and Richard D Smith. 2012. "Mass Spectrometry Based Proteomics: Existing Capabilities and Future Directions." *Chemical Society Reviews* 41: 3912–28.

Antunes, J. Lobo, Peter W. Carmel, Edgar M. Housepian, and Michel Ferin. 1979. "Luteinizing Hormone-Releasing Hormone in Human Pituitary Blood." *Journal of Neurosurgery* 34 (4): 313–15.

Apweiler, Rolf, Amos Bairoch, Lydie Bougueleret, Severine Altairac, Valeria Amendolia, Andrea Auchincloss, Ghislaine Argoud-Puy, et al. 2009. "The Universal Protein Resource (UniProt) 2009." *Nucleic Acids Research* 37 (SUPPL. 1): 169–74.

Arnold, Melina, Mark J. Rutherford, Aude Bardot, Jacques Ferlay, Therese M.L. Andersson, Tor Åge Myklebust, Hanna Tervonen, et al. 2019. "Progress in Cancer Survival, Mortality, and Incidence in Seven High-Income Countries 1995–2014 (ICBP SURVMARK-2): A Population-Based Study." *The Lancet Oncology* 20 (11): 1493–1505.

Asiabi, Parinaz, Kohneh Shahri, Maria Costanza Chiti, and Christiani A Amorim. 2019. "Isolation and Characterization of the Human Ovarian Cell Population for Transplantation into an Artificial Ovary." *Animal Reproduction Science* 16 (1): 39–44.

Avolio, Elisa, Valeria V. Alvino, Mohamed T. Ghorbel, and Paola Campagnolo. 2017. "Perivascular Cells and Tissue Engineering: Current Applications and Untapped Potential." *Pharmacology and Therapeutics* 171: 83–92.

Baca, Manuel, and Luciano Zamboni. 1967. "The Fine Structure of Human Follicular Oocytes." *Journal of Ultrasructure Research* 19: 354–81.

Bachelot, Anne, Carole Nicolas, Maud Bidet, Jérôme Dulon, Monique Leban, Jean Louis Golmard,

Michel Polak, and Philippe Touraine. 2017. “Long-Term Outcome of Ovarian Function in Women with Intermittent Premature Ovarian Insufficiency.” *Clinical Endocrinology* 86 (2): 223–28.

Bainbridge, P. 2013. “Wound Healing and the Role of Fibroblasts.” *Journal of Wound Care* 22 (8): 407–12.

Barrett, Susan L., Lonnie D. Shea, and Teresa K. Woodruff. 2010. “Noninvasive Index of Cryorecovery and Growth Potential for Human Follicles in Vitro.” *Biology of Reproduction* 82 (6): 1180–89.

Bedoschi, Giuliano, Paula Andrea Navarro, and Kutluk Oktay. 2016. “Chemotherapy-Induced Damage to Ovary: Mechanisms and Clinical Impact.” *Future Oncology* 12 (19): 2333–44.

Berkholtz, Courtney B, Bonnie E Lai, Teresa K Woodruff, and Lonnie D Shea. 2006. “Distribution of Extracellular Matrix Proteins Type I Collagen, Type IV Collagen, Fibronectin, and Laminin in Mouse Folliculogenesis.” *Histochemistry and Cell Biology* 126 (5): 583–92.

Bidet, Maud, Anne Bachelot, Estelle Bissauge, Jean Louis Golmard, Solenne Gricourt, Jeŕoḿe Dulon, Christiane Coussieu, Yasmina Badachi, and Philippe Touraine. 2011. “Resumption of Ovarian Function and Pregnancies in 358 Patients with Premature Ovarian Failure.” *Journal of Clinical Endocrinology and Metabolism* 96 (12): 3864–72.

Bidet, Maud, Anne Bachelot, and Philippe Touraine. 2008. “Premature Ovarian Failure: Predictability of Intermittent Ovarian Function and Response to Ovulation Induction Agents.” *Current Opinion in Obstetrics and Gynecology* 20 (4): 416–20.

Billig, Hakan, Itsuko Furuta, and Aaron J W Hsueh. 1993. “Estrogens Inhibit and Androgens Enhance Ovarian Granulosa Cell Apoptosis.” *Endocrinology* 133 (5): 2204–12.

Birgit, Borgström, Hreinsson Julius, Rasmussen Carsten, Sheikhi Maryam, Fried Gabriel, Keros Victoria, Fridström Margareta, and Hovatta Outi. 2009. “Fertility Preservation in Girls with Turner Syndrome: Prognostic Signs of the Presence of Ovarian Follicles.” *Journal of Clinical Endocrinology and Metabolism* 94 (1): 74–80.

Blaustein, Ancel. 1982. *Blaustein’s Pathology of the Female Genital Tract*. Edited by Robert J. Kurkman, Lora Hedrick Ellenson, and Brigitte M. Ronett. *Blaustein’s Pathology of the Female Genital Tract*. Springer International Publishing.

Bourret, Rodolphe, Eric Martinez, François Vialla, Chloé Giquel, Aurélie Thonnat-Marin, and John De Vos. 2016. “Human-Animal Chimeras: Ethical Issues about Farming Chimeric Animals Bearing Human Organs.” *Stem Cell Research and Therapy* 7 (1).

Brando, Bruno, David Barnett, George Janossy, Francis Mandy, Brigitte Autran, Gregor Rothe, Barbara Scarpati, et al. 2000. “Cytofluorometric Methods for Assessing Absolute Numbers of Cell Subsets in Blood.” *Communications in Clinical Cytometry* 42 (6): 327–46.

Braw-Tal, R., and Z. Roth. 2005. “Gene Expression for LH Receptor, 17α-Hydroxylase and StAR in the Theca Interna of Preantral and Early Antral Follicles in the Bovine Ovary.” *Reproduction* 129 (4): 453–61.

Briley, Shawn M., Susmita Jasti, Jennifer M. McCracken, Jessica E. Hornick, Barbara Fegley, Michele T. Pritchard, and Francesca E. Duncan. 2016. “Reproductive Age-Associated Fibrosis in the Stroma of the Mammalian Ovary.” *Reproduction* 152 (3): 245–60.

Brink, Susanne C van den, Fanny Sage, Abel Vertesy, Bastiaan Spanjaard, Josi Peterson-Maduro, Chloe S Baron, Catherine Robin, and Alexander van Oudenaarden. 2017. “Single-Cell Sequencing Reveals Dissociation-Induced Gene Expression in Tissue Subpopulations.” *Nature Methods* 14 (10): 935–36.

Britt, Kara L., Ann E. Drummond, Victoria A. Cox, Mitzilee Dyson, Nigel G. Wreford, Margaret E.E. Jones, Evan R. Simpson, and Jock K. Findlay. 2000. “An Age-Related Ovarian Phenotype in Mice with Targeted Disruption of the Cyp 19 (Aromatase) Gene.” *Endocrinology* 141 (7): 2614–23.

Britt, Kara L., Philippa K. Saunders, Stephen J. McPherson, Marie L. Misso, Evan R. Simpson, and Jock K. Findlay. 2004. “Estrogen Actions on Follicle Formation and Early Follicle

Development1." *Biology of Reproduction* 71 (5): 1712–23.
Byrne, Julianne, Thomas R. Fears, Mitchell H. Gail, David Pee, Roger R. Connelly, Donald F. Austin, Grace F. Holmes, et al. 1992. "Early Menopause in Long-Term Survivors of Cancer during Adolescence." *American Journal of Obstetrics and Gynecology* 166 (3): 788–93.
Camp, Tamara A, Jason O Rahal, and Kelly E Mayo. 1991. "Cellular Localization and Hormonal Regulation of Follicle-Stimulating Hormone and Luteinizing Hormone Receptor Messenger RNAs in the Rat Ovary." *Molecular Endocrinology* 5 (10): 1405–17.
Cancer Research UK. n.d. "Cancer Survival Statistics for All Cancers Combined | Cancer Research UK." Accessed December 24, 2020. https://www.cancerresearchuk.org/health-professional/cancer-statistics/survival/all-cancers-combined#heading-One.
Cao, Hongguo, Pan Yang, Yong Pu, Xueping Sun, Huiqun Yin, Yu Zhang, Yunhai Zhang, et al. 2012. "Characterization of Bovine Induced Pluripotent Stem Cells by Lentiviral Transduction of Reprogramming Factor Fusion Proteins." *International Journal of Biological Sciences* 8 (4): 498–511.
Castrillon, Diego H., Lili Miao, Ramya Kollipara, James W. Horner, and Ronald A. DePinho. 2003. "Suppression of Ovarian Follicle Activation in Mice by the Transcription Factor Foxo3a." *Science* 301 (5630): 215–18.
Castrillon, Diego H, Bradley J Quade, T Y Wang, Catherine Quigley, Christopher P Crum, Mackay Memorial Hospital, and Taiwan D Communicated by Jean Wilson. 2000. "The Human VASA Gene Is Specifically Expressed in the Germ Cell Lineage." *PNAS* 97 (17): 9585–90.
Cen, Changhuo, Min Chen, Jingjing Zhou, Lianjun Zhang, Shuguang Duo, Lin Jiang, Xiaohui Hou, and Fei Gao. 2020. "Inactivation of Wt1 Causes Pre-Granulosa Cell to Steroidogenic Cell Transformation and Defect of Ovary Development." *Biology of Reproduction* 103 (1): 60–69.
Chand, A. L., C. A. Harrison, and A. N. Shelling. 2009. "Inhibin and Premature Ovarian Failure." *Human Reproduction Update* 16 (1): 39–50.
Chen, K, Barbara S. Mallon, Ronald D.G. McKay, and Pamela G. Robey. 2017. "Optimized Template Detection and Extraction Algorithm for Web Scraping of Dynamic Web Pages." *Global Journal of Pure and Applied Mathematics* 13 (2): 973–1768.
Chiti, Maria Costanza, Marie-Madeleine Dolmans, Maria Hobeika, Alice Cernogoraz, Jacques Donnez, and Christiani Andrade Amorim. 2017. "A Modified and Tailored Human Follicle Isolation Procedure Improves Follicle Recovery and Survival." *Journal of Ovarian Research* 10 (71).
Chiti, Maria Costanza, Marie-Madeleine Dolmans, Lucie Mortiaux, Flanco Zhuge, Emna Ouni, Parinaz Asiabi, Kohneh Shahri, et al. 2018. "A Novel Fibrin-Based Artificial Ovary Prototype Resembling Human Ovarian Tissue in Terms of Architecture and Rigidity." *Journal of Assisted Reproduction and Genetics* 35: 41–48.
Cho, Eun, Yoon Young Kim, Kevin Noh, and Seung Yup Ku. 2019. "A New Possibility in Fertility Preservation: The Artificial Ovary." *Journal of Tissue Engineering and Regenerative Medicine* 13 (8): 1294–1315.
Christofolini, Denise Maria, Emerson Barchi Cordts, Fernando Santos-Pinheiro, Erika Azuma Kayaki, Mayla Cristina Fernandes Dornas, Monise de Castro Santos, Bianca Bianco, and Caio Parente Barbosa. 2017. "How Polymorphic Markers Contribute to Genetic Diseases in Different Populations? The Study of Inhibin A for Premature Ovarian Insufficiency." *Einstein (Sao Paulo, Brazil)* 15 (3): 269–72.
Clarkson, Yvonne L, Marie Mclaughlin, Martin Waterfall, Cheryl E Dunlop, Paul A Skehel, Richard A Anderson, and Evelyn E Telfer. 2018. "Initial Characterisation of Adult Human Ovarian Cell Populations Isolated by DDX4 Expression and Aldehyde Dehydrogenase Activity." *Scientific Reports* 8 (6953).
Cohen, Dena E, and Douglas Melton. 2011. "Turning Straw into Gold: Directing Cell Fate for Regenerative Medicine." *Nature Reviews Genetics* 12: 243–52.

Coleman, M L, and M F Olson. 2002. “Rho GTPase Signalling Pathways in the Morphological Changes Associated with Apoptosis.” *Cell Death and Differentiation* 9: 493–504.

Condorelli, Margherita, and Isabelle Demeestere. 2019. “Challenges of Fertility Preservation in Non-Oncological Diseases.” *Acta Obstetricia et Gynecologica Scandinavica* 98 (5): 638–46.

Conneely, Orla M., Biserka Mulac-Jericevic, and John P. Lydon. 2003. “Progesterone-Dependent Regulation of Female Reproductive Activity by Two Distinct Progesterone Receptor Isoforms.” *Steroids* 68 (10–13): 771–78.

Corre, Tanguy, Julia Schuettler, Silvia Bione, Anna Marozzi, Luca Persani, Raffaella Rossetti, Francesca Torricelli, Irene Giotti, Peter Vogt, and Daniela Toniolo. 2009. “A Large-Scale Association Study to Assess the Impact of Known Variants of the Human INHA Gene on Premature Ovarian Failure.” *Human Reproduction* 24 (9): 2023–28.

Coulam, Carolyn B., Steven C. Adamson, and Annegers John F. F. 1986. “Incidence of Premature Ovarian Failure.” *Obstetrics & Gynecology* 67 (4): 604–6.

Couse, John F., Jonathan Lindzey, Kaj Grandien, Jan Åke Gustafsson, and Kenneth S. Korach. 1997. “Tissue Distribution and Quantitative Analysis of Estrogen Receptor-α (ERα) and Estrogen Receptor-β (ERβ) Messenger Ribonucleic Acid in the Wild-Type and ERα-Knockout Mouse.” *Endocrinology* 138 (11): 4613–21.

Craig, Jesse, Makoto Orisaka, Hongmei Wang, Sanae Orisaka, Winston Thompson, Cheng Zhu, Fumikazu Kotsuji, and Benjamin K Tsang. 2007. “Gonadotropin and Intra-Ovarian Signals Regulating Follicle Development and Atresia: The Delicate Balance between Life and Death.” *Frontiers in Bioscience* 12: 3628–39.

Davidson, Ben, Reuven Reich, Viive M Howell, Angela Cho, and Emily K Colvin. 2015. “The Extracellular Matrix in Epithelial Ovarian Cancer – a Piece of a Puzzle.” *Frontiers in Oncology* 5: 245.

DerVen, H. Van, J. Liebenthron, M. Beckmann, B. Toth, M. Korell, J. Krüssel, T. Frambach, et al. 2016. “Ninety-Five Orthotopic Transplantations in 74 Women of Ovarian Tissue after Cytotoxic Treatment in a Fertility Preservation Network: Tissue Activity, Pregnancy and Delivery Rates.” *Human Reproduction* 31 (9): 2031–41.

Desai, Swapna S, Binita Sur Roy, and Smita D Mahale. 2013. “Mutations and Polymorphisms in FSH Receptor: Functional Implications in Human Reproduction.” *Reproduction* 146: 235–48.

Dierich, Andree, M. Ram Sairam, Lucia Monaco, Gian Maria Fimia, Anne Gansmuller, Marianne Lemeur, and Paolo Sassone-Corsi. 1998. “Impairing Follicle-Stimulating Hormone (FSH) Signaling in Vivo: Targeted Disruption of the FSH Receptor Leads to Aberrant Gametogenesis and Hormonal Imbalance.” *Proceedings of the National Academy of Sciences of the United States of America* 95 (23): 13612–17.

Dittmar, Manuela, and George J. Kahaly. 2003. “Polyglandular Autoimmune Syndromes: Immunogenetics and Long-Term Follow-Up.” *Journal of Clinical Endocrinology and Metabolism* 88 (7): 2983–92.

Dixit, H, M Deendayal, and L Singh. 2004. “Mutational Analysis of the Mature Peptide Region of Inhibin Genes in Indian Women with Ovarian Failure.” *Human Reproduction* 19 (8): 1760–64.

Dixit, Hridesh, Lakshmi K. Rao, Venkata V. Padmalatha, Murthy Kanakavalli, Mamata Deenadayal, Nalini Gupta, Baidyanath Chakrabarty, and Lalji Singh. 2006. “Missense Mutations in the BMP15 Gene Are Associated with Ovarian Failure.” *Human Genetics* 119 (4): 408–15.

Doherty, Elaine, Pirjo Pakarinen, Aila Tiitinen, Anna Kiilavuori, Ilpo Huhtaniemi, Susan Forrest, and Kristiina Aittomäki. 2002. “A Novel Mutation in the FSH Receptor Inhibiting Signal Transduction and Causing Primary Ovarian Failure.” *Journal of Clinical Endocrinology and Metabolism* 87 (3): 1151–55.

Dolmans, Marie Madeleine, Valérie Luyckx, Jacques Donnez, Claus Yding Andersen, and Tine

Greve. 2013. “Risk of Transferring Malignant Cells with Transplanted Frozen-Thawed Ovarian Tissue.” *Fertility and Sterility* 99 (6): 1514–22.

Dolmans, Marie Madeleine, and Diego D Manavella. 2018. “Recent Advances in Fertility Preservation.” *The Journal of Obstetrics and Gynaecology Research* 45 (2): 266–79.

Dolmans, Marie Madeleine, Nathalie Michaux, Alessandra Camboni, Belen Martinez-Madrid, Anne Van Langendonckt, Stefania Annarita Nottola, and Jacques Donnez. 2006. “Evaluation of Liberase, a Purified Enzyme Blend, for the Isolation of Human Primordial and Primary Ovarian Follicles.” *Human Reproduction* 21 (2): 413–20.

Dong, J., D. F. Albertini, K. Nishimori, T. R. Kumar, N. Lu, and M. M. Matzuk. 1996. “Growth Differentiation Factor-9 Is Required during Early Ovarian Folliculogenesis.” *Nature* 383 (6600): 531–35.

Drummond, Ann E. 2006. “The Role of Steroids in Follicular Growth.” *Reproductive Biology and Endocrinology* 4 (16).

Drummond, Ann E, and Jock K Findlay. 1999. “The Role of Estrogen in Folliculogenesis.” *Molecular and Cellular Endocrinology* 151 (1999): 57–64.

Dube, Jennifer L., Pei Wang, Julia Elvin, Karen M. Lyons, Anthony J. Celeste, and Martin M. Matzuk. 1998. “The Bone Morphogenetic Protein 15 Gene Is X-Linked and Expressed in Oocytes.” *Molecular Endocrinology* 12 (12): 1809–17.

Duffin, K, R A L Bayne, A J Childs, C Collins, and R A Anderson. 2009. “The Forkhead Transcription Factor FOXL2 Is Expressed in Somatic Cells of the Human Ovary Prior to Follicle Formation.” *Molecular Human Reproduction* 15 (12): 771–77.

Duguay, Duke, Ramsey A. Foty, and Malcolm S. Steinberg. 2003. “Cadherin-Mediated Cell Adhesion and Tissue Segregation: Qualitative and Quantitative Determinants.” *Developmental Biology* 253 (2): 309–23.

Dunham, Wade H., Michael Mullin, and Anne Claude Gingras. 2012. “Affinity-Purification Coupled to Mass Spectrometry: Basic Principles and Strategies.” *Proteomics* 12 (10): 1576–90.

Durlinger, Alexandra L. L., Piet Kramer, Bas Karels, Frank H. de Jong, Jan Th. J. Uilenbroek, J. Anton Grootegoed, and Axel P. N. Themmen. 1999. “Control of Primordial Follicle Recruitment by Anti-Müllerian Hormone in the Mouse Ovary1.” *Endocrinology* 140 (12): 5789–96.

Durlinger, Alexandra L.L., Maria J.G. Gruijters, Piet Kramer, Bas Karels, Holly A. Ingraham, Mark W. Nachtigal, Jan Th J. Uilenbroek, J. Anton Grootegoed, and Axel P.N. Themmen. 2002. “Anti-Müllerian Hormone Inhibits Initiation of Primordial Follicle Growth in the Mouse Ovary.” *Endocrinology* 143 (3): 1076–84.

El-Hayek, Stephany, Qin Yang, Laleh Abbassi, Greg FitzHarris, and Hugh J. Clarke. 2018. “Mammalian Oocytes Locally Remodel Follicular Architecture to Provide the Foundation for Germline-Soma Communication.” *Current Biology* 28 (7): 1124-1131.e3.

Elsheikh, M., D. B. Dunger, G. S. Conway, and J. A. H. Wass. 2002. “Turner’s Syndrome in Adulthood.” *Endocrine Reviews* 23 (1): 120–40.

Eppig, John J, and Karen Wigglesworth. 2000. “Development of Mouse and Rat Oocytes in Chimeric Reaggregated Ovaries after Interspecific Exchange of Somatic and Germ Cell Components.” *Biology of Reproduction* 63: 1014–23.

Eppig, John J, Karen Wigglesworth, and Frank L Pendola. 2002. “The Mammalian Oocyte Orchestrates the Rate of Ovarian Follicular Development.” *PNAS* 99 (5): 2890–94.

Erickson, Gregory F., Dennis A. Magoffin, Cheryl A. Dyer, and Chris Hofeditz. 1985. “The Ovarian Androgen Producing Cells: A Review of Structure/Function Relationships.” *Endocrine Reviews* 6 (3): 371–99.

Faddy, M. J. 2000. “Follicle Dynamics during Ovarian Ageing.” *Molecular and Cellular Endocrinology* 163 (1–2): 43–48.

Faddy, M J, and R G Gosden. 1996. “A Model Conforming the Decline in Follicle Numbers to the

Age of Menopause in Women." *Human Reproduction* 11 (7): 1484–86.
Fagerberg, Linn, Kalle Jonasson, Gunnar Von Heijne, Mathias Uhlén, and Lisa Berglund. 2010. "Prediction of the Human Membrane Proteome." *Proteomics* 10 (6): 1141–49.
Familiari, Giuseppe, Alberto Caggiati, Stefania A. Nottola, Michele Ermini, Maria Rita Di Benedetto, and Pietro M. Motta. 1993. "Infertility: Ultrastructure of Human Ovarian Primordial Follicles after Combination Chemotherapy for Hodgkin's Disease." *Human Reproduction* 8 (12): 2080–87.
Fan, X, M Bialecka, I Moustakas, E Lam, V Torrens-Juaneda, N V Borggreven, L Trouw, et al. 2019. "Single-Cell Reconstruction of Follicular Remodeling in the Human Adult Ovary." *Nature Communications* 10 (3164).
Fauque, Patricia, Anis Ben Amor, Christiane Joanne, Germain Agnani, Jean Luc Bresson, and Christophe Roux. 2007. "Use of Trypan Blue Staining to Assess the Quality of Ovarian Cryopreservation." *Fertility and Sterility* 87 (5).
Fauser, Bart C J M, and Arne M Van Heusden. 1997. "Manipulation of Human Ovarian Function: Physiological Concepts and Clinical Consequences." *Endocrine Reviews* 18 (1).
Faustino, L. R., R. R. Santos, C. M.G. Silva, L. C. Pinto, J. J.H. Celestino, C. C. Campello, J. R. Figueiredo, and A. P.R. Rodrigues. 2010. "Goat and Sheep Ovarian Tissue Cryopreservation: Effects on the Morphology and Development of Primordial Follicles and Density of Stromal Cell." *Animal Reproduction Science* 122 (1–2): 90–97.
Felici, Massimo De. 2013. "Origin, Migration, and Proliferation of Human Primordial Germ Cells." In *Oogenesis*, 19–37. Springer-Verlag London Ltd.
Feng, Yan Min, Gui Jin Liang, Bo Pan, Xun Si Qin, Xi Feng Zhang, Chun Lei Chen, Lan Li, Shun Feng Cheng, Massimo De Felici, and Wei Shen. 2014. "Notch Pathway Regulates Female Germ Cell Meiosis Progression and Early Oogenesis Events in Fetal Mouse." *Cell Cycle* 13 (5): 782–91.
Findlay, John K, Karla J Hutt, Martha Hickey, and Richard A Anderson. 2015. "How Is the Number of Primordial Follicles in the Ovarian Reserve Established?" *Biology of Reproduction* 93 (5): 111–12.
Fisher, Carolyn R., Kathy H. Graves, Albert F. Parlow, and Evan R. Simpson. 1998. "Characterization of Mice Deficient in Aromatase (ArKO) Because of Targeted Disruption of the Cyp19 Gene." *Proceedings of the National Academy of Sciences of the United States of America* 95 (12): 6965–70.
Flaws, Jodi A., Fady I. Sharara, Ellen K. Silbergeld, and Anne N. Hirshfield. 2000. "Environmental Exposures and Women's Reproductive Health." In *Women and Health*, edited by Marlene B. Goldman and Maureen C. Hatch, 625–33. Academic Press.
Forges, T., P. Monnier-Barbarino, G. C. Faure, and M. C. Béné. 2004. "Autoimmunity and Antigenic Targets in Ovarian Pathology." *Human Reproduction Update* 10 (2): 163–75.
Fraison, Eloise, Giselle Crawford, Gabrielle Casper, Victoria Harris, and William Ledger. 2019. "Pregnancy Following Diagnosis of Premature Ovarian Insufficiency: A Systematic Review." *Reproductive BioMedicine Online* 39 (3): 467–76.
Gallardo, Miguel, Fernanda Paulini, Ariadna Corral, Marcin Balcerzyk, Carolina M. Lucci, Jérôme Ambroise, Marta Merola, et al. 2018. "Evaluation of a New Freezing Protocol Containing 20% Dimethyl Sulphoxide Concentration to Cryopreserve Human Ovarian Tissue." *Reproductive BioMedicine Online* 37 (6): 653–65.
Georges, Adrien, Aurelie Auguste, Laurianne Bessière, Anne Vanet, Anne Laure Todeschini, and Reiner A. Veitia. 2014. "FOXL2: A Central Transcription Factor of the Ovary." *Journal of Molecular Endocrinology* 52 (1): 17–33.
Gittens, J. E. I., and Gerald M. Kidder. 2005. "Differential Contributions of Connexin37 and Connexin43 to Oogenesis Revealed in Chimeric Reaggregated Mouse Ovaries." *Journal of Cell Science* 118 (21): 5071–78.
Gondos, Bernard, Lars Westergaard, and Anne Grete Byskov. 1986. "Initiation of Oogenesis in

the Human Fetal Ovary: Ultrastructural and Squash Preparation Study." *American Journal of Obstetrics and Gynecology* 155 (1): 189–95.
Gook, Debra A., D. H. Edgar, J. Borg, and M. Martic. 2008. "Detection of Zona Pellucida Proteins during Human Folliculogenesis." *Human Reproduction* 23 (2): 394–402.
Gook, Debra A, D H Edgar, and C Stern. 1999. "Effect of Cooling Rate and Dehydration Regimen on the Histological Appearance of Human Ovarian Cortex Following Cryopreservation in 1,2-Propanediol." *Human Reproduction* 14 (8): 2061–68.
Gosden, R. G. 2000. "Low Temperature Storage and Grafting of Human Ovarian Tissue." *Molecular and Cellular Endocrinology* 163 (1–2): 125–29.
Goswami, Deepti, and Gerard S. Conway. 2005. "Premature Ovarian Failure." *Human Reproduction Update* 11 (4): 391–410.
Gougeon, A. 1986. "Dynamics of Follicular Growth in the Human: A Model from Preliminary Results." *Human Reproduction* 1 (2): 81–87.
Gougeon, Alain. 1996. "Regulation of Ovarian Follicular Development in Primates: Facts and Hypotheses." *Endocrine Reviews* 17 (2): 121–55.
Graham, J. Dinny, and Christine L. Clarke. 1997. "Physiological Action of Progesterone in Target Tissues." *Endocrine Reviews* 18 (4): 502–19.
Grasa, Patricia, Heidy Kaune, and Suzannah A. Williams. 2012. "Embryos Generated from Oocytes Lacking Complex N- and O-Glycans Have Compromised Development and Implantation." *Reproduction* 144 (4): 455–65.
Grieve, Kelsey M., Marie McLaughlin, Cheryl E. Dunlop, Evelyn E. Telfer, and Richard A. Anderson. 2015. "The Controversial Existence and Functional Potential of Oogonial Stem Cells." *Maturitas* 82 (3): 278–81.
Griffin, Jeanine, Benjamin R Emery, Ivan Huang, Matthew Peterson, and Douglas T Carrell. 2006. "Comparative Analysis of Follicle Morphology and Oocyte Diameter in Four Mammalian Species (Mouse, Hamster, Pig, and Human)." *Experimental and Clinical Assisted Reproduction* 3 (2).
Grosbois, J., and I. Demeestere. 2018. "Dynamics of PI3K and Hippo Signaling Pathways during in Vitro Human Follicle Activation." *Human Reproduction* 33 (9): 1705–14.
Grynberg, Michal El, Maud Bidet, Julie Benard, Marine Poulain, Charlotte Sonigo, Isabelle C Edrin-Durnerin, and Michel Polak. 2016. "Fertility Preservation in Turner Syndrome." *Fertility and Sterility* 105 (1): 13–19.
Gustafson, Eric A., and Gary M. Wessel. 2010. "Vasa Genes: Emerging Roles in the Germ Line and in Multipotent Cells." *BioEssays* 32 (7): 626–37.
Guzel, Yilmaz, Yilda Arzu Aba, Kayhan Yakin, and Ozgur Oktem. 2017. "Menstrual Cycle Characteristics of Young Females with Occult Primary Ovarian Insufficiency at Initial Diagnosis and One-Year Follow-up with Serum Amh Level and Antral Follicle Count." *PLoS One* 12 (11).
Hagen, Casper P, Kaspar Sørensen, Lise Aksglaede, Annette Mouritsen, Mikkel G Mieritz, Jeanette Tinggaard, Christine Wohlfart-Veje, et al. 2014. "Pubertal Onset in Girls Is Strongly Influenced by Genetic Variation Affecting FSH Action." *Scientific Reports* 4 (6412).
Hashimoto, Hisashi, Tamotsu Sudo, Yoshiki Mikami, Mieko Otani, Masaoki Takano, Hiroshi Tsuda, Hiroaki Itamochi, Hidetaka Katabuchi, Masaharu Ito, and Ryuichiro Nishimura. 2008. "Germ Cell Specific Protein VASA Is Over-Expressed in Epithelial Ovarian Cancer and Disrupts DNA Damage-Induced G2 Checkpoint." *Gynecologic Oncology* 111 (2): 312–19.
Hayashi, Masaru, E. A. McGee, Gyesik Min, Cynthia Klein, Ursula M. Rose, Marcel Van Duin, and Aaron J.W. Hsueh. 1999. "Recombinant Growth Differentiation Factor-9 (GDF-9) Enhances Growth and Differentiation of Cultured Early Ovarian Follicles." *Endocrinology* 140 (3): 1236–44.
Heeren, A. Marijne, Liesbeth Van Iperen, Daniëlle B. Klootwijk, Ana De Melo Bernardo, Matthias S. Roost, Maria M.Gomes Fernandes, Leonie A. Louwe, et al. 2015. "Development of the

Follicular Basement Membrane during Human Gametogenesis and Early Folliculogenesis." *BMC Developmental Biology* 15 (1): 1–13.

Heller, Carl G., and Emily J. Heller. 1939. "Gonadotropic Hormone: Urine Assays of Normally Cycling, Menopausal, Castrated, and Estrin Treated Human Females 1." *Journal of Clinical Investigation* 18 (2): 171–78.

Hennet, Margo L., and Catherine M.H. Combelles. 2012. "The Antral Follicle: A Microenvironment for Oocyte Differentiation." *International Journal of Developmental Biology* 56 (10–12): 819–31.

Hikabe, Orie, Nobuhiko Hamazaki, Go Nagamatsu, Yayoi Obata, Yuji Hirao, Norio Hamada, So Shimamoto, et al. 2016. "Reconstitution in Vitro of the Entire Cycle of the Mouse Female Germ Line." *Nature* 539: 299–303.

Himelstein, Braw R., A. G. Byskov, H. Peters, and M. Faber. 1976. "Follicular Atresia in the Infant Human Ovary." *Journal of Reproduction and Fertility* 46 (1): 55–59.

Hirshfield, Anne Newman. 1991. "Development of Follicles in the Mammalian Ovary." *International Review of Cytology* 124: 43–101.

Homcha, Christine, and H Paul Ehrlich. 2011. "Fibroblast Expression of α-Smooth Muscle Actin, A2β1 Integrin and Avβ3 Integrin: Influence of Surface Rigidity." *Experimental and Molecular Pathology* 91: 394–99.

Hornick, J E, F E Duncan, L D Shea, and T K Woodruff. 2012. "Isolated Primate Primordial Follicles Require a Rigid Physical Environment to Survive and Grow in Vitro." *Human Reproduction* 27 (6): 1801–10.

Hovatta, Outi, Rene Silye, Thomas Krausz, Ronit Abir, Raul Margara, Geoffrey Trew, Amir Lass, and Robert M L Winston. 1996. "Cryopreservation of Human Ovarian Tissue Using Dimethylsulphoxide and Propanediol-Sucrose as Cryoprotectants." *Human Reproduction* 11 (6): 1268–72.

Hovatta, Outi, Catherine Wright, Thomas Krausz, Kate Hardy, and Robert M.L. Winston. 1999. "Human Primordial, Primary and Secondary Ovarian Follicles in Long-Term Culture: Effect of Partial Isolation." *Human Reproduction* 14 (10): 2519–24.

Høyer, Poul Erik, Anne Grete Byskov, and Kjeld Møllgård. 2005. "Stem Cell Factor and C-Kit in Human Primordial Germ Cells and Fetal Ovaries." *Molecular and Cellular Endocrinology* 234 (1–2): 1–10.

Hreinsson, Julius Gisli, Marjut Otala, Margareta Fridström, Birgit Borgström, Carsten Rasmussen, Monalill Lundqvist, Timo Tuuri, et al. 2002. "Follicles Are Found in the Ovaries of Adolescent Girls with Turner's Syndrome." *Journal of Clinical Endocrinology and Metabolism* 87 (8): 3618–23.

Hreinsson, Julius, Pu Zhang, Marja Liisa Swahn, Kjell Hultenby, and Outi Hovatta. 2003. "Cryopreservation of Follicles in Human Ovarian Cortical Tissue. Comparison of Serum and Human Serum Albumin in the Cryoprotectant Solutions." *Human Reproduction* 18 (11): 2420–28.

Hu, Yueh Chiang, Peng Hui Wang, Shuyuan Yeh, Ruey Sheng Wang, Chao Xie, Qingquan Xu, Xinchang Zhou, Hsiang Tai Chao, Meng Yin Tsai, and Chawnshang Chang. 2004. "Subfertility and Defective Folliculogenesis in Female Mice Lacking Androgen Receptor." *PNAS* 101 (31): 11209–14.

Huang, Wenling, Ying Cao, and Lei Shi. 2019. "Effects of FSHR Polymorphisms on Premature Ovarian Insufficiency in Human Beings: A Meta-Analysis." *Reproductive Biology and Endocrinology* 17 (80).

Hummitzsch, Katja, Richard A. Anderson, Dagmar Wilhelm, Ji Wu, Evelyn E. Telfer, Darryl L. Russell, Sarah A. Robertson, and Raymond J. Rodgers. 2015. "Stem Cells, Progenitor Cells, and Lineage Decisions in the Ovary." *Endocrine Reviews* 36 (1): 65–91.

Jacobs, Patricia A., A. G. Baikie, W. M.Court Brown, T. N. MacGregor, N. Maclean, and D. G. Harnden. 1960. "Evidence for the Existence of the Human 'Super Female.'" *Obstetrical and*

*Gynecological Survey* 15 (3): 440–41.

Jager, Lindsey D., PhD, Claire-Marie A. Canda, Crystal A. Hall, Cassandra L. Heilingoetter, Joann Huynh, Susanna S. Kwok, Jin H. Kwon, Jacob R. Richie, and MS Jensen, Matthew B. MD. 2017. "Effect of Enzymatic and Mechanical Methods of Dissociation on Neural Progenitor Cells Derived from Induced Pluripotent Stem Cells." *Physiology & Behavior* 176 (12): 139–48.

Jahr, H., G. Pfeiffer, B. J. Hering, K. Federlin, and R. G. Bretzel. 1999. "Endotoxin-Mediated Activation of Cytokine Production in Human PBMCs by Collagenase and Ficoll." In *Journal of Molecular Medicine*, 77:118–20. Springer Verlag.

Jennison, Marshall W. 1945. "BACTERIAL COLLAGENASE."

Jewelewicz, Raphael, and Moshe Schwartz. 1986. "Premature Ovarian Failure." *The Bulletin of New York Academy of Medicine* 62 (3).

Jia, Xiao Chi, Bruce Kessel, Thomas H. Welsh, and Aaron J.W. Hsueh. 1985. "Androgen Inhibition of Follicle-Stimulating Hormone-Stimulated Luteinizing Hormone Receptor Formation in Cultured Rat Granulosa Cells." *Endocrinology* 117 (1): 13–22.

Jiang, Min, Kristiina Aittomaki, Christel Nilsson, Pirjo Pakarinen, Antti Iitia, Toni Torresani, Henrik Simonsen, et al. 1998. "The Frequency of an Inactivating Point Mutation (566C-->T) of the Human Follicle-Stimulating Hormone Receptor Gene in Four Populations Using Allele-Specific Hybridization and Time-Resolved Fluorometry." *Journal of Clinical Endocrinology and MetabolismEndocrinology* 83 (12): 4338–43.

Jiang, Xuliang, James A. Dias, and Xiaolin He. 2014. "Structural Biology of Glycoprotein Hormones and Their Receptors: Insights to Signaling." *Molecular and Cellular Endocrinology* 382 (1): 424–51.

John, George B, Teresa D Gallardo, Lane J Shirley, and Diego H Castrillon. 2008. "Foxo3 Is a PI3K-Dependent Molecular Switch Controlling the Initiation of Oocyte Growth." *Developmental Biology* 321: 197–204.

Josso, Nathalie, Isabelle Lamarre, Jean Yves Picard, Philippe Berta, Norman Davies, Nicole Morichon, Marc Peschanski, and Roland Jeny. 1993. "Anti-Müllerian Hormone in Early Human Development." *Early Human Development* 33 (2): 91–99.

Julian, Linda, and Michael F Olson. 2014. "Rho-Associated Coiled-Coil Containing Kinases (ROCK): Structure, Regulation, and Functions. Small GTPases." *Landes Bioscience* 5.

Kaivo-Oja, Noora, Jonas Bondestam, Meerit Kämäräinen, Janne Koskimies, Ursula Vitt, Mark Cranfield, Kaisa Vuojolainen, et al. 2003. "Growth Differentiation Factor-9 Induces Smad2 Activation and Inhibin B Production in Cultured Human Granulosa-Luteal Cells." *Journal of Clinical Endocrinology and Metabolism* 88 (2): 755–62.

Kasteren, Y M Van, and J Schoemaker. 1999. "Premature Ovarian Failure: A Systematic Review on Therapeutic Interventions to Restore Ovarian Function and Achieve Pregnancy." *Human Reproduction* 5 (5): 483–92.

Kaune, Heidy, Sairah Sheikh, and Suzannah A. Williams. 2017. "Analysis of in Vitro Follicle Development during the Onset of Premature Ovarian Insufficiency in a Mouse Model." *Reproduction, Fertility and Development* 29 (8): 1538–44.

Kawamura, Kazuhiro, Yuan Cheng, Nao Suzuki, Masashi Deguchi, Yorino Sato, Seido Takae, Chi Hong Ho, et al. 2013. "Hippo Signaling Disruption and Akt Stimulation of Ovarian Follicles for Infertility Treatment." *PNAS* 110 (43): 17474–79.

Kendrick, Nancy, Costel C. Darie, Matt Hoelter, Ginny Powers, and Jon Johansen. 2019. "2D SDS PAGE in Combination with Western Blotting and Mass Spectrometry Is a Robust Method for Protein Analysis with Many Applications." *Advances in Experimental Medicine and Biology* 1140: 563–74.

Kessel, Bruce, V X Liu, X C Jia, and Aaron J W Hsueh2. 1985. "Autocrine Role of Estrogens in the Augmentation of Luteinizing Hormone Receptor Formation in Cultured Rat Granulosa Cells1." *Biology of Reproduction* 32: 1038–50.

Kheansaard, Wasinee, Prapaporn Panichob, Suthat Fucharoen, and Dalina I Tanyong. 2011. "Cytokine-Induced Apoptosis of Beta-Thalassemia/ Hemoglobin E Erythroid Progenitor Cells via Nitric Oxide-Mediated Process in Vitro." *Acta Haematol* 126: 224–30.

Kim, Ki Hyung, Yun-Jeong Kang, Jin-Ok Jo, Mee Sun Ock, Soo Hyun Moon, Dong Soo Suh, Man Soo Yoon, et al. 2014. "DDX4 (DEAD Box Polypeptide 4) Colocalizes with Cancer Stem Cell Marker CD133 in Ovarian Cancers." *Biochemical and Biophysical Research Communications* 447: 315–22.

Kim, Sooyoung, Younji Lee, Sanghoon Lee, and Tak Kim. 2018. "Ovarian Tissue Cryopreservation and Transplantation in Patients with Cancer." *Obstetrics and Gynecology Science* 61 (4): 431–42.

Kirkpatrick, C. J., I. Melzner, and T. Göller. 1985. "Comparative Effects of Trypsin, Collagenase and Mechanical Harvesting on Cell Membrane Lipids Studied in Monolayer-Cultured Endothelial Cells and a Green Monkey Kidney Cell Line." *BBA - Molecular Cell Research* 846 (1): 120–26.

Knecht, Michael, Jean Marie Darbon, Tapio Ranta, Albert J. Baukal, and Kevin J. Catt. 1984. "Estrogens Enhance the Adenosine 3',5'-Monophosphate- Mediated Induction of Follicle-Stimulating Hormone and Luteinizing Hormone Receptors in Rat Granulosa Cells." *Endocrinology* 115 (1): 41–49.

Knoepfler, Paul S. 2009. "Deconstructing Stem Cell Tumorigenicity: A Roadmap to Safe Regenerative Medicine." *Stem Cells* 27: 1050–56.

Komorowska, Beata. 2016. "Autoimmune Premature Ovarian Failure." *Menopause Review* 15 (4): 210–14.

Konagaya, Shuhei, Takeshi Ando, Toshiaki Yamauchi, Hirofumi Suemori, and Hiroo Iwata. 2015. "Long-Term Maintenance of Human Induced Pluripotent Stem Cells by Automated Cell Culture System." *Scientific Reports* 5: 1–9.

Kozhukhar, V G. 2011. "Mammalian and Human Primordial Germ Cells : Differentiation , Identification , Migration." *Cell and Tissue Biology* 5 (3): 203–13.

Krege, John H., Jeffrey B. Hodgin, John F. Couse, Eva Enmark, Margaret Warner, Joel F. Mahler, Madhabananda Sar, Kenneth S. Korach, Jan Åke Gustafsson, and Oliver Smithies. 1998. "Generation and Reproductive Phenotypes of Mice Lacking Estrogen Receptor β." *Proceedings of the National Academy of Sciences of the United States of America* 95 (26): 15677–82.

Kreuser, Ernst-Dietrich, Wulf-Dieter Hetzel, Daniela Oliva Billia, and Eckhard Thiel. 1990. "Gonadal Toxicity Following Cancer Therapy in Adults: Significance,Diagnosis,Prevention and Treatment." *Cancer Treatment Reviews* 17: 169–75.

Kristensen, Stine Gry, Annette Rasmussen, Anne Grete Byskov, and Claus Yding Andersen. 2011. "Isolation of Pre-Antral Follicles from Human Ovarian Medulla Tissue." *Human Reproduction* 26 (1): 157–66.

Kumar, T. Rajendra, Yan Wang, Naifang Lu, and Martin M. Matzuk. 1997. "Follicle Stimulating Hormone Is Required for Ovarian Follicle Maturation but Not Male Fertility." *Nature Genetics* 3 (11): 3–8.

Laissue, Paul, Sophie Christin-Maitre, Philippe Touraine, Frederique Kuttenn, Olli Ritvos, Kristiina Aittomaki, Nathalie Bourcigaux, et al. 2006. "Mutations and Sequence Variants in GDF9 and BMP15 in Patients with Premature Ovarian Failure." *European Journal of Endocrinology* 154 (5): 739–44.

Lakhoo, K., J. Davies, S. Chakraborty, S. Berg, R. Tennyson, D. Fowler, S. Manek, C. Verrill, and S. Lane. 2019. "Development of a New Reproductive Tissue Cryopreservation Clinical Service for Children: The Oxford Programme." *Pediatric Surgery International* 35 (11): 1271–78.

Lasko, Paul. 2013. "The DEAD-Box Helicase Vasa: Evidence for a Multiplicity of Functions in RNA Processes and Developmental Biology." *Biochimica et Biophysica Acta* 1829 (8): 810–16.

Lee, Hye Nam, and Eun Mi Chang. 2019. "Primordial Follicle Activation as New Treatment for

Primary Ovarian Insufficiency." *Clin Exp Reprod Med* 46 (2): 43–49.
Lierman, Sylvie, Kelly Tilleman, Maria Cornelissen, Winnok H De Vos, Steven Weyers, Guy T'sjoen, Claude A Cuvelier, and Petra De Sutter. 2015. "Follicles of Various Maturation Stages React Differently to Enzymatic Isolation: A Comparison of Different Isolation Protocols." *Reproductive BioMedicine Online* 30: 181–90.
Lind, A. K., B. Weijdegård, P. Dahm-Kähler, J. Mölne, K. Sundfeldt, and M. Brännström. 2006. "Collagens in the Human Ovary and Their Changes in the Perifollicular Stroma during Ovulation." *Acta Obstetricia et Gynecologica Scandinavica* 85 (12): 1476–84.
Linder, Patrick, and Eckhard Jankowsky. 2011. "Spliceosome From Unwinding to Clamping-the DEAD Box RNA Helicase Family." *Nature Reviews Molecular Cell Biology* 12: 505.
Liu, Meng na, Kun Zhang, and Tian min Xu. 2019. "The Role of BMP15 and GDF9 in the Pathogenesis of Primary Ovarian Insufficiency." *Human Fertility* 14: 1–8.
Lo, Belinda K M, Sairah Sheikh, and Suzannah A Williams. 2019. "In Vitro and in Vivo Mouse Follicle Development in Ovaries and Reaggregated Ovaries." *Reproduction* 157: 135–48.
Loutradis, Dimitris, Eleni Patsoula, Konstantinos Stefanidis, Peter Drakakis, Georgios Antonakis, Ritsa Bletsa, Aris Antsaklis, and Stylianos Michalas. 2006. "Follicle-Stimulating Hormone Receptor Gene Mutations Are Not Evident in Greek Women with Premature Ovarian Failure and Poor Responders." In *Gynecologic and Obstetric Investigation*, 61:56–60. Gynecol Obstet Invest.
Lu, Cuiling, Li Lin, Huiping Tan, Hao Wu, Stephanie L Sherman, Fei Gao, Peng Jin, and Dahua Chen. 2012. "Fragile X Premutation RNA Is Sufficient to Cause Primary Ovarian Insufficiency in Mice." *Human Molecular Genetics* 21 (23): 5039–47.
Luque-Garcia, Jose L., Ge Zhou, Daniel S. Spellman, Tung-Tien Sun, and Thomas A. Neubert. 2009. "Analysis of Electroblotted Proteins by Mass Spectrometry: Protein Identification after Western Blotting." *Mollecular and Cellular Proteomics* 7 (2): 308–14.
Lygoe, Kate A., Ivan Wall, Philip Stephens, and Mark P. Lewis. 2007. "Role of Vitronectin and Fibronectin Receptors in Oral Mucosal and Dermal Myofibroblast Differentiation." *Biology of the Cell* 99 (11): 601–14.
MacDonald, Julie A., Yasushi Takai, Osamu Ishihara, Hiroyuki Seki, Dori C. Woods, and Jonathan L. Tilly. 2019. "Extracellular Matrix Signaling Activates Differentiation of Adult Ovary-Derived Oogonial Stem Cells in a Species-Specific Manner." *Fertility and Sterility* 111 (4): 794–805.
Manuel, Sharron L., Elena Antonova, Jessica E. Hornick, Farners Amargant Riera, Jian-Jun Wei, Mary Ellen Pavone, Michele T. Pritchard, and Francesca E. Duncan. 2019. "Collagen and Hyaluronan Matrices Undergo Age-Related Changes in the Human Ovary." *Fertility and Sterility* 112 (3): e252–53.
Marlow, Florence. 2015. "Primordial Germ Cell Specification and Migration." *F1000 Research*.
Marozzi, A., C. Porta, W. Vegetti, P. G. Crosignani, M. G. Tibiletti, L. Dalprà, and E. Ginelli. 2002. "Mutation Analysis of the Inhibin Alpha Gene in a Cohort of Italian Women Affected by Ovarian Failure." *Human Reproduction* 17 (7): 1741–45.
Marques, Pedro, Karolina Skorupskaite, Jyothis T George, and Richard A Anderson. 2000. *Physiology of GNRH and Gonadotropin Secretion*. *Endotext*. MDText.com, Inc.
Marsella, Tiziana, Paola Sena, Susanna Xella, Antonio La Marca, Simone Giulini, Anto De Pol, Annibale Volpe, and Laura Marzona. 2008. "Human Ovarian Tissue Cryopreservation: Effect of Sucrose Concentration on Morphological Features after Thawing." *Reproductive BioMedicine Online* 16 (2): 257–67.
Martinez-Madrid, Belen, Marie-Madeleine Dolmans, Anne Van Langendonckt, Sylvie Defrère, Anne-Sophie Van Eyck, and Jacques Donnez. 2004. "Ficoll Density Gradient Method for Recovery of Isolated Human Ovarian Primordial Follicles." *Fertility and Sterility* 82 (6): 1648–53.
Matoba, Shogo, and Atsuo Ogura. 2011. "Generation of Functional Oocytes and Spermatids

from Fetal Primordial Germ Cells after Ectopic Transplantation in Adult Mice." *Biology of Reproduction* 84 (4): 631–38.

McGee, Elizabeth A., and Aaron J. W. Hsueh. 2000. "Initial and Cyclic Recruitment of Ovarian Follicles." *Endocrine Reviews* 21 (2): 200–214.

Mckinnon, Katherine M. 2018. "Flow Cytometry: An Overview." *Current Protocols in Immunology* 120 (1).

McNatty, K. P., W. M. Hunter, A. S. McNeilly, and R. S. Sawers. 1975. "Changes in the Concentration of Pituitary and Steroid Hormones in the Follicular Fluid of Human Graafian Follicles throughout the Menstrual Cycle." *Journal of Endocrinology* 64 (3): 555–71.

Meirow, D., J. Dor, B. Kaufman, A. Shrim, J. Rabinovici, E. Schiff, H. Raanani, J. Levron, and E. Fridman. 2007. "Cortical Fibrosis and Blood-Vessels Damage in Human Ovaries Exposed to Chemotherapy. Potential Mechanisms of Ovarian Injury." *Human Reproduction* 22 (6): 1626–33.

Meirow, Dror. 2000. "Reproduction Post-Chemotherapy in Young Cancer Patients." *Molecular and Cellular Endocrinology* 169: 123–31.

Meskhi, Apollo, and Mourad W Seif. 2006. "Premature Ovarian Failure." *Current Opinion in Obstetrics and Gynecology* 18 (4): 418–26.

Mihm, M., and A. C.O. Evans. 2008. "Mechanisms for Dominant Follicle Selection in Monovulatory Species: A Comparison of Morphological, Endocrine and Intraovarian Events in Cows, Mares and Women." *Reproduction in Domestic Animals* 43 (SUPPL.2): 48–56.

Modi, D. N., S. Sane, and D. Bhartiya. 2003. "Accelerated Germ Cell Apoptosis in Sex Chromosome Aneuploid Fetal Human Gonads." *Molecular Human Reproduction* 9 (4): 219–25.

Montanelli, Lucia, Joost J.J. Van Durme, Guillaume Smits, Marco Bonomi, Patrice Rodien, Eric J. Devor, Kristin Moffat-Wilson, Leonardo Pardo, Gilbert Vassart, and Sabine Costagliola. 2004. "Modulation of Ligand Selectivity Associated with Activation of the Transmembrane Region of the Human Follitropin Receptor." *Molecular Endocrinology* 18 (8): 2061–73.

Moore, R. Kelly, Fumio Otsuka, and Shunichi Shimasaki. 2003. "Molecular Basis of Bone Morphogenetic Protein-15 Signaling in Granulosa Cells." *Journal of Biological Chemistry* 278 (1): 304–10.

Motta, Pietro M, Sayoko Makabe, and Stefania A Nottola. 1997. "The Ultrastructure of Human Reproduction. I. The Natural History of the Female Germ Cell: Origin, Migration and Differentiation inside the Developing Ovary." *Human Reproduction Update* 3 (3): 281–95.

Mouloungui, Elodie, Tristan Zver, Christophe Roux, and Clotilde Amiot. 2018. "A Protocol to Isolate and Qualify Purified Human Preantral Follicles in Cases of Acute Leukemia, for Future Clinical Applications." *Journal of Ovarian Research* 11 (4).

Mulac-Jericevic, B., R. A. Mullinax, F. J. DeMayo, J. P. Lydon, and O. M. Conneely. 2000. "Subgroup of Reproductive Functions of Progesterone Mediated by Progesterone Receptor-B Isoform." *Science* 289 (5485): 1751–54.

Mulac-Jericevic, Biserka, John P. Lydon, Francesco J. DeMayo, and Orla M. Conneely. 2003. "Defective Mammary Gland Morphogenesis in Mice Lacking the Progesterone Receptor B Isoform." *PNAS* 100 (17): 9744–49.

Murray, Anna, Minouk J. Schoemaker, Claire E. Bennett, Sarah Ennis, James N. MacPherson, Michael Jones, Danielle H. Morris, et al. 2014. "Population-Based Estimates of the Prevalence of FMR1 Expansion Mutations in Women with Early Menopause and Primary Ovarian Insufficiency." *Genetics in Medicine* 16 (1): 19–24.

Nakamura, M, H Katabuchi, T Y Ohba Fukumatsu -H Okamura, and T Y Ohba Fukumatsu H Okamura. 1994. "Isolation, Growth and Characteristics of Human Ovarian Surface Epithelium." *Virchows Archiv* 424: 59–67.

Nandedkar, T. D., and S. R. Munshi. 1981. "Effect of Dihydrotestosterone on Follicular Development, Ovulation and Reproductive Capacity of Mice." *Journal of Reproduction and*

*Fertility* 62 (1): 21–24.
Nelson, Lawrence M. 2009. “Clinical Practice. Primary Ovarian Insufficiency.” *The New England Journal of Medicine* 360 (6): 606–14.
Nelson, Lawrence M., Sharon N. Covington, and Robert W. Rebar. 2005. “An Update: Spontaneous Premature Ovarian Failure Is Not an Early Menopause.” *Fertility and Sterility* 83 (5): 1327–32.
Nelson, Lawrence M, James N Anasti, Lorene M Kimzey, Ruby A Defensor, Kenneth J Lipetz, Beverly J White, Thomas H Shawker, and Maria J Merino. 1994. “Development of Luteinized Graafian Follicles in Patients with Karyotypically Normal Spontaneous Premature Ovarian Failure.” *Journal of Clinical Endocrinology and Metabolism* 79 (5): 1470–75.
Nelson, P N, G M Reynolds, E E Waldron, E Ward, K Giannopoulos, and P G Murray. 2000. “Demystified... Monoclonal Antibodies.” *Journal of Clinical Pathology* 53: 111–17.
Niu, Wanbao, and Allan C. Spradling. 2020. “Two Distinct Pathways of Pregranulosa Cell Differentiation Support Follicle Formation in the Mouse Ovary.” *PNAS* 117 (33): 20015–26.
Novosad, Judy A, Sophia N Kalantaridou, Zhi-Bin Tong, and Lawrence M Nelson. 2003. “Ovarian Antibodies as Detected by Indirect Immunofluorescence Are Unreliable in the Diagnosis of Autoimmune Premature Ovarian Failure: A Controlled Evaluation.” *BioMed Central* 3 (2).
Novus Biologicals. “Cytokeratin 13 Antibody.” Accessed August 14, 2020. https://www.novusbio.com/products/cytokeratin-13-antibody-3g4_nbp2-37468#reviews-publications.
Ohno, S., and J. B. Smith. 1964. “Role of Fetal Follicular Cells in Meiosis of Mammalian Oöcytes.” *Cytogenetic and Genome Research* 3 (5): 324–33.
Oktay, Kutluk, Giuliano Bedoschi, Karen Berkowitz, Richard Bronson, Banafsheh Kashani, Peter McGovern, Lubna Pal, Gwendolyn Quinn, and Karen Rubin. 2016. “Fertility Preservation in Women with Turner Syndrome: A Comprehensive Review and Practical Guidelines.” *Journal of Pediatric and Adolescent Gynecology* 29 (5): 409–16.
Oktay, Kutluk, David Briggs, and Roger G. Gosden. 1997. “Ontogeny of Follicle-Stimulating Hormone Receptor Gene Expression in Isolated Human Ovarian Follicles.” *Journal of Clinical Endocrinology and Metabolism* 82 (11): 3748–51.
Oktay, Kutluk, David Nugent, Helen Newton, Osama Salha, Prasad Chatterjee, and Roger G. Gosden. 1997. “Isolation and Characterization of Primordial Follicles from Fresh and Cryopreserved Human Ovarian Tissue.” *Fertility and Sterility* 67 (3): 481–86.
Olsen, Jesper V., Shao En Ong, and Matthias Mann. 2004. “Trypsin Cleaves Exclusively C-Terminal to Arginine and Lysine Residues.” *Molecular and Cellular Proteomics* 3 (6): 608–14.
Oskam, Irma C., Babak A. Asadi, and Regiane R. Santos. 2010. “Histologic and Ultrastructural Features of Cryopreserved Ovine Ovarian Tissue: Deleterious Effect of 1,2-Propanediol Applying Different Thawing Protocols.” *Fertility and Sterility* 93 (8): 2764–66.
Ouni, Emna, Didier Vertommen, Maria Costanza Chiti, Marie-Madeleine Dolmans, and Christiani A Amorim. 2019. “A Draft Map of the Human Ovarian Proteome for Tissue Engineering and Clinical Applications.” *The American Society for Biochemistry and Molecular Biology* 18.
Pais, Helio, Katia Ruggero, Jing Zhang, Osama Al-Assar, Nicolas Bery, Ravneet Bhuller, Victoria Weston, et al. 2019. “Surfaceome Interrogation Using an RNA-Seq Approach Highlights Leukemia Initiating Cell Biomarkers in an LMO2 T Cell Transgenic Model.” *Scientific Reports* 9 (1): 1–16.
Pan, Bo, and Julang Li. 2019. “The Art of Oocyte Meiotic Arrest Regulation.” *Reproductive Biology and Endocrinology* 17 (8).
Pan, Zezheng, Mengli Sun, Jia Li, Fangyue Zhou, Xia Liang, Jian Huang, Tuochen Zheng, Liping Zheng, and Yuehui Zheng. 2015. “The Expression of Markers Related to Ovarian Germline Stem Cells in the Mouse Ovarian Surface Epithelium and the Correlation with Notch

Signaling Pathway." *Cellular Physiology and Biochemistry* 37 (6): 2311–22.
Pankhurst, Michael W. 2017. "A Putative Role for Anti-Müllerian Hormone (AMH) in Optimising Ovarian Reserve Expenditure." *Journal of Endocrinology* 233 (1): R1–13.
Pankhurst, Michael W., and Ian S. McLennan. 2013. "Human Blood Contains Both the Uncleaved Precursor of Anti-Müllerian Hormone and a Complex of the NH2- and COOH-Terminal Peptides." *American Journal of Physiology - Endocrinology and Metabolism* 305 (10): 1241–47.
Park, Chang-Eun, Dongryul Lee, Kyeoung-Hwa Kim, and Kyung-Ah Lee. 2006. "Establishment of Ovarian Reconstruction System in Culture for Functional Genomic Analysis." *Journal of Bioscience and Bioengineering* 102 (5): 396–401.
Pasquino, Anna Maria, Franca Passeri, Ida Pucarelli, Maria Segni, and Giovanna Municchi. 1997. "Spontaneous Pubertal Development in Turner's Syndrome." *Journal of Clinical Endocrinology and Metabolism* 82 (6): 1810–13.
Patel, Bhavin M.D., Greg Ph.D. Potts, Leigh B.S Foster, Alex M.S. Behling, John M.S Bucci, and John Ph.D. Rogers. "Characterization of Antibody Specificity Using Immunoprecipitation and Mass Spectrometry | Thermo Fisher Scientific - GR." Accessed December 24, 2020. https://www.thermofisher.com/gr/en/home/life-science/antibodies/antibodies-learning-center/antibodies-resource-library/antibody-application-notes/characterization-antibody-specificity-using-ip-ms.html.
Patino, Liliana C., Kelly L. Walton, Thomas D. Mueller, Katharine E. Johnson, William Stocker, Dulama Richani, David Agapiou, Robert B. Gilchrist, Paul Laissue, and Craig A. Harrison. 2017. "BMP15 Mutations Associated with Primary Ovarian Insufficiency Reduce Expression, Activity, or Synergy with Gdf9." *Journal of Clinical Endocrinology and Metabolism* 102 (3): 1009–19.
Pearson, Terry, and Leigh Anderson. 1980. "Analytical Techniques for Cell Fractions. Isoelectric Point Standards for Two-Dimensional Electrophoresis." *Analytical Biochemistry* 101 (2): 377–86.
Pedersen, T., and H. Peters. 1968. "Proposal for a Classification of Oocytes and Follicles in the Mouse Ovary." *Journal of Reproduction and Fertility* 17 (3): 555–57.
Peek, Ronald, Myra Schleedoorn, Dominique Smeets, Guillaume Van De Zande, Freek Groenman, Didi Braat, Janielle Van Der Velden, and Kathrin Fleischer. 2019. "Ovarian Follicles of Young Patients with Turner's Syndrome Contain Normal Oocytes but Monosomic 45,X Granulosa Cells." *Human Reproduction* 34 (9): 1686–96.
Peng, Jia, Qinglei Li, Karen Wigglesworth, Adithya Rangarajan, Chandramohan Kattamuri, Randall T. Peterson, John J. Eppig, Thomas B. Thompson, and Martin M. Matzuk. 2013. "Growth Differentiation Factor 9:Bone Morphogenetic Protein 15 Heterodimers Are Potent Regulators of Ovarian Functions." *PNAS* 110 (8).
Pepling, Melissa E., and Allan C. Spradling. 2001. "Mouse Ovarian Germ Cell Cysts Undergo Programmed Breakdown to Form Primordial Follicles." *Developmental Biology* 234 (2): 339–51.
Perdrix, Anne, Bertrand MacE, Jean-Pierre SC Milazzo, AgnEs Liard-Zmuda, Marc Baron, and Nathalie Rives. 2010. "Ovarian Tissue Thawing: A Comparison of Two Conditions." *Fertility and Sterility* 93: 307–10.
Peters, H., A. G. Byskov, S. Lintern-Moore, M. Faber, and M. Andersen. 1973. "The Effect of Gonadotrophin on Follicle Growth Initiation in the Neonatal Mouse Ovary." *Journal of Reproduction and Fertility* 35 (1): 139–41.
Picton, Helen, David Briggs, and Roger Gosden. 1998. "The Molecular Basis of Oocyte Growth and Development." *Molecular and Cellular Endocrinology* 145 (1–2): 27–37.
Podfigurna, Agnieszka, and Błażej Męczekalski. 2018. "Cardiovascular Health in Patients with Premature Ovarian Insufficiency. Management of Long-Term Consequences." *Menopause Review* 17 (3): 109–11.

Poirot, Catherine, Laurence Brugieres, Karima Yakouben, Marie Prades-Borio, Flora Marzouk, Guenolee de Lambert, Helene Pacquement, et al. 2019. “Ovarian Tissue Cryopreservation for Fertility Preservation in 418 Girls and Adolescents up to 15 Years of Age Facing Highly Gonadotoxic Treatment. Twenty Years of Experience at a Single Center.” *Acta Obstetricia et Gynecologica Scandinavica* 98 (5): 630–37.

Popat, Vaishali B., Karim A. Calis, Vien H. Vanderhoof, Giovanni Cizza, James C. Reynolds, Nancy Sebring, James F. Troendle, and Lawrence M. Nelson. 2009. “Bone Mineral Density in Estrogen-Deficient Young Women.” *Journal of Clinical Endocrinology and Metabolism* 94 (7): 2277–83.

Qu, Jianping, Pierre Arnaud Godin, Michelle Nisolle, and Jacques Donnez. 2000. “Distribution and Epidermal Growth Factor Receptor Expression of Primordial Follicles in Human Ovarian Tissue before and after Cryopreservation.” *Human Reproduction* 15 (2): 302–10.

Reddy, Pradeep, Lian Liu, Deepak Adhikari, Krishna Jagarlamudi, Singareddy Rajareddy, Yan Shen, Chun Du, et al. 2008. “Oocyte-Specific Deletion of Pten Causes Premature Activation of the Primordial Follicle Pool.” *Science* 319 (5863): 611–13.

Reggeti, F, and D Bienzle. 2011. “Flow Cytometry in Veterinary Oncology.” *Veterinary Pathology* 48 (1): 223–35.

Revel, Ariel, Moriah Koler, Alex Simon, Aby Lewin, Neri Laufer, and Anat Safran. 2003. “Oocyte Collection during Cryopreservation of the Ovarian Cortex.” *Fertility and Sterility* 79 (5): 1237–39.

Revel, Ariel, Neri Laufer, Assaf Ben Meir, Meital Lebovich, and Eduardo Mitrani. 2011. “Micro-Organ Ovarian Transplantation Enables Pregnancy: A Case Report.” *Human Reproduction* 26 (5): 1097–1103.

Revel, Ariel, Shoshana Revel-Vilk, Einat Aizenman, Anat Porat-Katz, Anat Safran, Assaf Ben-Meir, Michael Weintraub, Michael Shapira, Hanna Achache, and Neri Laufer. 2009. “At What Age Can Human Oocytes Be Obtained?” *Fertility and Sterility* 92 (2): 458–63.

Reynaud, Karine, Rita Cortvrindt, Franciska Verlinde, Jean De Schepper, Claire Bourgain, and Johan Smitz. 2004. “Number of Ovarian Follicles in Human Fetuses with the 45,X Karyotype.” *Fertility and Sterility* 81 (4): 1112–19.

Richardson, Sandra J, Vyta Senikas, and James F Nelsonf. 1987. “Follicular Depletion During the Menopausal Transition: Evidence for Accelerated Loss and Ultimate Exhaustion*.” *Journal of Clinical Endocrinology and Metabolism* 65 (6): 1231–37.

Rifé, M., A. Nadal, Montserrat Milà, and R. Willemsen. 2004. “Immunohistochemical FMRP Studies in a Full Mutated Female Fetus.” *American Journal of Medical Genetics* 124 A (2): 129–32.

Roh, Jae Sook, Jonas Bondestam, Sabine Mazerbourg, Noora Kaivo-Oja, Nigel Groome, Olli Ritvos, and Aaron J.W. Hsueh. 2003. “Growth Differentiation Factor-9 Stimulates Inhibin Production and Activates Smad2 in Cultured Rat Granulosa Cells.” *Endocrinology* 144 (1): 172–78.

Roness, Hadassa, Zohar Gavish, Yoram Cohen, and Dror Meirow. 2013. “Ovarian Follicle Burnout: A Universal Phenomenon?” *Cell Cycle* 12 (20): 3245–46.

Rosario, Roseanne, Andrew J. Childs, and Richard A. Anderson. 2017. “RNA-Binding Proteins in Human Oogenesis: Balancing Differentiation and Self-Renewal in the Female Fetal Germline.” *Stem Cell Research* 21: 193–201.

Rosario, Roseanne, Panagiotis Filis, Victoria Tessyman, Hazel Kinnell, Andrew J. Childs, Nicola K. Gray, and Richard A. Anderson. 2016. “FMRP Associates with Cytoplasmic Granules at the Onset of Meiosis in the Human Oocyte.” Edited by Barbara Bardoni. *PLOS One* 11 (10): e0163987.

Rossetti, Raffaella, Ilaria Ferrari, Ilaria Bestetti, Silvia Moleri, Francesco Brancati, Luisa Petrone, Palma Finelli, and Luca Persani. 2020. “Fundamental Role of BMP15 in Human Ovarian Folliculogenesis Revealed by Null and Missense Mutations Associated with Primary

Ovarian Insufficiency." *Human Mutation* 41 (5): 983–97.
Roussou, Paraskevi, Nikolaos J Tsagarakis, Dimitrios Kountouras, Sarantis Livadas, and Evanthia Diamanti-Kandarakis. 2013. "Beta-Thalassemia Major and Female Fertility: The Role of Iron and Iron-Induced Oxidative Stress." *Anemia* 2013.
Ruby, John R., Robert F. Dyer, Raymond F. Gasser, and Richard G. Skalko. 1970. "Intercellular Connections between Germ Cells in the Developing Human Ovary." *Zeitschrift Für Zellforschung Und Mikroskopische Anatomie* 105 (2): 252–58.
Rudnicka, Ewa, Jagoda Kruszewska, Klaudia Klicka, Joanna Kowalczyk, Grymowicz, Jolanta Skorska, Wojciech Pieta, and Roman Smolarczyk. 2018. "Premature Ovarian Insufficiency – Aetiopathology, Epidemiology, and Diagnostic Evaluation." *Menopause Review* 17 (3): 105–8.
Rungsiwiwut, Ruttachuk, Chirawattana Manolertthewan, Pranee Numchaisrika, Vichuda Ahnonkitpanit, Pramuan Virutamasen, Mongkol Techakumphu, and Kamthorn Pruksananonda. 2013. "The ROCK Inhibitor Y-26732 Enhances the Survival and Proliferation of Human Embryonic Stem Cell-Derived Neural Progenitor Cells upon Dissociation." *Cells Tissues Organs* 198 (2): 127–38.
Saier, Milton H., Can V. Tran, and Ravi D. Barabote. 2006. "TCDB: The Transporter Classification Database for Membrane Transport Protein Analyses and Information." *Nucleic Acids Research* 34: 181–86.
Scherer, William F., Jerome T. Syverton, and George O. Gey. 1953. "Studies on the Propagation in Vitro of Poliomyelitis Viruses: IV. Viral Multiplication in a Stable Strain of Human Malignant Epithelial Cells (Strain Hela) Derived from an Epidermoid Carcinoma of the Cervix." *Journal of Experimental Medicine* 97 (5): 695–710.
Schipper, Izaäk, Wim C.J. Hop, and Bart C.J.M. Fauser. 1998. "The Follicle-Stimulating Hormone (FSH) Threshold/Window Concept Examined by Different Interventions with Exogenous FSH during the Follicular Phase of the Normal Menstrual Cycle: Duration, Rather than Magnitude, of FSH Increase Affects Follicle Development." *Journal of Clinical Endocrinology and Metabolism* 83 (4): 1292–98.
Schmidt, Dirk, Catherine E. Ovitt, Katrin Anlag, Sandra Fehsenfeld, Lars Gredsted, Anna Corina Treier, and Mathias Treier. 2004. "The Murine Winged-Helix Transcription Factor Foxl2 Is Required for Granulosa Cell Differentiation and Ovary Maintenance." *Development* 131 (4): 933–42.
Schmidt, K. L.T., N. Kryger-Baggesen, A. G. Byskov, and C. Yding Andersen. 2005. "Anti-Müllerian Hormone Initiates Growth of Human Primordial Follicles in Vitro." *Molecular and Cellular Endocrinology* 234 (1–2): 87–93.
Schmidt, K L T, A G Byskov, A Nyboe Andersen, J Mu, and Yding Andersen. 2003. "Density and Distribution of Primordial Follicles in Single Pieces of Cortex from 21 Patients and in Individual Pieces of Cortex from Three Entire Human Ovaries." *Human Reproduction* 18 (6): 1158–64.
Schmidt, Viola Maria, Evgenia Isachenko, Gunter Rappl, Gohar Rahimi, Bettina Hanstein, Bernd Morgenstern, Peter Mallmann, and Vladimir Isachenko. 2018a. "Construction of Human Artificial Ovary from Cryopreserved Ovarian Tissue: Appearance of Apoptosis and Necrosis after Enzymatic Isolation of Follicles." *Cryobiology* 84: 10–14.
Schmidt, Viola Maria, Vladimir Isachenko, Gunter Rappl, Gohar Rahimi, Bettina Hanstein, Bernd Morgenstern, Peter Mallmann, and Evgenia Isachenko. 2018b. "Comparison of the Enzymatic Efficiency of Liberase TM and Tumor Dissociation Enzyme: Effect on the Viability of Cells Digested from Fresh and Cryopreserved Human Ovarian Cortex." *Reproductive Biology and Endocrinology* 16 (57).
Schomberg, David W., John F. Couse, Abir Mukherjee, Dennis B. Lubahn, M. Sar, Kelly E. Mayo, and Kenneth S. Korach. 1999. "Targeted Disruption of the Estrogen Receptor-α Gene in Female Mice: Characterization of Ovarian Responses and Phenotype in the Adult."

*Endocrinology* 140 (6): 2733–44.
Schupbach, Trudi, and Eric Wieschaus. 1989. "Female Sterile Mutations on the Second Chromosome of Drosophila Melanogaster. I. Maternal Effect Mutations." *Genetics* 121: 101–17.
Shaw, N. D., S. N. Histed, S. S. Srouji, J. Yang, H. Lee, and Janet E. Hall. 2010. "Estrogen Negative Feedback on Gonadotropin Secretion: Evidence for a Direct Pituitary Effect in Women." *Journal of Clinical Endocrinology and Metabolism* 95 (4): 1955–61.
Shelling, Andrew N. 2000. "X Chromosome Defects and Premature Ovarian Failure." *Australian and New Zealand Journal of Medicine* 30 (1): 5–7.
Shelling, Andrew N., Karen A. Burton, Ashwini L. Chand, Cynthia C. Van Fe, John T. France, Cynthia M. Farquhar, Stella R. Milsom, et al. 2000. "Inhibin: A Candidate Gene for Premature Ovarian Failure." *Human Reproduction* 15 (12): 2644–49.
Shelling, Andrew N. 2010. "Premature Ovarian Failure." *Reproduction* 140 (5): 633–41.
Shi, Shaolin, Suzannah A. Williams, Antti Seppo, Henry Kurniawan, Wei Chen, Zhengyi Ye, Jamey D. Marth, and Pamela Stanley. 2004. "Inactivation of the Mgat1 Gene in Oocytes Impairs Oogenesis, but Embryos Lacking Complex and Hybrid N-Glycans Develop and Implant." *Molecular and Cellular Biology* 24 (22): 9920–29.
Shimizu, Ken, Tomoko Nakamura, Bayasula, Natsuki Nakanishi, Yukiyo Kasahara, Takashi Nagai, Tomohiko Murase, et al. 2019. "Molecular Mechanism of FSHR Expression Induced by BMP15 in Human Granulosa Cells." *Journal of Assisted Reproduction and Genetics* 36 (6): 1185–94.
Shirasawa, Hiromitsu, and Yukihiro Terada. 2017. "In Vitro Maturation of Human Immature Oocytes for Fertility Preservation and Research Material." *Reproductive Medicine and Biology* 16 (3): 258–67.
Silvestris, Erica, Paola Cafforio, Stella D'oronzo, Claudia Felici, Franco Silvestris, and Giuseppe Loverro. 2018. "In Vitro Differentiation of Human Oocyte-like Cells from Oogonial Stem Cells: Single-Cell Isolation and Molecular Characterization." *Human Reproduction* 33 (3): 464–73.
Sirard, Marc André, François Richard, Patrick Blondin, and Claude Robert. 2006. "Contribution of the Oocyte to Embryo Quality." *Theriogenology* 65 (1): 126–36.
Skinner, Michael K. 2005. "Regulation of Primordial Follicle Assembly and Development." *Human Reproduction Update* 11 (5): 461–71.
Snow, Christopher. 2004. "Flow Cytometer Electronics." *Cytometry* 57A (2): 63–69.
Society, European, and Human Reproduction. 2015. "Management of Women with Premature Ovarian Insufficiency." *Guideline of the European Society of Human Reproduction and Embryology POI*, 2015.
Steiner, Debora, Hanita Khaner, Malkiel Cohen, Sharona Even-Ram, Yaniv Gil, Pavel Itsykson, Tikva Turetsky, et al. 2010. "Derivation, Propagation and Controlled Differentiation of Human Embryonic Stem Cells in Suspension." *Nature Biotechnology* 28 (4): 361–64.
Stenn, Kurt S., Richard Link, Gisela Moellmann, Joseph Madri, and Elizabeth Kuklinska. 1989. "Dispase, a Neutral Protease from Bacillus Polymyxa, Is a Powerful Fibronectinase and Type IV Collagenase." *Journal of Investigative Dermatology* 93 (2): 287–90.
Stimpfel, Martin, Thomas Skutella, Branko Cvjeticanin, Marija Meznaric, Peter Dovc, Srdjan Novakovic, Petra Cerkovnik, Eda Vrtacnik-Bokal, and Irma Virant-Klun. 2013. "Isolation, Characterization and Differentiation of Cells Expressing Pluripotent/Multipotent Markers from Adult Human Ovaries." *Cell Tissue Research* 354: 593–607.
Styhler, Sylvia, Akira Nakamura, Andrew Swan, Beat Suter, and Paul Lasko. 1998. "Vasa Is Required for GURKEN Accumulation in the Oocyte, and Is Involved in Oocyte Differentiation and Germline Cyst Development." *Development* 125 (9): 1569–78.
Sugawara, Nobuo, Machiko Maeda, Tomomi Manome, Rie Nagai, and Yasuhisa Araki. 2013. "Patients with 47, XXX Karyotype Who Experienced Premature Ovarian Failure (POF): Two

Case Reports." *Reproductive Medicine and Biology* 12 (4): 193–95.
Sugimoto, Kazuhiro, Eitetsu Koh, Ho-Su Sin, Yuji Maeda, Kazutaka Narimoto, Koji Izumi, Yoshitomo Kobori, et al. 2009. "Tissue-Specific Differentially Methylated Regions of the Human VASA Gene Are Potentially Associated with Maturation Arrest Phenotype in the Testis." *Journal of Human Genetics* 54: 450–56.
Sullivan, Shannon D., Corrine Welt, and Stephanie Sherman. 2011. "FMR1 and the Continuum of Primary Ovarian Insufficiency." *Seminars in Reproductive Medicine* 29 (4): 299–307.
Sundblad, Victoria, Violeta A. Chiauzzi, Luz Andreone, Stella Campo, Eduardo H. Charreau, and Liliana Dain. 2006. "Controversial Role of Inhibin α-Subunit Gene in the Aetiology of Premature Ovarian Failure." *Human Reproduction* 21 (5): 1154–60.
Suzuki, Nao, Nobuhito Yoshioka, Seido Takae, Yodo Sugishita, Midori Tamura, Shu Hashimoto, Yoshiharu Morimoto, and Kazuhiro Kawamura. 2015. "Successful Fertility Preservation Following Ovarian Tissue Vitrification in Patients with Primary Ovarian Insufficiency." *Human Reproduction* 30 (3): 608–15.
Takahashi, Kazutoshi, Koji Tanabe, Mari Ohnuki, Megumi Narita, Tomoko Ichisaka, Kiichiro Tomoda, and Shinya Yamanaka. 2007. "Induction of Pluripotent Stem Cells from Adult Human Fibroblasts by Defined Factors." *Cell* 131 (5): 861–72.
Takahashi, Kazutoshi, and Shinya Yamanaka. 2006. "Induction of Pluripotent Stem Cells from Mouse Embryonic and Adult Fibroblast Cultures by Defined Factors." *Cell* 126 (4): 663–76.
Tanaka, Satomi S, Yayoi Toyooka, Ryuko Akasu, Yuko Katoh-Fukui, Yoko Nakahara, Rika Suzuki, Minesuke Yokoyama, and Toshiaki Noce. 2000. "The Mouse Homolog of Drosophila Vasa Is Required for the Development of Male Germ Cells." *Genes & Development* 14: 841–53.
Tanghe, Sofie, Ann Van Soom, Hans Nauwynck, Marc Coryn, and Aart De Kruif. 2002. "Minireview: Functions of the Cumulus Oophorus during Oocyte Maturation, Ovulation, and Fertilization." *Molecular Reproduction and Development* 61 (3): 414–24.
Telfer, Evelyn E, Marie Mclaughlin, Christina Ding, and K Joo Thong. 2008. "A Two-Step Serum-Free Culture System Supports Development of Human Oocytes from Primordial Follicles in the Presence of Activin." *Human Reproduction* 23 (5): 1151–58.
The Practice Committee of the American Society for Reproductive Medicine. 2013. "Mature Oocyte Cryopreservation: A Guideline." *Fertility and Sterility* 99 (1): 37–43.
The Practice Committee of the American Society for Reproductive Medicine, American Society for Reproductive Medicine. 2014. "Ovarian Tissue Cryopreservation: A Committee Opinion." *Fertility and Sterility* 101 (5): 1237–43.
Thomas, Fiona H., and Barbara C. Vanderhyden. 2006. "Oocyte-Granulosa Cell Interactions during Mouse Follicular Development: Regulation of Kit Ligand Expression and Its Role in Oocyte Growth." *Reproductive Biology and Endocrinology* 4: 1–8.
Thomas, Frédéric, François Renaud, Eric Benefice, Thierry De Meeüs, and Jean-François Guegan. 2001. "International Variability of Ages at Menarche and Menopause: Patterns and Main Determinants." *Human Biology*. Vol. 73.
Torrealday, Saioa, Pinar Kodaman, and Lubna Pal. 2019. "Open Peer Review Premature Ovarian Insufficiency-an Update on Recent Advances in Understanding and Management." *F1000 Research* 6 (2069).
Touraine, P., I. Beau, A. Gougeon, G. Meduri, A. Desroches, C. Pichard, M. Detoeuf, et al. 1999. "New Natural Inactivating Mutations of the Follicle-Stimulating Hormone Receptor: Correlations between Receptor Function and Phenotype." *Molecular Endocrinology* 13 (11): 1844–54.
Toyooka, Yayoi, Naoki Tsunekawa, Yoshihiko Takahashi, Yasuhisa Matsui, Michio Satoh, and Toshiaki Noce. 2000. "Expression and Intracellular Localization of Mouse Vasa-Homologue Protein during Germ Cell Development." *Mechanisms of Development* 93 (1–2): 139–49.
Tracy, Lauren E, Raquel A Minasian, and E J Caterson. 2016. "Extracellular Matrix and Dermal Fibroblast Function in the Healing Wound." *Wound Healing Society* 5 (3): 119–36.

Trama, Annalisa, Alice Bernasconi, Martin G. McCabe, Marcela Guevara, Gemma Gatta, Laura Botta, Lynn Ries, and Archie Bleyer. 2019. "Is the Cancer Survival Improvement in European and American Adolescent and Young Adults Still Lagging behind That in Children?" *Pediatric Blood and Cancer* 66 (1): 1–9.

Tuck, Astrud R, Rebecca L Robker, Robert J Norman, Wayne D Tilley, and Theresa E Hickey. 2015. "Discovery of Dachshund 2 Protein as a Novel Biomarker of Poor Prognosis in Epithelial Ovarian Cancer." *Journal of Ovarian Research* 8 (31).

Tung, L, M K Mohamed, J P Hoeffler, G S Takimoto, and K B Horwitz. 1993. "Antagonist-Occupied Human Progesterone B-Receptors Activate Transcription without Binding to Progesterone Response Elements and Are Dominantly Inhibited by A-Receptors." *Molecular Endocrinology* 7 (10): 1256–65.

Uda, Manuela, Chris Ottolenghi, Laura Crisponi, Jose Elias Garcia, Manila Deiana, Wendy Kimber, Antonino Forabosco, Antonio Cao, David Schlessinger, and Giuseppe Pilia. 2004. "Foxl2 Disruption Causes Mouse Ovarian Failure by Pervasive Blockage of Follicle Development." *Human Molecular Genetics* 13 (11): 1171–81.

Vanacker, Julie, Alessandra Camboni, Catherine Dath, Anne Van Langendonckt, Marie-Madeleine Dolmans, Jacques Donnez, and Christiani A Amorim. 2011. "Enzymatic Isolation of Human Primordial and Primary Ovarian Follicles with Liberase DH: Protocol for Application in a Clinical Setting." *Fertility and Sterility* 96 (2): 379–83.

Vasseur, Claudine, Patrice Rodien, Isabelle Beau, Agnes Desroches, Capucine Gerard, Loic de Poncheville, Stephanie Chaplot, et al. 2003. "A Chorionic Gonadotropin-Sensitive Mutation in the Follicle-Stimulating Hormone Receptor as a Cause of Familial Gestational Spontaneous Ovarian Hyperstimulation Syndrome." *The New England Journal of Medicine* 349: 753–59.

Vegeto, Elisabetta, Manouchehr M. Shahbaz, Dawn X. Wen, Mark E. Goldman, Bert W. O'Malley, and Donald P. McDonnell. 1993. "Human Progesterone Receptor A Form Is a Cell- and Promoter-Specific Repressor of Human Progesterone Receptor B Function." *Molecular Endocrinology* 7 (10): 1244–55.

Venn, Alison, Lyndsey Florence Watson, Elina Hemminki, David Healy, and Fiona Jane Bruinsma. 2001. "Mortality in a Cohort of IVF Patients." *Human Reproduction* 16 (12): 1359–72.

Volk, Susan W, Yanjian Wang, Elizabeth A Mauldin, Kenneth W Liechty, and Sherrill L Adams. 2011. "Diminished Type III Collagen Promotes Myofibroblast Differentiation and Increases Scar Deposition in Cutaneous Wound Healing." *Cells Tissues Organs* 194: 25–37.

Vujovic, Svetlana. 2009. "Aetiology of Premature Ovarian Failure." *Menopause International* 15 (2): 72–75.

Wagner, Magdalena, Masahito Yoshihara, Iyadh Douagi, Anastasios Damdimopoulos, Sarita Panula, Sophie Petropoulos, Haojiang Lu, et al. 2020. "Single-Cell Analysis of Human Ovarian Cortex Identifies Distinct Cell Populations but No Oogonial Stem Cells." *Nature Communications* 11 (1147).

Walker, Charlotte A, Briet D Bjarkadottir, Muhammad Fatum, Sheila Lane, and Suzannah A Williams. 2019. "Variation in Follicle Health and Development in Cultured Cryopreserved Ovarian Cortical Tissue: A Study of Ovarian Tissue from Patients Undergoing Fertility Preservation." *Human Fertility* 23: 1–11.

Wartenberg, H. 1982. "Development of the Early Human Ovary and Role of the Mesonephros in the Differentiation of the Cortex." *Anatomy and Embryology* 165 (2): 253–80.

Wassarman, Paul M., and Wendy J. Josefowicz. 1978. "Oocyte Development in the Mouse: An Ultrastructural Comparison of Oocytes Isolated at Various Stages of Growth and Meiotic Competence." *Journal of Morphology* 156 (2): 209–35.

Wassarman, Paul M., and Eveline S. Litscher. 2012. "Influence of the Zona Pellucida of the Mouse Egg on Folliculogenesis and Fertility." *International Journal of Developmental Biology* 56 (10–12): 833–39.

Watanabe, Kiichi, Morio Ueno, Daisuke Kamiya, Ayaka Nishiyama, Michiru Matsumura, Takafumi Wataya, Jun B Takahashi, et al. 2007. “A ROCK Inhibitor Permits Survival of Dissociated Human Embryonic Stem Cells.” *Nature Biotechnology* 25 (6): 681–86.

Webber, L, M Davies, R Anderson, J Bartlett, D Braat, B Cartwright, R Cifkova, et al. 2016. “ESHRE Guideline: Management of Women with Premature Ovarian Insufficiency. The ESHRE Guideline Group on POI.” *Human Reproduction* 31 (5): 926–37.

Weenen, Christien, Joop S E Laven, Anne R M Von Bergh, Mark Cranfield, Nigel P Groome, Jenny A Visser, Piet Kramer, Bart C J M Fauser, and Axel P N Themmen. 2004. “Anti-Muellerian Hormone Expression Pattern in the Human Ovary: Potential Implications for Initial and Cyclic Follicle Recruitment.” *Molecular Human Reproduction* 10 (2): 77–83.

Weiland, Florian, Carla M. Zammit, Frank Reith, and Peter Hoffmann. 2014. “High Resolution Two-Dimensional Electrophoresis of Native Proteins.” *Electrophoresis* 35 (12–13): 1893–1902.

Weiss, Lester. 1971. “Additional Evidence of Gradual Loss of Germ Cells in the Pathogenesis of Streak Ovaries in Turner’s Syndrome.” *Journal of Medical Genetics* 8: 540.

Welt, Corrine K. 2008. “Primary Ovarian Insufficiency: A More Accurate Term for Premature Ovarian Failure.” *Clinical Endocrinology* 68 (4): 499–509.

White, Yvonne A R, Dori C Woods, Yasushi Takai, Osamu Ishihara, Hiroyuki Seki, and Jonathan L Tilly. 2012. “Oocyte Formation by Mitotically Active Germ Cells Purified from Ovaries of Reproductive Age Women.” *Nature Medicine* 18 (3): 413–21.

Willecke, Klaus, Jürgen Eiberger, Joachim Degen, Dominik Eckardt, Alessandro Romualdi, Martin Güldenagel, Urban Deutsch, and Goran Söhl. 2002. “Structural and Functional Diversity of Connexin Genes in the Mouse and Human Genome.” *Biological Chemistry* 383 (5): 725–37.

Williams, Suzannah A., and Pamela Stanley. 2008. “Mouse Fertility Is Enhanced by Oocyte-specific Loss of Core 1-derived O-glycans.” *The FASEB Journal* 22 (7): 2273–84.

Williams, Suzannah A., and Pamela Stanley. 2011. “Premature Ovarian Failure in Mice with Oocytes Lacking Core 1-Derived O-Glycans and Complex N-Glycans.” *Endocrinology* 152 (3): 1057–66.

Williams, Suzannah A., Lijun Xia, Richard D. Cummings, Rodger P. McEver, and Pamela Stanley. 2007. “Fertilization in Mouse Does Not Require Terminal Galactose or N-Acetylglucosamine on the Zona Pellucida Glycans.” *Journal of Cell Science* 120 (8): 1341–49.

Woad, Kathryn J., Deborah Prendergast, Ingrid M. Winship, and Andrew N. Shelling. 2013. “FSH Receptor Gene Variants Are Rarely Associated with Premature Ovarian Failure.” *Reproductive BioMedicine Online* 26 (4): 396–99.

Woad, Kathryn J., Wendy J. Watkins, Deborah Prendergast, and Andrew N. Shelling. 2006. “The Genetic Basis of Premature Ovarian Failure.” *Australian and New Zealand Journal of Obstetrics and Gynaecology* 46 (3): 242–44.

Woodruff, Teresa K, and Lonnie D Shea. 2011. “A New Hypothesis Regarding Ovarian Follicle Development: Ovarian Rigidity as a Regulator of Selection and Health.” *Journal of Assisted Reproduction and Genetics* 28: 3–6.

World Health Organisation. 2010. *Antiretroviral Therapy For HIV Infection In Infants And Children: Towards Universal Access*. *WHO Library Cataloguing-in-Publication Data*. Vol. 4911.

Wu, Xuemei, Lei Chen, Christopher A. Brown, Changning Yan, and Martin M. Matzuk. 2004. “Interrelationship of Growth Differentiation Factor 9 and Inhibin in Early Folliculogenesis and Ovarian Tumorigenesis in Mice.” *Molecular Endocrinology* 18 (6): 1509–19.

Xu, Min, Susan L. Barrett, Erin West-Farrell, Laxmi A. Kondapalli, Sarah E. Kiesewetter, Lonnie D. Shea, and Teresa K. Woodruff. 2009. “In Vitro Grown Human Ovarian Follicles from Cancer Patients Support Oocyte Growth.” *Human Reproduction* 24 (10): 2531–40.

Yajima, Mamiko, and Gary M. Wessel. 2015. “Essential Elements for Translation: The Germline

Factor Vasa Functions Broadly in Somatic Cells." *Development (Cambridge)* 142 (11): 1960–70.

Yamada, Shigetoshi, Hiroshi Fujiwara, Tetsuro Honda, Toshihiro Higuchi, Takahiro Nakayama, Takuya Inoue, Michiyuki Maeda, and Shingo Fujii. 1999. "Human Granulosa Cells Express Integrin A2 and Collagen Type IV: Possible Involvement of Collagen Type IV in Granulosa Cell Luteinization." *Molecular Human Reproduction* 5 (7): 607–17.

Yan, Changning, Pei Wang, Janet Demayo, Francesco J. Demayo, Julia A. Elvin, Cecilia Carino, Sarvamangala V. Prasad, et al. 2001. "Synergistic Roles of Bone Morphogenetic Protein 15 and Growth Differentiation Factor 9 in Ovarian Function." *Molecular Endocrinology* 15 (6): 854–66.

Zarate-Garcia, Larissa, Simon I R Lane, Julie A Merriman, and Keith T Jones. 2016. "FACS-Sorted Putative Oogonial Stem Cells from the Ovary Are Neither DDX4-Positive nor Germ Cells." *Scientific Reports* 6 (27991).

Zhai, Jun, Guidong Yao, Fangli Dong, Zhiqin Bu, Yuan Cheng, Yorino Sato, Linli Hu, et al. 2016. "In Vitro Activation of Follicles and Fresh Tissue Auto-Transplantation in Primary Ovarian Insufficiency Patients." *Journal of Clinical Endocrinology and Metabolism* 101 (11): 4405–12.

Zhang, Kun, and Jianfeng Chen. 2012. "The Regulation of Integrin Function by Divalent Cations." *Cell Adhesion & Migration* 6 (1): 20–29.

Zhang, Yingying, Xin Chen, Cyril Gueydan, and Jiahuai Han. 2017. "Plasma Membrane Changes during Programmed Cell Deaths." *Cell Research* 28: 9–21.

Zhou, Feng, Li Bing Shi, and Song Ying Zhang. 2017. "Ovarian Fibrosis: A Phenomenon of Concern." *Chinese Medical Journal* 130 (3): 365–71.

Zou, Kang, Lin Hou, Kejing Sun, Wenhai Xie, and Ji Wu. 2011. "Improved Efficiency of Female Germline Stem Cell Purification Using Fragilis-Based Magnetic Bead Sorting." *Stem Cells and Development* 20 (12).

Zver, Tristan, Elodie Mouloungui, Aurélie Berdin, Christophe Roux, and Clotilde Amiot. 2017. "Validation of an Automated Technique for Ovarian Cortex Dissociation: Isolation of Viable Ovarian Cells and Their Qualification by Multicolor Flow Cytometry." *Journal of Ovarian Research* 10 (38).

# APPENDICES

# Appendix I.

## An analytical method to reflect age differences based on live cell yield isolated from human frozen/thawed ovarian cortex (Chapter 4, Section 4.4.4)

## INTRODUCTION

One of the aims in Chapter 4 was to investigate the effect of age on the dissociation of human frozen/thawed ovarian cortical tissue. Prior to addressing this aim, it was important to first determine two age groups. This was addressed by using the median split approach which was discussed in Chapter 4 (Section 4.4.4). Additionally, I wanted to explore if a split in age can be defined using a biological approach (i.e. are there differences in the efficacy of dissociation methods used in Chapter 4). To this end, I compared the differences in live-cell yield between the three different dissociation methods used in Chapter 4 (Table 4. 1) for each patient.

## MATERIALS AND METHODS

***Methods used to dissociate human frozen/thawed ovarian cortical tissue***

Frozen/thawed ovarian cortical tissue obtained from 10 patients aged 13- to 33-years (n=10) was dissociated using three different methods; 'Shaker L15', 'L15' and 'PBS', as described in Chapter 4 (Section 4.3.5) and viability was assessed as described (Chapter 2).

***Calculation of the difference in live-cell yield between dissociation methods used per patient***

Difference in live-cell yield was calculated and expressed as a percentage between method L15 and PBS (blue equation), Shaker L-15 and PBS (green equation) and Shaker L-15 and L15 (orange).

$$\text{Difference (\%)} = \frac{Number\ of\ Viable\ cells\ in\ L15 - Number\ of\ Viable\ cells\ in\ PBS}{Number\ of Viable\ cells\ in\ L15 + Number\ of\ Viable\ cells\ in\ PBS}$$

$$\text{Difference (\%)} = \frac{Number\ of\ Viable\ cells\ in\ Shaker\ L15 - Number\ of\ Viable\ cells\ in\ PBS}{Number\ of\ Viable\ cells\ in\ Shaker\ L15 + Number\ of\ Viable\ cells\ in\ PBS}$$

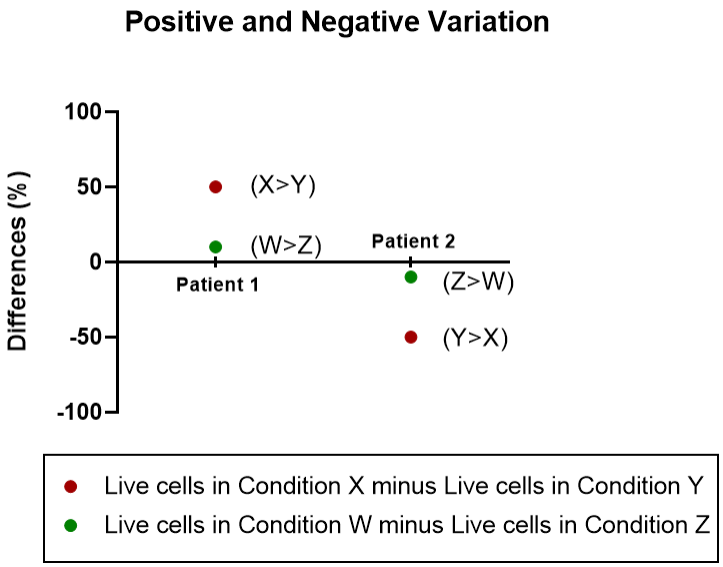
$$\text{Difference (\%)} = \frac{Number\ of\ Viable\ cells\ in\ Shaker\ L15 - Number\ of\ Viable\ cells\ in\ L15}{Number\ of\ Viable\ cells\ in\ Shaker\ L15 + Number\ of\ Viable\ cells\ in\ L15}$$

The quantified differences (%) per patient were presented in a graph as dots (see below). High variation was determined as the case where at least one difference/dot (in a patient) fell within the range ±50% to ±100%, otherwise patients were grouped into the low variation group (0% to 50%). Fifty percent was used as the threshold to determine high or low variation because 50% represents the middle value within a given range of 0% to 100%.

***The meaning of absolute positive and negative difference (%) – An Example***

If the number of viable cells in the first condition of the equation is bigger than the second condition of the equation (patient 1 in Supplementary Figure 1), then the difference (%) calculated is a positive number and this indicates that the first condition is more effective than the second for the patient analysed. For a positive difference (%), the dot is presented above the x-axis, i.e. red dot in patient 1; dissociation condition X is more effective to dissociation condition Y (X>Y), and green dot in patient 1; dissociation condition W is more effective to dissociation condition Z (W>Z) (Supplementary Figure 1).

On the contrary, if the number of viable cells in the second condition of the equation is bigger than the first condition of the equation (Patient 2 in Supplementary Figure 1), then the difference (%) is negative and this indicates that the second condition is more effective. For a negative difference (%), the dot is presented below x-axis, i.e. for patient 2; green dot; dissociation condition Z is more effective than dissociation condition W (Z>W), and red dot; dissociation condition Y is more effective than dissociation condition X (Y>X) (Supplementary Figure 1). Thus, differences in cell viability per patient between dissociation methods might reveal a pattern of the efficacy of the dissociation methods used.

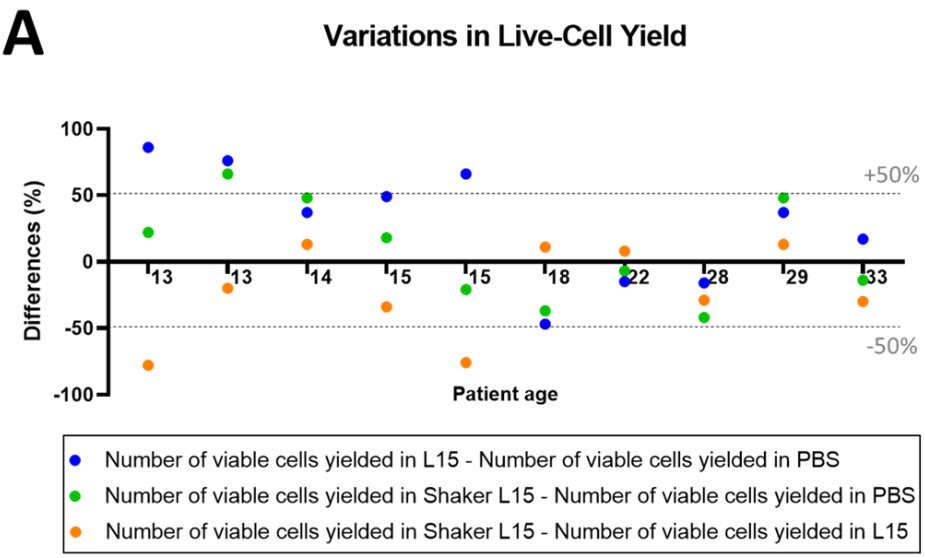



**Supplementary Figure 1. Difference (%) in live-cell yield between method X/Y and W/Z per patient.** For patient 1, the difference (%) is positive for both equations (red and green), whereas for patient 2 the difference (%) is negative for both equations (red and green). For patient 1, the most effective method is X, whereas for patient 2 is method Y. One equation represents one 'pair' of methods analysed per patient.

# RESULTS

A natural split in age between 15 and 18 years of age was revealed (Supplementary Figure 2A) with patients aged 13-15 years (younger patients) showing higher variation with 3 of 5 patients showing differences above ±50% (Supplementary Figure 2B). In patients aged over 18 years (older patients), variation was low; below 50% (Supplementary Figure 2).

**A**




**B**

| Patient | (+ / -) % | | |
|---|---|---|---|
| | Shaker L15 - L15 | Shaker L15 - PBS | L15 - PBS |
| 13 | -78 | 22 | 86 |
| 13 | -20 | 66 | 76 |
| 14 | 13 | 48 | 37 |
| 15 | -34 | 18 | 49 |
| 15 | -76 | -21 | 66 |
| 18 | 11 | -37 | -47 |
| 22 | 8 | -7 | -15 |
| 28 | -29 | -42 | -16 |
| 29 | 13 | 48 | 37 |
| 33 | -30 | -14 | 17 |

**Supplementary Figure 2. Analysis of the differences in live-cell yield per patient.** The difference in the number of viable cells/g isolated from each patient using Shaker L15, L15 and PBS was calculated and expressed as percentage (%). No statistical analysis was performed.

Based on this analysis, patients could be allocated into a Younger or Older category. Patients younger than 18 years of age were assigned to the Younger group and patients ≥18 years of age were assigned to the Older group.

## DISCUSSION

The age of the patients included to investigate the dissociation of frozen/thawed ovarian cortex in Chapter 4 widely ranged from 13-33 years. For this reason, I explored if a patient-focused analysis based on live-cell yield per gram of tissue using the three dissociation methods would reveal any similarities in the efficacy of dissociation between patients of similar ages.

Analysis of variation of live-cell yield revealed a split in age; patients aged 13-15 years showed high variation, and patients aged 18-33 years showed low variation. What is more, data differed between patients aged 15 years. This might be due to the fact that the age of menarche varies in healthy girls (the average age at menarche is 13.8 years ranging from 9 to 18 years (Flaws et al. 2000)) and is susceptible to many factors, some of which are still unknown (F. Thomas et al. 2001; Hagen et al. 2014). Therefore, different patients at the same chronological age could be at different developmental stages and thus, the pace of ovarian development might be different too. Interpatient variation and heterogeneity within patients have been demonstrated (K. L. T. Schmidt et al. 2003; Walker et al. 2019). This was evident in two out of four patients at the same age used in this study where the difference in live-cell yield between the three dissociation methods used was not similar; however, the efficacy of dissociation methods used was similar.

Information on the stage of puberty (i.e. Tanner scale) for patients included in this thesis was not available and patients were classified as pre- or post-pubertal (World Health Organisation 2010). As a result, differences in the ovarian ECM composition at different developmental stages may affect the dissociation of the ovarian cortex, which could explain the variation in the efficacy of dissociation for the 13-15-year-old patients. In the Older group there weren't any patients at the same age included and therefore, differences in the efficacy of dissociation methods between Older patients at the same ages could not be analysed; if more patients at the same age are included in the Older group, then differences in the efficacy of the three dissociation methods used may be revealed.

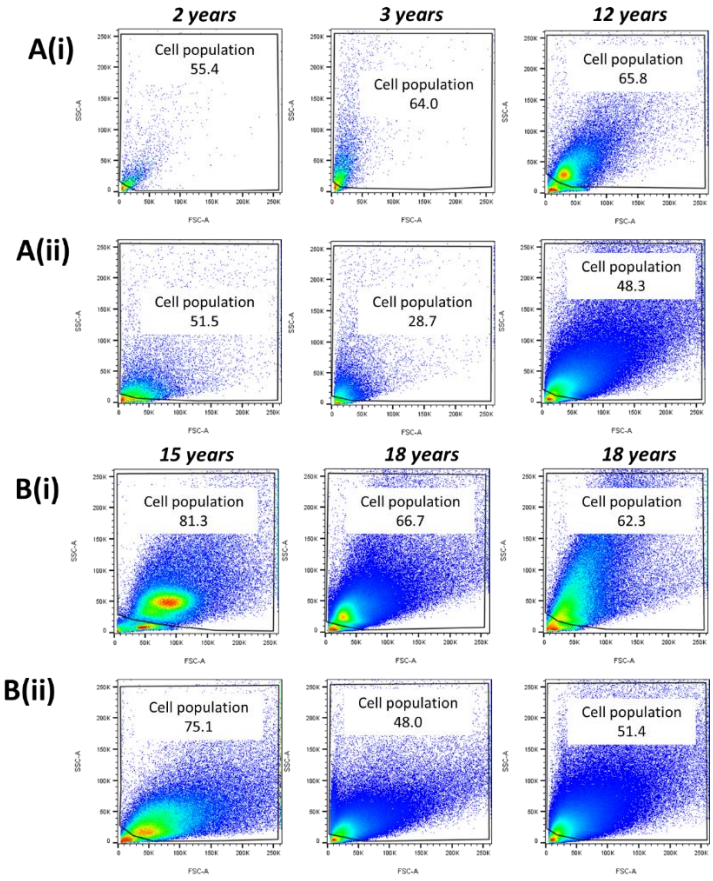
# CONCLUSIONS

This study showed that the analytical method developed here could be used to reveal a split in biological age based on differences in live-cell yield isolated from human frozen/thawed ovarian cortical tissue in future studies. Future studies should consider recruiting a larger cohort of patients, including patients at the same age, to explore how age affects the efficacy of dissociation of human frozen/thawed ovarian cortical tissue and how interpatient variation affects the efficacy of tissue dissociation using a patient-focused approach. Nevertheless, data obtained from this analytical study were consistent with the median split approach (Chapter 4) where patients younger than 16 years of age were assigned to the Younger group and those older than 16 years of age to the Older group.

# Appendix IIa.

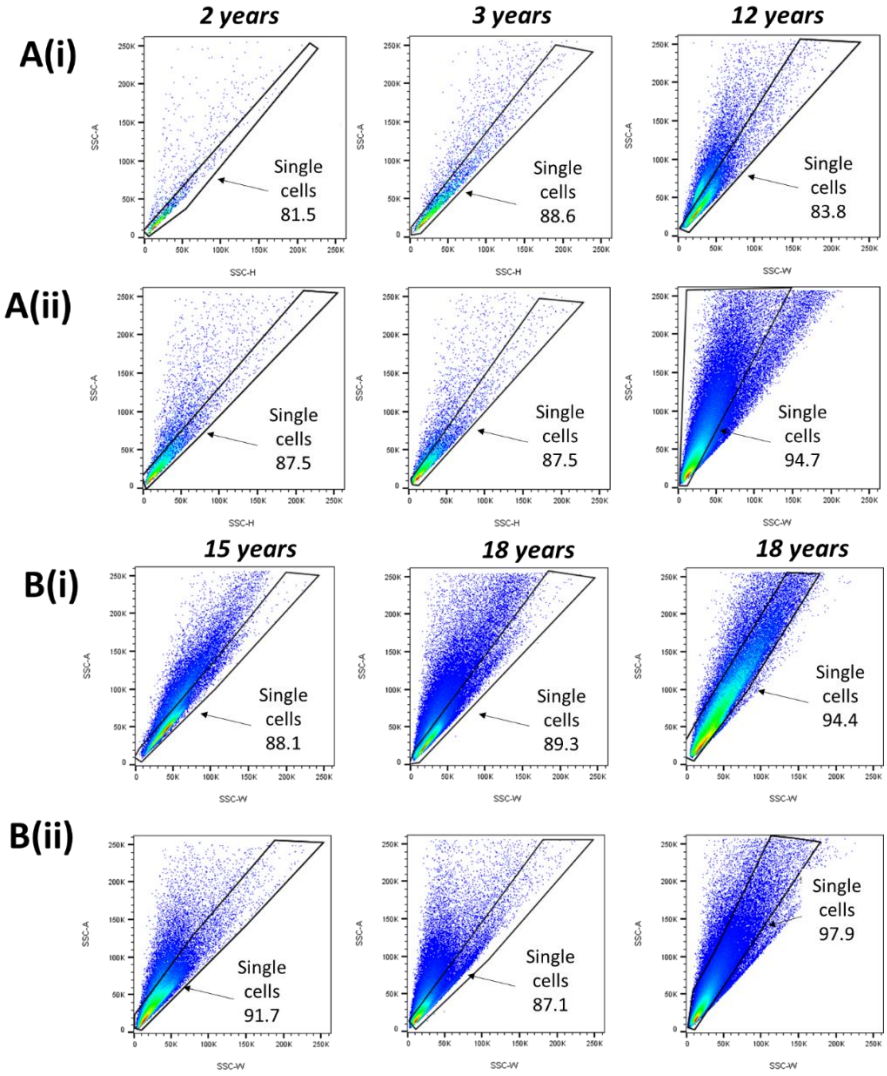
## Identification of the total cell population, single cell population and gating of positive cells based on isotype controls obtained from human fresh ovarian remnant tissue as measured by flow cytometry (FC) – Chapter 5

Cells obtained from human fresh ovarian remnants were analysed using FC (Section 5.4.2.1). Debris was excluded from the main cell population obtained from pre- and post-pubertal patients and the percentage of the total cell population was identified (Supplementary Figure 3.).



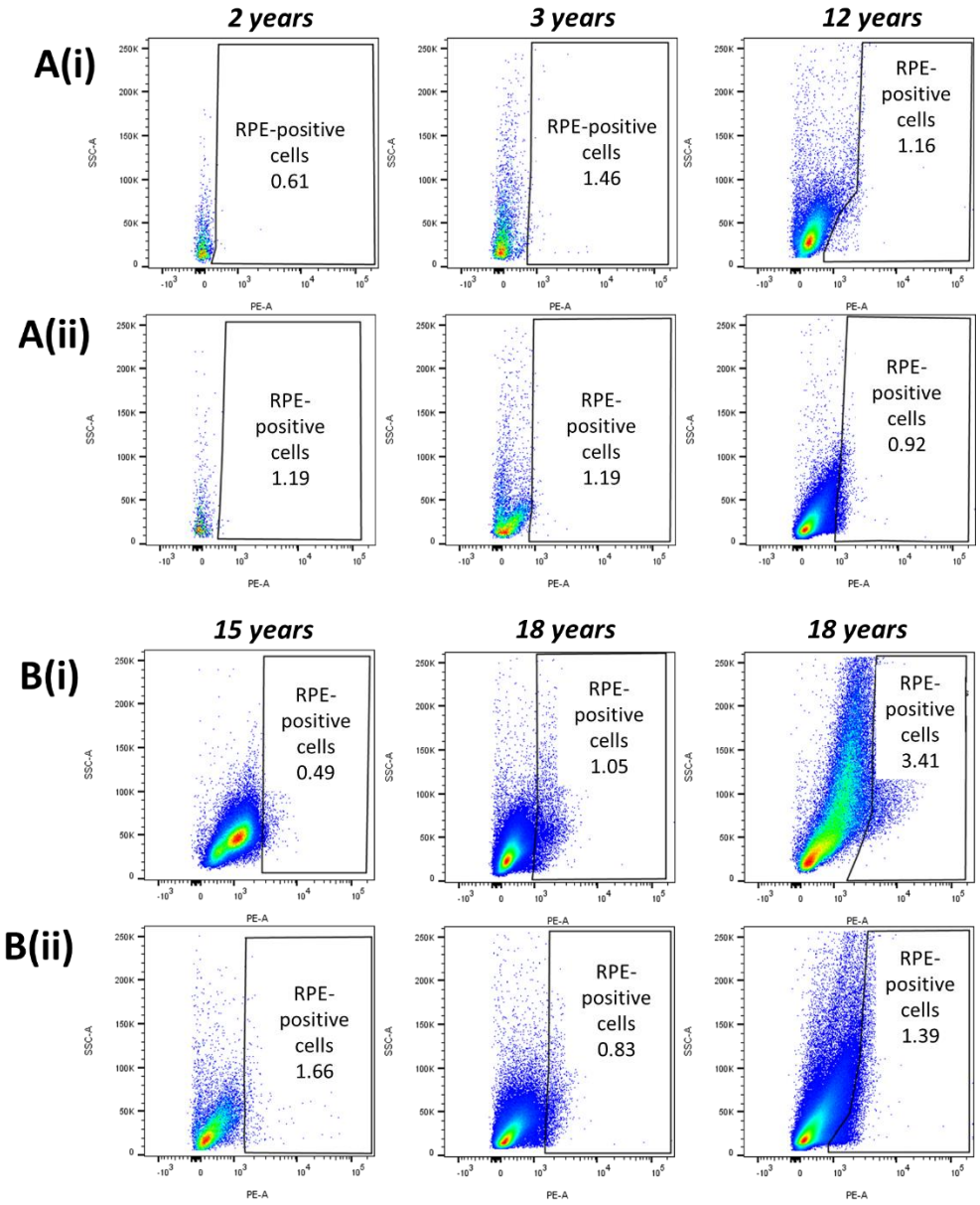

**Supplementary Figure 3. Total cell population from human fresh ovarian remnant tissue measured by FC.** Cells from pre-pubertal (A(i): ND-group; A(ii): D group) and post-pubertal (B(i): ND-group; B(ii): D-group) patients were analysed using FC. Data is displayed using a SSC-A versus FSC-A dot plot and a gate was drawn around the main cell population to exclude cell debris. Data shows the percentage of the total cell population analysed for each patient. SSC-A: side scatter area; FSC-A: forward scatter area.

Cells obtained from human fresh ovarian remnants were analysed using FC (Section 5.4.2.1). Doublets were excluded from the total cell population obtained from pre- and post-pubertal patients and the percentage of single cells was identified (Supplementary Figure 4.).




**Supplementary Figure 4. Identification of the single cell population from human fresh remnant ovarian tissue measured by FC.** Cells as identified in the total cell population from pre-pubertal (A(i): ND-group; A(ii): D group) and post-pubertal (B(i): ND-group; B(ii): D-group) patients were displayed on an SSC-A versus SSC-W dot plot to eliminate doublets. Data shows the percentage of single cells analysed for each patient. SSC-A: side scatter area; SSC-W: side scatter weight.

Cells obtained from human fresh ovarian remnants were analysed using FC (Section 5.4.2.3). Viable single cells were labelled with anti-IgG1 isotype control and R-Phycoerythrin (RPE). Cells were analysed on a SSC-A vs. IgG1-PE (PE-A) and a gate was drawn at ~1% of RPE-positive cells (Supplementary Figure 5.).

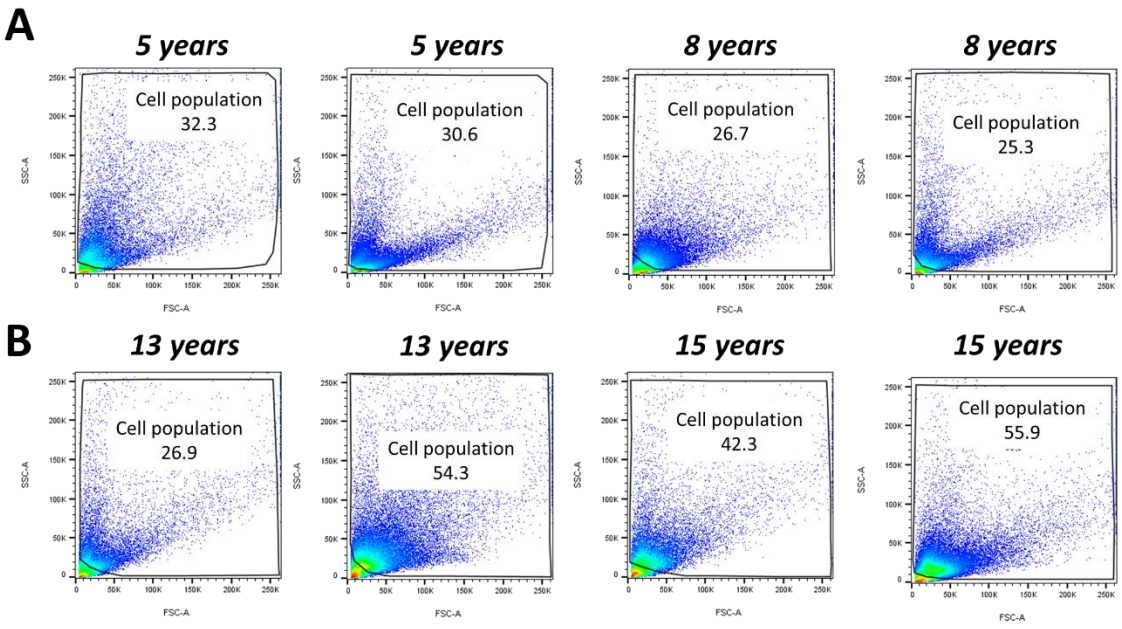



**Supplementary Figure 5. Isotype controls used to set a gate at ~1% of RPE-positive cells obtained from human fresh ovarian remnant tissue measured by FC.** Viable single cells obtained from pre-pubertal (A(i): ND-group; A(ii): D group) and post-pubertal (B(i): ND-group; B(ii): D-group) patients as identified in the total cell population were labelled with anti-IgG1 and displayed on SSC-A versus IgG1-PE (PE-A) density scatter plots, and a gate was set at 0.1% – 3.4%. Data shows the percentage of IgG1-RPE-positive cells (RPE-positive cells) analysed for each patient. SSC-A: side scatter area; RPE: secondary antibody conjugated to R-Phycoerythrin; PE-A: R-phycoerythrin area.

# Appendix IIb.

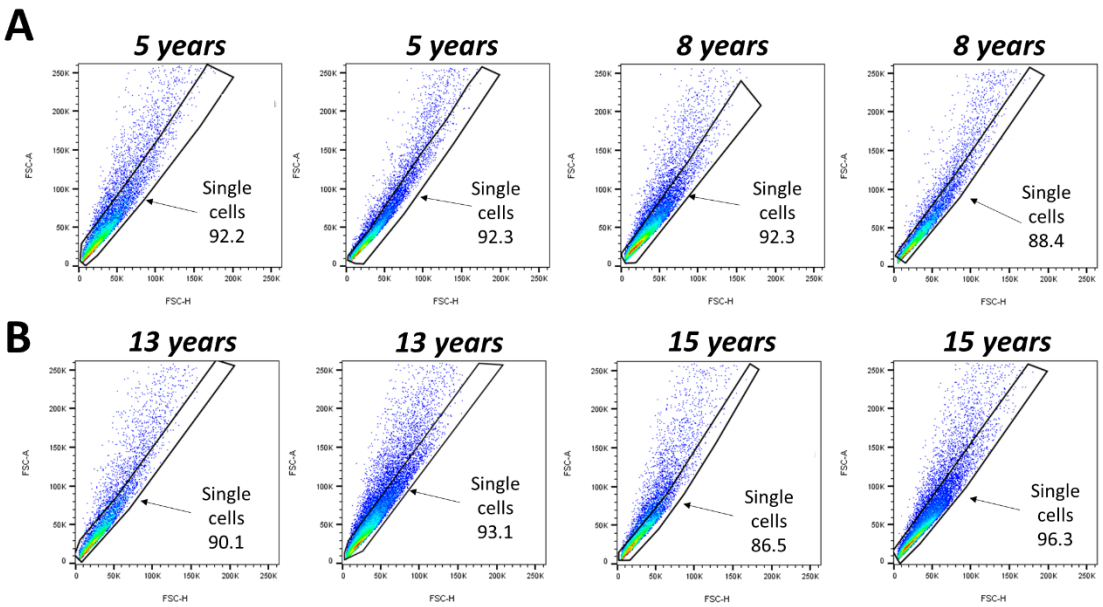
## Identification of the total cell population, single cell population and gating of positive cells based on isotype controls obtained from human frozen/thawed ovarian cortex as measured by flow cytometry (FC) – Chapter 5

Cells obtained from human frozen/thawed ovarian cortical tissue were analysed using FC (Section 5.4.3.1). Debris was excluded from the main cell population obtained from pre- and post-pubertal patients and the percentage of the total cell population was identified (Supplementary Figure 6.).



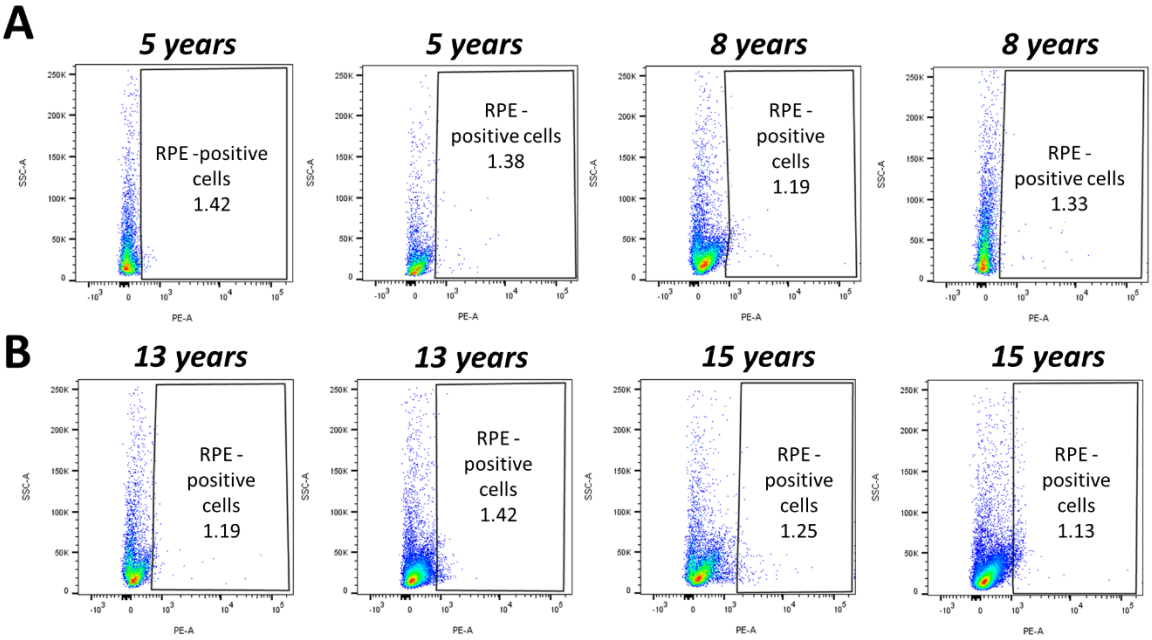

**Supplementary Figure 6. Total cell population from human frozen/thawed ovarian cortical tissue measured using FC.** Dissociated cells from pre-pubertal (A) and post-pubertal (B) patients were analysed using FC. Data was displayed using a SSC-A versus FSC-A dot plot and a gate was drawn around the main population to exclude cell debris. Data shows the percentage of the main cell population analysed for each patient. SSC-A: side scatter area; FSC-A: forward scatter area.

Cells obtained from human frozen/thawed ovarian cortical tissue were analysed using FC (Section 5.4.3.1). Doublets were excluded from the total cell population obtained from pre- and post-pubertal patients and the percentage of single cells was identified (Supplementary Figure 7.).




**Supplementary Figure 7. Identification of the single cell population from human frozen/thawed ovarian cortical tissue measured by FC.** Dissociated cells as identified in the total cell population from pre-pubertal (A) and post-pubertal (B) patients were displayed on an SSC-A versus SSC-W dot plot to eliminate doublets. Data shows the percentage of single cells analysed for each patient. SSC-A: side scatter area; SSC-W: side scatter weight.

Cells obtained from human frozen/thawed ovarian cortex were analysed using FC (Section 5.4.3.3). Viable single cells were labelled with anti-IgG1 isotype control and R-Phycoerythrin (RPE). Cells were analysed on a SSC-A versus. IgG1-PE (PE-A) and a gate was drawn at ~1% of RPE-positive cells (Supplementary Figure 8.).




**Supplementary Figure 8. Isotype controls used to set a gate at ~1% of RPE-positive cells obtained from human frozen/thawed ovarian cortex measured by FC.** Viable single cells obtained from pre-pubertal (A) and post-pubertal (B) patients as identified in the total cell population were labelled with anti-IgG1 and displayed on SSC-A versus IgG1-PE (PE-A) density scatter plots, and a gate was set at ~1%. Data shows the percentage of IgG1-RPE-positive cells (positive cells) analysed for each patient. SSC-A: side scatter area; RPE: secondary antibody conjugated to R-Phycoerythrin; PE-A: R-phycoerythrin area.

# Appendix III

## Demonstration of the *in vitro* mouse RO method – Chapter 6

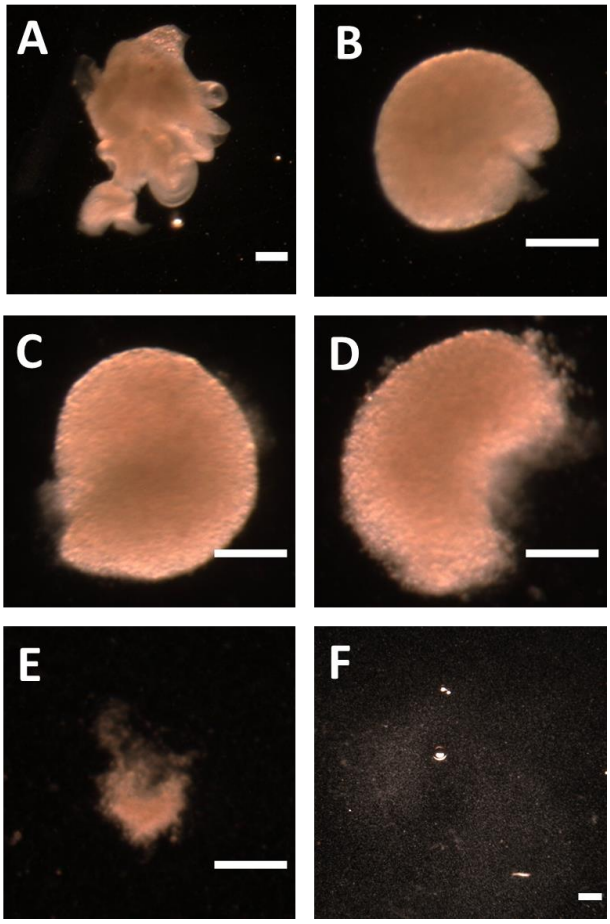
## MATERIALS AND METHODS

To demonstrate I could perform clean separation of follicular somatic cells and oocytes using differential adhesion as routinely used in the RO method, ovaries were obtained from CD1xROSA26*LacZ* or ROSA26*LacZ* mice at postnatal day 3 to 8 and dissociated into a single cell suspension as described (Chapter 2). Germ and somatic cells were separated using differential adhesion and combined to form a pellet, which was then cultured on a polycarbonate membrane in a 24-well culture plate for 7 days as described (Chapter 2). *LacZ*$^{+}$ germ cells were combined with *LacZ*$^{-}$ somatic cells to form a RO. To assess clean separation of germ cells from somatic cells, cultured ROs (n=3) were harvested, fixed in 10% formalin, and stained using the X-gal method as described (Chapter 2).

To demonstrate follicle development *in vitro* in the RO, ovaries were obtained from CD1xROSA26*LacZ* mice at postnatal day 5 to 7 and processed to generate a RO as described above. ROs were cultured on a polycarbonate membrane in a 24-well culture plate for 14 days as described (Chapter 2). To assess follicle development, cultured ROs (n=6) were harvested, fixed in 10% neutral buffered formalin and processed for histological analysis (see below).

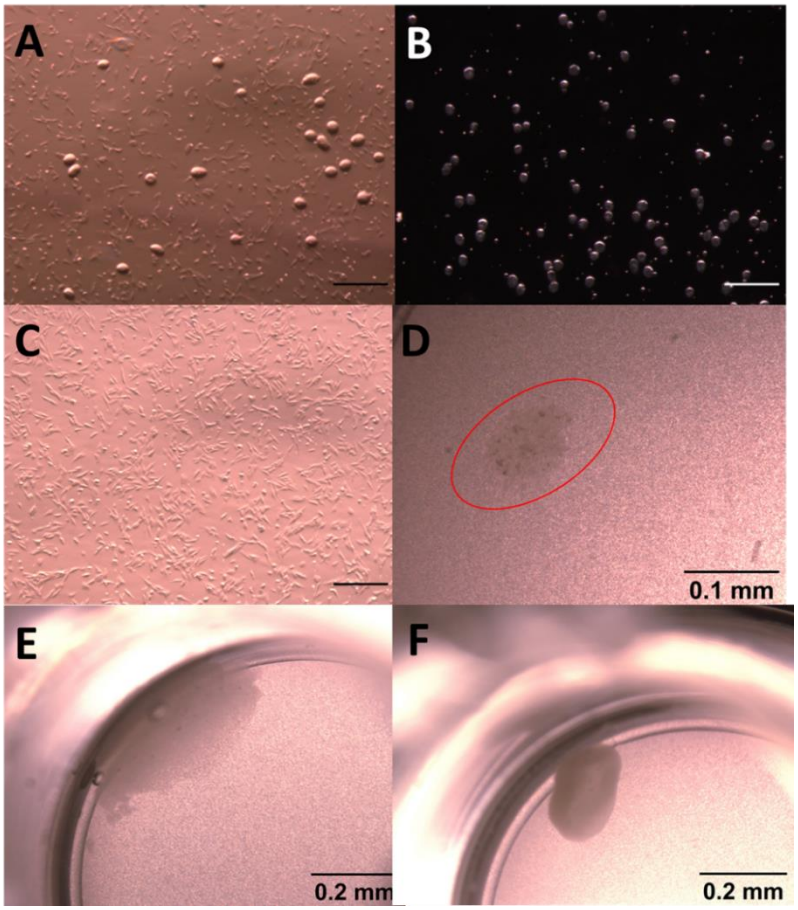
# RESULTS

Ovaries were transferred to the laboratory (Supplementary Figure 9.A), cleaned of the bursa and fat (Supplementary Figure 9.B), and enzymatically digested. Gradual dissociation of the ovaries was observed at 15 min (Supplementary Figure 9.C), 20 min (Supplementary Figure 9.D) and 25 min (Supplementary Figure 9.E). At 30 min of enzymatic digestion, ovaries had fully dissociated into a single cell suspension (Supplementary Figure 9.F).



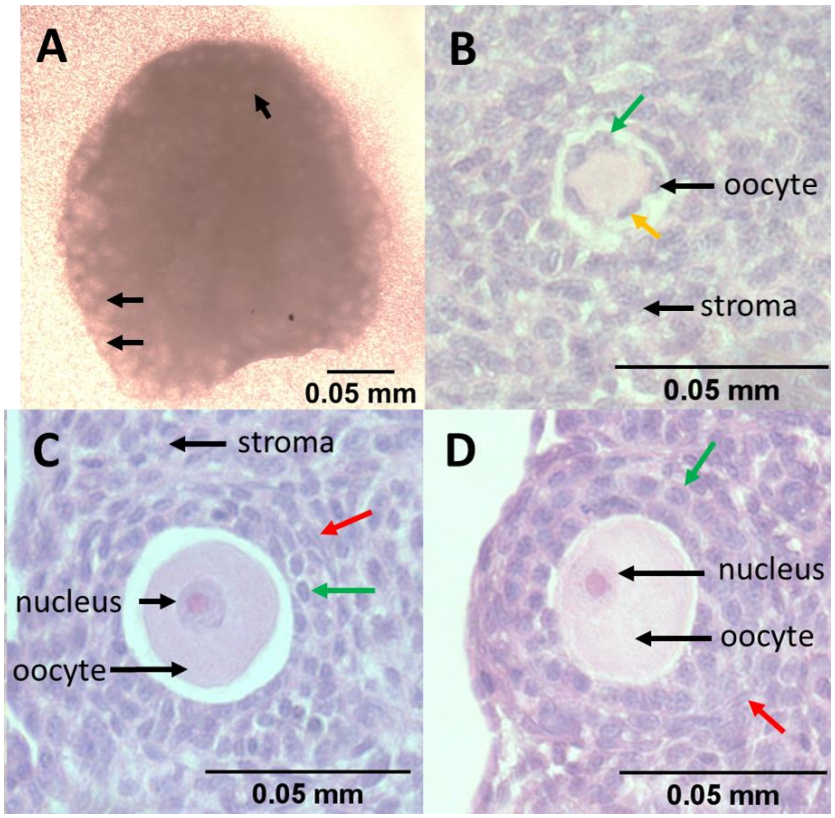

**Supplementary Figure 9. Representative images of neonatal mouse ovaries at different stages of dissociation using the RO method.** Ovaries were obtained from mice at postnatal day 4 (A), and bursa and fat were removed leaving the clean ovary (B). Ovaries were digested enzymatically for 30 min. To aid dissociation the digestion mixture was mixed by gentle pipetting at 15- (C), 20- (D) and 25 min (E). At 30 min of digestion ovaries were completely dissociated (F). Scale bar: 50 µm.

The next stage in the RO method was to achieve differential adhesion and pellet formation. Somatic cells successfully adhered to the bottom of the culture plate after the first differential separation (overnight incubation, Supplementary Figure 10.A) and second differential separation (6 hours of incubation, Supplementary Figure 10.C) while, as anticipated, germ cells did not (first differential separation (Supplementary Figure 10.A) and second differential separation (Supplementary Figure 10.B)). Therefore, after successful differential adhesion, germ and somatic cells were aggregated and a pellet was formed (Supplementary Figure 10.D). To aid the rounding process, the pellet was placed at the edge of culture membrane and incubated overnight (Supplementary Figure 10.E); the rounded pellet was characterised as an RO (Supplementary Figure 10.F).



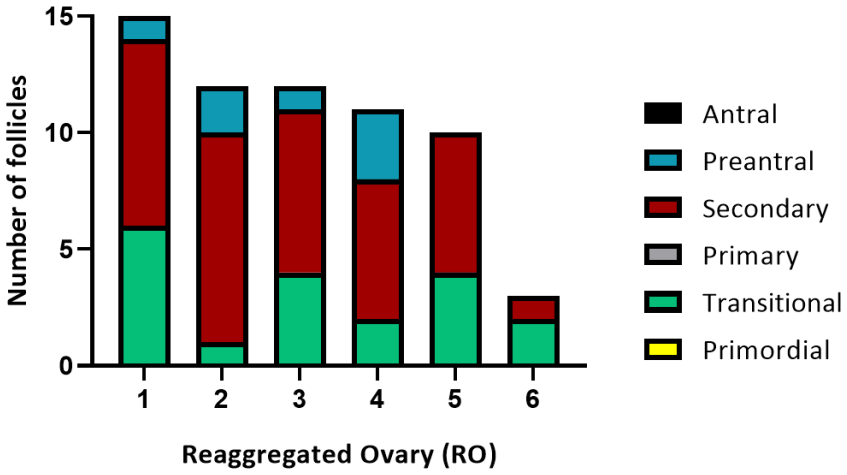

**Supplementary Figure 10. Representative images of stages in the generation of a RO using mouse cells.** A single cell suspension was obtained after dissociation of mouse ovaries and cultured overnight to allow for somatic cell adhesion; first separation. Floating germ cells and adhered somatic cells (A) were each collected, re-plated in separate culture plates and incubated for another 6 hours at 37°C in an atmosphere of 5% $CO_2$ with 95% air to allow for clean separation; second separation (B; floating germ cells, C; adhered somatic cells). Germ and somatic cells were reagregated to form a pellet (D) that was placed at the edge of culture membrane in a 24-well culture plate with culture medium overnight to aid the rounding process (E). The rounded pellet; the RO (F), was further cultured for 7 or 14 days. Scale bar: 50 µm (if not indicated otherwise).

To investigate whether the ROs produced follicles, ROs were cultured for 14 days *in vitro*. Follicles were observed in all ROs generated (n=6) (Supplementary Figure 11.), and after histological analysis follicles were classified into transitional, secondary or preantral as described (Chapter 2).




**Supplementary Figure 11. Representative images of transitional, secondary and preantral follicles in a RO cultured for 14 days.** Germ cells and somatic cells obtained after dissociation of neonatal mouse ovaries were reaggregated to generate a RO and cultured for 14 days to allow for follicle development. Follicles resembled bubble-like structures (black arrows) in the RO after 14 days (A). ROs were processed and analysed histologically using Haemotoxylin and Eosin staining (B, C, D). Transitional follicles (B) were characterised by a single layer of mixed flattened pre-granulosa cells (yellow arrows) and cuboidal granulosa cells (GCs) (green arrows). In secondary follicles (C), the oocyte was surrounded by up to 2 complete layers of cuboidal GCs and some theca cells (TCs) (red arrows), and preantral follicles (D) had at least 3 complete layers of GCs and some TCs. The oocyte, oocyte nucleus and stroma are also indicated (B, C, D). Scale bar: 50 µm.

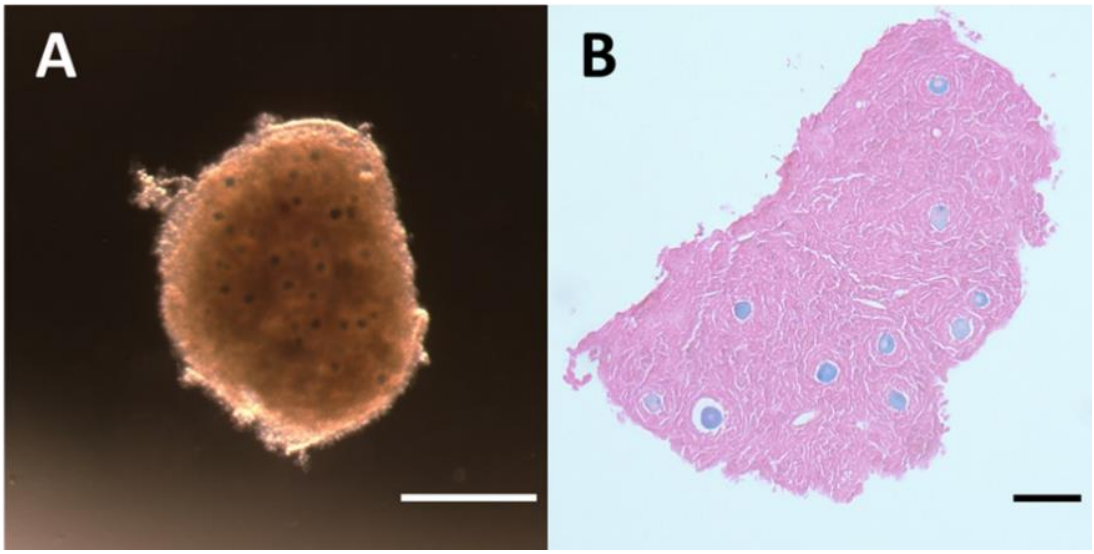
Of the 6 ROs analysed, 5 had 10 or more follicles at different stages of development (Supplementary Figure 12.). A total of 63 follicles were identified and of these, 19 were at the transitional stage of development and 37 at the secondary stage of development. Seven pre-antral follicles were identified in 4 of the 6 ROs studied. No primordial, primary, or antral follicles were observed (Supplementary Figure 12.). Furthermore, all of the analysed ROs had incomplete theca cell (TCs) layers.




**Supplementary Figure 12. Stages of follicle development observed *in vitro* in ROs.** Mouse germ cells were aggregated with mouse somatic cells and cultured *in vitro* for 14 days using the RO method. Follicle development was assessed, and follicles were categorised into primordial, transitional, primary, secondary, preantral and antral follicles. Data shows the number of follicles analysed in each developmental stage. N=63.

This analysis confirmed that I was able to produce functional ROs that supported follicle development up to preantral stage *in vitro*. This finding was in accordance with other studies carried out in our laboratory (Lo, Sheikh, and Williams 2019).

To examine if clean separation of germ cells from somatic cells was achieved, ROs were cultured for 7 days *in vitro*. The ROs analysed here (n=3) were generated using *LacZ*$^{+}$ germ cells and *LacZ*$^{-}$ somatic cells. To detect *LacZ*$^{+}$ cells, ROs were stained using the X-gal method as described (Chapter 2). This analysis showed that oocytes were *LacZ*$^{+}$ and stained blue while somatic cells were LacZ$^{-}$ and did not stain blue in all the ROs studied (n=3) (Supplementary Figure 13.A,B). This data indicated that clean separation of oocytes from somatic cells obtained from *LacZ*$^{+}$ mouse ovaries, and clean separation of somatic cells from oocytes obtained from *LacZ*$^{-}$ ovaries was achieved using differential separation.




**Supplementary Figure 13. Representative images of RO processed to detect blue *LacZ*$^+$ cells.** ROs were cultured for 7 days, harvested, and processed for analysis. The X-gal staining method was used to detect *LacZ*$^+$ germ cells in ROs before (A) and after eosin staining (B). Blue: *LacZ*$^+$ cells; pink: eosin-positive cells (extracellular matrix and cytoplasm). Scale bar: 50 µm.

Here it was shown that the RO method was successfully reproduced by myself with clean separation and follicle development. Clean separation was demonstrated using mouse LacZ$^+$ germ cells, indicating that a pure mouse germ cell population (not contaminated with mouse somatic cells) could be isolated using the RO method. Thus, generation of FibROs using mouse germ cells (which would generate mouse oocytes) and human dermal fibroblasts (which would replace the mouse somatic cells to support follicle formation and development).